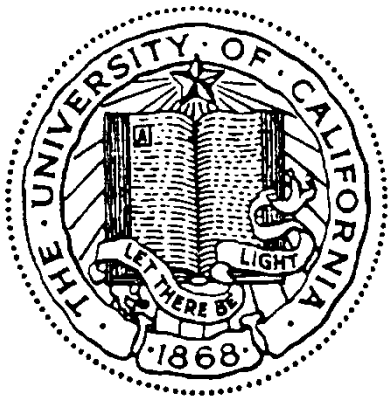

STRUCTURAL SYSTEMS

RESEARCH PROJECT

Report No.
SSRP–16/05

MSBRIDGE: OPENSEES PUSHOVER AND EARTHQUAKE ANALYSIS OF MULTI-SPAN BRIDGES - USER MANUAL

by

ABDULLAH ALMUTAIRI

JINCHI LU

AHMED ELGAMAL

KEVIN MACKIE

Final Report Submitted to the California Department of Transportation (Caltrans) under Contract No. 65A0530.

January 2019

Department of Structural Engineering
University of California, San Diego
La Jolla, California 92093-0085

University of California, San Diego
Department of Structural Engineering
Structural Systems Research Project

Report No. SSRP-16/05

MSBridge: OpenSees Pushover and Earthquake Analysis of Multi-span Bridges - User Manual

by

Abdullah Almutairi
Graduate Student Researcher, UC San Diego

Jinchi Lu
Associate Project Scientist, UC San Diego

Ahmed Elgamal
Professor of Geotechnical Engineering, UC San Diego

Kevin Mackie
Associate Professor of Structural Engineering,
University of Central Florida

Final Report Submitted to the California Department of Transportation under Contract No. 65A0530

Department of Structural Engineering
University of California, San Diego
La Jolla, California 92093-0085

January 2019

Technical Report Documentation Page

1. Report No.	2. Government Accession No.	3. Recipient's Catalog No.

4. Title and Subtitle	5. Report Date
MSBridge: OpenSees Pushover and Earthquake Analysis of Multi-span Bridges - User Manual	January 2019
	6. Performing Organization Code

7. Author(s)	8. Performing Organization Report No.
Abdullah Almutairi, Jinchi Lu, Ahmed Elgamal and Kevin Mackie	UCSD / SSRP-16/05

9. Performing Organization Name and Address	10. Work Unit No. (TRAIS)
Department of Structural Engineering School of Engineering University of California, San Diego La Jolla, California 92093-0085	11. Contract or Grant No. 65A0530

12. Sponsoring Agency Name and Address	13. Type of Report and Period Covered
California Department of Transportation Division of Engineering Services 1801 30th St., MS-9-2/5i Sacramento, California 95816	Final Report
	14. Sponsoring Agency Code

15. Supplementary Notes

Prepared in cooperation with the State of California Department of Transportation.

16. Abstract

MSBridge is a PC-based graphical pre- and post-processor (user-interface) for conducting nonlinear Finite Element (FE) studies for a wide range of multi-span bridge systems. FE computations are conducted using OpenSees (http://opensees.berkeley.edu), an open source framework (for simulating the seismic response of structural and geotechnical systems) developed by the Pacific Earthquake Engineering Research (PEER) Center. MSBridge allows users (e.g., structural engineers) to rapidly build a bridge model, run the FE analysis, and evaluate the performance of the bridge-ground system. Main capabilities of MSBridge include: i) horizontal and vertical alignments, with different skew angles for bents/abutments; ii) nonlinear beam-column elements with fiber section for bridge columns and/or piles; iii) deck hinges, isolation bearings, steel jackets, and abutment models; and iv) foundation represented by foundation matrix (6x6) or soil springs (p-y, t-z, and q-z). The analysis options available in MSBridge include: i) pushover analysis; ii) mode shape analysis; iii) 3D base input acceleration analysis (for suites of ground motions, built-in and/or user-defined); iv) equivalent static analysis (ESA); and v) PBEE analysis (with PBEE outcomes in terms of repair cost, time and carbon footprint).

17. Key Words	18. Distribution Statement
Finite Element, Time History Analysis	Unlimited

19. Security Classification (of this report)	20. Security Classification (of this page)	21. No. of Pages	22. Price
Unclassified	Unclassified		

Form DOT F 1700.7 (8-72) Reproduction of completed page authorized

DISCLAIMER

This document is disseminated in the interest of information exchange. The contents of this report reflect the views of the authors who are responsible for the facts and accuracy of the data presented herein. The contents do not necessarily reflect the official views or policies of the State of California or the Federal Highway Administration. This publication does not constitute a standard, specification or regulation. This report does not constitute an endorsement by the California Department of Transportation of any product described herein.

For individuals with sensory disabilities, this document is available in Braille, large print, audiocassette, or compact disk. To obtain a copy of this document in one of these alternate formats, please contact Division of Research and Innovation, MS-83, California Department of Transportation, P.O. Box 942873, Sacramento, CA 94273-0001.

ACKNOWLEDGMENTS

The research described in this report was primarily supported by the California Department of Transportation (Caltrans) with Dr. Charles Sikorsky as the project manager. Additional funding was provided by the Pacific Earthquake Engineering Research Center (PEER). These supports are most appreciated. In addition, we are grateful for the valuable technical suggestions, comments, and contributions provided by Caltrans engineers, particularly Dr. Charles Sikorsky, Dr. Toorak Zokaie, Mr. Yeo (Tony) Yoon, Dr. Mark Mahan, Dr. Anoosh Shamsabadi, and Mr. Steve Mitchell.

ABSTRACT

MSBridge is a PC-based graphical pre- and post-processor (user-interface) for conducting nonlinear Finite Element (FE) studies for a wide range of multi-span bridge systems. FE computations are conducted using OpenSees (http://opensees.berkeley.edu), an open source framework (for simulating the seismic response of structural and geotechnical systems) developed by the Pacific Earthquake Engineering Research (PEER) Center. MSBridge allows users (e.g., structural engineers) to rapidly build a bridge model, run the FE analysis, and evaluate the performance of the bridge-ground system. Main capabilities of MSBridge include: i) horizontal and vertical alignments, with different skew angles for bents/abutments; ii) nonlinear beam-column elements with fiber section for bridge columns and/or piles; iii) deck hinges, isolation bearings, steel jackets, and abutment models; and iv) foundation represented by foundation matrix (6x6) or soil springs (p-y, t-z, and q-z). The analysis options available in MSBridge include: i) pushover analysis; ii) mode shape analysis; iii) 3D base input acceleration analysis (for suites of ground motions, built-in and/or user-defined); iv) equivalent static analysis (ESA); and v) PBEE analysis (with PBEE outcomes in terms of repair cost, time and carbon footprint).

TABLE OF CONTENTS

LIST OF FIGURES

LIST OF TABLES

1 INTRODUCTION

1.1 Overview

MSBridge is a PC-based graphical pre- and post-processor (user-interface) for conducting nonlinear Finite Element (FE) studies for multi-span bridge systems. Main capabilities include:

i) Horizontal and vertical alignments, with different skew angles for bents/abutments
ii) Nonlinear beam-column element with fiber section for bridge columns and piles
iii) Deck hinges, isolation bearings, and steel jackets
iv) Foundation represented by Foundation matrix or soil springs (p-y, t-z and q-z)
v) Advanced abutment models (Elgamal *et al.* 2014; Aviram 2008a, 2008b)
vi) Automatic mesh generation of multi-span bridge systems
vii) Management of ground motion suites
viii) Simultaneous execution of nonlinear Time History Analysis (THA) for multiple motions
ix) PBEE outcomes in terms of repair cost, time and carbon footprint
x) Visualization and animation of response time histories

FE computations in **MSBridge** are conducted using OpenSees (currently ver. 2.5.0 is employed). OpenSees is an open source software framework (McKenna et al. 2010; Mazzoni et al. 2009) for simulating the seismic response of structural and geotechnical systems. OpenSees has been developed as the computational platform for research in performance-based earthquake engineering (PBEE) at the Pacific Earthquake Engineering Research (PEER) Center. For more information about OpenSees, please visit http://opensees.berkeley.edu/.

The analysis options available in **MSBridge** include:

i) Pushover Analysis
ii) Mode Shape Analysis
iii) Single and Multiple 3D Base Input Acceleration Analysis
iv) Equivalent Static Analysis (ESA)
v) PBEE Analysis

1.2 What's New in Current Updated Version

A number of capabilities and features have been added in the current version of MSBridge. These added features mainly allow MSBridge to address possible variability in the bridge deck, bent cap, column, foundation, or soil configuration/properties (on a bent-by-bent basis). For the complete list of the added capabilities and features, please see Appendix A.

1.3 Units

MSBridge supports analysis in both the US/English and SI unit systems, and the default system is US/English units. This unit option can be interchanged during model creation, and MSBridge will convert all input data to the desired unit system. For conversion between SI and English Units, please check:
http://www.unit-conversion.info/

Some commonly used quantities can be converted as follows:

1 kPa	=	0.14503789 psi
1 psi	=	6.89475 kPa
1 m	=	39.37 in
1 in	=	0.0254 m

1.4 Coordinate Systems

The global coordinate system employed in **MSBridge** is shown in Fig. 1. The origin is located at the left deck-end of the bridge. The bridge deck direction in a straight bridge is referred to as "longitudinal direction (X)," while the horizontal direction perpendicular to the longitudinal direction is referred to as "transverse direction (Y)." At any time, "Z" denotes the vertical direction.

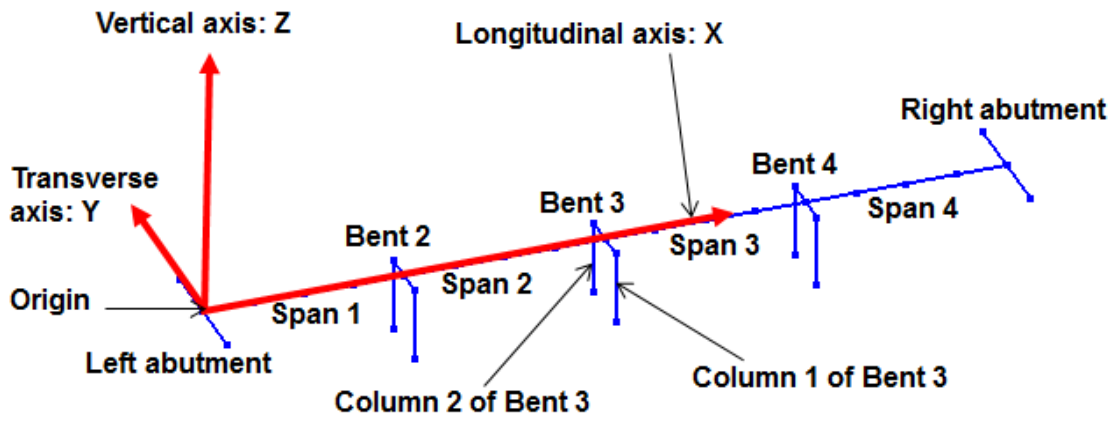

Fig. 1. Global coordinate system employed in **MSBridge**

Bridge component numbering and names used in **MSBridge** follow designations as follows: The left abutment (see Fig. 1) is designated "Abutment 1". The bents are numbered consecutively (starting with Bent 2). The right abutment is designated "Right Abutment" or "Abutment *N*" (where *N* is the last Bent number plus one, e.g., the right abutment shown in Fig. 1 can be referred to as "Abutment 5"). The spans are numbered similar to the abutment and bent numbering, e.g., Span 1 is between Abutment 1 and Bent 2, Span 2 is between Bents 2 and 3.

For multi-column scenarios, the columns are numbered consecutively along the transverse (Y) direction, starting from 1 in the most negative side. e.g., in Fig. 1, the

column at the negative side of the transverse (Y) direction is referred to as Column 1 while the one at the positive side is called Column 2. For Bent 3, there are "Column 1 of Bent 3" and "Column 2 of Bent 3" (Fig. 1).

Local coordinate systems will also be used in this document to describe certain components, e.g., deck hinges, isolation bearings, distributed spring abutment models with a skew angle, etc. In that case, labels of "1", "2" and "3" (or lower case "x," "y" and "z") will be used. Please refer to the appropriate section for the corresponding description.

In **MSBridge**, maximum response quantities (e.g., displacement, acceleration) are reported in the local coordinate system. For a straight bridge, the local coordinate system is parallel to the global one. For a curved bridge, the local coordinate system is defined in such a way that the local longitudinal axis (x) is tangent to the bridge curve at a given superstructure location while the transverse axis (y) is another horizontal direction that is perpendicular to the longitudinal axis (x). The z-axis in a local coordinate system is perpendicular to the x- and y-axes and positive upwards.

1.5 System Requirements

MSBridge runs on PC-compatible systems running Windows (7, 8, 10 or Server). The system should have a minimum hardware configuration appropriate to the particular operating system. For best results, the system's video should be set to 1024 by 768 or higher.

1.6 Acknowledgment

Development of **MSBridge** was funded primarily by the California Department of Transportation (Caltrans). Additional funding was provided by the Pacific Earthquake Engineering Research Center (PEER), a multi-institutional research and education center with headquarters at the University of California, Berkeley.

MSBridge was written in Microsoft .NET Framework (Windows Presentation Foundation or WPF). OpenTK (OpenGL) library (https://opentk.github.io/) was used for visualization of FE mesh and OxyPlot package (https://github.com/oxyplot) was employed for x-y plotting. In addition, 3D extruded view of a bridge model was implemented by using Helix Toolkit (https://github.com/helix-toolkit).

For questions or remarks about **MSBridge**, please send email to Dr. Ahmed Elgamal (elgamal@ucsd.edu), or Dr. Jinchi Lu (jinlu@ucsd.edu).

2 GETTING STARTED

2.1 Start-Up

On Windows, start **MSBridge** from the Start button or the **MSBridge** icon on your desktop. To Start **MSBridge** from the Start button:

i) Click Start, and then select the **MSBridge** folder
ii) Click on **MSBridge** (icon:)

The **MSBridge** main window is shown in Fig. 2.

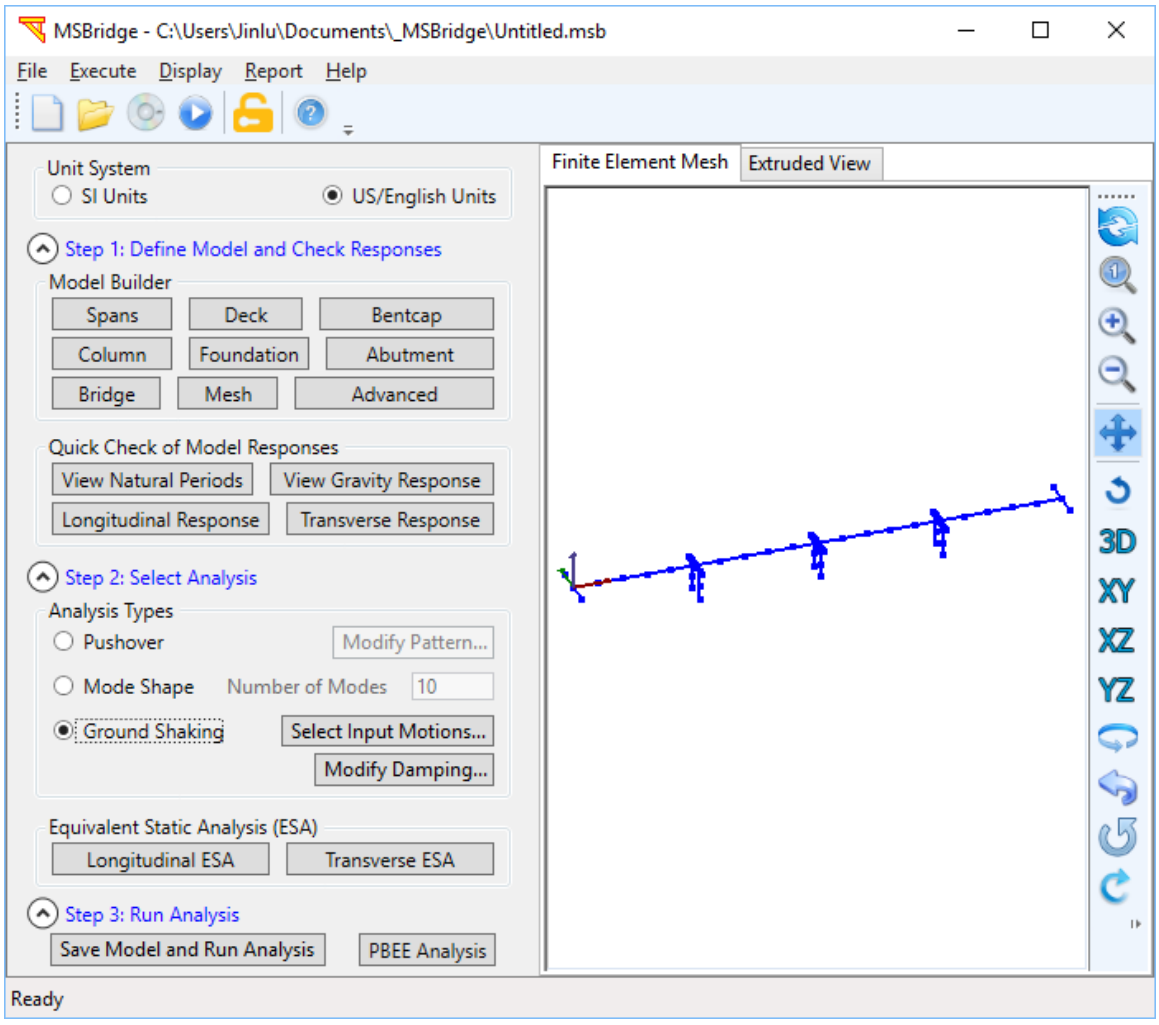

Fig. 2. MSBridge main window

2.2 Interface

There are three main regions in the **MSBridge** window – menu bar, the model input, and the FE mesh.

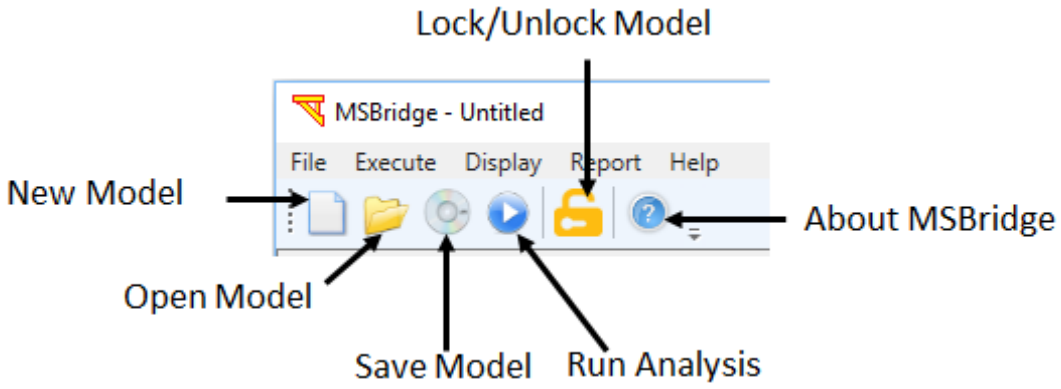

a)

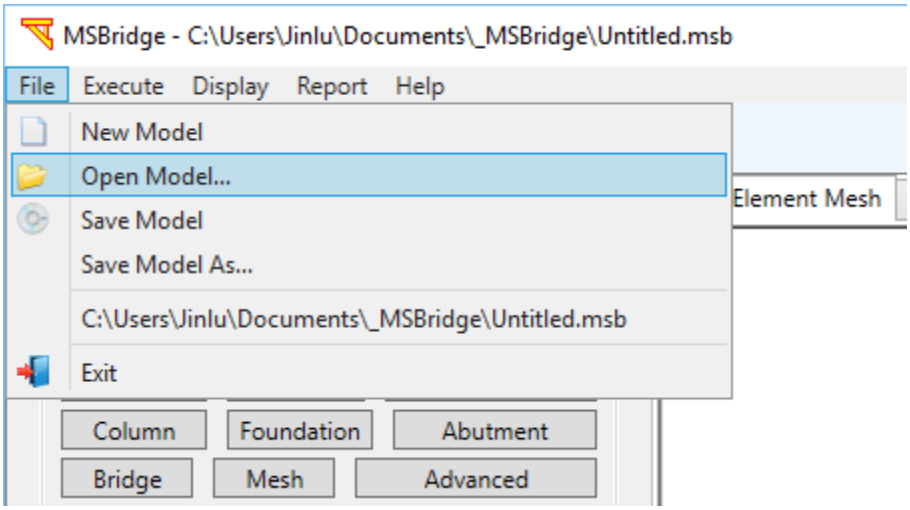

b)

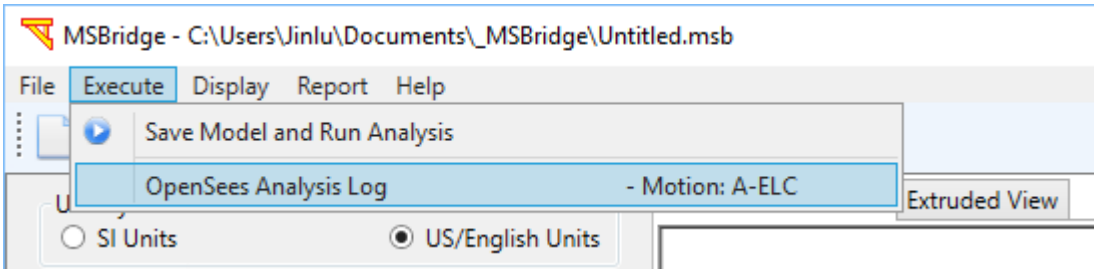

c)

Fig. 3. Toolbar and file-related submenus: a) toolbar; b) submenu **File**; c) submenu **Execute**

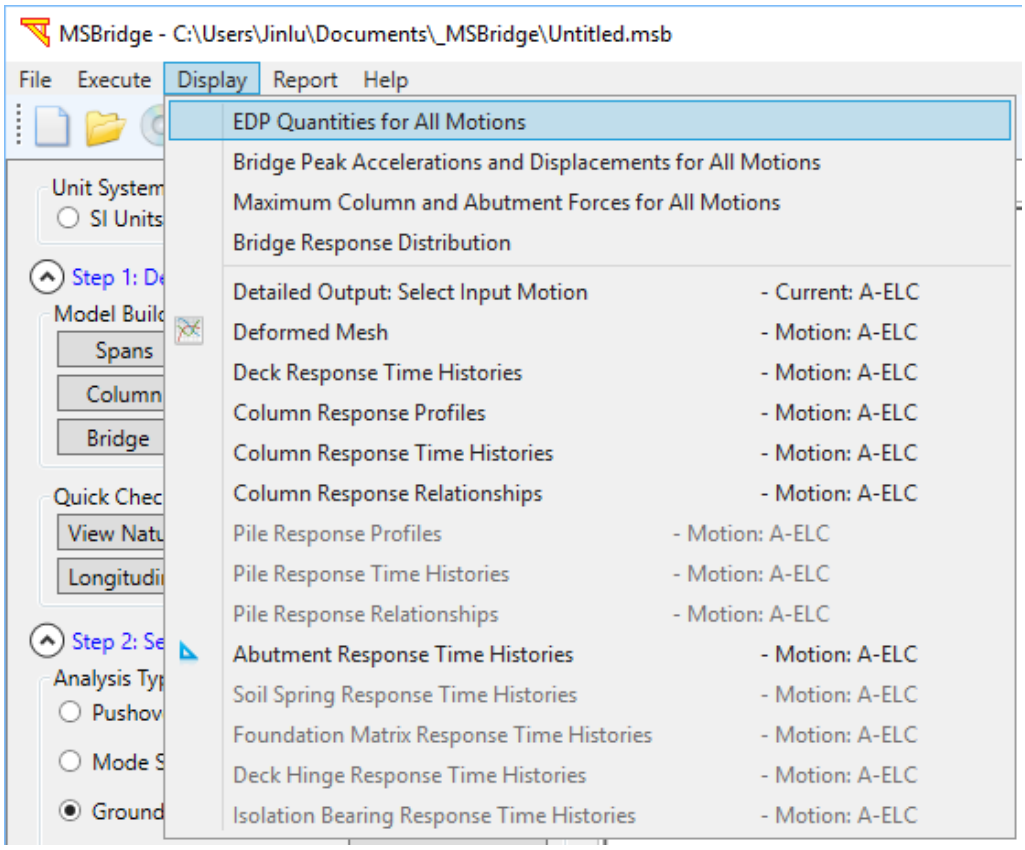

a)

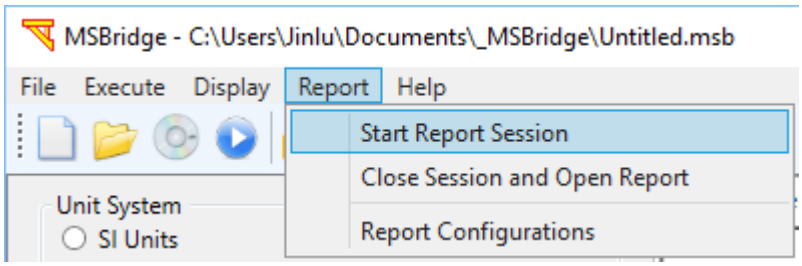

b)

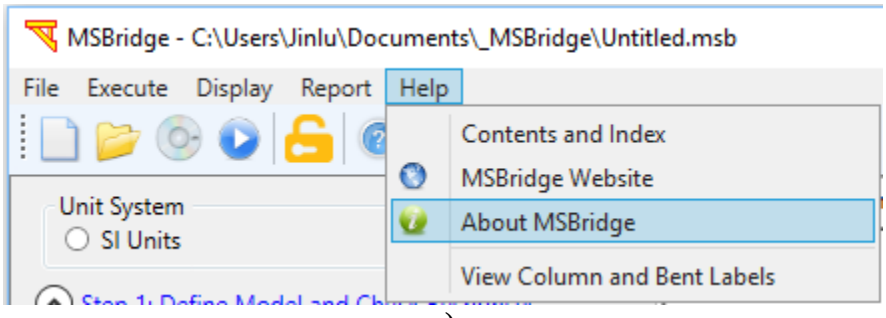

c)

Fig. 4. Result-related submenus: a) submenu **Display**; b) submenu **Report**; and c) submenu **Help**

2.2.1 Menu Bar

The menu bar, shown in Fig. 3 and Fig. 4, offers rapid access to most **MSBridge** main features. The main features in **MSBridge** are organized into the following submenus:

- **File:** Controls opening, saving of model definition parameters, and exiting **MSBridge**.
- **Execute:** Controls running analyses and displaying OpenSees analysis log.
- **Display:** Controls displaying analysis results.
- **Report:** Controls creating an analysis report in Microsoft Word format
- **Help:** Visit the **MSBridge** website and display the copyright/acknowledgment message (Fig. 5).

Note that Fig. 3a shows a "Lock Model" button which is a toggle button that prevents from overwriting analysis results after an analysis is done. If the model is in "Locked Mode," the OK buttons (and Apply buttons) in all dialog windows in **MSBridge** are disabled, and users cannot make changes to the current model. To unlock the model, users need to click the "Lock Model" button. If the model is in "Unlocked Mode," any result will be overwritten if a new analysis is launched.

2.2.2 Model Input Region

The model input region controls definitions of the model and analysis options, which are organized into three regions (Fig. 2):

Step 1: Define Model & Check Responses: Controls definitions of bridge parameters including material properties. Meshing parameters are also defined in this step.
Step 2: Select an Analysis Option: Controls analysis types (pushover analysis, mode shape analysis or ground shaking). Equivalent Static Analysis (ESA) option is also available.
Step 3: Run FE Analysis: Controls execution of the FE analysis and displaying of the analysis progress bar.

2.2.3 FE Mesh Region

The FE mesh region (Fig. 2) displays the generated mesh. In this window**,** the mesh can be manipulated by clicking buttons shown in Fig. 6.

The FE mesh shown in **MSBridge** is automatically generated. The user can also click the button at the top-right corner (shown in Fig. 6) to re-draw FE mesh (based on the input data entered).

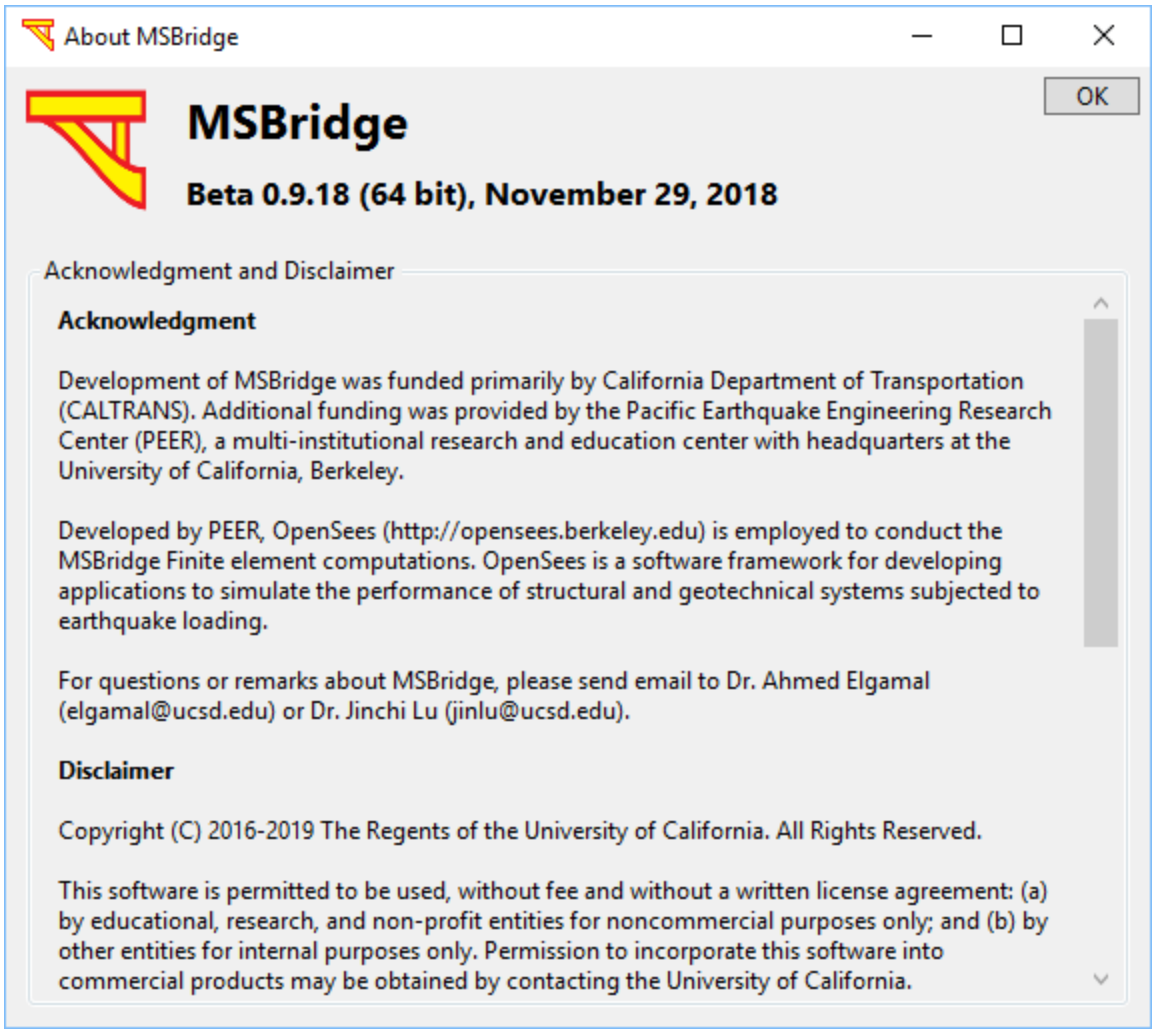

Fig. 5. MSBridge copyright and acknowledgment window

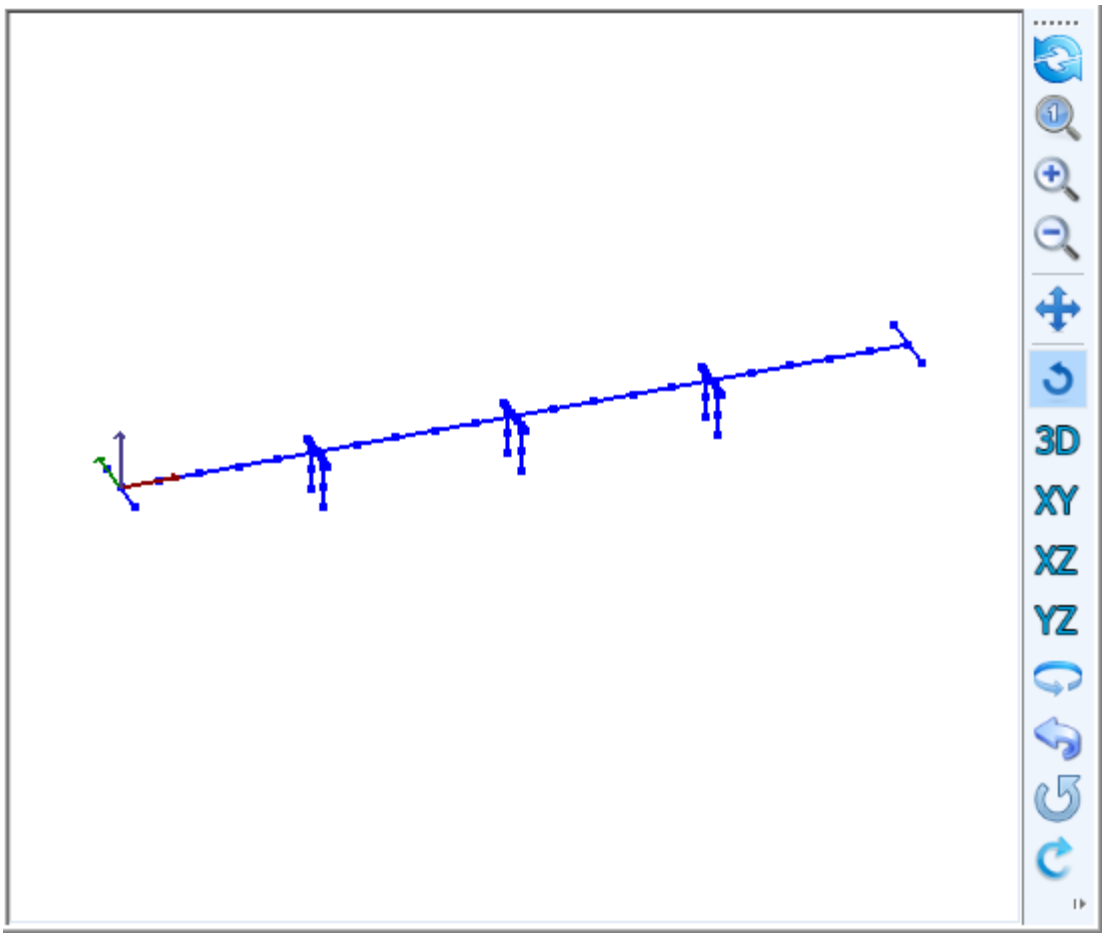

Fig. 6. Buttons available in the FE Mesh window

3 BRIDGE MODEL

In **MSBridge**, bridge deck, columns, and bentcaps are modeled using beam-column elements. The foundation is rigid-base type by default (Fig. 2 shows a bridge model with a rigid-base foundation). Other available foundation types including soil springs and foundation matrix are modeled using zeroLength elements.

To define a bridge model, click a corresponding button in Fig. 7. To include a deck hinge, isolation bearing or use a non-zero skew angle for any bent or abutment, click **Advanced**. To change the numbers of beam-column element used for deck, bentcap or columns, click **Mesh**. Fig. 8 shows a bridge model with soil springs and a deck hinge included.

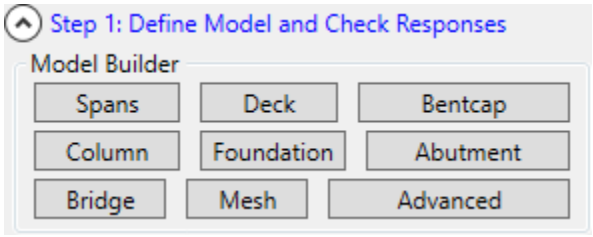

Fig. 7. Model builder buttons

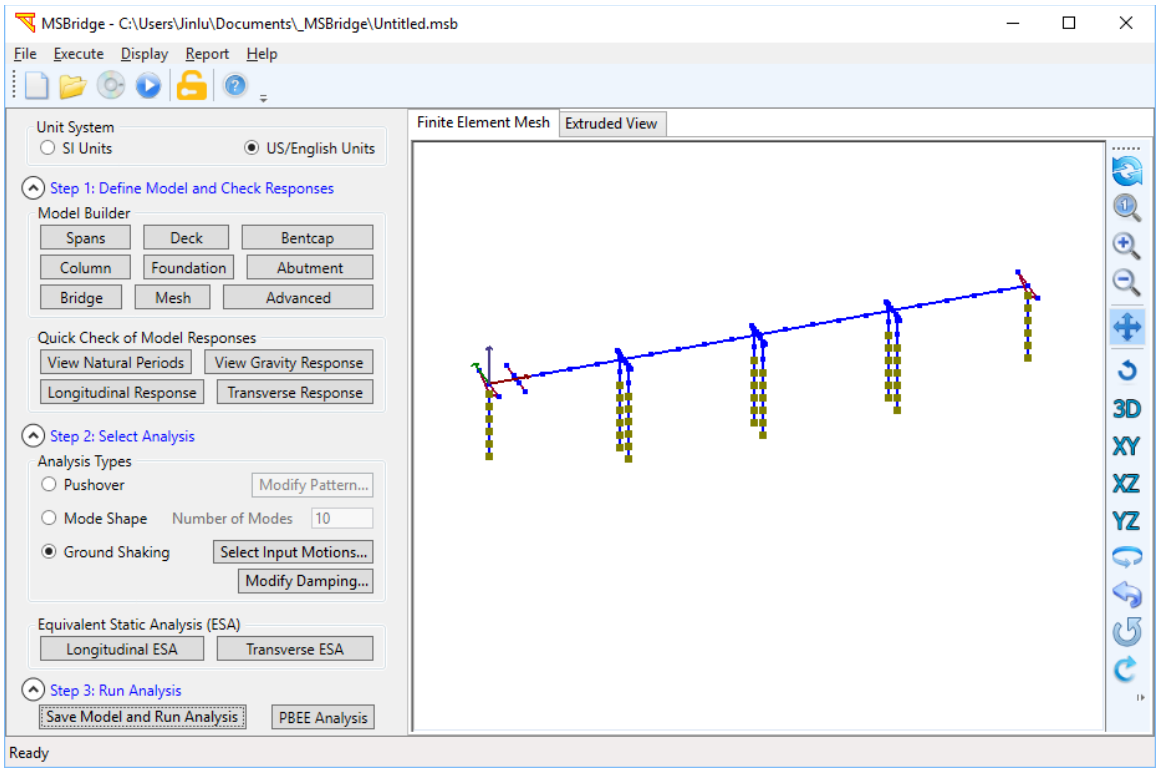

Fig. 8. MSBridge main window (bridge model with soil springs and a deck hinge included)

3.1 Spans

To change the number of spans, click **Spans** in the main window (Fig. 7 and Fig. 9).

> **Number of Spans**: The total number of spans for a multi-span bridge. The minimum is 2, and the maximum is 100.

MSBridge supports models for both straight bridge and curved bridge options.

3.1.1 Straight Bridge

If the bridge has equal span lengths, click **Equal Span Length** and specify the span length (Fig. 9).

If the bridge has varied span lengths, click **Varied Span Length** and then **Modify Span Lengths** to specify span lengths (Fig. 10). Fig. 11 shows a straight bridge model with varied span lengths.

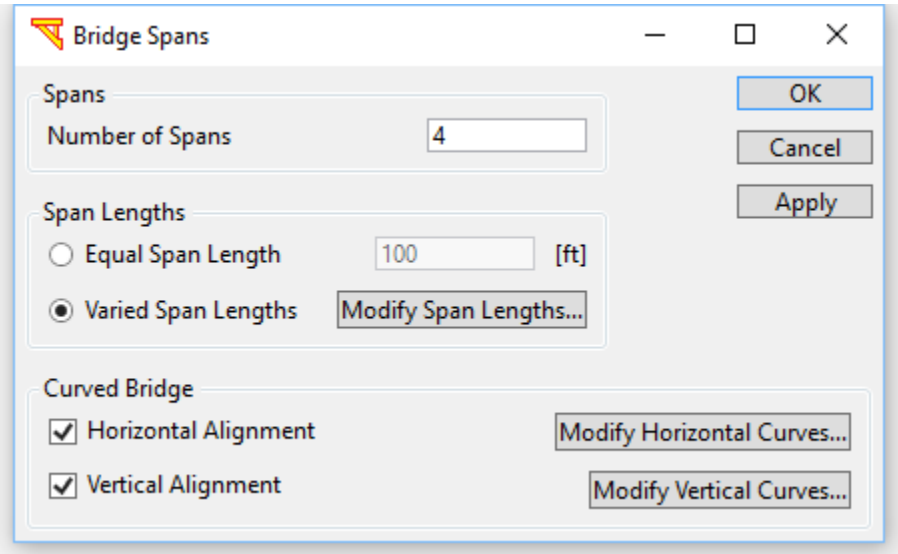

Fig. 9. Bridge span definition

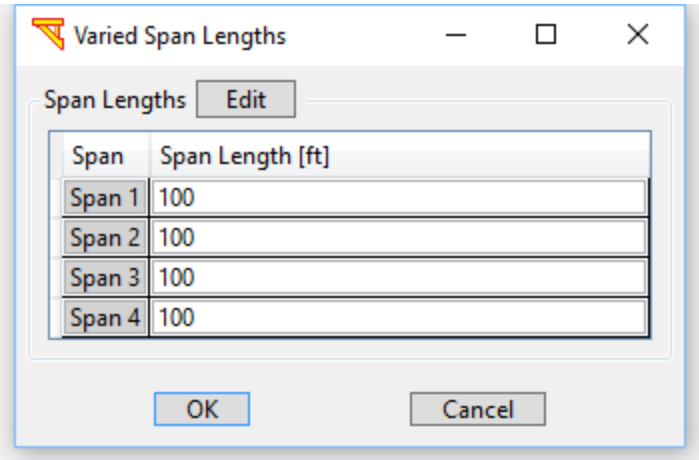

Fig. 10. Varied span lengths

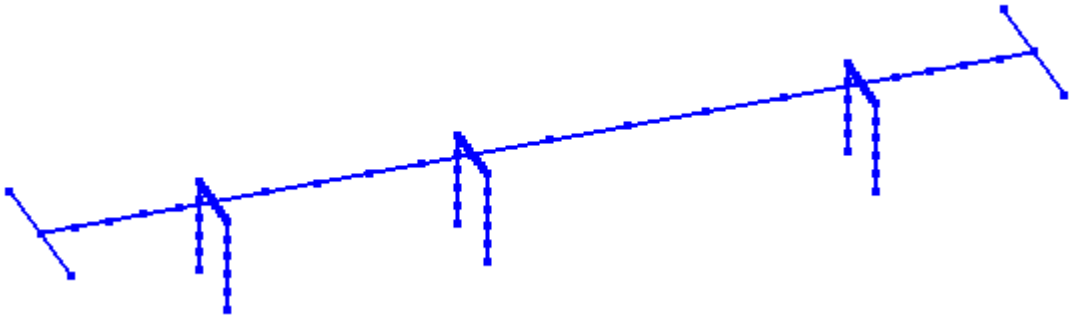

Fig. 11. Straight bridge with different span lengths

3.1.2 Curved Bridge

To define a curved bridge, please check **Horizontal Alignment** and/or **Vertical Alignment** in Fig. 9.

3.1.2.1 Horizontal Curved Bridge

To define a horizontally curved bridge, check **Horizontal Alignment** in Fig. 9. Fig. 12 shows the window to define horizontal curves. **Begin Curve Length** refers to the starting location of a horizontal curve (see Fig. 13a). **Curve Radius** refers to the radius of the horizontal curve; **Curve Length** refers to the arc length of the horizontal curve. The directions (**Left** or **Right**) refers to the arc rotation direction relative to the starting location (**Right**: clockwise rotation in XY plan view; **Left**: counter-clockwise in XY plan view). Click **Insert Curve** to add a horizontal curve and click **Delete Curve** to remove a chosen curve. Fig. 15 shows bridge examples of horizontal alignment.

3.1.2.2 Vertical Curved Bridge

To define a vertically curved bridge, check **Vertical Alignment** in Fig. 9. Fig. 14 shows the window to define vertical curves. **Begin Curve Length** refers to the starting location of the beginning slope of a vertical curve (see Fig. 13b). **Curve Length** refers to the length of the vertical curve. **End CurveSlope** refers to the slope of the end slope. Note that the slope value can be negative, zero or positive. Similarly, Click **Insert Curve** to add a vertical curve and click **Delete Curve** to remove a chosen vertical curve. Fig. 16 shows bridge examples of vertical alignment.

Note that a horizontal curve/alignment employs a circular arc while a vertical curve/alignment employs a parabolic equation. Any two (horizontal or vertical) curves cannot be overlapped, and any newly added curves must be located outside all previous curves.

For detailed information on the horizontal and vertical alignments, please refer to Highway Design Manual by Caltrans (2018).

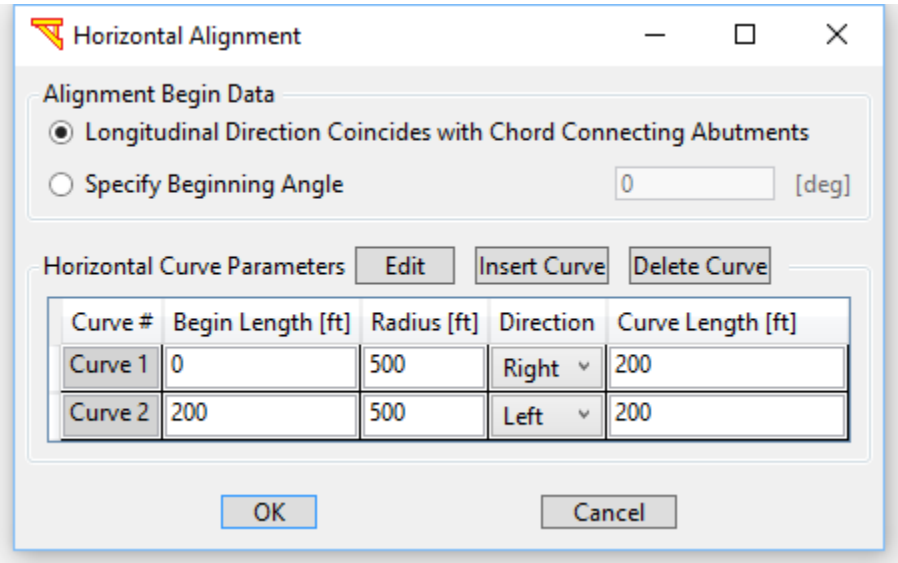

Fig. 12. Horizontal alignment

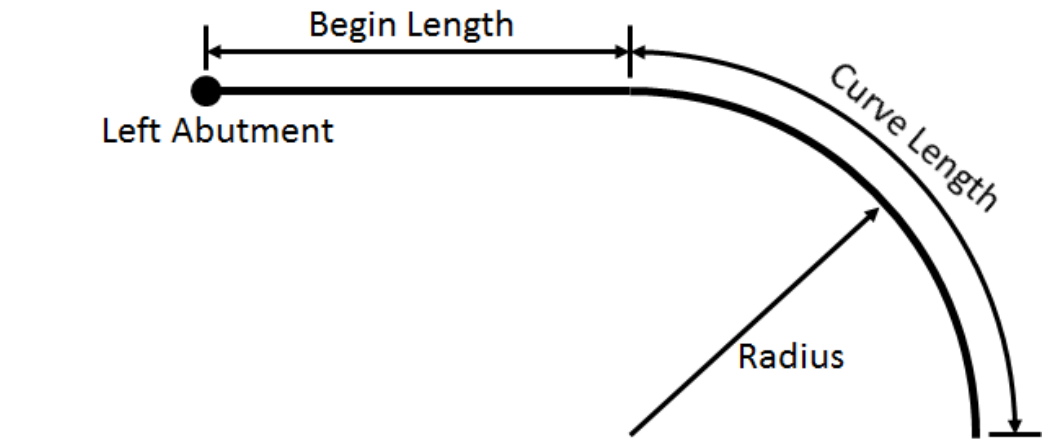

a)

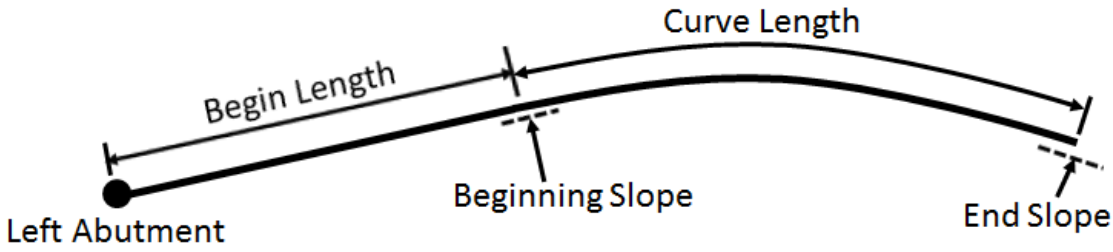

b)

Fig. 13. Horizontal and vertical alignments: a) horizontal alignment (plan view); b) vertical alignment (side view)

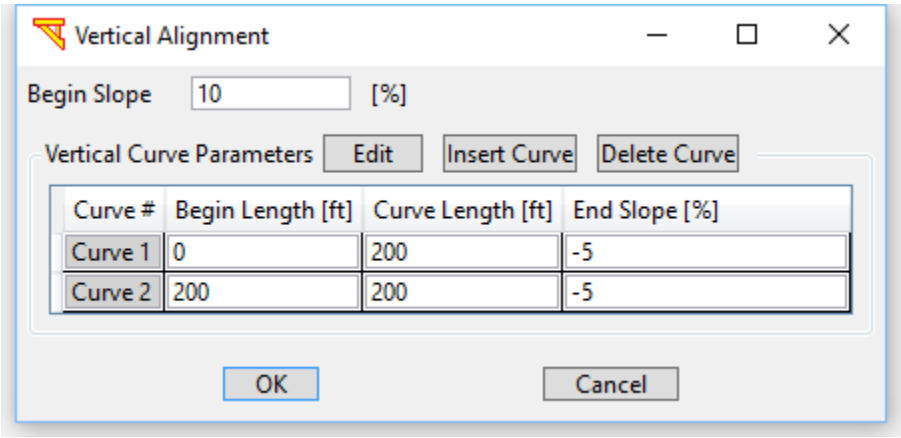

Fig. 14. Vertical alignment

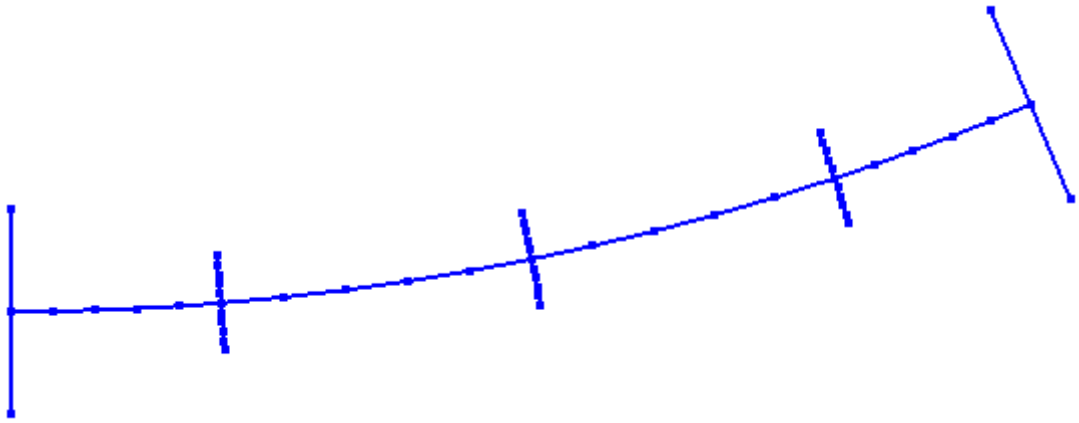

a)

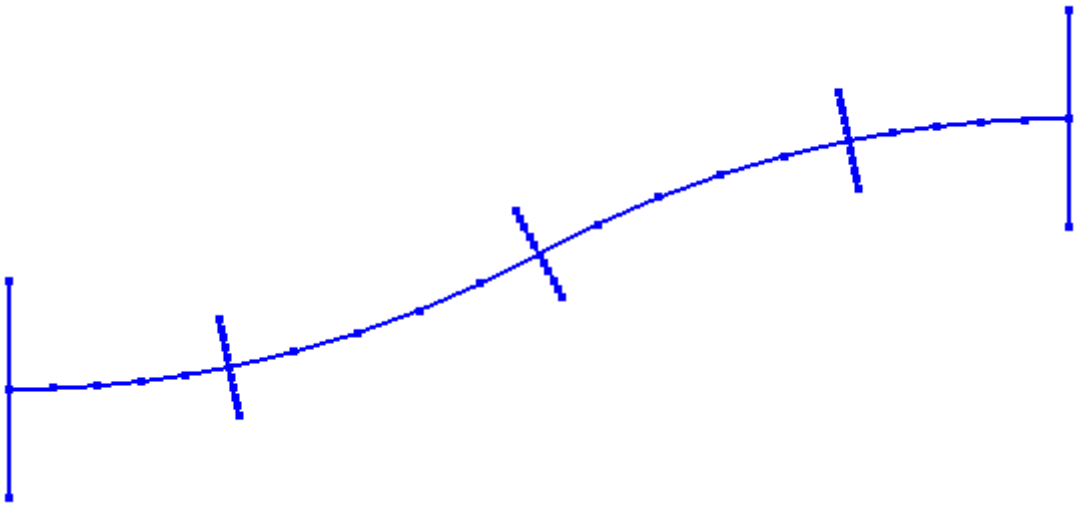

b)

Fig. 15. Examples of horizontally curved bridges (horizontal alignment): a) single horizontal curve; b) multiple horizontal curves.

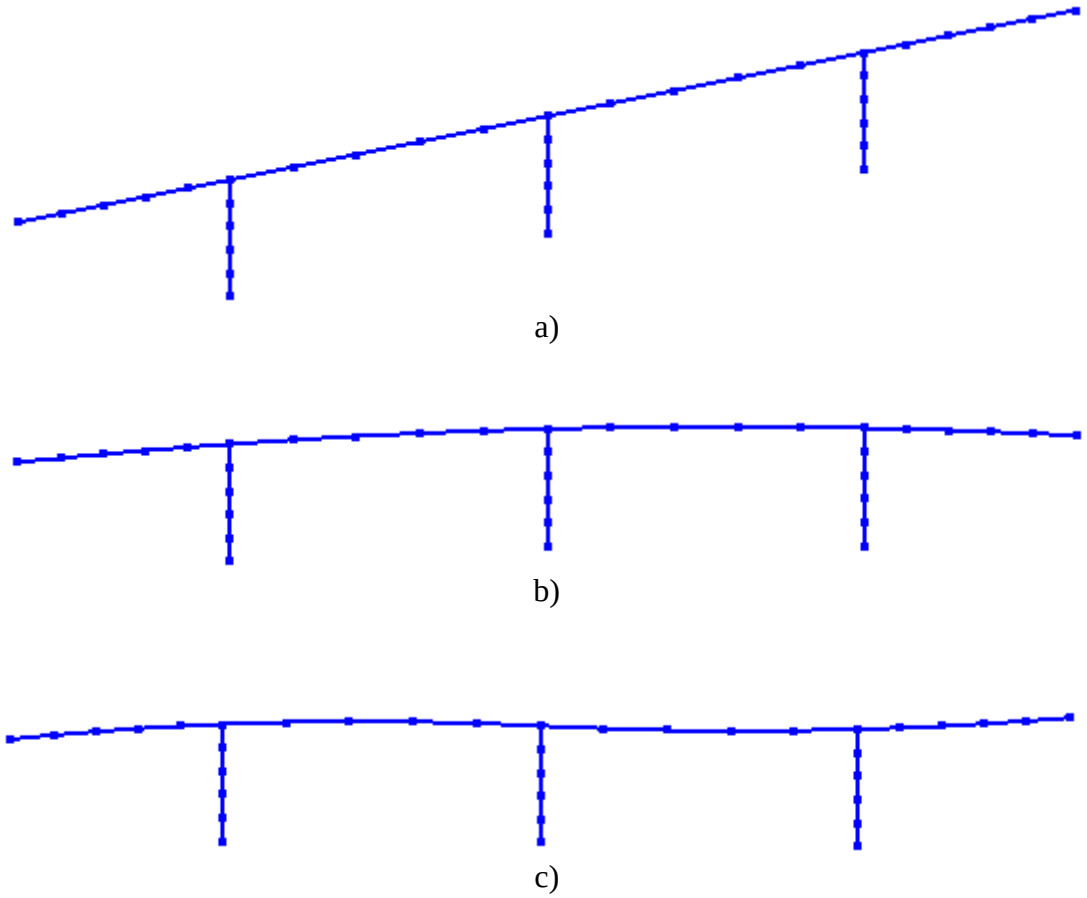

Fig. 16. Examples of vertically curved bridges (vertical alignment): a) single slope; b) begin and end slopes; c) multiple slopes.

3.2 Deck Sections

To change Deck properties, click **Deck** in Fig. 7. Fig. 17 shows the window to modify material and section properties of a deck section (e.g., Deck 1 as shown in Fig. 17).

MSBridge uses an elastic material model for bridge deck elements. Fig. 17 shows the default values for deck material properties including **Youngs Modulus**, **Shear Modulus**, and **Unit Weight**.

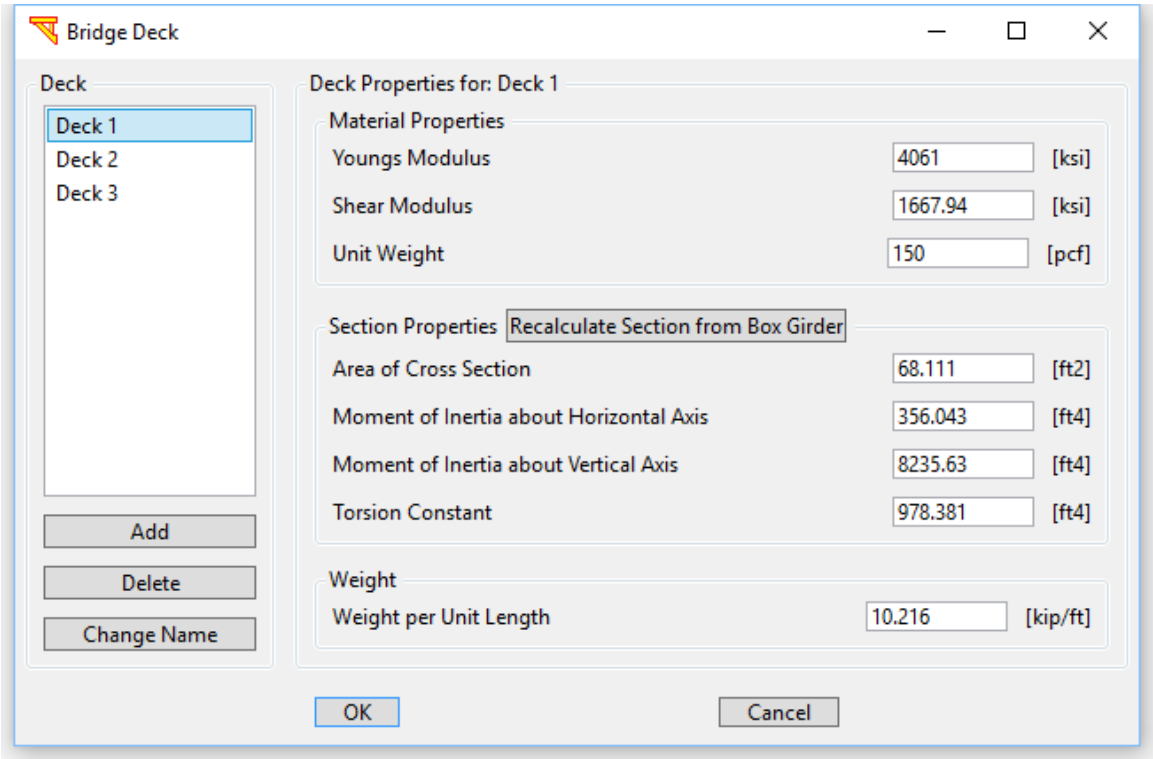

Fig. 17. Deck material and section properties

Fig. 17 also shows deck Section properties. Section properties can be input directly in Fig. 17, if available. If this information is not available, **MSBridge** will calculate properties based on general box girder section dimensions. Click **Recalculate Section from Box Girder** in Fig. 17 to define a new box girder shape (Fig. 18). The default values of geometrical properties are of typical for a four-cell reinforced concrete box girder deck configuration. Click **OK** in Fig. 18 if the user would like to use the defined cross-section. Corresponding entries in Fig. 17 will be updated. **Weight per Unit Length** is equal to the **Area of Cross Section** times the **Unit Weight** defined in Fig. 17.

Note that the **Box Width** defined in Fig. 18 will be used as the deck width of the bridge. To use a different deck width, the user needs to modify the **Box Width** (Fig. 18).

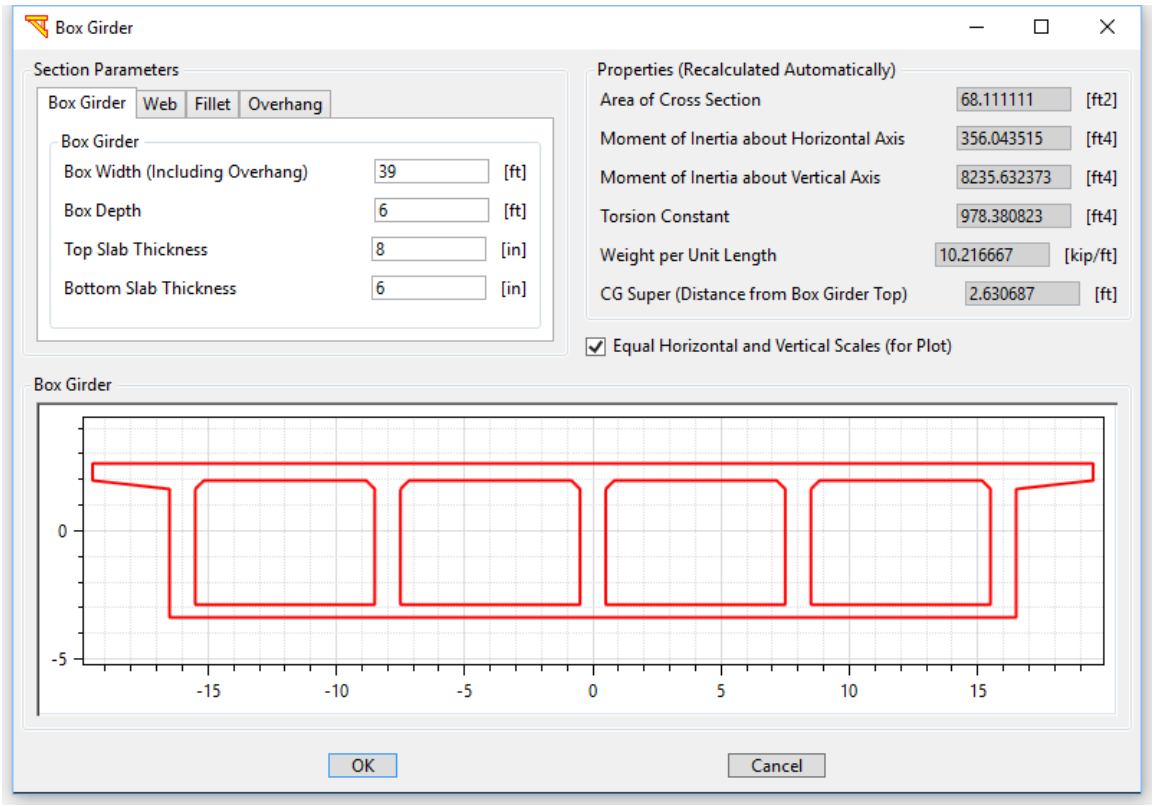

Fig. 18. Box girder shape employed for a bridge deck section

3.3 Bentcap Sections

To change bent cap properties, click **Bentcap** in Fig. 7. Fig. 19 shows the window to modify material and section properties of a bentcap section (e.g., Bentcap 1 as shown in Fig. 19)

MSBridge uses an elastic material model for bridge bentcap elements. Fig. 19 shows the default values for bentcap material properties including **Youngs Modulus**, **Shear Modulus**, and **Unit Weight**.

Fig. 19 also shows the default bentcap section properties which can be modified directly. If bentcap section properties are not available, **MSBridge** will calculate properties based on rectangular section dimensions specified. Click **Recalculate Section from Rectangular** in Fig. 19 to define a new rectangular shape (Fig. 20). Click **OK** in Fig. 18 if the user would like to use the defined cross-section. Corresponding entries in Fig. 19 will be updated. **Weight per Unit Length** is equal to the **Area of Cross Section** times the **Unit Weight** (Fig. 19).

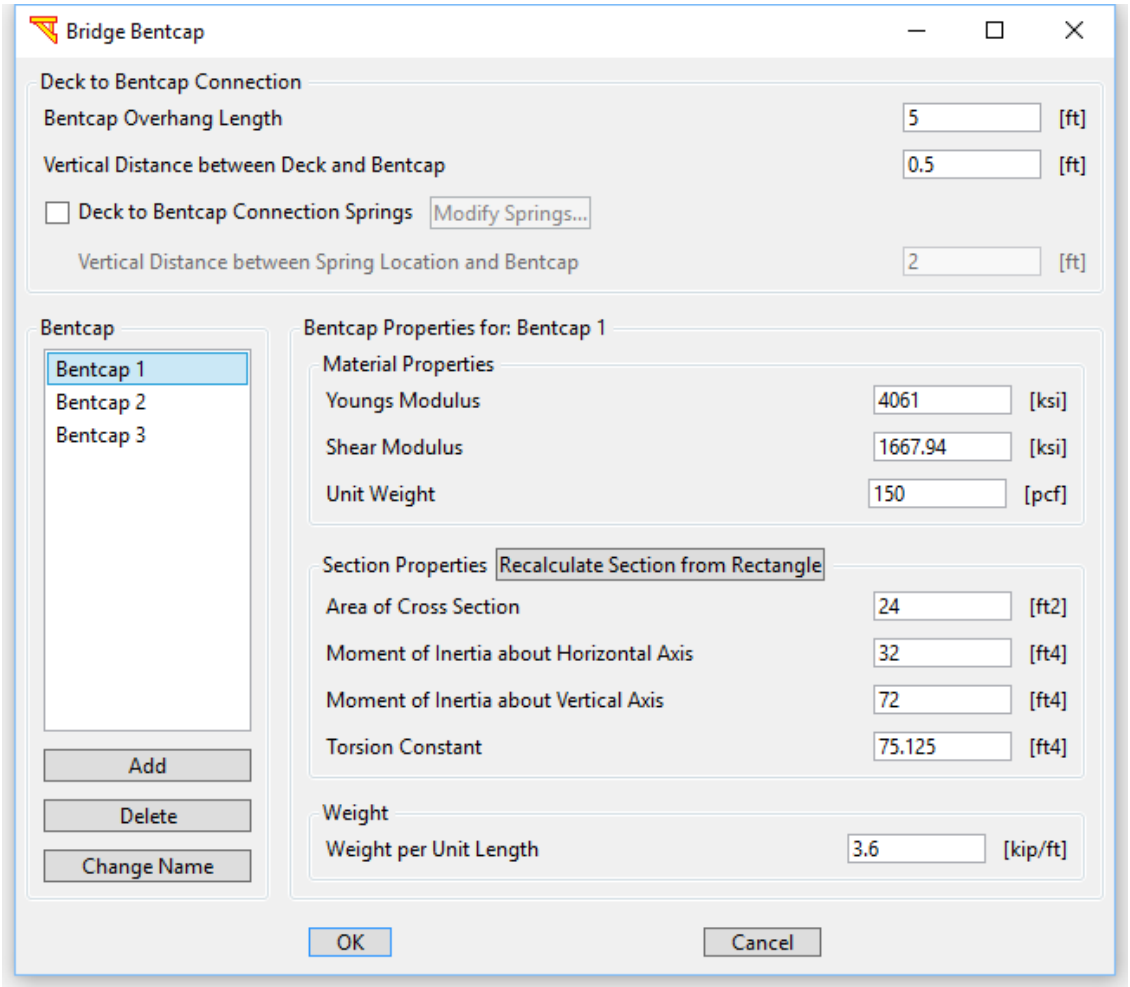

Fig. 19. Bentcap material and section properties

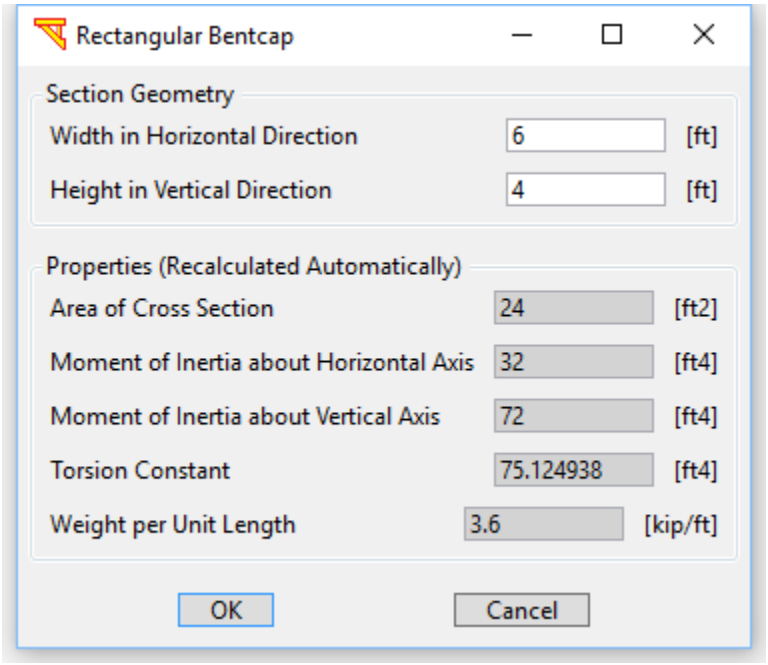

Fig. 20. Rectangular shape employed for a bentcap section

3.4 Column Cross Sections

To define material and geometrical properties of bridge columns, click **Column** in Fig. 7. Users can choose to use linearly elastic or nonlinear Fiber section for a column section. By default, nonlinear Fiber section is used (Fig. 21). Note that each bridge column is limited to one column cross section (for now in the current version).

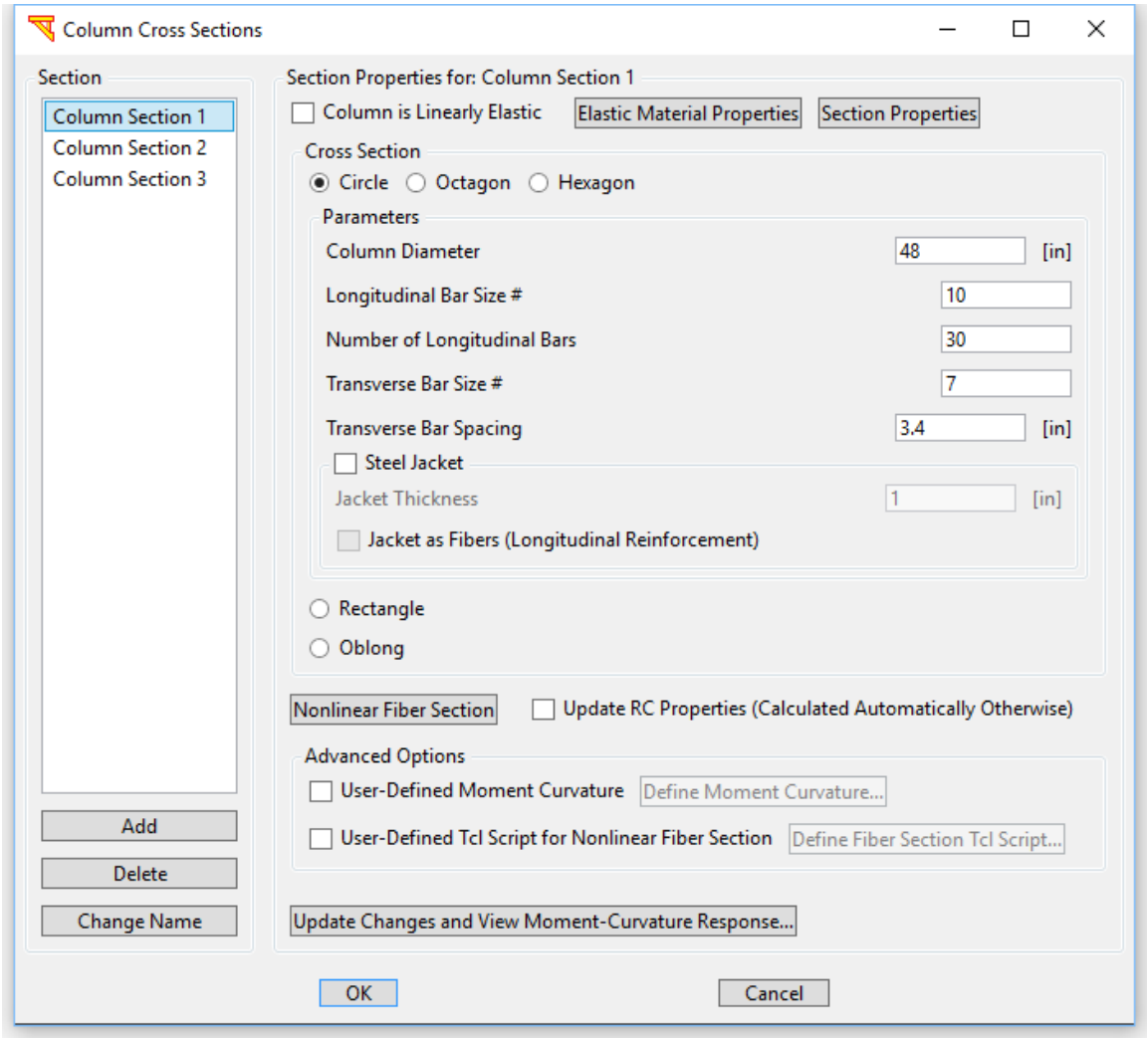

Fig. 21. Column section properties

3.4.1 Cross-section Shapes

The cross-section types currently available for columns are **Circle**, **Octagon**, **Hexagon,** and **Rectangle** (Fig. 21). For the Circular, Octagonal and Hexagonal sections, the user needs to define the **Column Diameter**. For Rectangular section, the user needs to define the widths in bridge longitudinal and transverse directions (Fig. 21).

3.4.2 Cross Section Properties

Four options available to define a bridge column section: i) linear elastic, ii) nonlinear Fiber Section, iii) user-defined moment curvature, and iv) user-defined Tcl script for nonlinear Fiber section.

3.4.2.1 Linearly Elastic

To activate the linearly elastic option for a column section, check the checkbox **Column is Linearly Elastic** (Fig. 22). Elastic beam-column element (**elasticBeamColumn**, McKenna et al. 2010) is used for the column section in this case. Click **Elastic Material Properties** to define **Youngs Modulus, Shear Modulus** and **Unit Weight** of the column section (Fig. 23). Click **Section Properties** to change the column section properties (by changing cracked section factors) as shown in Fig. 24.

3.4.2.2 Nonlinear Fiber Section

To use nonlinear Fiber section for a column section, click **Nonlinear Fiber Section** (Fig. 21). The window for defining the Fiber section is shown in Fig. 25. Click **Material Properties** buttons to display or modify the material properties for the rebars (Fig. 26), the core and the cover concrete (Fig. 27).

Nonlinear beam-column elements with fiber section (Fig. 28) are used to simulate the column in this case. The fiber layout for the octagonal and hexagonal cross sections are similar to that of the circular cross section except for the cover. Fig. 29 shows a slight treatment of the fiber layout for the octagonal and hexagon cross sections. For Rectangular section, the number of rebars refers to the number of reinforcing bars around the section perimeter (equal spacing).

The material options available for the rebars include **Elastic**, **Steel01**, **Steel02,** and **ReinforcingSteel**. The material options available for the concrete include **Elastic**, **ENT** (Elastic-No Tension), **Concrete01**, and **Concrete02**. The default material properties of a column section are shown in Tables 1-3.

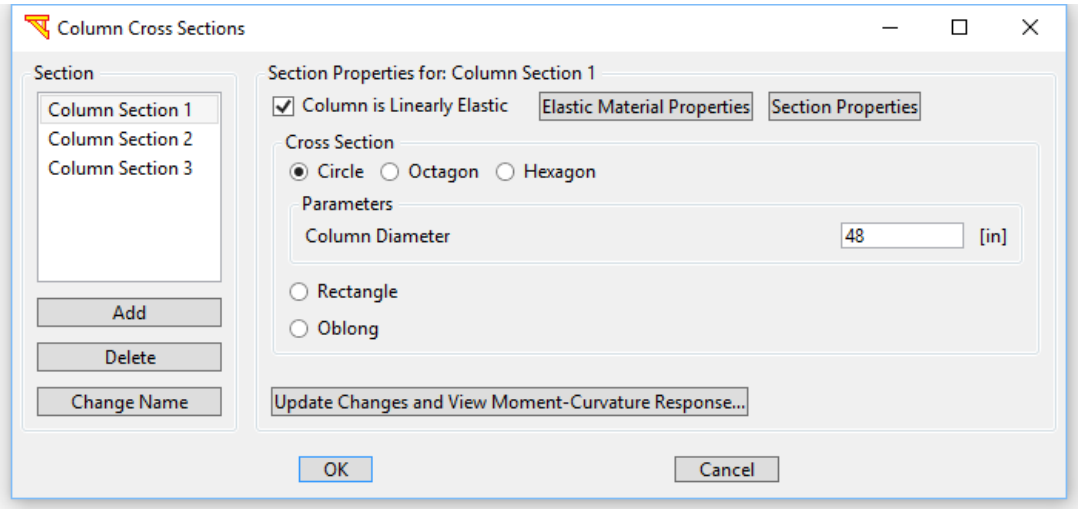

Fig. 22. Definition of linear column

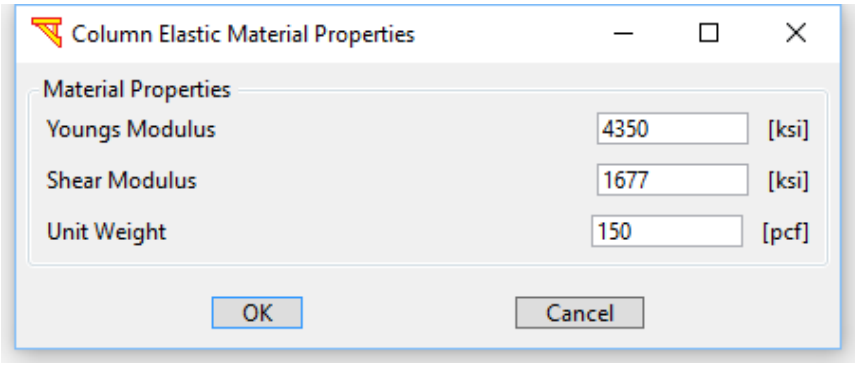

Fig. 23. Column elastic material properties

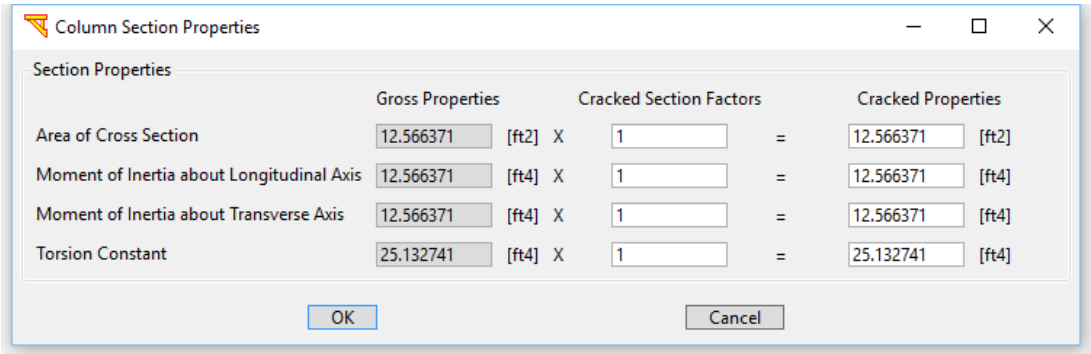

Fig. 24. Column section properties

By default, the Steel02 material in OpenSees (McKenna et al. 2010) is employed to simulate the rebars, and Concrete02 material is used for the concrete (core and cover). Steel02 is a uniaxial Giuffré-Menegotto-Pinto material that allows for isotropic strain hardening. Concrete02 is a uniaxial material with linear tension softening. The

Concrete02 material parameters were obtained from the Mander (1988) constitutive relationships for confined and unconfined concrete. More details on the derivation of the default values and the OpenSees uniaxialMaterial definitions used for each material are shown in Appendix A.

Fig. 30, Fig. 31, and Fig. 32 show the stress-strain curves of the steel, core, and cover concrete materials, respectively. These plots can be obtained for updated material properties directly from the interface by clicking on a corresponding **View Stress-Strain** button in the Column Fiber Section window (Fig. 25). The moment-curvature response for a column section is shown in Fig. 33 (a vertical compressive load of 2,500 kips is applied). For comparison, XSECTION (Caltrans 1999) result is also available (Fig. 33).

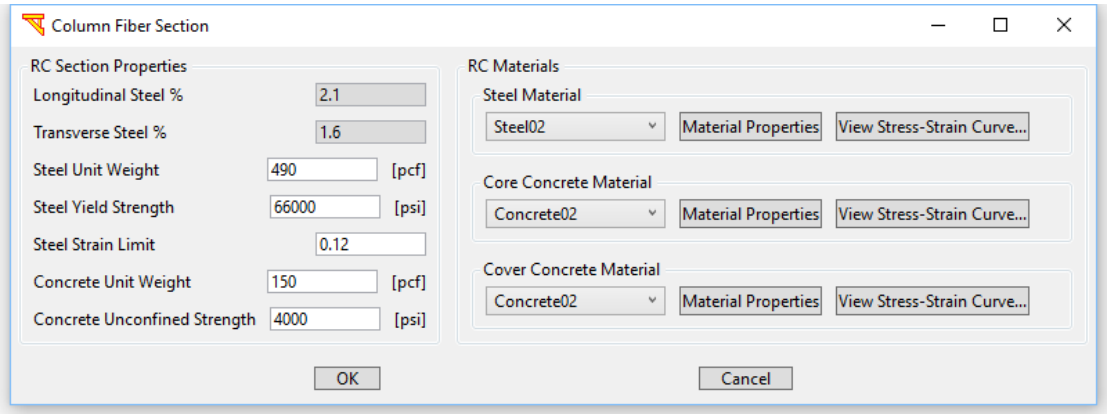

Fig. 25. Nonlinear Fiber Section window

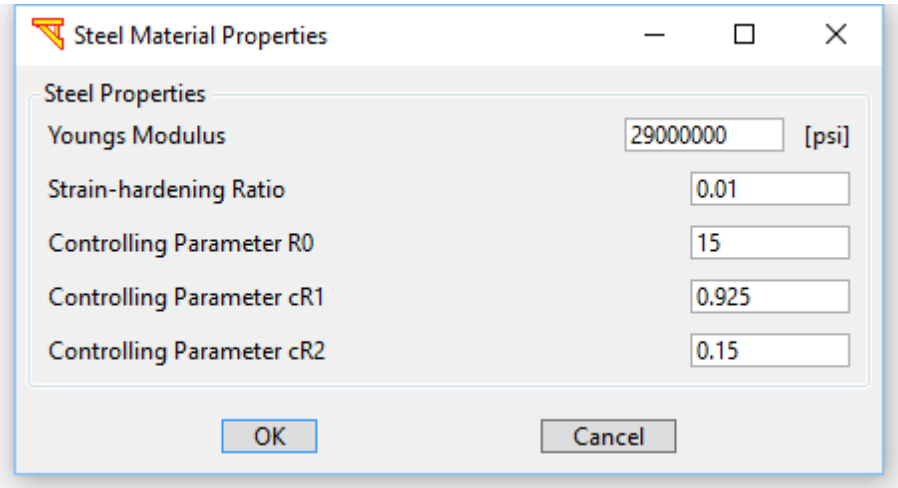

a)

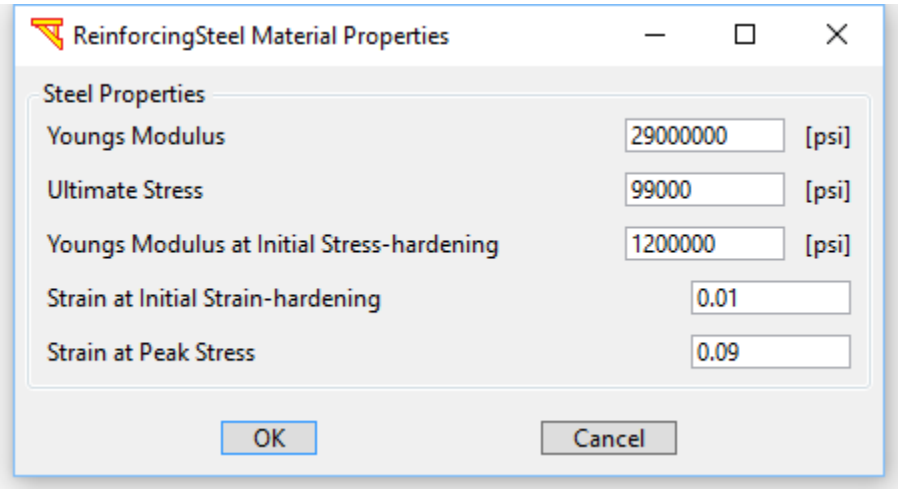

b)

Fig. 26. Rebar material properties: a) Steel02 material; b) ReinforcingSteel material

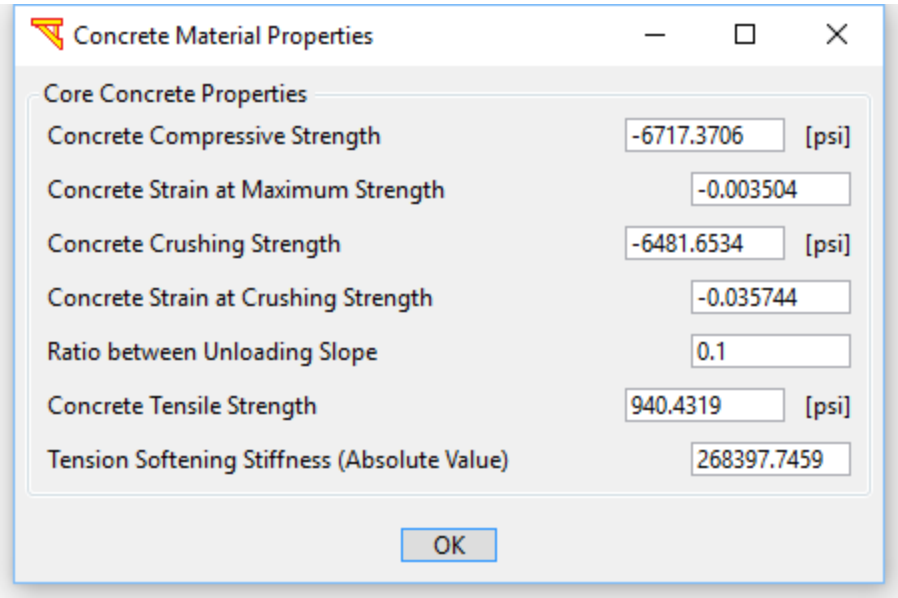

a)

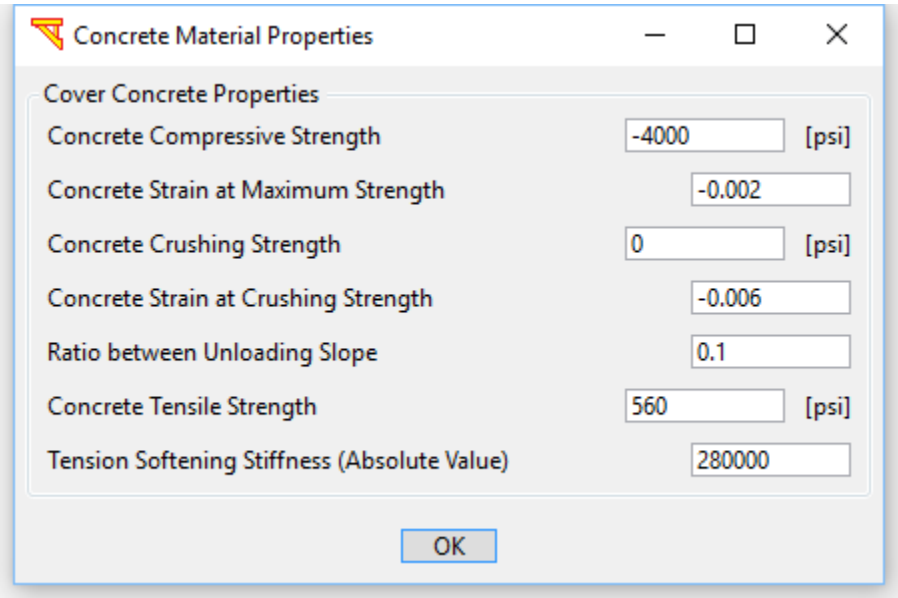

b)

Fig. 27. Concrete material properties: a) Concrete02 material for the core concrete; b) Concrete02 material for the cover concrete

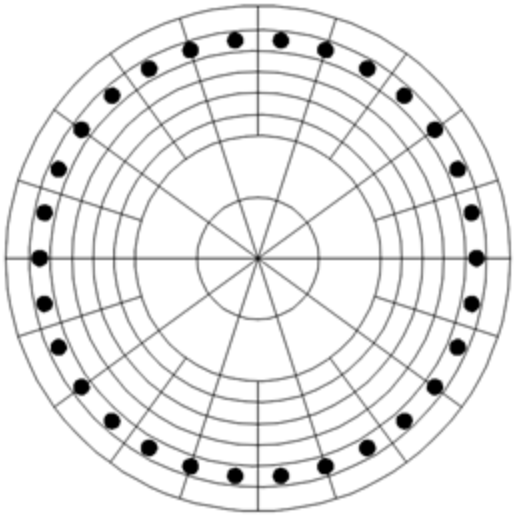

Fig. 28. Fiber discretization of a circular section (based on the report by Berry and Eberhard (2007))

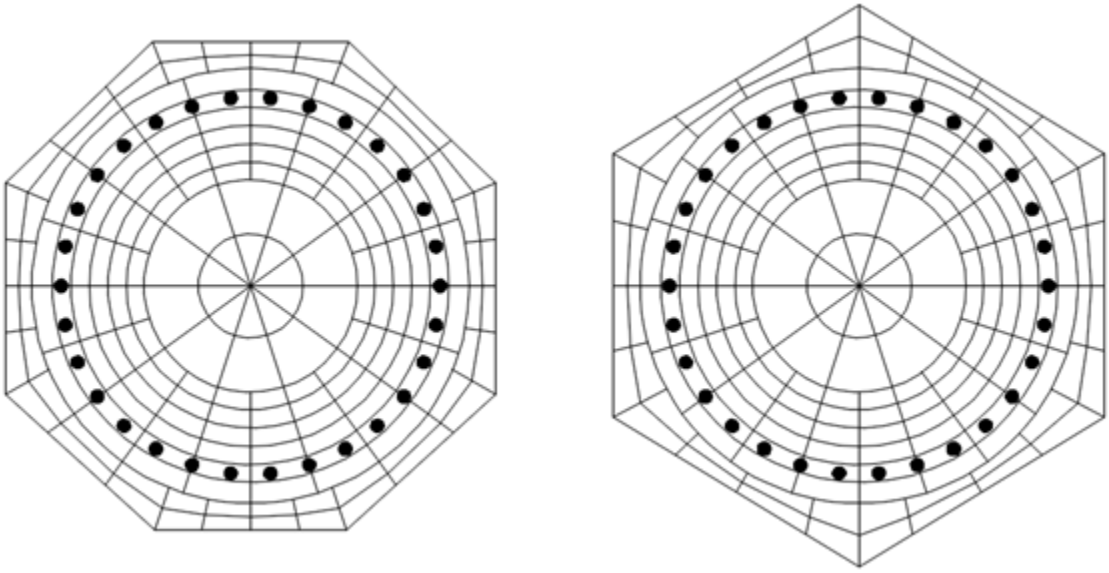

a) b)

Fig. 29. Fiber discretization of a column section: a) octagon shape; and b) hexagon shape

Table 1. Default values for reinforced concrete (RC) section properties

Parameter	Value
Longitudinal bar size (US #)	10
Longitudinal steel %	2
Transverse bar size (US #)	7
Transverse steel %	1.6
Steel unit weight (pcf)	490
Steel yield strength (psi)	66717.5
Concrete unit weight (pcf)	145
Concrete unconfined strength (psi)	4000

Table 2. Default values for Steel02 material properties

Parameter	Value	Typical range
Steel yield strength (psi)	66717.5	50,000-68,000
Young's modulus (psi)	29,000,000	-
Strain-hardening ratio*	0.01	0.005-0.025
Controlling parameter R0**	15	10-20
Controlling parameter cR1**	0.925	--
Controlling parameter cR2**	0.15	--

*The strain-hardening ratio is the ratio between the post-yield stiffness and the initial elastic stiffness.
**The constants R0, cR1, and cR2 are parameters to control the transition from elastic to plastic branches.

Table 3. Default values for Concrete02 material properties

Parameter	Core	Cover
Elastic modulus (psi)	3,644,147	3,644,147
Compressive strength (psi)	-6,739	-4000
Strain at maximum strength	-0.0037	-0.002
Crushing strength (psi)	-6,538	0
Strain at crushing strength	-0.036	-0.006
Ratio between unloading slope	0.1	0.1
Tensile strength (psi)	943.49	560
Tensile softening stiffness (psi)	255,090	280,000

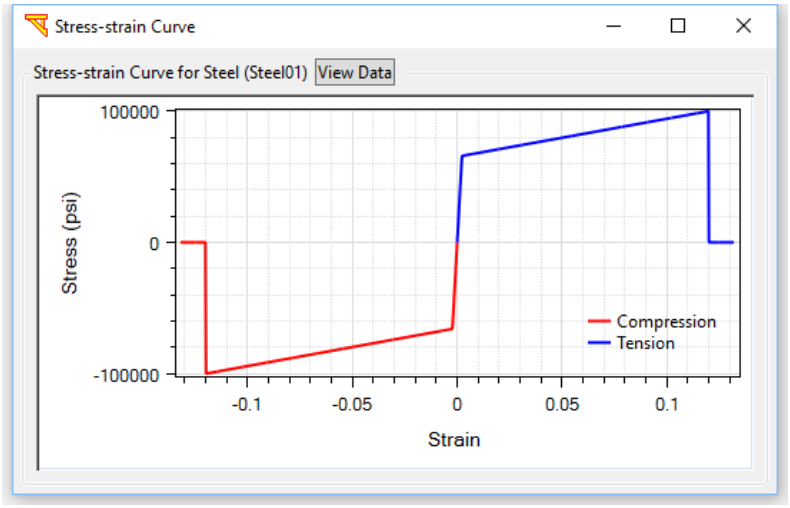

a)

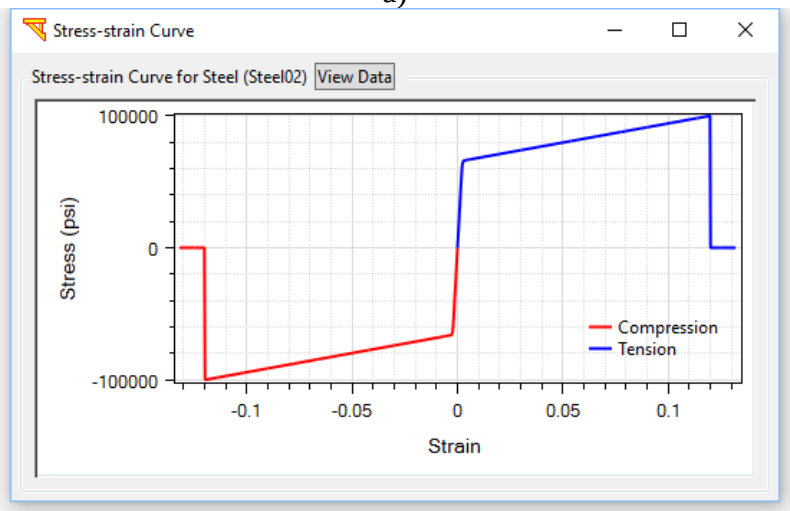

b)

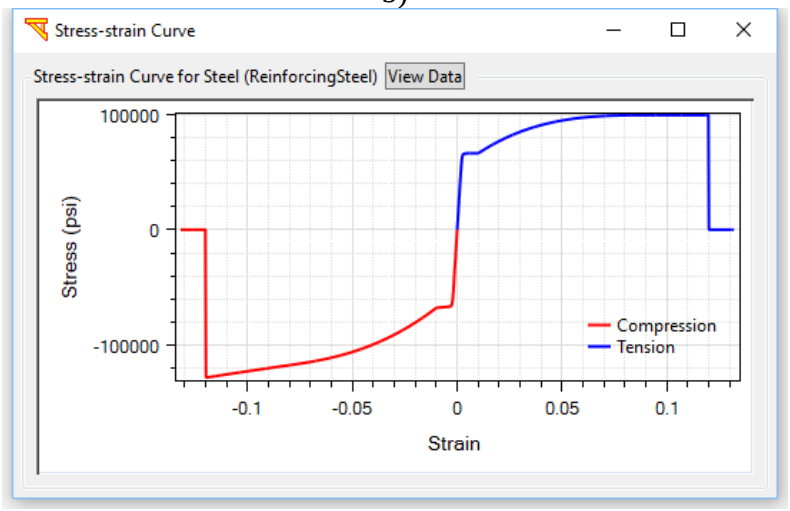

c)

Fig. 30. Stress-strain curve for a steel material (default values employed; with a strain limit of 0.12): a) Steel01; b) Steel02; and c) ReinforcingSteel

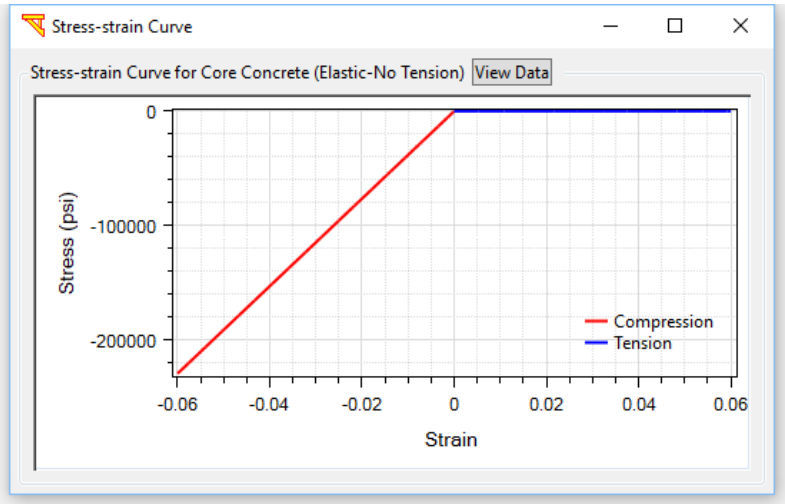

a)

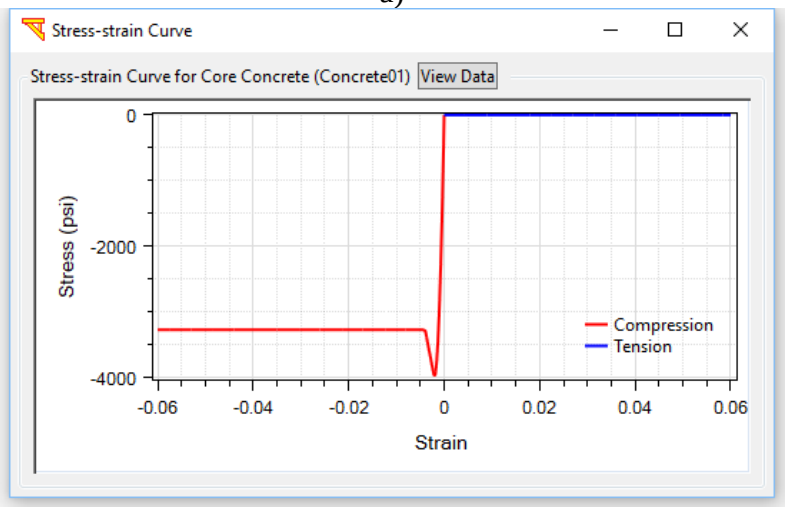

b)

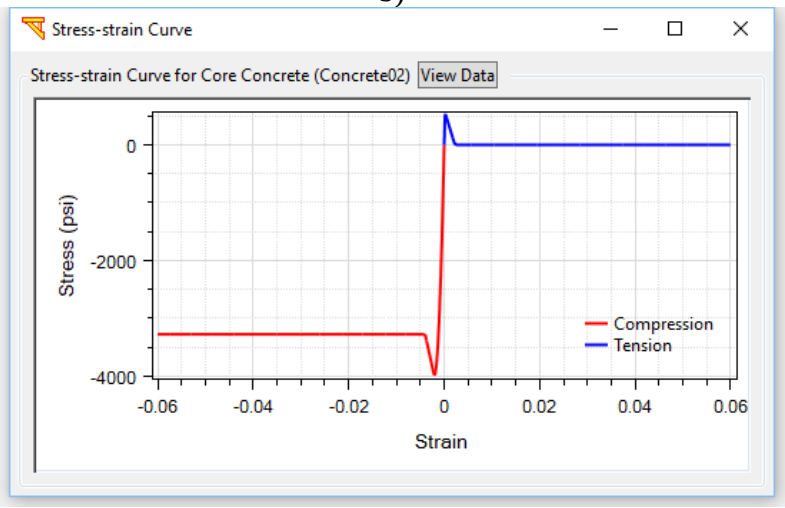

c)

Fig. 31. Stress-strain curve of a core concrete material (default values employed): a) Elastic-No Tension; b) Concrete01; and c) Concrete02

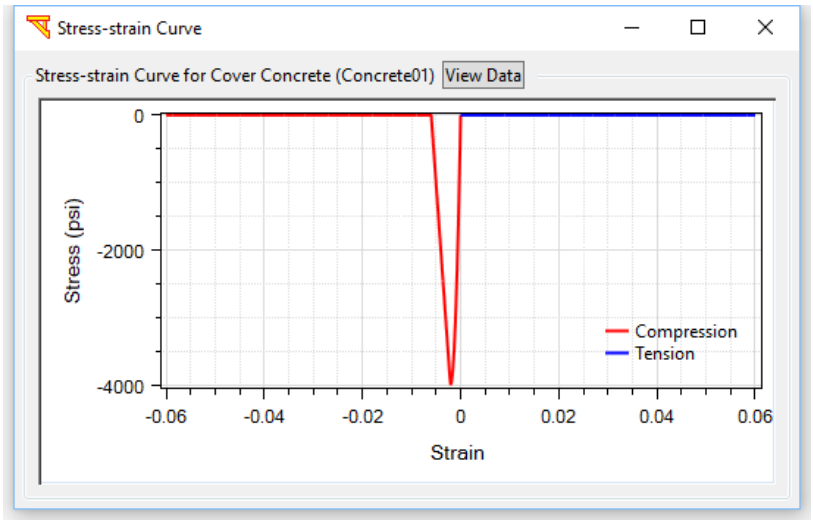

a)

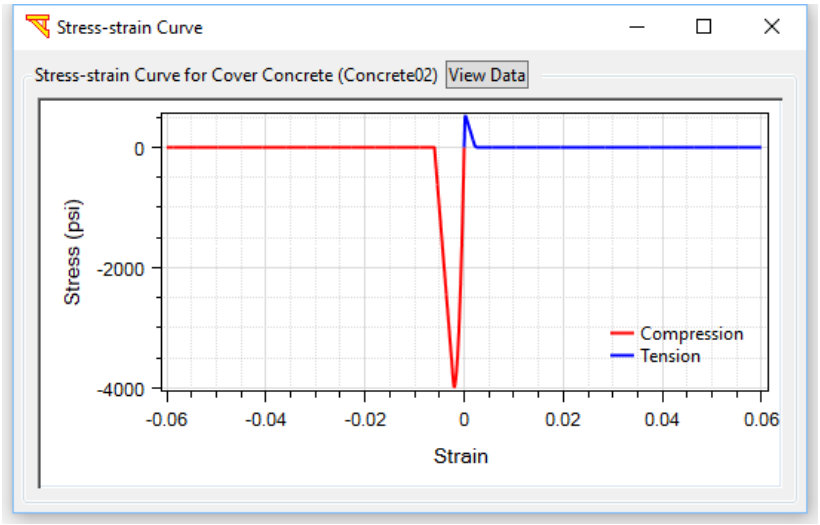

b)

Fig. 32. Stress-strain curve of a cover concrete material (default values employed): a) Concrete01; and b) Concrete02

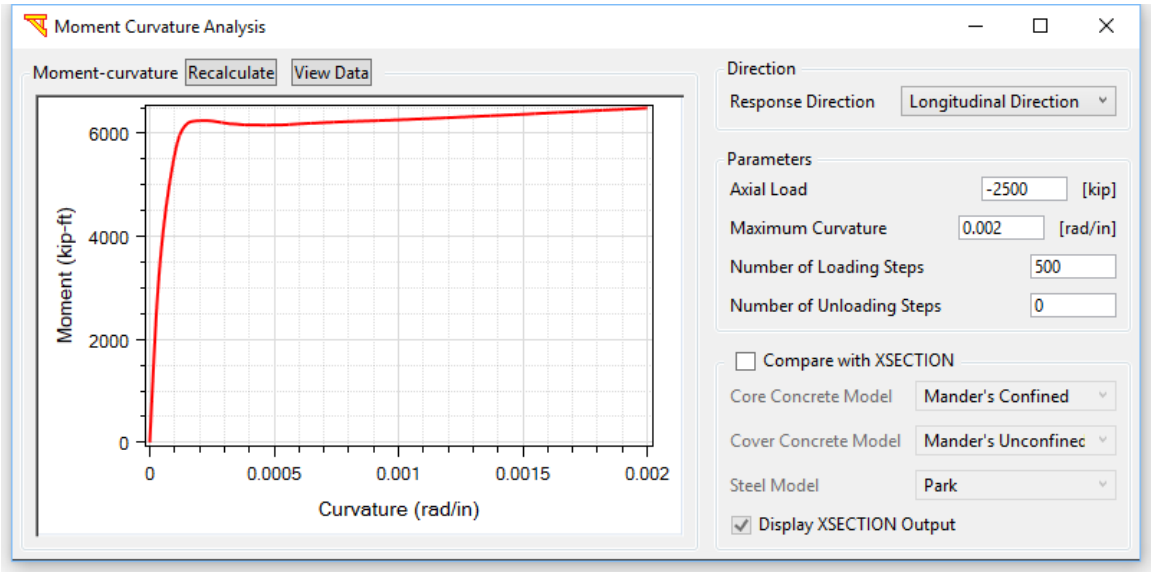

Fig. 33. Moment-curvature response for a column section (with default steel and concrete parameters)

3.4.2.3 User-defined Moment Curvature

To use moment-curvature curves for a column section, click **User-Defined Moment Curvatures** (Fig. 21). The window to define the section is shown in Fig. 34. Using this option, the user can define the cross section by simply entering moment-curvature data.

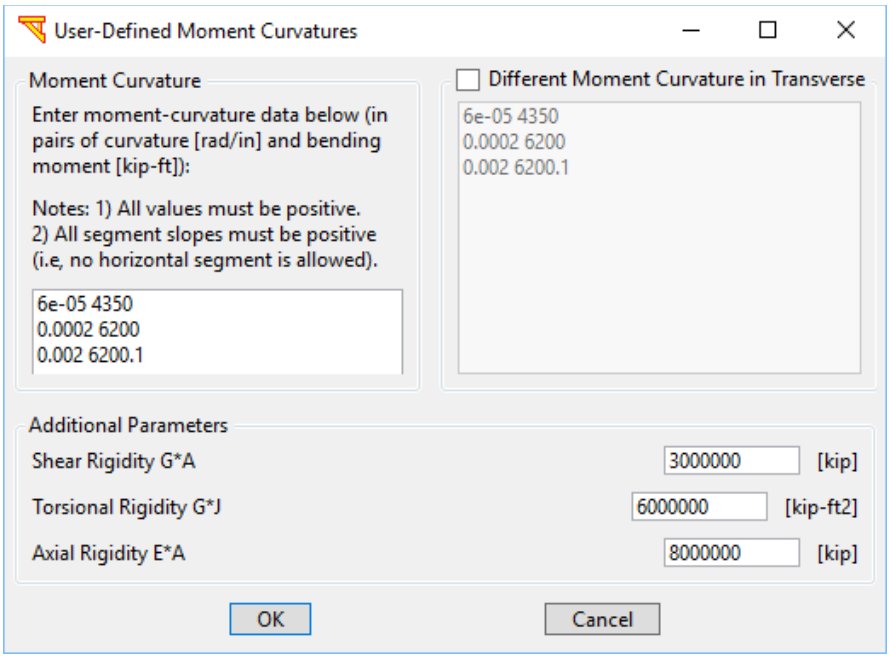

Fig. 34. User-defined moment curvature

3.4.2.4 User-defined Tcl Script for Nonlinear Fiber Section

To use used-defined Fiber section for a column section, click **User-Defined Fiber Section** (Fig. 21). The window for defining the Fiber section is shown in Fig. 35. Using this option, the user can use a Tcl code snippet to define a complex cross section.

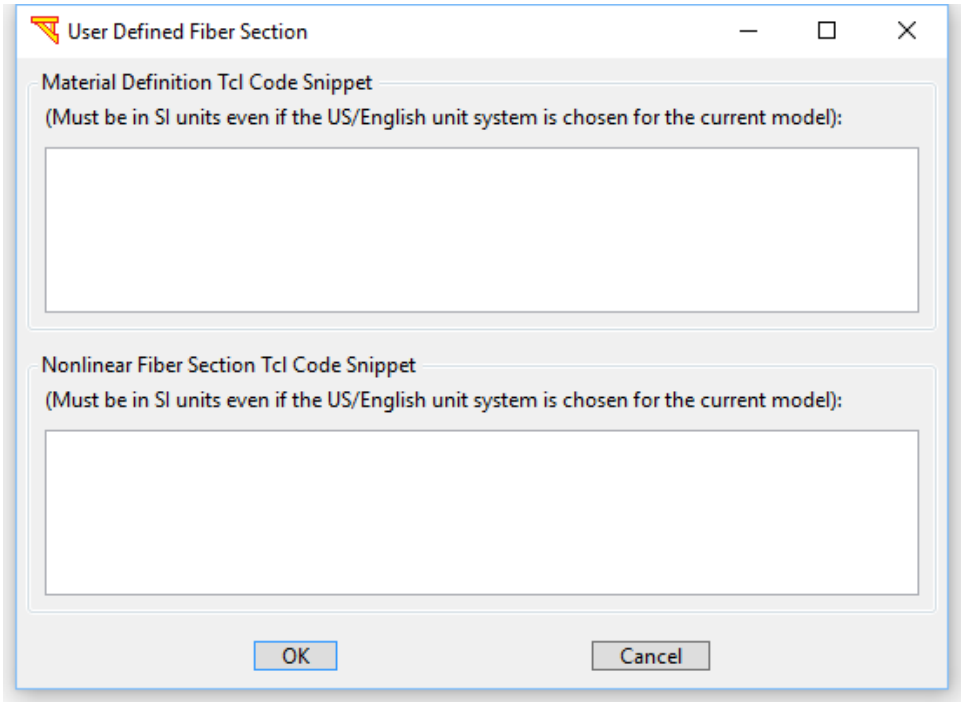

Fig. 35. User-defined Tcl script for nonlinear fiber section

3.5 Foundation

This section presents three ways to define and model the bridge foundation to account for the soil-structure interaction (SSI) in the analysis. There are three types of foundations available (Fig. 36): **Rigid Base**, **Soil Springs,** and **Foundation Matrix**.

3.5.1 Rigid Base

If Rigid Base is chosen, all column bases will be fixed (in three translational and three rotational directions). In that case, the "fixity" nodes of the abutment models are also fixed.

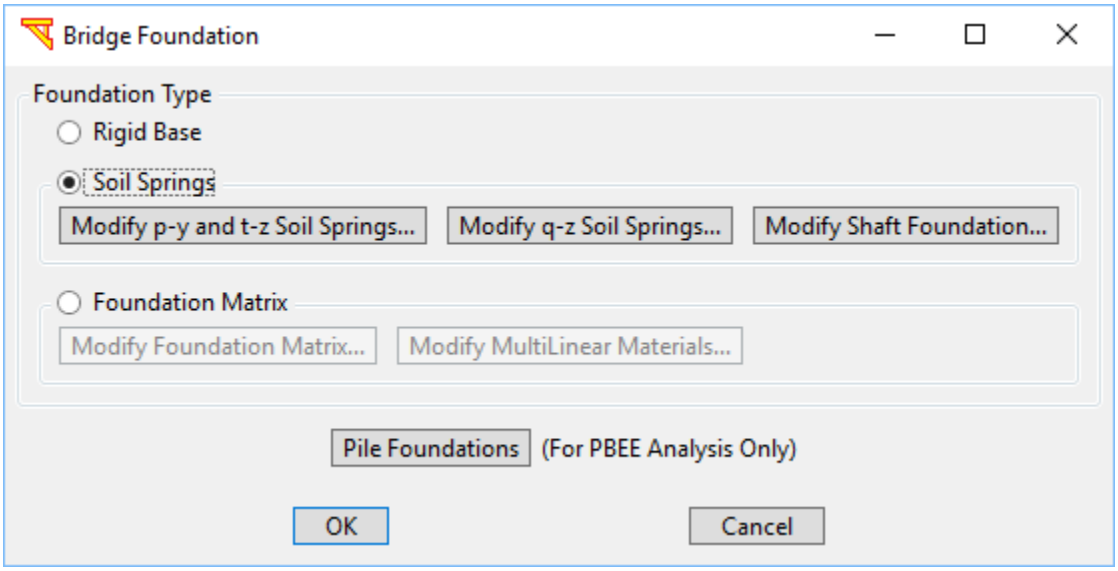

Fig. 36. Foundation types available in **MSBridge**

3.5.2 Soil Springs

To define soil springs, choose **Soil Springs** (Fig. 36) and then click **Modify Soil Springs** to define soil spring data or click **Modify Shaft Foundation** to define pile shaft data (Fig. 36). It is possible to exclude or include a shaft foundation at a particular bent or abutment; simply check the box to turn off/on shaft foundation for a bent/abutment (Fig. 37).

Parameters defining the pile foundation include (Fig. 37):

> **Stemwall Height**: the height of the stem wall (only available for abutments)
> **Pile Group Layout** (see Fig. 37). This option allows defining the numbers of the piles as well as the spacing (in the bridge longitudinal and transverse directions). Note that this option is only available for both abutments for now. For a bent, one single pile is assumed (for now in the current version).

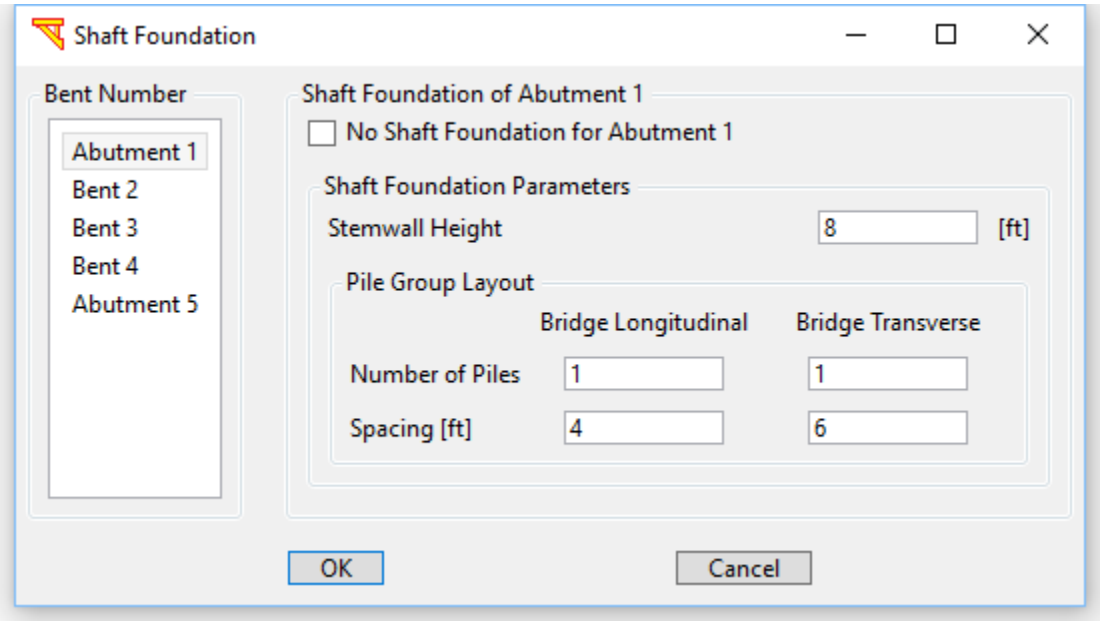

Fig. 37. Shaft foundation for abutments and bents

Fig. 38 shows the scheme of the pile foundation model for an abutment. The "abutment nodes" (Fig. 38) are referred to as "fixities" (see section ABUTMENT MODELS).

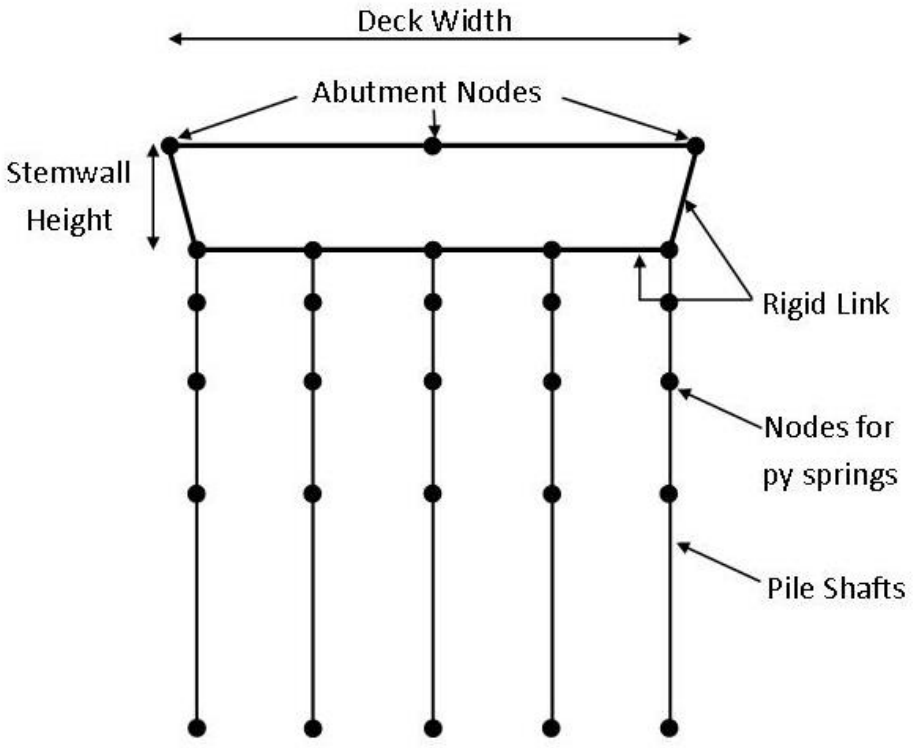

Fig. 38. Pile foundation model for an abutment

Parameters defining soil springs are shown in Fig. 39. Two identical horizontal soil springs (one for the bridge longitudinal direction and the other one for the transverse direction) will be applied at each depth. Button **Insert Depth** inserts a depth after the current depth being highlighted. Button **Delete Depth** removes the current depth being highlighted (associated soil spring data will be deleted as well).

To calculate the soil spring data based on p-y equations, click **Select from p-y Curves** (Fig. 39). For now, four types of soil p-y curves are available: **Soft Clay (Matlock), Stiff Clay with no Free Water (Reese), Sand (Reese), and Liquefied Soil (Rollins).** Fig. 40 - Fig. 43 show the calculated p-y curves for the above-mentioned soil materials, respectively. The procedures to calculate these p-y curves are described in Reese and van Impe (2001).

To use the soil spring data calculated based on p-y curves, click **OK** and then click **Yes**. The soil spring data chosen will replace existing soil spring data if any (Fig. 44). An example bridge model with the foundation of soil springs is shown in Fig. 45.

In addition, an option of user-defined p-y curves is available (Fig. 46). Options of defining t-z and q-z curves are shown in Fig. 47 and Fig. 48, respectively.

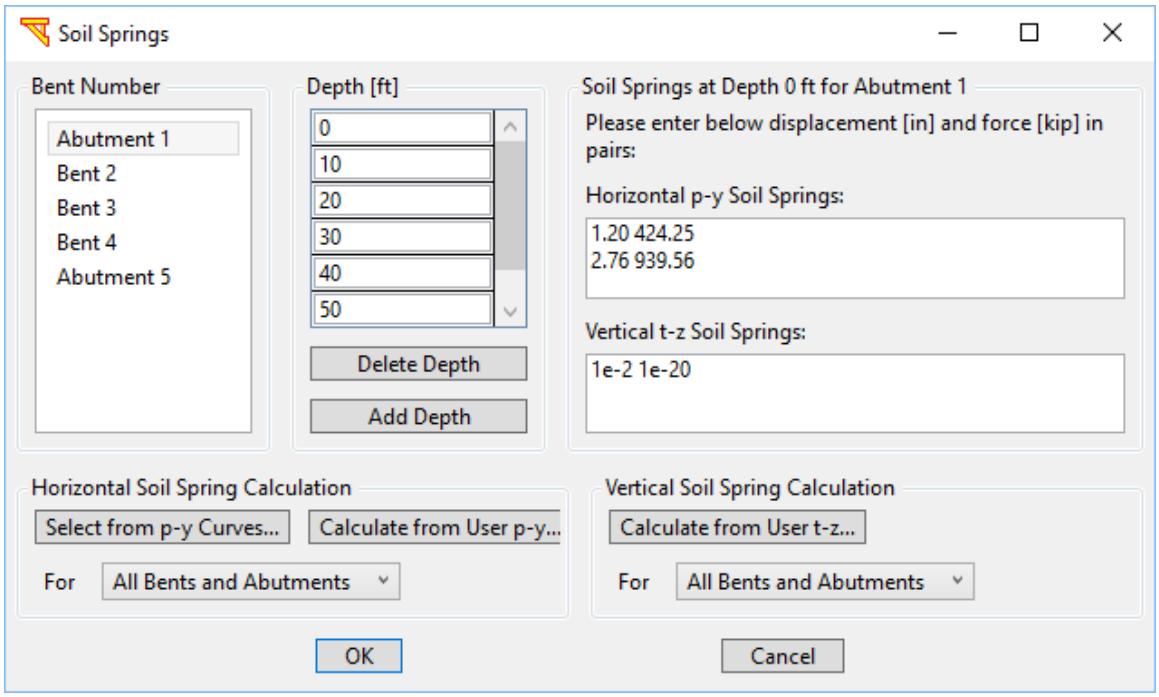

Fig. 39. Soil springs

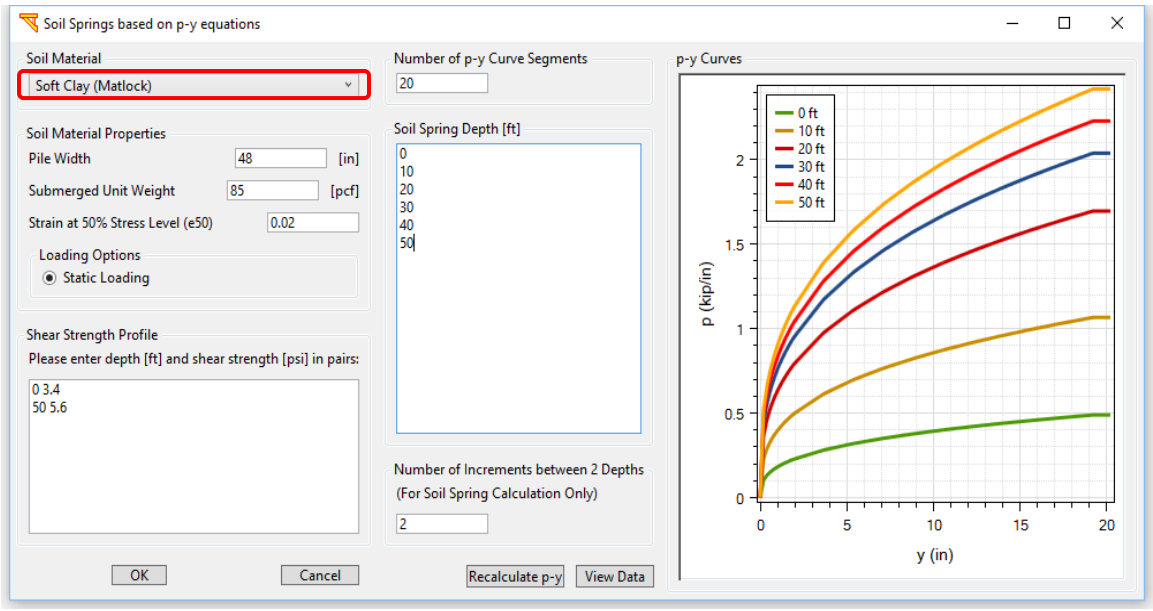

Fig. 40. Soft Clay (Matlock) p-y model

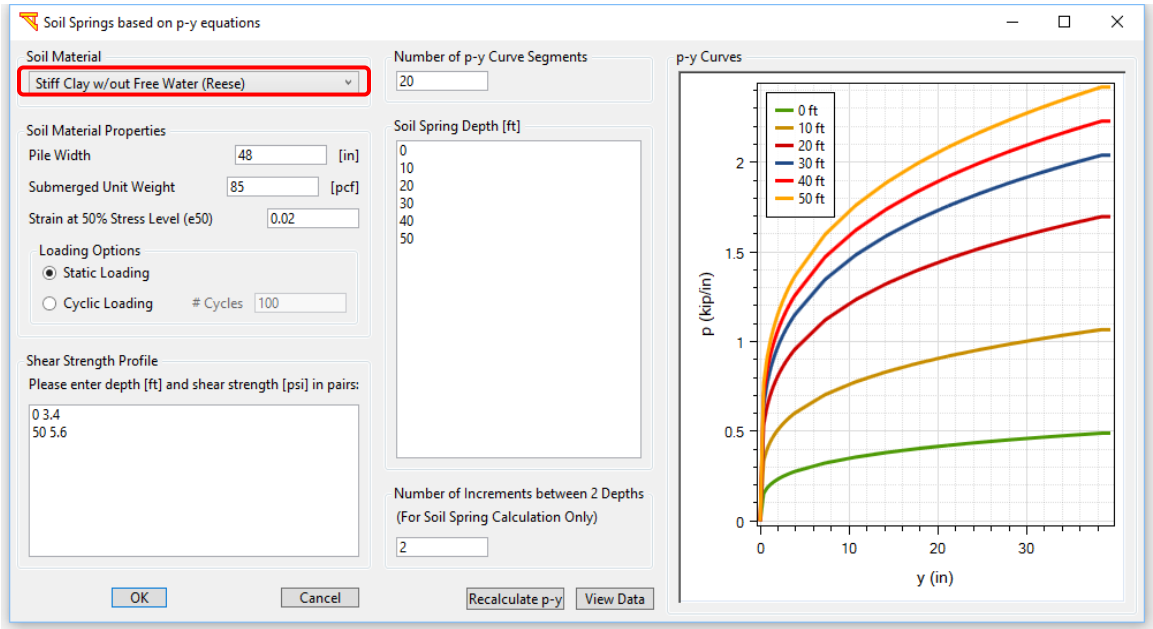

Fig. 41. Stiff Clay without Free Water (Reese) p-y model

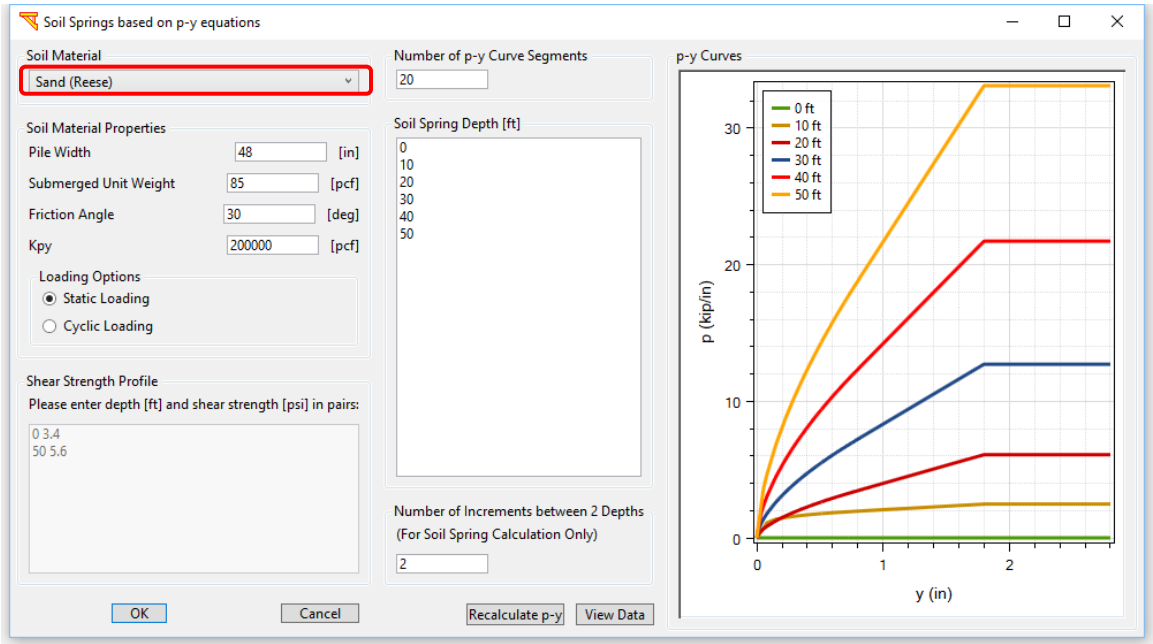

Fig. 42. Sand (Reese) p-y model

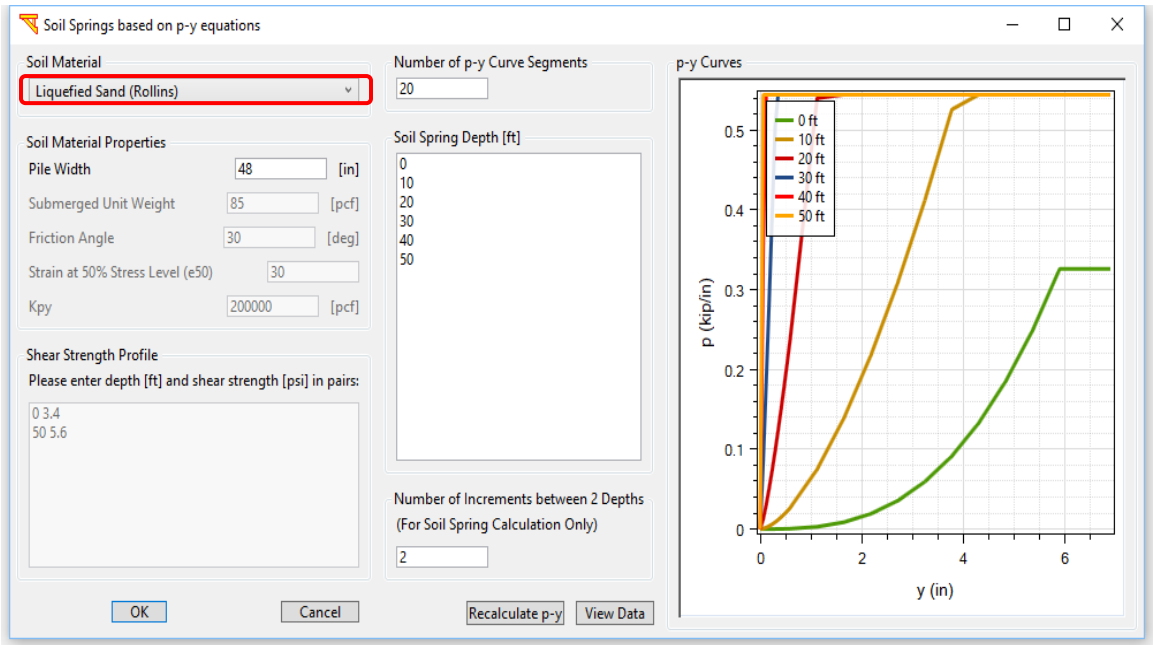

Fig. 43. Liquefied Sand (Rollins) p-y model

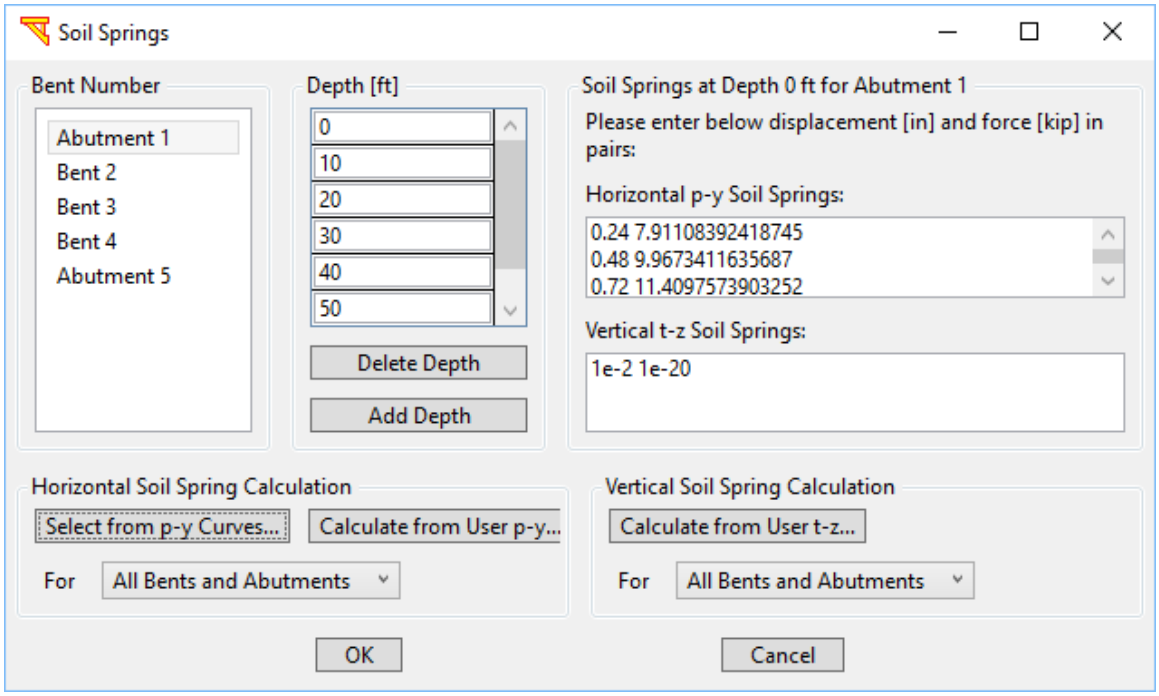

Fig. 44. Soil spring definition window after using the soil spring data calculated based on p-y equations

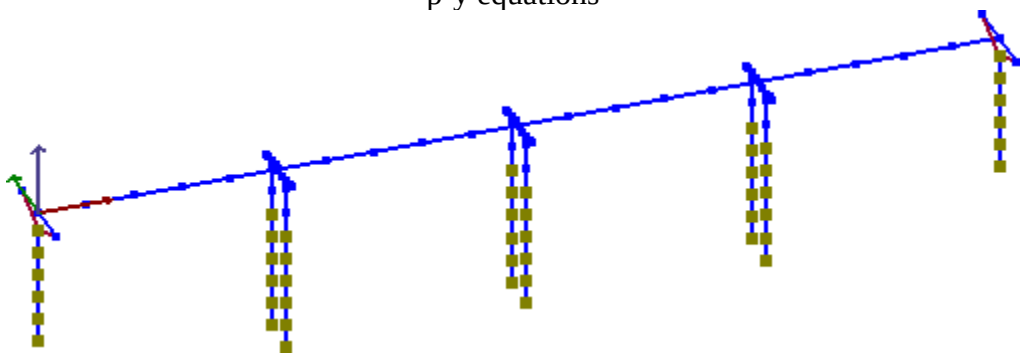

Fig. 45. FE mesh of a bridge model with soil springs included

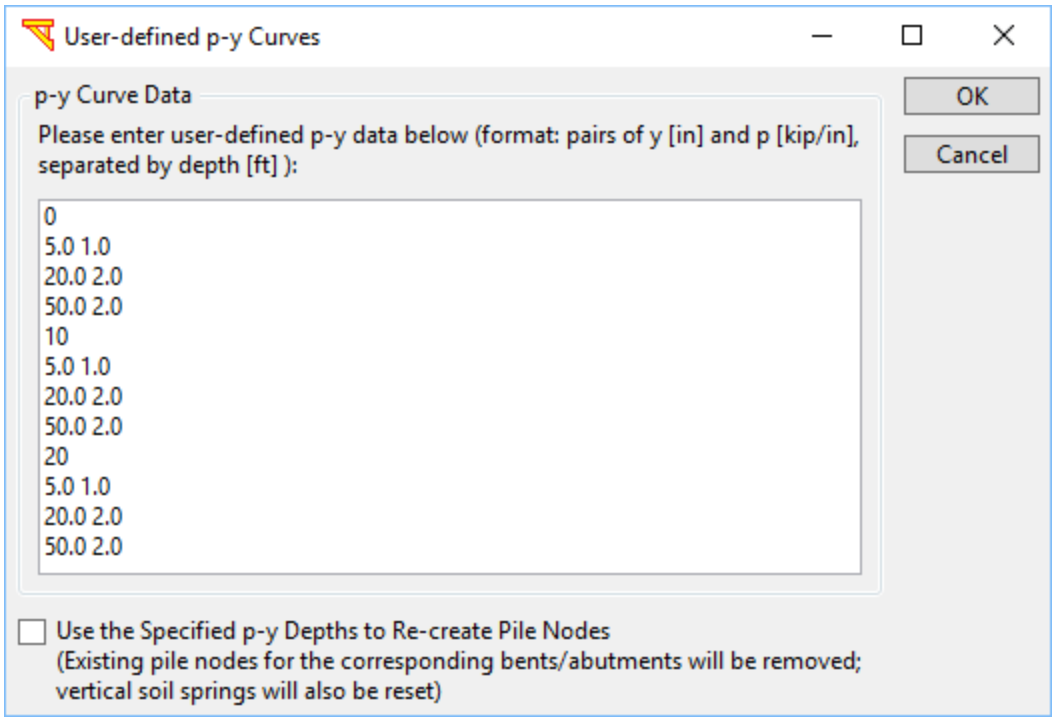

Fig. 46. User-defined p-y curves

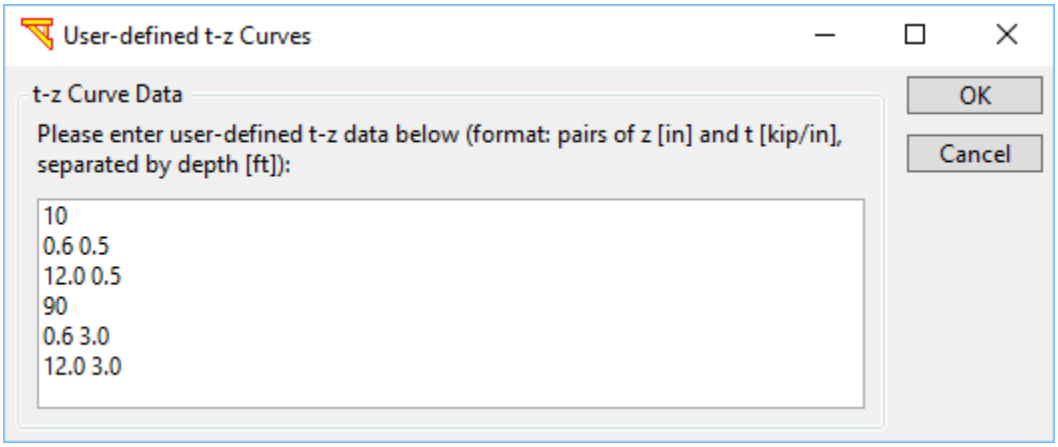

Fig. 47. User-defined t-z curves

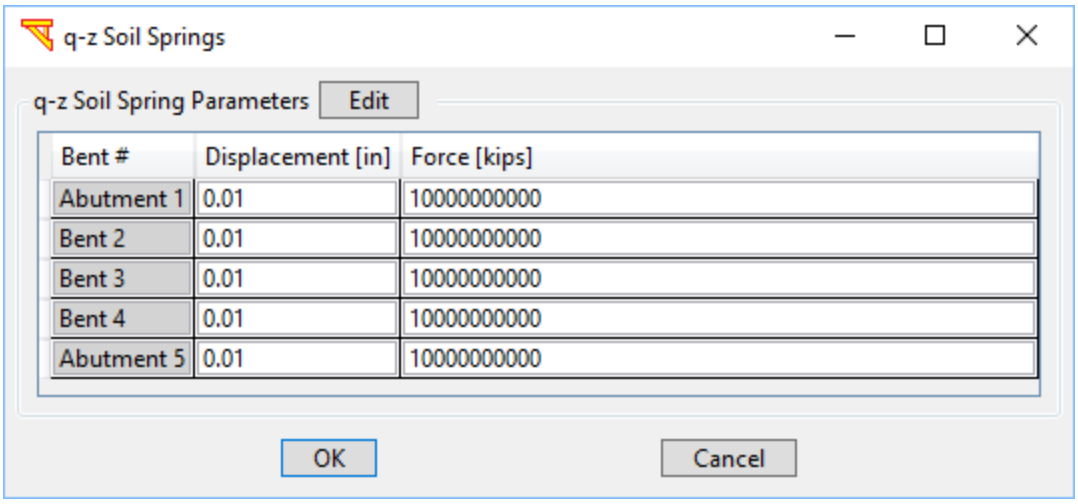

Fig. 48. User-defined q-z soil springs

3.5.3 Foundation Matrix

The third foundation type available is **Foundation Matrix** (Fig. 36, Li and Conte 2013). In this case, the foundation (only for bent columns) is represented by the coupled foundation stiffness matrix (Lam and Martin 1986). Specifically, the stiffness of a single pile is represented by a 6 x 6 matrix representing stiffness associated with all six degrees of freedom at the pile head. The local coordinate system employed for the foundation matrix is parallel to the global coordinate system (Fig. 49).

To define a foundation matrix, select **Foundation Matrix** and then click **Modify Foundation Matrix** (Fig. 36). Fig. 50 shows the window defining a foundation matrix, where Fx and Fy can be provided by nonlinear materials (Fig. 51). Fig. 52 shows the definition of pile foundations (for PBEE analysis only for now in the current version).

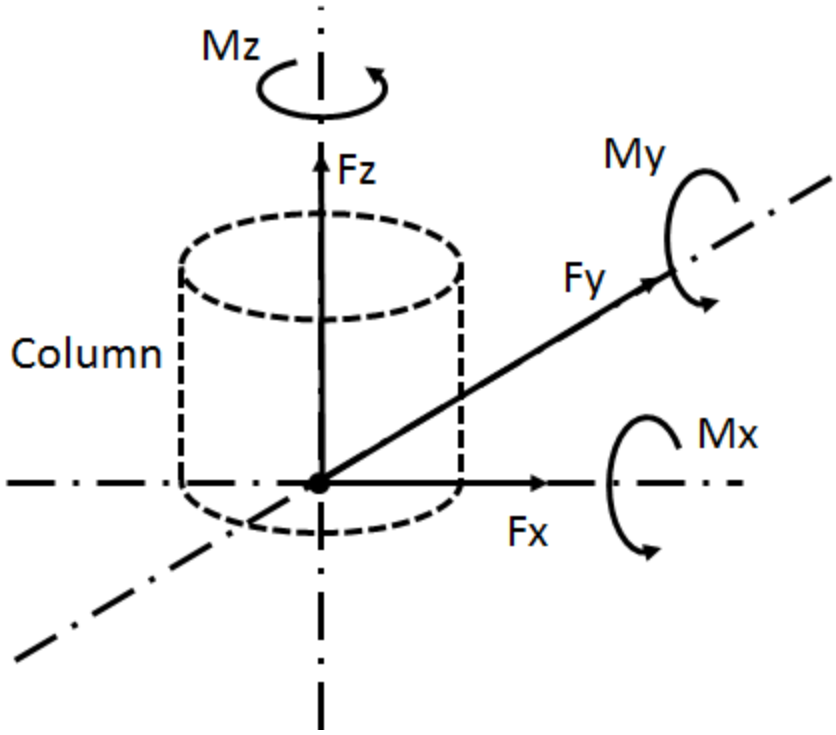

Fig. 49. Local coordination system for a foundation matrix

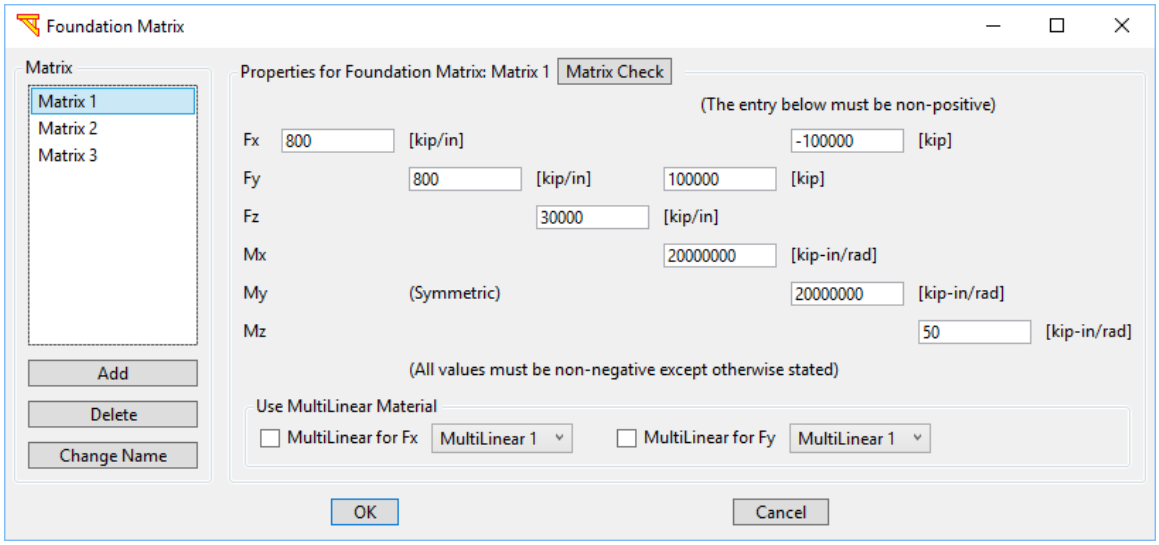

Fig. 50. Foundation matrix definition

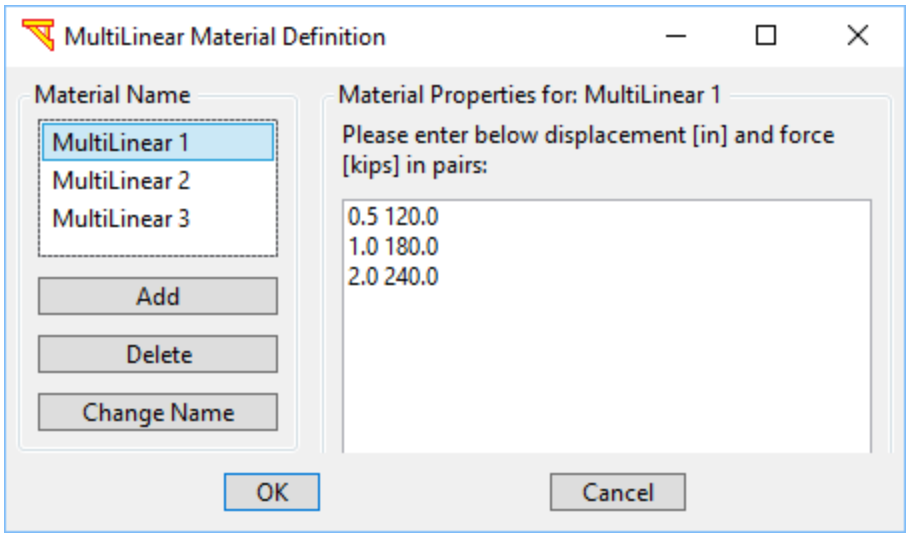

Fig. 51. Multi-linear material definition

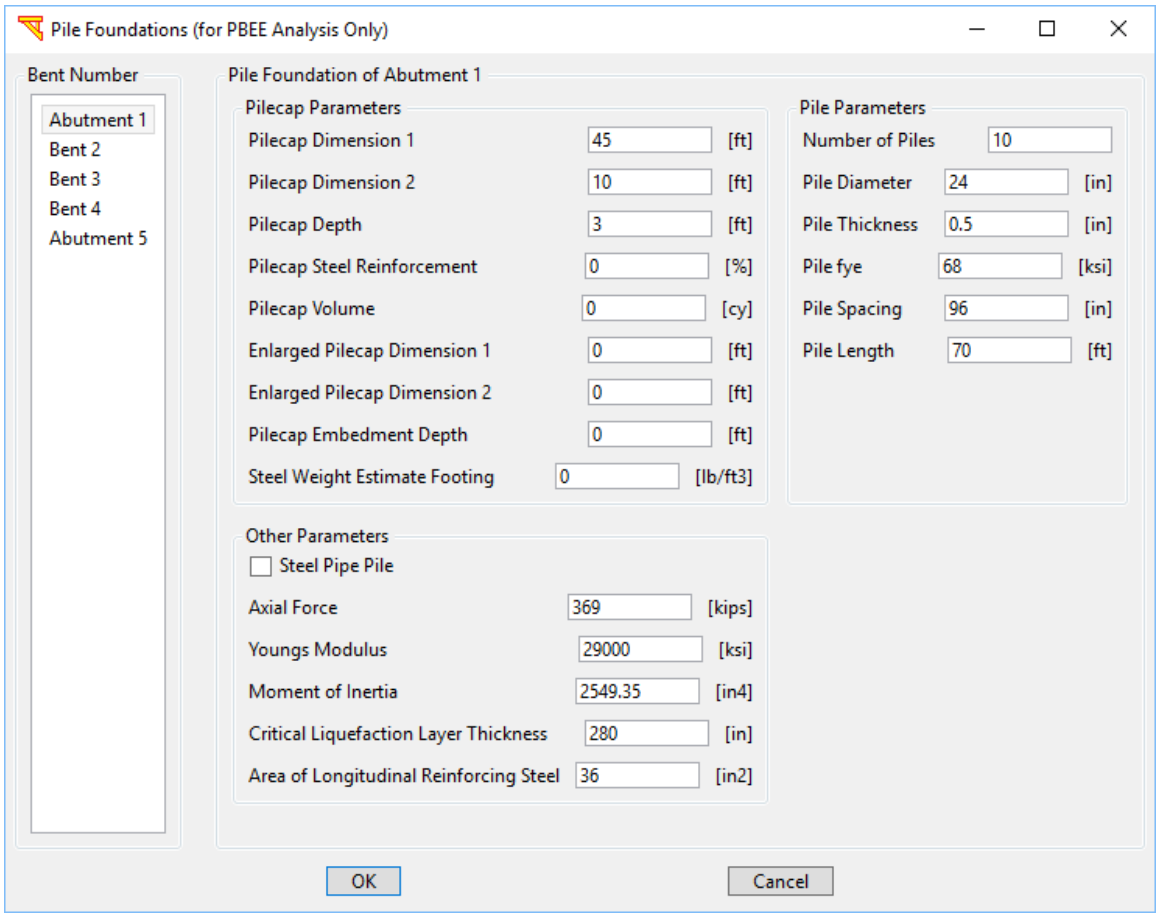

Fig. 52. Definition of pile foundations (for PBEE analysis only)

3.6 Abutment

To define an abutment model, click **Abutments** in Fig. 7. A window for defining an abutment model is shown in Fig. 53. More details about the abutment model will be further explained in the next chapter (see Chapter ABUTMENT MODELS)

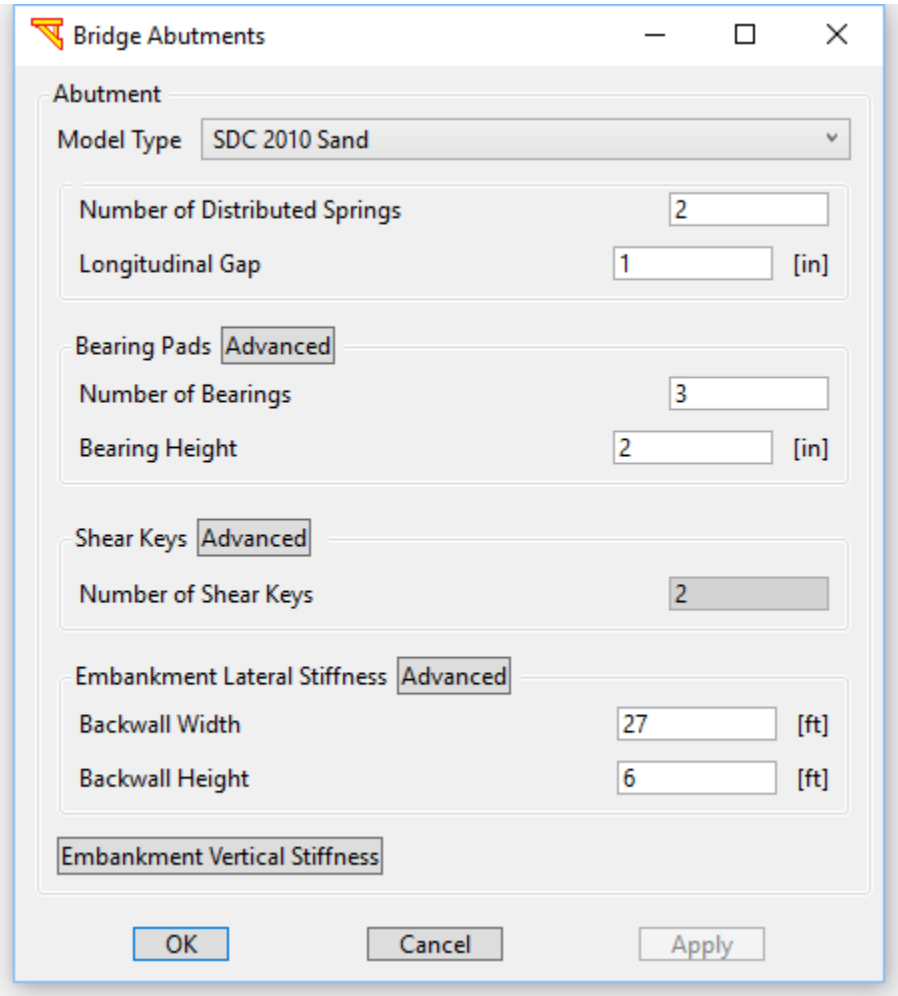

Fig. 53. Definition of an abutment model

3.7 Bridge Model

To define a bridge model, click **Bridge** in Fig. 7. A window for defining a bridge model is shown in Fig. 54. The user will assign the defined sections to corresponding bridge components. In addition, the column heights and column connection types are also defined.

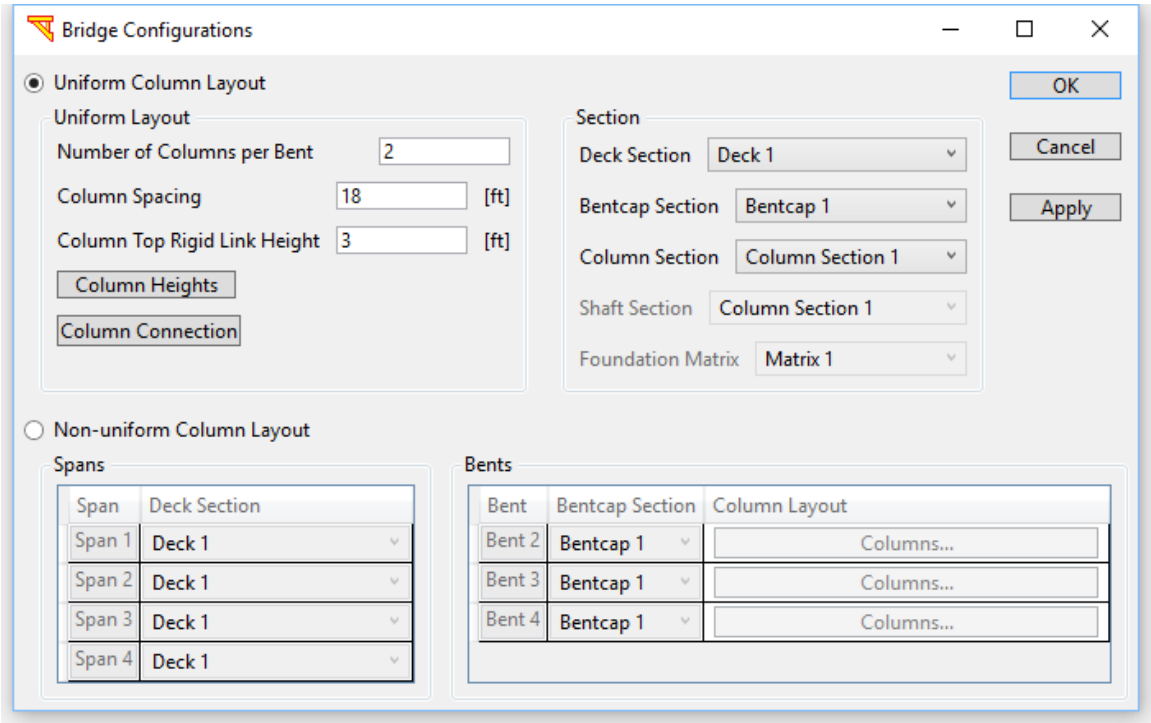

Fig. 54. Definition of a bridge model

3.7.1 Uniform Column Layout

If the **Uniform Column Layout** option is selected, all bents will have the same number of columns (with the same **Column Spacing** for each bent**)**. If **Number of Column for Each Bent** is 1, **Column Spacing** will be ignored (Fig. 55).

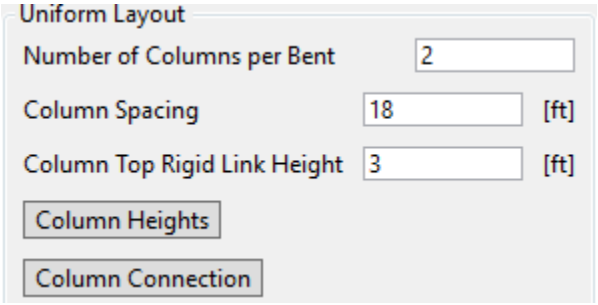

Fig. 55. Uniform column layout

3.7.1.1 Column Heights

To define column heights, click **Column Heights** in Fig. 55. A window for defining column heights will appear (Fig. 56).

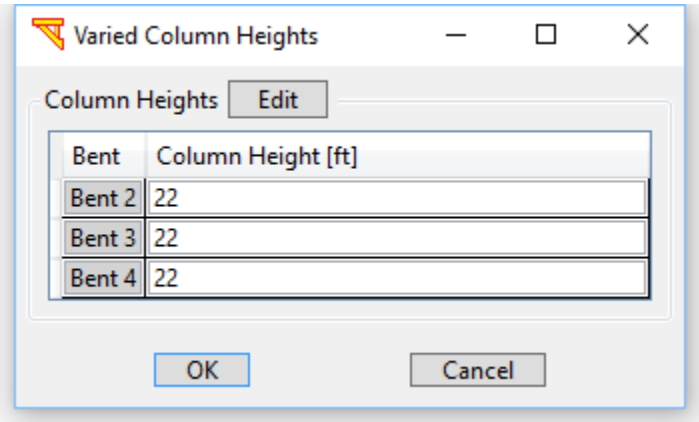

Fig. 56. Column heights

3.7.1.2 Column Connection

In a multi-column case (the number of columns per bent is equal to 2 or more), the user can specify the boundary connection conditions of the columns. Click **Column Connection** (in Fig. 55) to select the boundary condition for the columns and bent cap connection. Three options are available (Fig. 57): i) fixed at top / pinned at base, ii) pinned at top / fixed base, and iii) fixed at both top and base. **Note:** In a single column case (the number of columns per bent is equal to 1), both column top and base are assumed fixed.

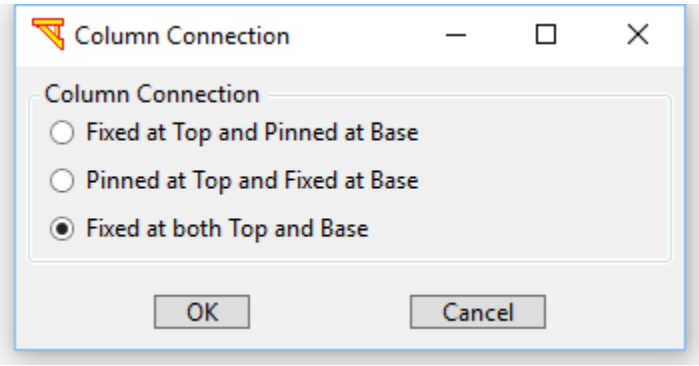

Fig. 57. Column boundary conditions

3.7.2 Non-uniform Column Layout

If the **Non-uniform Column Layout** option is selected, the user can have the flexibility to define a different number of columns on a bent-by-bent basis (Fig. 58).

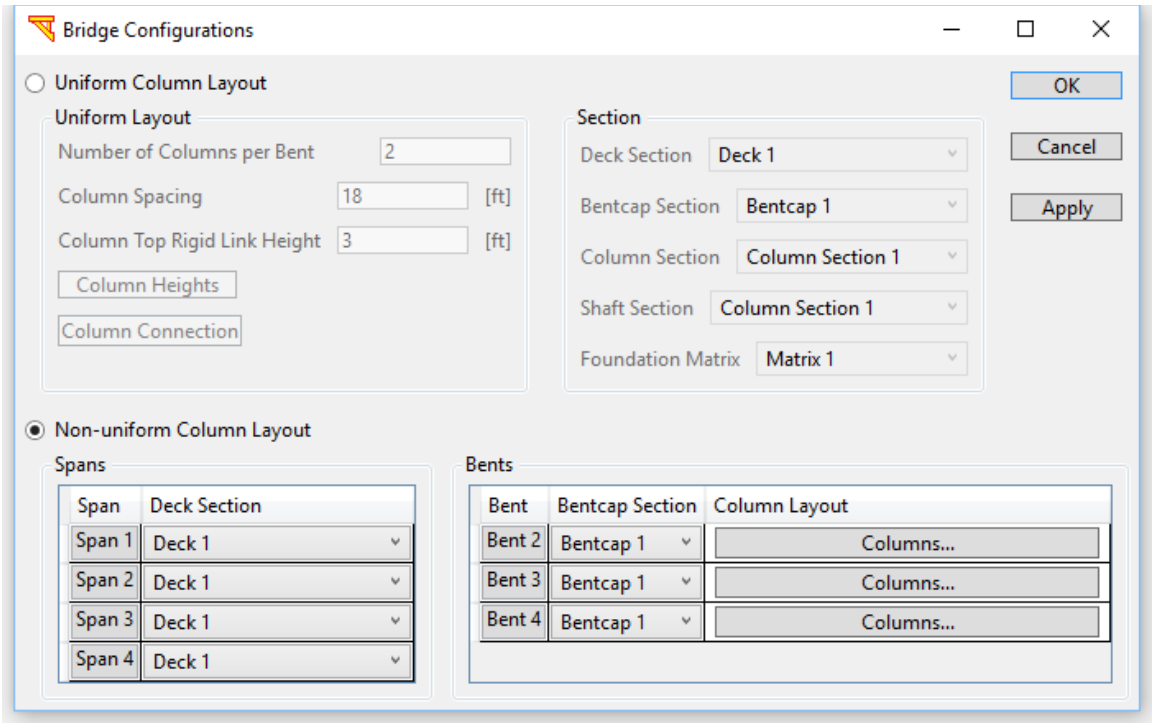

a)

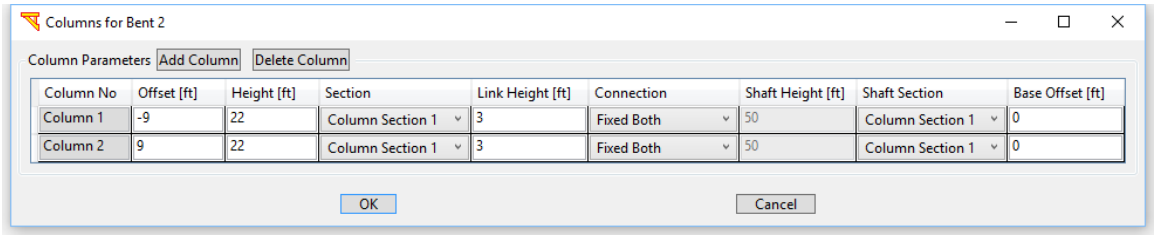

b)

Fig. 58. Bridge configuration: a) general options; b) column layout definition

3.8 Advanced Options

The advanced options in **MSBridge** mainly include Deck Hinges, Isolation Bearings, Steel Jacket, and Skew Angles. Click **Advanced** in Fig. 7 to include any of these options as shown in Fig. 59 into the bridge model.

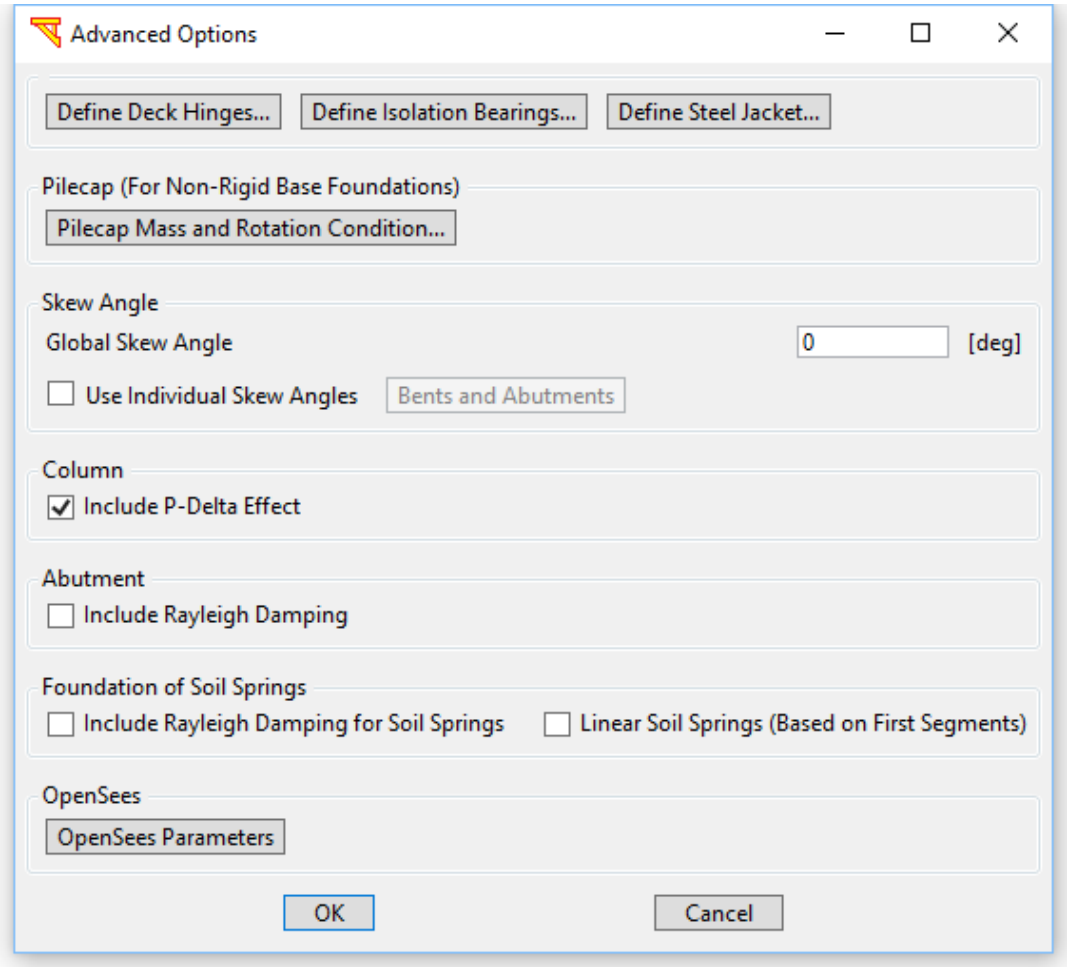

Fig. 59. Advanced options

3.8.1 Deck Hinges

To define deck hinges, click **Define Deck Hinges** in Fig. 59 and a window for defining deck hinge properties will appear (Fig. 60). An example bridge model including two deck hinges is shown in Fig. 61.

To activate/define a deck hinge, check the checkbox immediately before the **Hinge #** (e.g., Hinge 2).

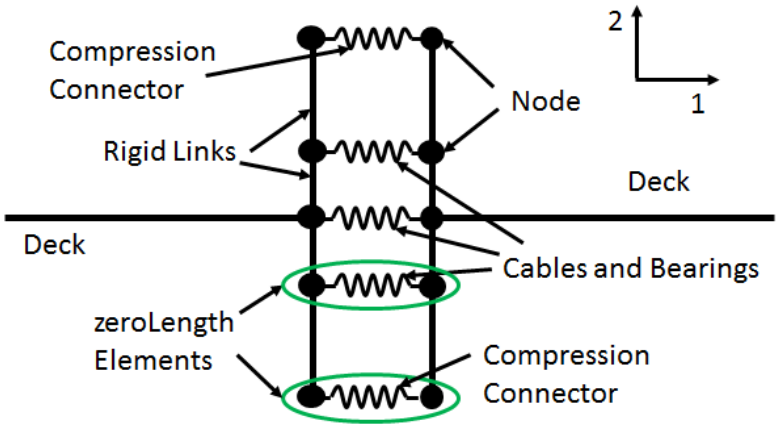

Fig. 62 shows the general scheme of a deck hinge, which consists of 2 compression connectors (located at both deck edges) and cables.

Distance to Bent: The distance to the nearest (left) bent. Foot and meter are used for English and SI units, respectively
Spacing: The space between transverse left and right deck compression connectors. This space should usually be approximately equal to the deck width.
Skew Angle: The skew angle of the deck hinge. A zero skew angle means the deck hinge is perpendicular to the bridge deck direction
# of Cables: The total number of cables for the deck hinge
Cable Spacing: The spacing between cables. A symmetric layout of cables is assumed. Foot and meter are used for English and SI units, respectively

As shown in Fig. 62, zeroLength elements are used for cables and compression connectors. The bearing pads are included in the cables. For each zeroLength element, both nodes interact in the longitudinal direction (denoted as direction "1" in Fig. 62) but tied in the vertical direction "3" (not shown in Fig. 62) as well as the transverse direction (denoted as direction "2" in Fig. 62). The above conditions would force both sides of deck segments to move in the same deck surface plane. Note that the local coordinate system 1-2-3 may or may not coincide with the global coordinate system X-Y-Z (Fig. 1).

In the longitudinal direction and as the load is applied at the right side of the hinge; only the bearings will resist the movement since the cables are loose, but once the cables start to be stretched the cables stiffness will add resistance to the movement. In addition, the connectors will be out of the picture since the gap is not closing while the load is tension. On the other hand, if the load is applied to the left side of the hinge; the gap will be closing and only the bearing will resist the movement until the gap is closed, then the connectors will make sure that the deck will move as one object. The cables are not playing any role in this process.

In the transverse direction, it does not matter at which direction the load will be applied, the hinge will act the same. Both nodes are tied and both sides of the deck segments will move in the same plane; even if the bearing stiffness is very low. However, as the two segments are moving in the transverse direction, they will rotate and this rotation will make

the nearest end in compression and the other end in tension. Therefore, the bearings and the connectors – if the gap is closed - will work longitudinally in the compression end, and the bearings and cables – if they are stretched – will act longitudinally in the tension end.

The default values of properties for the compression connectors, cables, bearing pads are also shown in Fig. 60.

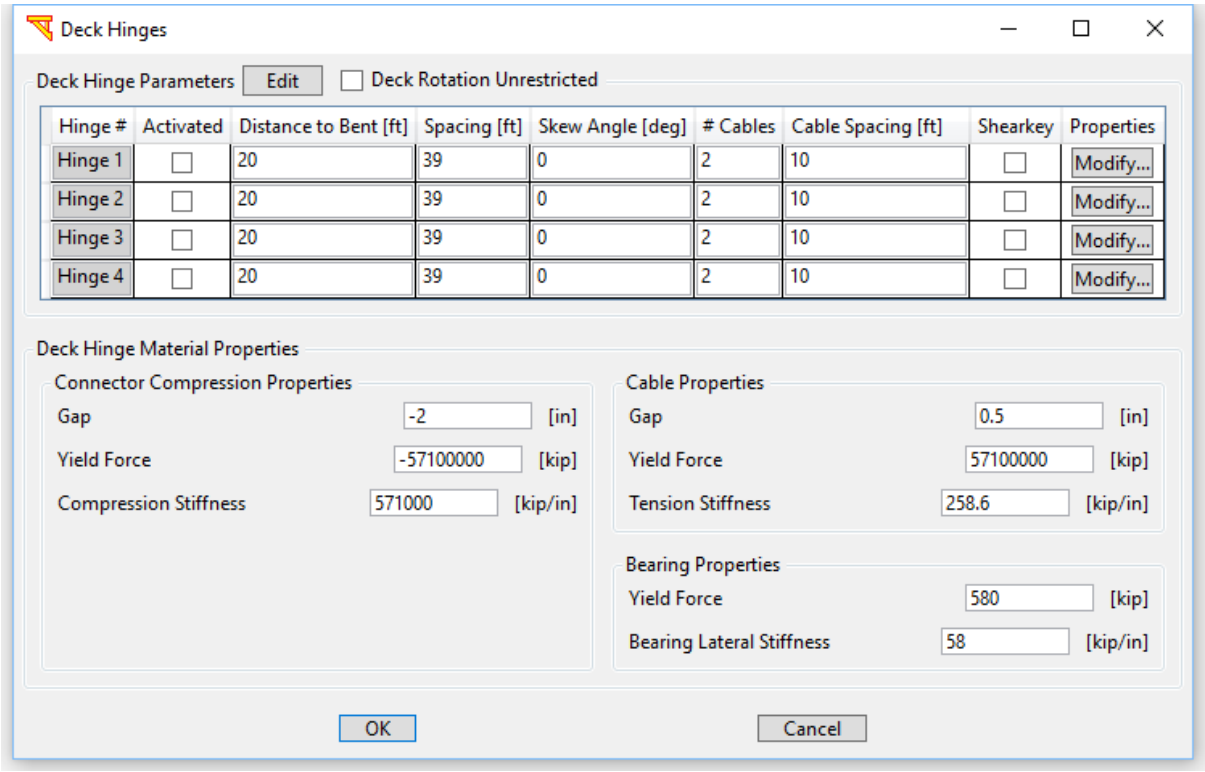

a)

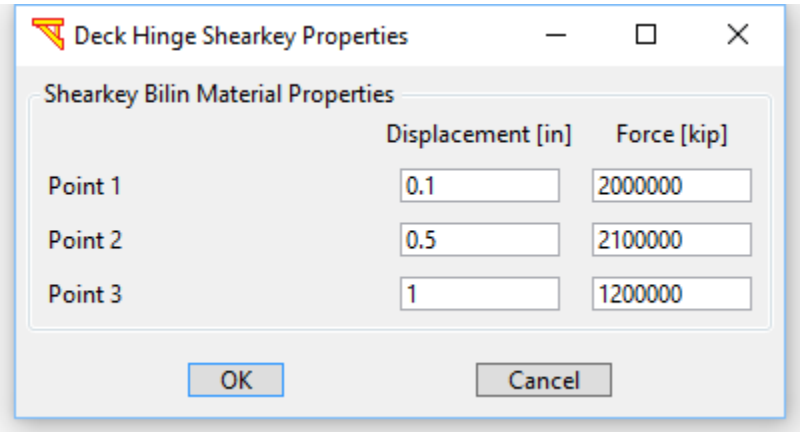

b)

Fig. 60. Definition of deck hinges

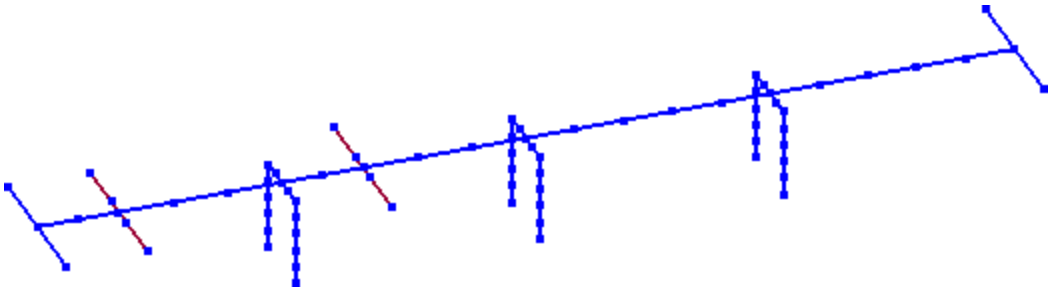

Fig. 61. FE mesh of a 4-span model with 2 deck hinges included

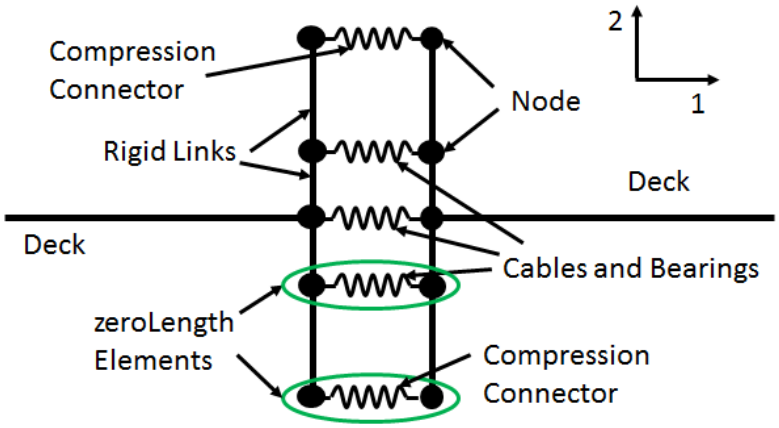

Fig. 62. OpenSees zeroLength elements for deck hinges (plan view)

3.8.2 Isolation Bearings

To define isolation bearings, click **Define Isolation Bearings** in Fig. 59 and a window for defining isolation bearing properties will appear (Fig. 63). An example bridge model including two isolation bearings on each bent cap is displayed in Fig. 64.

To activate/define isolation bearings on a bent cap, check the checkbox immediately before the **Bent #** (e.g., Bent 2).

> **# Bearings**: The total number of isolation bearings activated at the bent cap.
> **Spacing**: The spacing between isolation bearings. A symmetric layout of bearings is assumed.

Default values of material properties for the isolation bearings are also shown in Fig. 63. As shown in Fig. 65, zeroLength elements are used for the isolation bearings (Li and Conte 2013). For each zeroLength element, the two nodes interact in both horizontal directions (denoted as directions “1”(not shown) and “2” in Fig. 65) but tied in the vertical direction “3” (Fig. 65). Note that the local coordinate system 1-2-3 may or may not coincide with the global coordinate system X-Y-Z (Fig. 1).

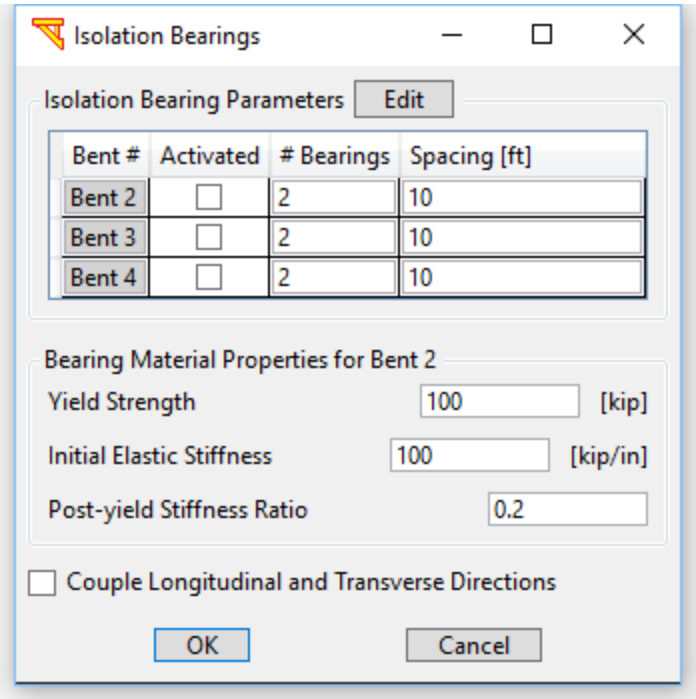

Fig. 63. Definition of isolation bearings

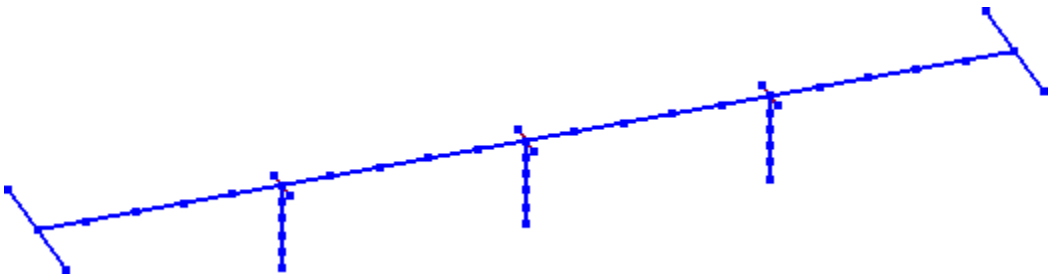

Fig. 64. FE mesh of a 4-span bridge model with two isolation bearings included on each bent cap

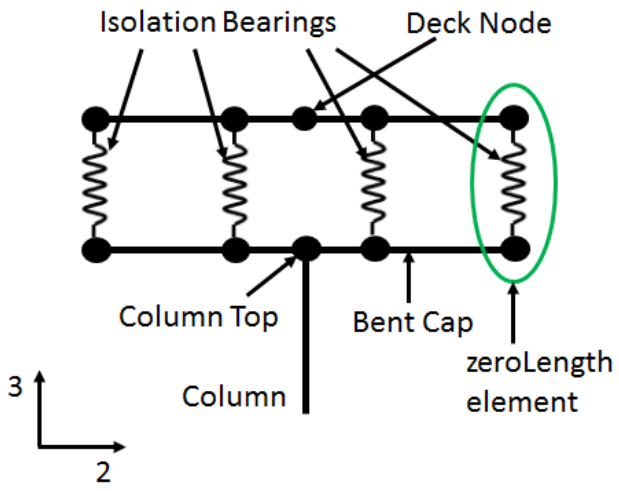

Fig. 65. OpenSees zeroLength elements for isolation bearings (side view of bentcap cut-plan)

3.8.3 Steel Jackets

To define steel jackets, click **Define Steel Jackets** in Fig. 59 and a window for defining steel jacket properties will appear (Fig. 66).

Note that the steel jacket option is only available for a circular column. To activate/define steel jacket for all columns for a bent, please enter nonzero values for the corresponding row (Fig. 66). In the case of partial length of steel jacket (Fig. 67), please specify enough number of elements for the column (since an equal element size is used for each column within a bent, for now).

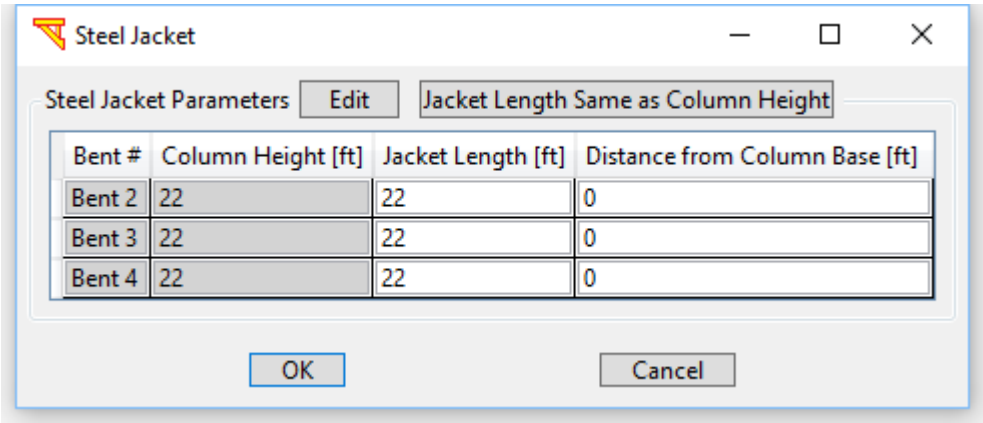

Fig. 66. Definition of steel jackets

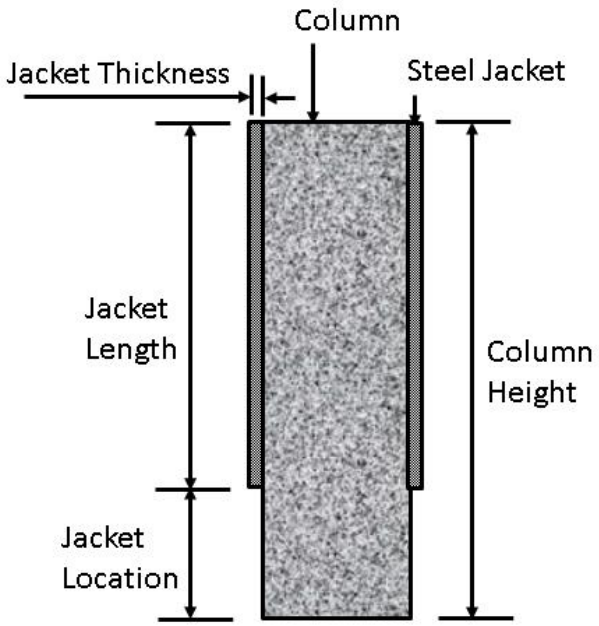

Fig. 67. Sketch of a steel jacket

3.8.4 Skew Angles

The user can choose to use a single (global) skew angle or individual skew angles for abutments and bents. By default, a zero global skew angle is assumed (Fig. 59). To define individual skew angles, check the checkbox **Use Individual Skew Angles** (Fig. 59).

To define individual skew angles, click **Bents and Abutments** in Fig. 68. A window for defining skew angle properties will appear (Fig. 68).

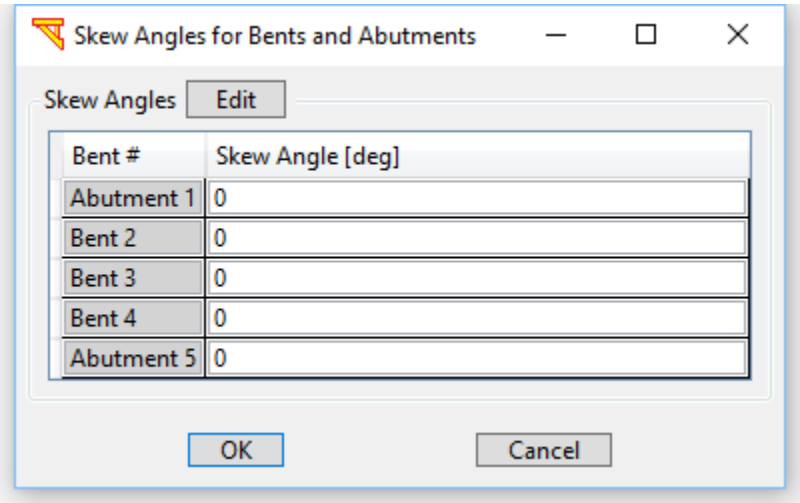

Fig. 68. Definition of skew angles

3.8.5 Pilecap Mass

To define pilecap mass, click **Pilecap Mass and Rotation Condition** in Fig. 59 and a window for defining pilecap mass properties will appear (Fig. 69).

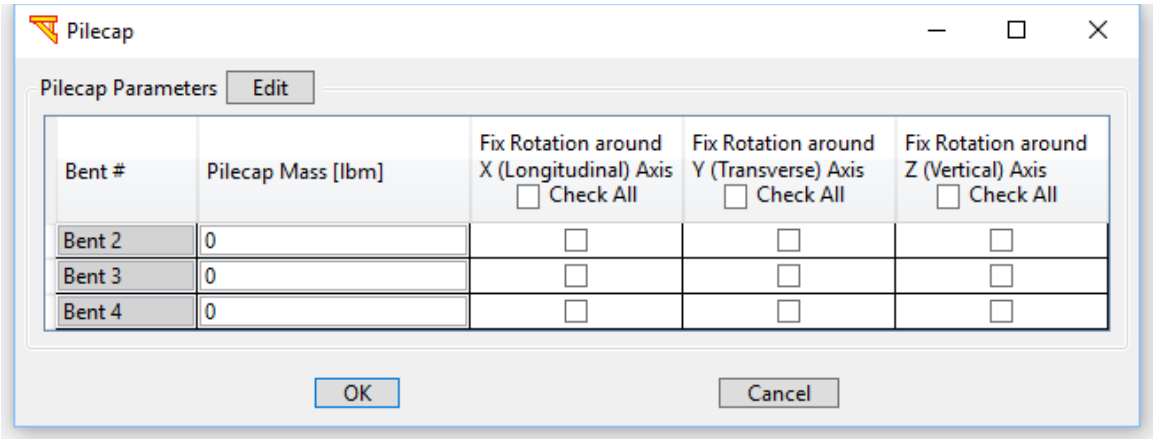

Fig. 69. Definition of pilecap mass

3.8.6 OpenSees Parameters

To modify OpenSees analysis parameters, click **OpenSees Parameters** in Fig. 59 and a window for modifying OpenSees analysis parameters will appear (Fig. 70).

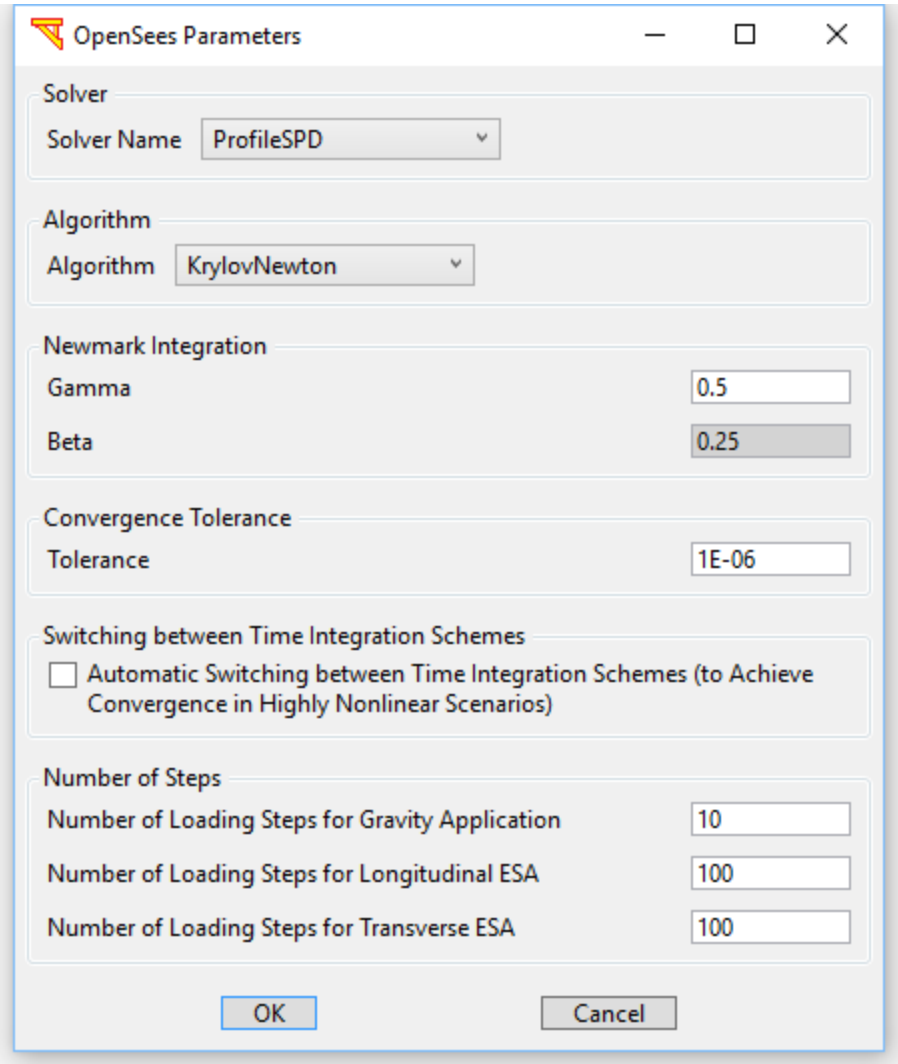

Fig. 70. Parameters for OpenSees analysis

3.9 Mesh Parameters

To change the number of beam-column elements for the bridge model, click **Mesh** in Fig. 7. Fig. 71 displays the **Mesh Parameters** window showing the default values. The number of beam-column elements for a deck segment (a span) must be least 2. For each bentcap segment between 2 neighboring columns, the number of elements must be even.

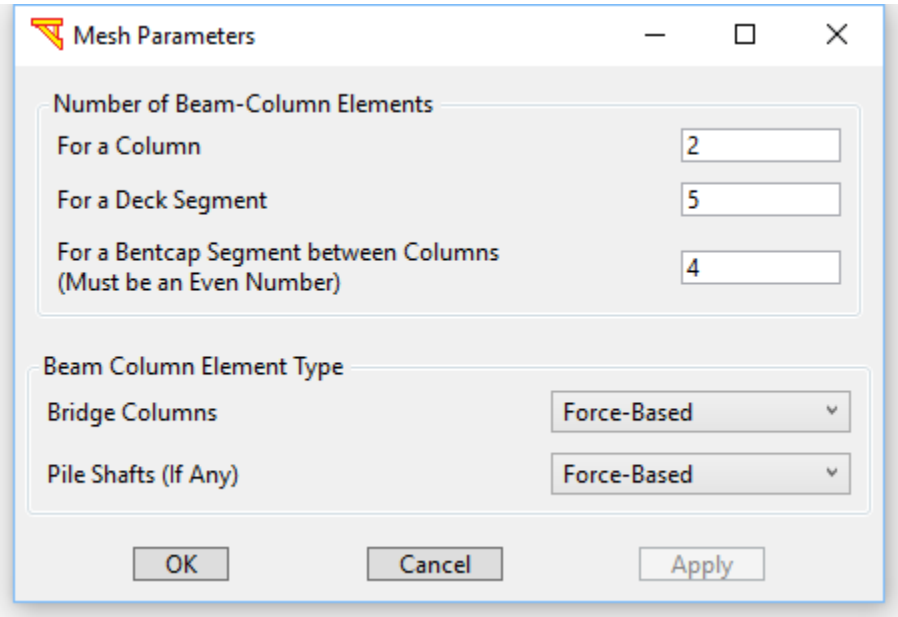

Fig. 71. Mesh parameters

Three types of nonlinear Beam-Column Elements are available for the column: **Beam With Hinges**, **Force-Based Beam-Column, and Displacement-based Beam-Column** (McKenna et al. 2010). By default, Forced-based beam-column elements (**nonlinearBeamColumn**, McKenna et al. 2010) are used (the number of integration points = 5).

When the **Beam With Hinges** Element is used, the calculation of the plastic hinge length (L_p) for the column is based on Eq. 7.25 of SDC (2010):

$$L_p = \begin{cases} 0.08L + 0.15 f_{ye} d_{bl} \geq 0.3 f_{ye} d_{bl} & (\text{in}, \text{ksi}) \\ 0.08L + 0.022 f_{ye} d_{bl} \geq 0.044 f_{ye} d_{bl} & (\text{mm}, \text{MPa}) \end{cases}$$

Where L is the column height, f_{ye} is the steel yield strength,d_{bl} is the longitudinal bar size. The plastic hinge length (L_p) is the equivalent length of the column over which the plastic curvature is assumed constant for estimating plastic rotation (SDC 2010).

4 ABUTMENT MODELS

Abutment behavior, soil-structure interaction, and embankment flexibility have been found by post-earthquake reconnaissance reports to significantly influence the response of the entire bridge system under moderate to strong intensity ground motions. Specifically, for Ordinary Standard bridge structures in California with short spans and relatively high superstructure stiffness, the embankment mobilization and the inelastic behavior of the soil material under high shear deformation levels dominate the response of the bridge and the intermediate column bents (Kotsoglu and Pantazopoulou 2006; Shamsabadi et al. 2007, 2010). Seven abutment models have been implemented in **MSBridge**. The abutment models are defined as Elastic, Roller, SDC 2004, SDC 2010 Sand, SDC 2010 Clay, EPP-Gap and HFD abutment models.

To define an abutment model, click **Abutment** in Fig. 7. A window for defining an abutment model is shown in Fig. 72.

4.1 Elastic Abutment Model

The Elastic Abutment Model consists of a series of 6 elastic springs (3 translational and 3 rotational) at each node at the end of the bridge (Fig. 73). To choose the Elastic Abutment Model, select **Elastic** for the Model Type in Fig. 72 (Fig. 74).The main window to define the Elastic Abutment Model is shown in Fig. 75. By default, no additional rotational springs are specified but can be added by the user.

As shown in Fig. 73 - Fig. 75, **MSBridge** allows the user to define multiple distributed springs (equal spacing within deck width). The values specified in Fig. 75 are the overall stiffness for each direction (translational or rotational). For the longitudinal direction (translational and rotational), each of the distributed (Elastic) springs carries its tributary amount.

e.g., Fig. 73 shows a case of 4 distributed springs. Each of the both end springs carries one-sixth of the load, and each of the middle springs carries one-third (Fig. 73a). The vertical components (translational and rotational) are similar to the longitudinal ones. i.e., each of the distributed springs carries its tributary amount in the vertical direction. However, the transverse component is different: only the both end-springs carry the load. In other words, each of the end springs carries half of the load along the transverse direction (translational and rotational).

By default, the number of distributed springs is 2. In this case, these two springs are located at the both ends of the Rigid element (the length of which is equal to deck width) shown in Fig. 73. However, due to the coupling of the longitudinal, and vertical translational springs, the option of using a single node at each abutment is possible, this gives the user full control over the true rotational stiffness apart from the translational stiffness.

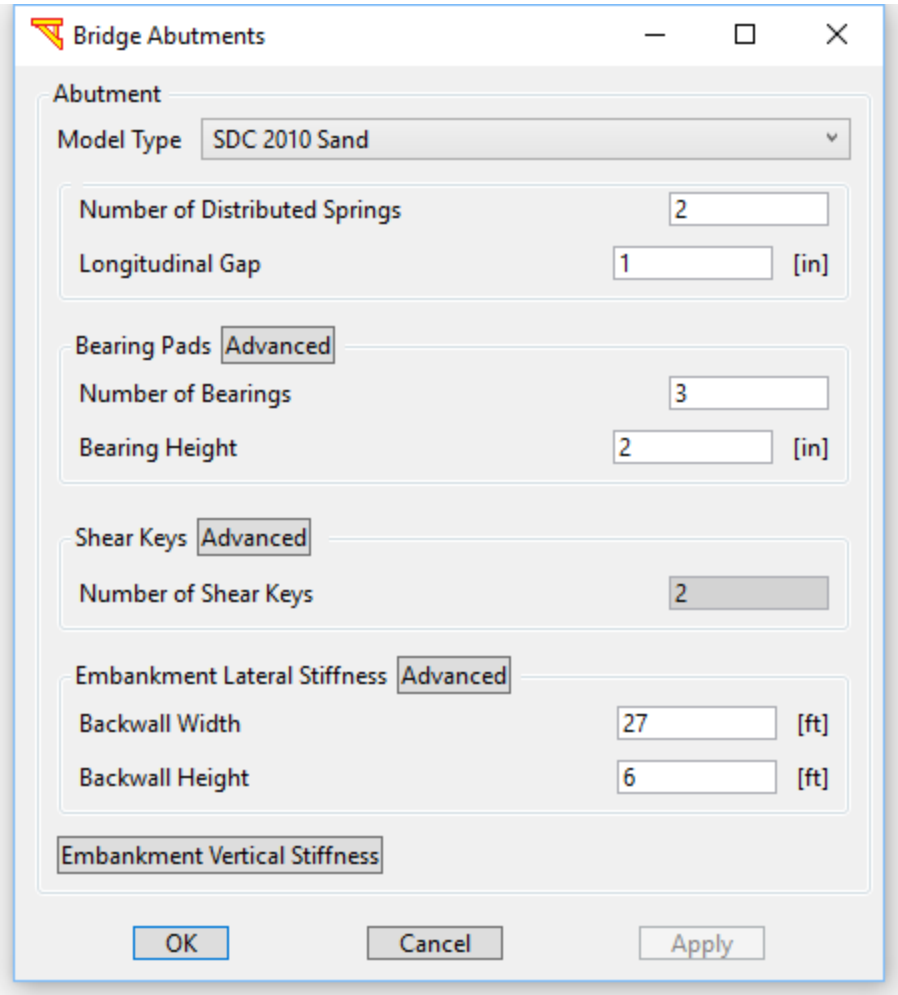

Fig. 72. Definition of an abutment model

The abutment will be rotated counter-clockwise if the skew angle is positive (rotated clockwise if negative). Fig. 76 shows the direction of longitudinal springs in a curved bridge with a non-zero skew angle. Fig. 77 shows a bridge model with five distributed abutment springs and a non-zero skew angle.

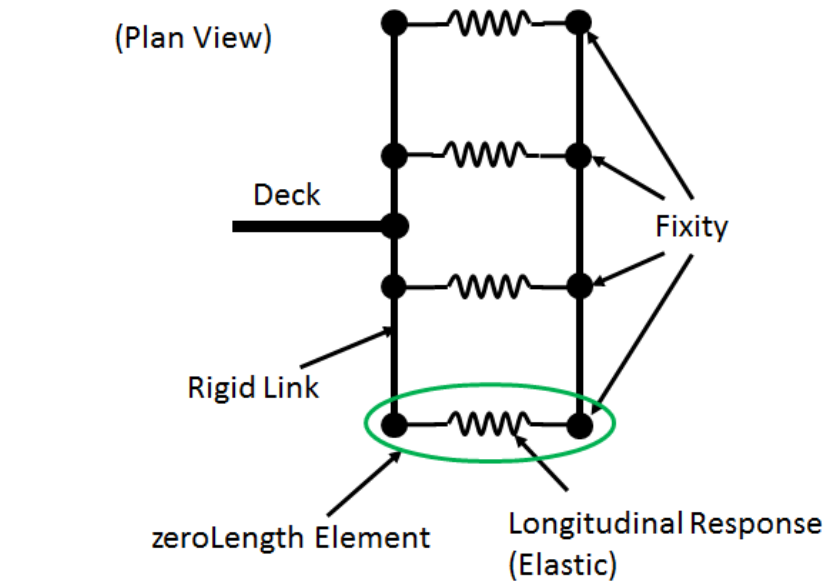

a)

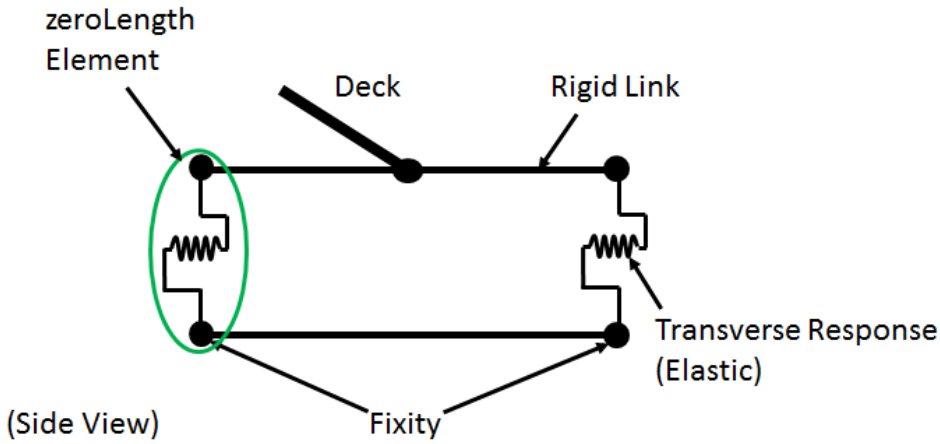

b)

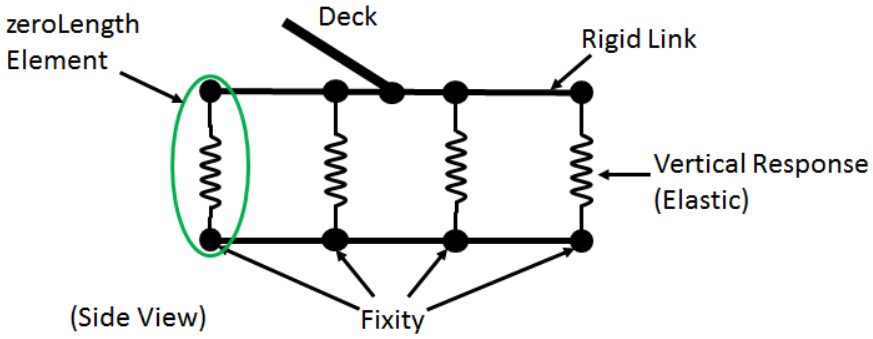

c)

Fig. 73. General scheme of the Elastic Abutment Model: a) longitudinal component; b) transverse component; c) vertical component

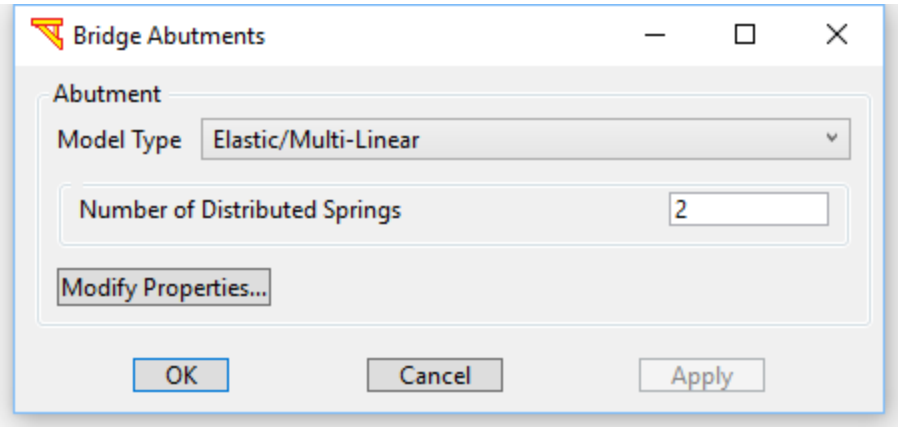

Fig. 74. Definition of the Elastic Abutment Model

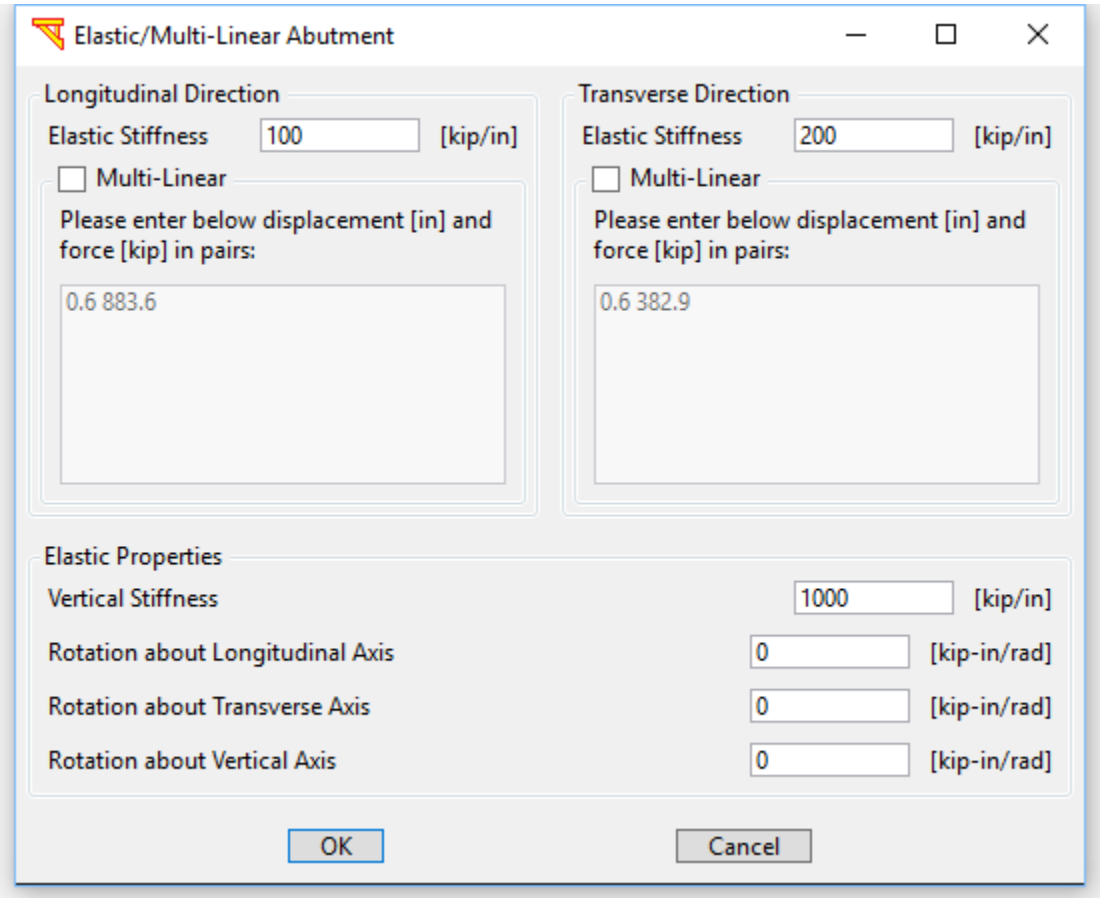

Fig. 75. Parameters of the Elastic Abutment Model

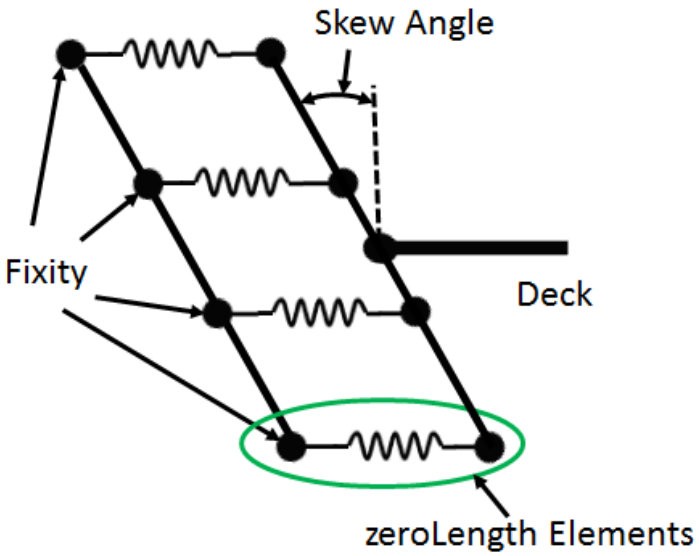

a)

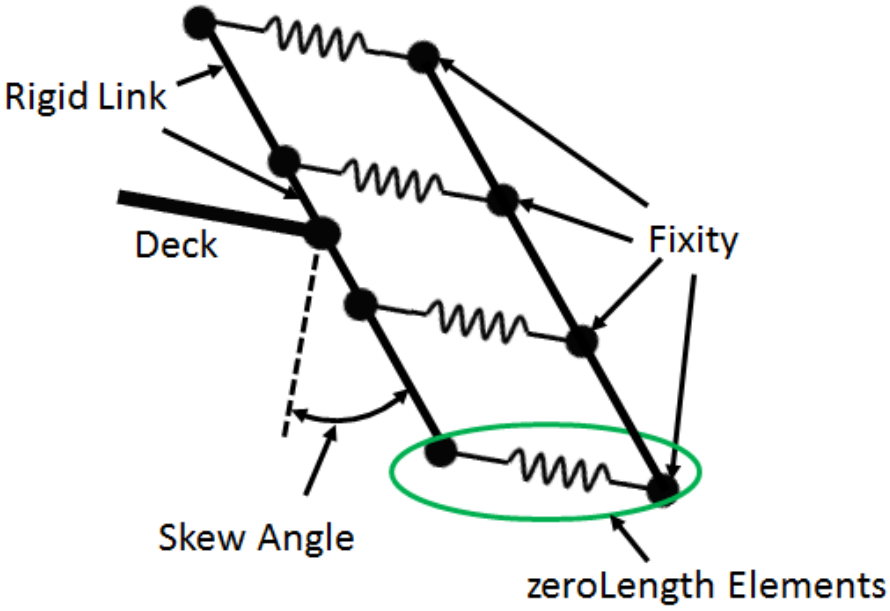

b)

Fig. 76. Longitudinal components of the Elastic Abutment Model in a curved bridge: a) left abutment; b) right abutment

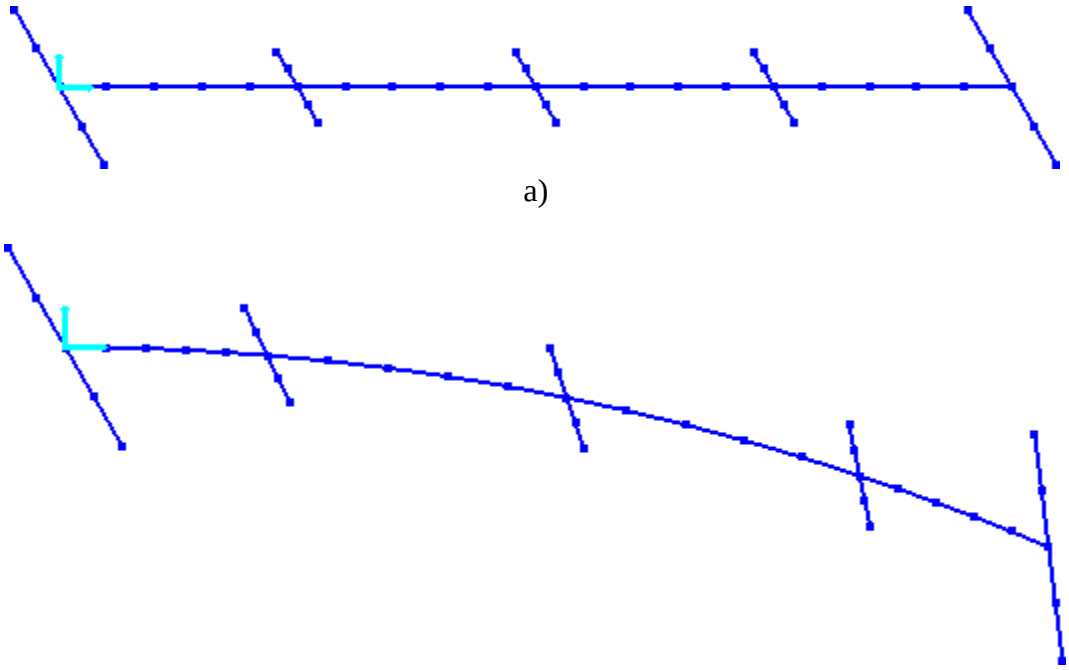

a)

b)

Fig. 77. Bridge model with multiple distributed springs and a positive skew angle: a) straight bridge; b) curved bridge

4.2 Roller Abutment Model

The Roller Abutment Model (Fig. 78) consists of rollers in the transverse and longitudinal directions, and a simple boundary condition module that applies single-point constraints against displacement in the vertical direction (i.e., bridge and abutment are rigidly connected in the vertical direction). These vertical restraints also provide a boundary that prevents rotation of the deck about its axis (torsion).

This model can be used to provide a lower-bound estimate of the longitudinal and transverse resistance of the bridge that may be displayed through a pushover analysis.

To choose the Roller Abutment Model, select **Roller** for the Model Type in Fig. 72 (and Fig. 79).

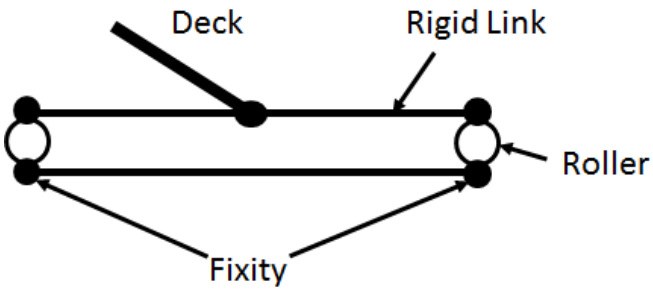

Fig. 78. General scheme of the Roller Abutment Model

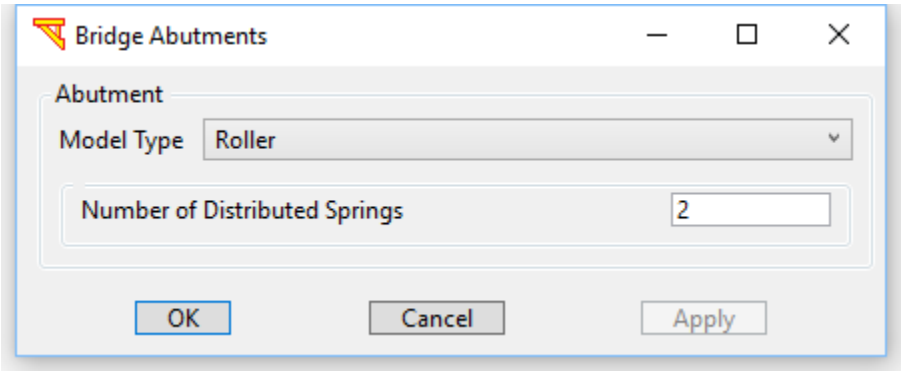

Fig. 79. Selection of the Roller Abutment Model

4.3 SDC 2004 Abutment Model

SDC 2004 Abutment Model was developed based on the Spring Abutment Model by Mackie and Stojadinovic (2006). This model includes sophisticated longitudinal, transverse, and vertical nonlinear abutment response. Detailed responses of the abutment model in the longitudinal, transverse, and vertical directions are described below.

4.3.1 Longitudinal Response

The longitudinal response is based on the system response of the elastomeric bearing pads, gap, abutment back wall, abutment piles, and soil backfill material. Prior to impact or gap closure, the superstructure forces are transmitted through the elastomeric bearing pads to the stem wall, and subsequently to the piles and backfill, in a series system. After gap closure, the superstructure bears directly on the abutment back wall and mobilizes the full passive backfill pressure. The detailed scheme of the longitudinal response is shown in Fig. 80a. The typical response of a bearing pad is shown in Fig. 80b. And the typical overall behavior is illustrated in Fig. 80c. The yield displacement of the bearings is assumed to be at 150% of the shear strain. The longitudinal backfill, back wall, and pile system response are accounted for by a series of zero-length elements between rigid element 2 and the fixity (Fig. 80a). The initial abutment stiffness (Kabt) and ultimate

passive pressure (Pabt) are obtained from equations 7.43 and 7.44 of SDC 2004. Fig. 81 shows the directions of zeroLength elements for a curved bridge with a skew angle.

Each bearing pad has a default height (h) of 0.0508 m (2 in) which can be modified by users and a side length (square) of 0.508 m (20 in). The properties of a bearing pad are listed in Table 4.

The abutment is assumed to have a nominal mass proportional to the superstructure dead load at the abutment, including a contribution from structural concrete as well as the participating soil mass. An average of the embankment lengths obtained from Zhang and Makris (2002) and Werner (1994) is included in the calculation of the participating mass due to the embankment of the abutment. The user can modify the lumped mass through the soil mass. For design purposes, this lumped mass can be ignored and set to be zero.

Table 4. Geometric and Material Properties of a Bearing Pad

Shear Modulus G	1034.2 kPa (0.15 ksi)
Young's Modulus E	34473.8 kPa (5 ksi)
Yield Displacement	150% shear strain
Lateral Stiffness	$\frac{GA}{h}$ (where A is the cross-section area, and h is the height)
Longitudinal gap	4 in
hardening ratio	1%
Vertical Stiffness	$\frac{EA}{h}$
Vertical Tearing Stress	15513.2 kPa (2.25 ksi)
Longitudinal gap	2 in

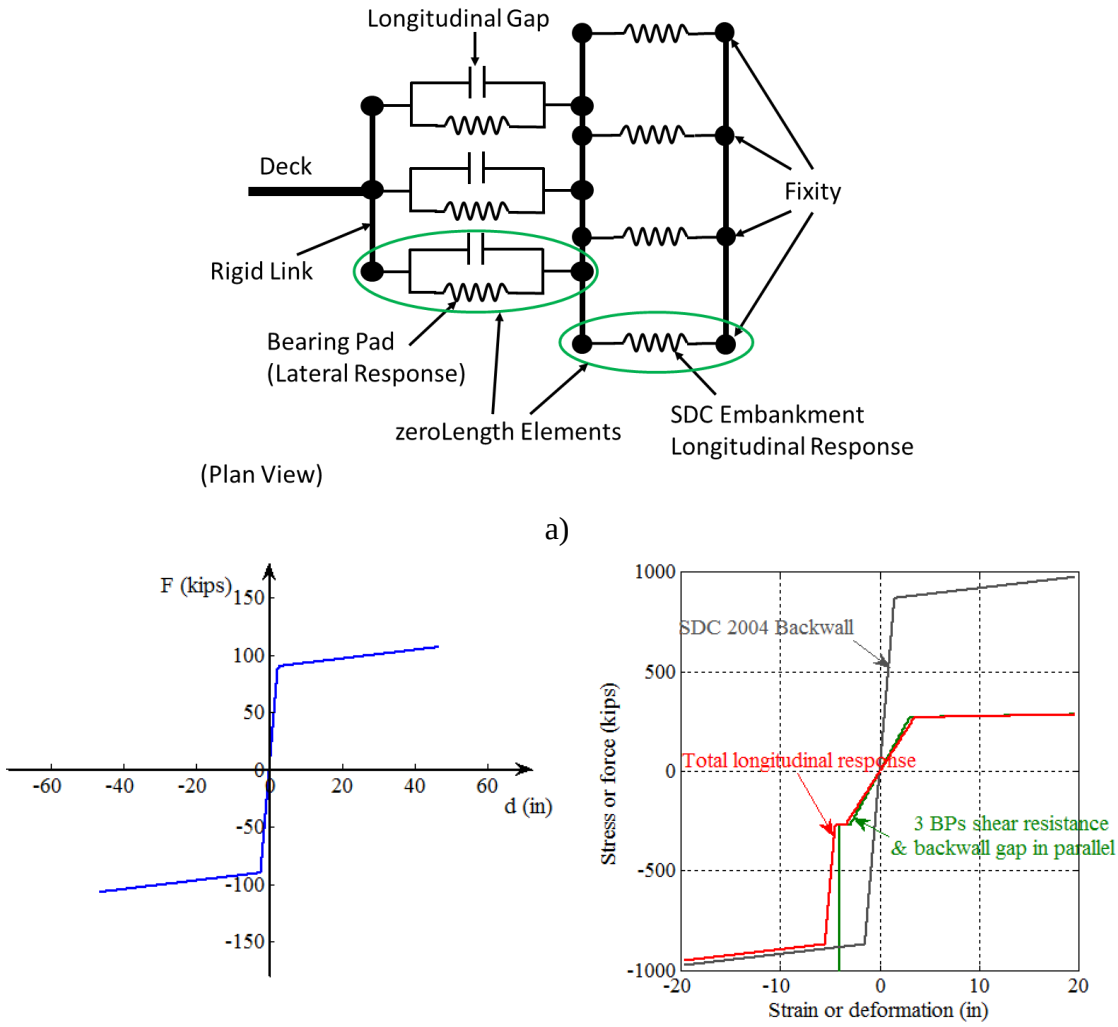

Fig. 80. Longitudinal response of the SDC 2004 Abutment Model: a) general scheme; b) longitudinal response of a bearing pad; c) total longitudinal response

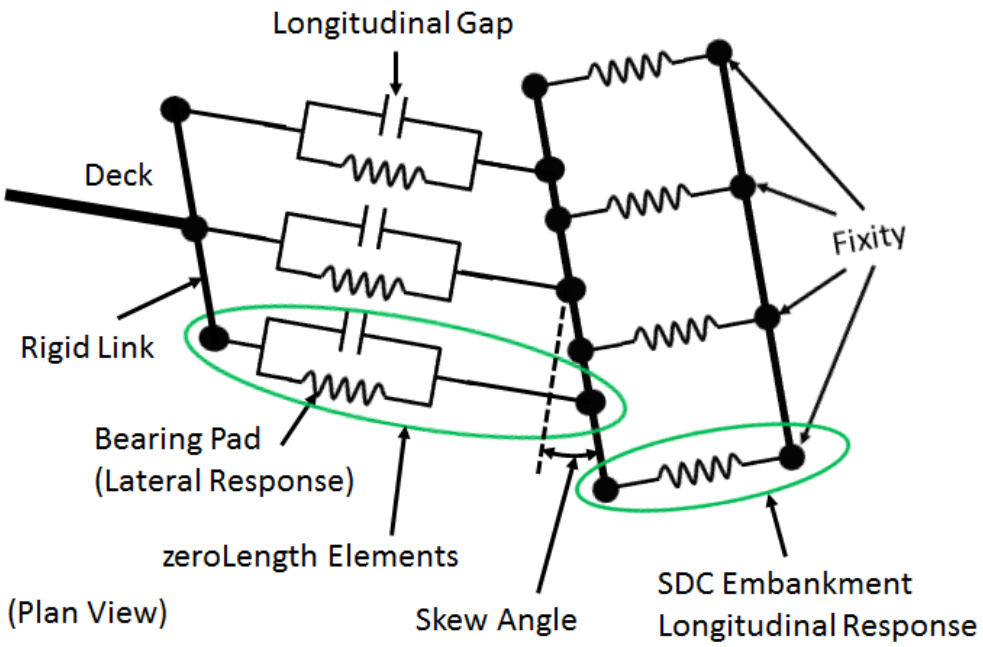

Fig. 81. Longitudinal response of the SDC 2004 Abutment Model for a curved bridge with a (positive) skew angle

4.3.2 Transverse Response

The transverse response is based on the system response of the elastomeric bearing pads, exterior concrete shear keys, abutment piles, wing walls, and backfill material. The bearing pad model discussed above is used with uncoupled behavior for the longitudinal direction. The constitutive model of the exterior shear keys is derived from experimental tests (Megally et al. 2003). Properties (yield and ultimate stresses) of shear keys depend on the ultimate capacity of the bridge which is defined as 30 percent of the dead load at abutment.

The detailed scheme of the transverse response is shown in Fig. 82a. The typical response of a bearing pad and a shear key is shown in Fig. 82b. And the typical overall behavior of the transverse response is illustrated in Fig. 82c. The superstructure forces are transmitted through the parallel system of bearing pads and shear keys (T_1) to the embankment (T_2) in series. The ultimate shear key strength is assumed to be 30% of the superstructure dead load, according to equation 7.47 of SDC 2004. A hysteretic material with trilinear response backbone curve is used with two hardening and one softening stiffness values. The initial stiffness is a series-system stiffness of the shear and flexural response of a concrete cantilever with shear key dimensions (16849 ksi). The hardening and softening branches are assumed to have magnitudes of 2.5% of the initial stiffness. The transverse stiffness and strength of the backfill, wing wall and pile system is calculated using a modification of the SDC procedure for the longitudinal direction.

Wingwall effectiveness (CL) and participation coefficients (CW) of 2/3 and 4/3 are used, according to Maroney and Chai (1994). The abutment stiffness (Kabt) and back wall strength (Pbw) obtained for the longitudinal direction from Section 7.8 of SDC 2004 are modified using the above coefficients. The wing wall length can be assumed 1/2–1/3 of the back wall length. The bearing pads and shear keys are assumed to act in parallel. Combined bearing pad- shear key system acts in series with the transverse abutment stiffness and strength.

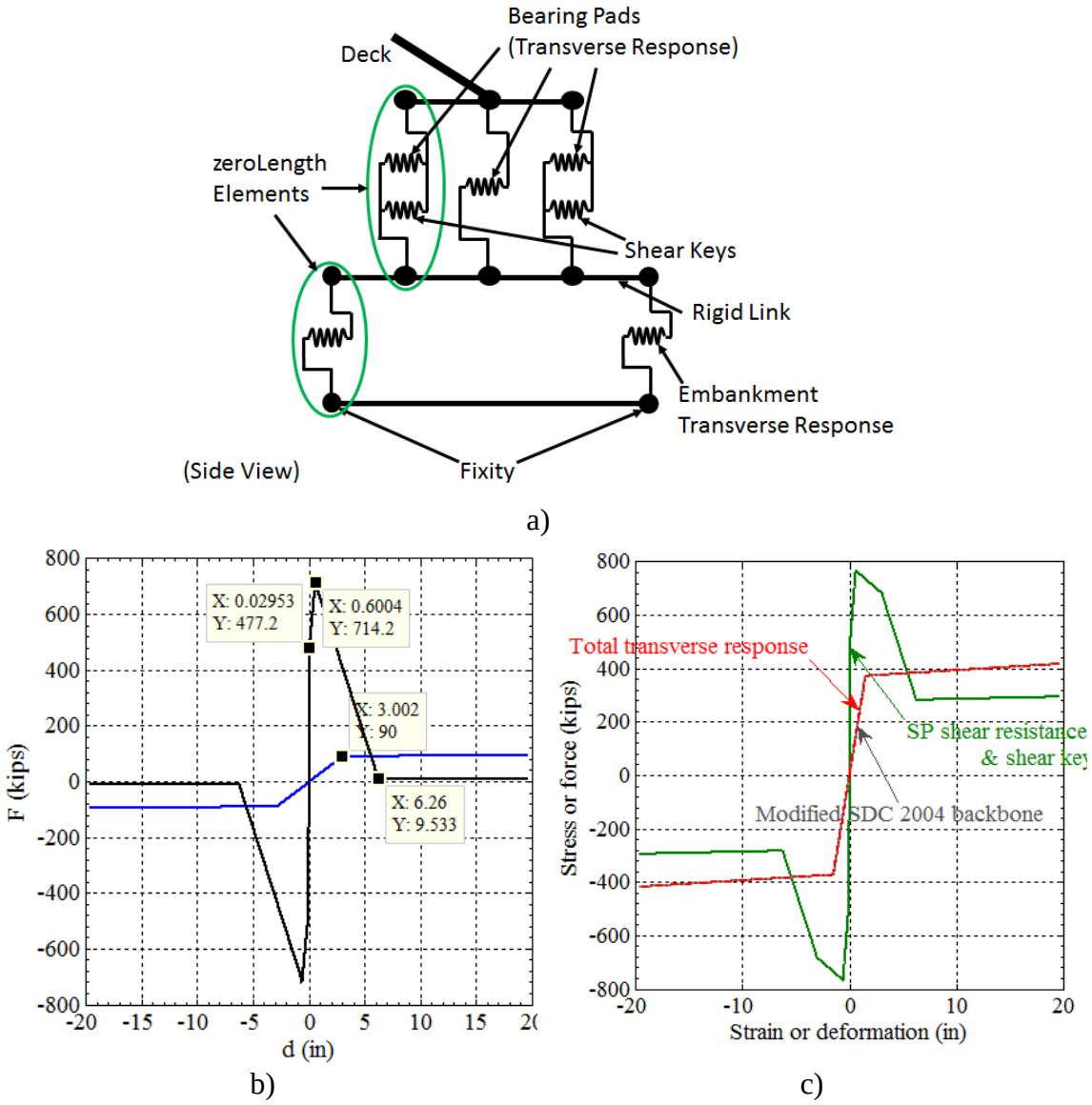

Fig. 82. Transverse response of the SDC 2004 Abutment Model: a) general scheme; b) response of a bearing pad and shear keys (curve with a higher peak value is the shear key response); c) total transverse response

4.3.3 Vertical Response

The vertical response of the abutment model includes the vertical stiffness of the bearing pads in series with the vertical stiffness of the trapezoidal. The detailed scheme of the vertical response is shown in Fig. 83a. The typical vertical response of a bearing pad is shown in Fig. 83b. And the typical overall behavior of the vertical response is illustrated in Fig. 83c.

A vertical gap (2-inch by default, which can be modified by the user) is employed for the vertical property of the bearing pads. The embankment stiffness per unit length was obtained from Zhang and Makris (2000) and modified using the critical length to obtain a lumped stiffness.

In the vertical direction, an elastic spring is defined at each end of the rigid link, with a stiffness corresponding to the vertical stiffness of the embankment soil mass. The embankment is assumed to have a trapezoidal shape and based on the effective length formulas from Zhang and Makris (2002), the vertical stiffness (K_v, unit: 1/m) can be calculated from (Zhang and Makris 2002):

$$K_v = \frac{E_s d_w}{z_0 \ln\left(\frac{z_0 + H}{z_0}\right)} L_c \qquad (3)$$

Where H is the embankment height, d_w is the deck width, $z_0 = 0.5 d_w S$, S is the embankment slope (parameter in window, see Fig. 20), $E_{sl} = 2.8G$, $G = \rho V_s^2$, ρ and V_s are the mass density and the shear wave velocity of the embankment soil, respectively.

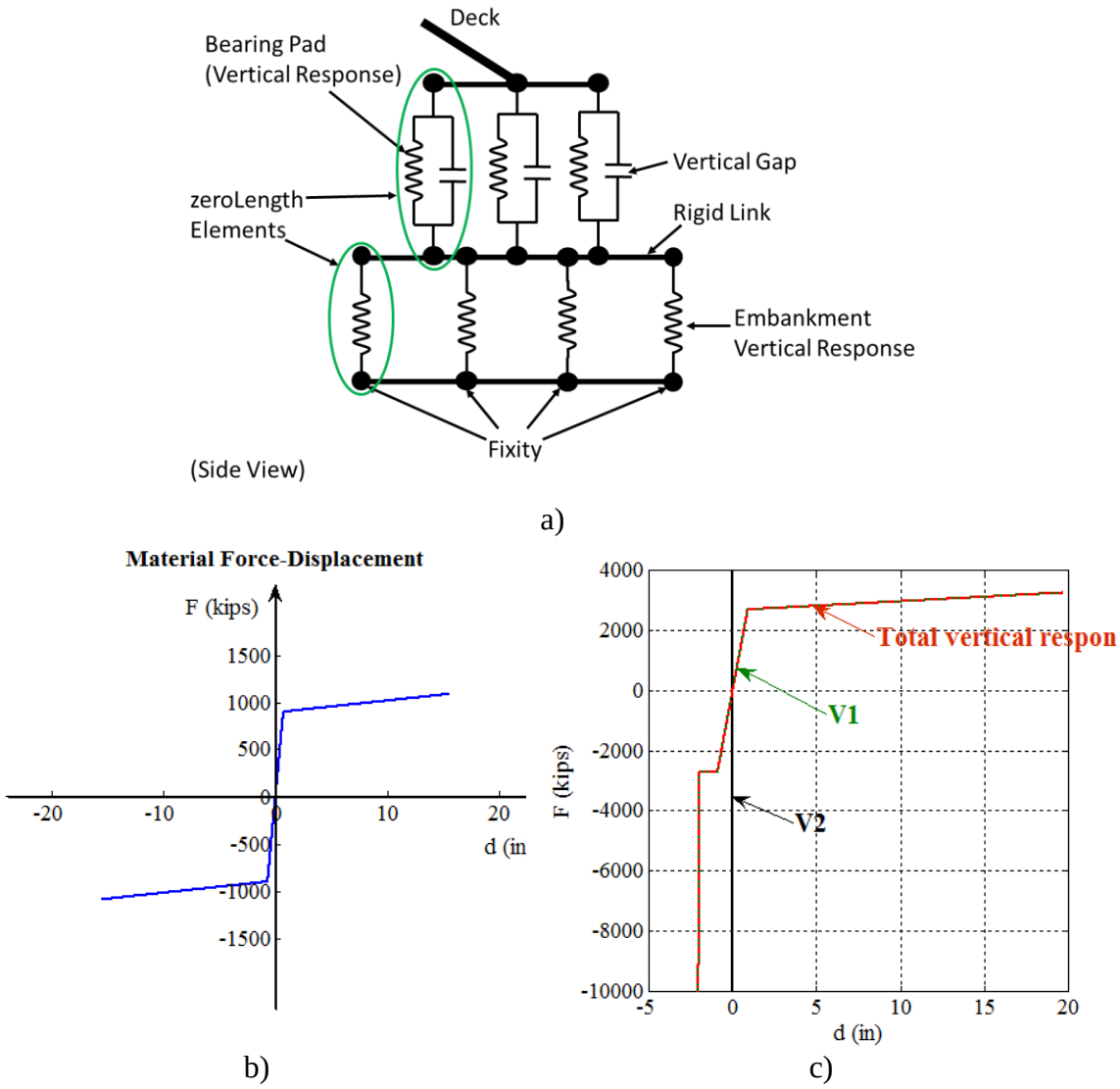

Fig. 83. Vertical response of the SDC 2004 Abutment Model: a) general scheme; b) vertical response of a bearing pad; c) total vertical response

4.3.4 Definition of the SDC 2004 Abutment Model

To define an SDC 2004 Abutment Model, please follow the steps shown in Fig. 84 and Fig. 85. To define an SDC 2004 Abutment Model, select **SDC 2004** for the abutment model type in Fig. 72.

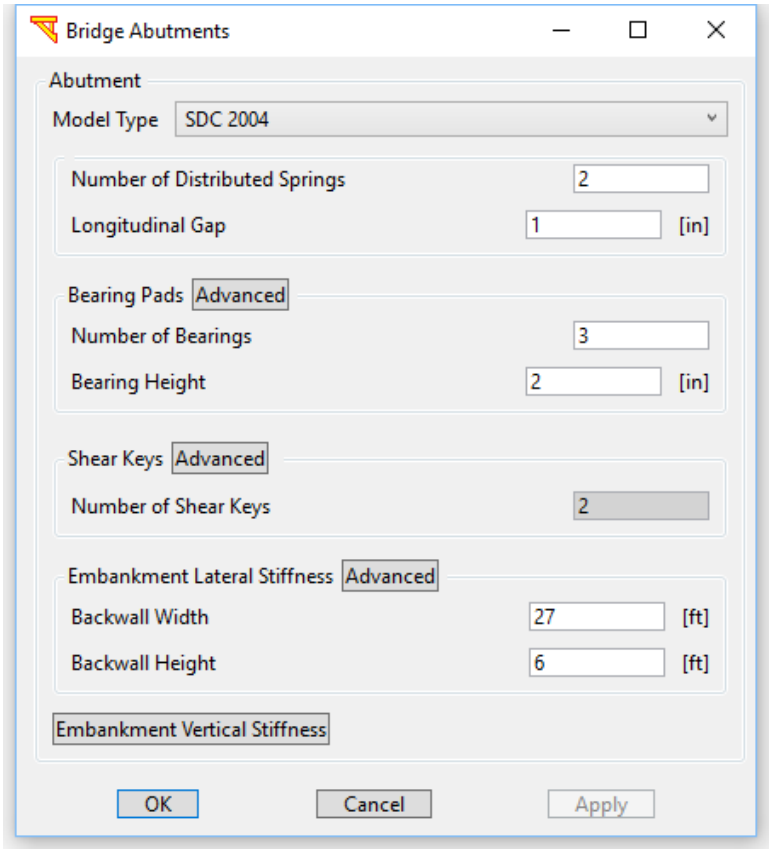

a)

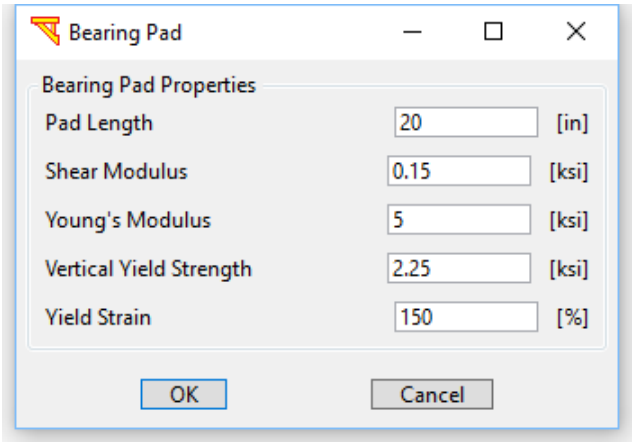

b)

Fig. 84. Definition of the SDC 2004 Abutment Model: a) main parameters; b) bearing pad properties

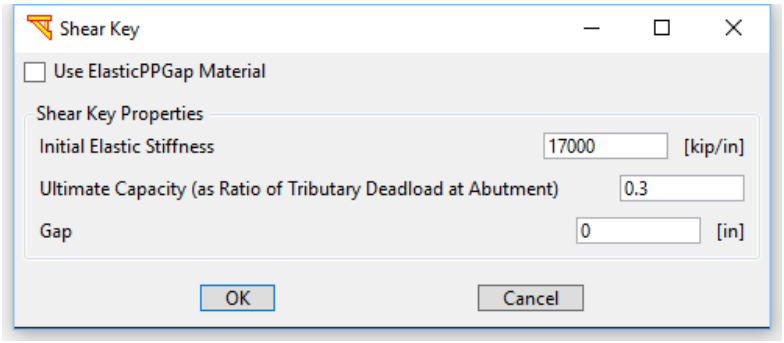

a)

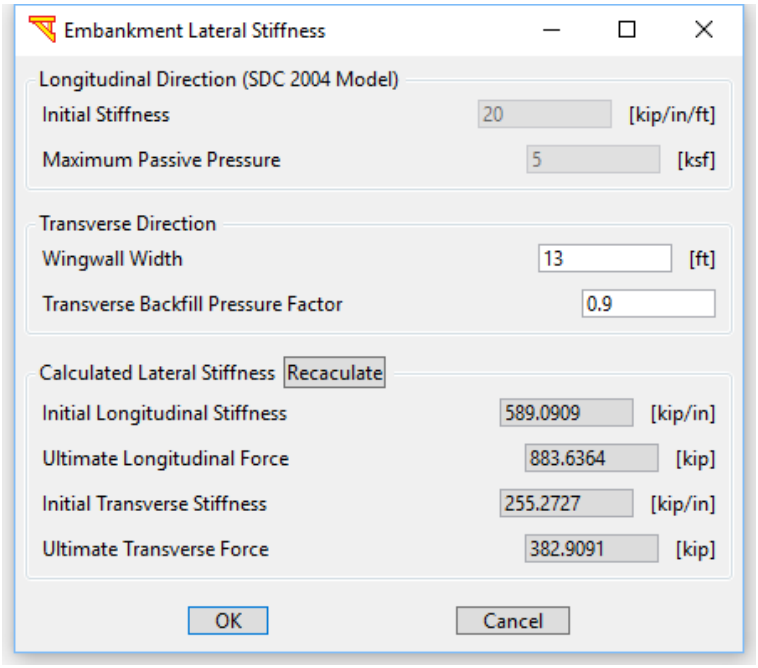

b)

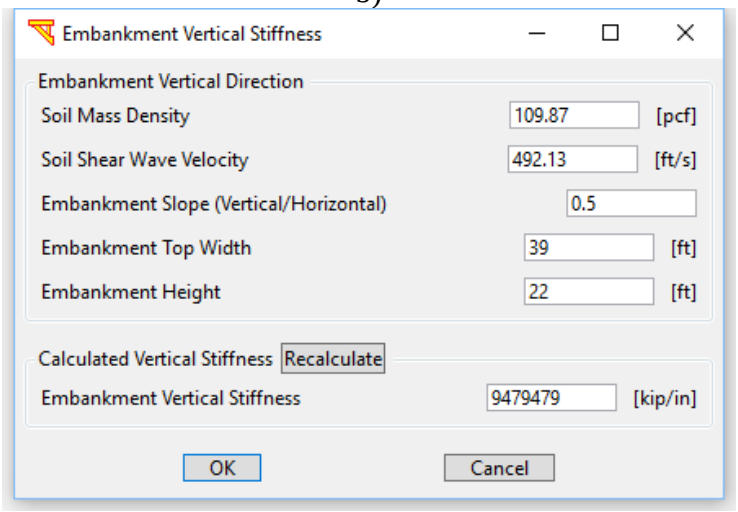

c)

Fig. 85. Definition of the SDC 2004 Abutment Model: a) shear key properties; b) SDC abutment properties; c) embankment properties

4.4 SDC 2010 Sand Abutment Model

This model is similar to the SDC 2004 abutment model but employs the parameters of the most recent SDC 2010 for a sand backfill Embankment (Fig. 86). To define an SDC 2010 Sand Abutment Model, select **SDC 2010 Sand** for the abutment model type in Fig. 72. Table 5 shows the initial stiffness and the maximum passive pressure employed for the SDC 2010 Sand Abutment Model, compared to other similar abutment models including SDC 2004, SDC 2010 Clay, EPP-Gap and HFD Models).

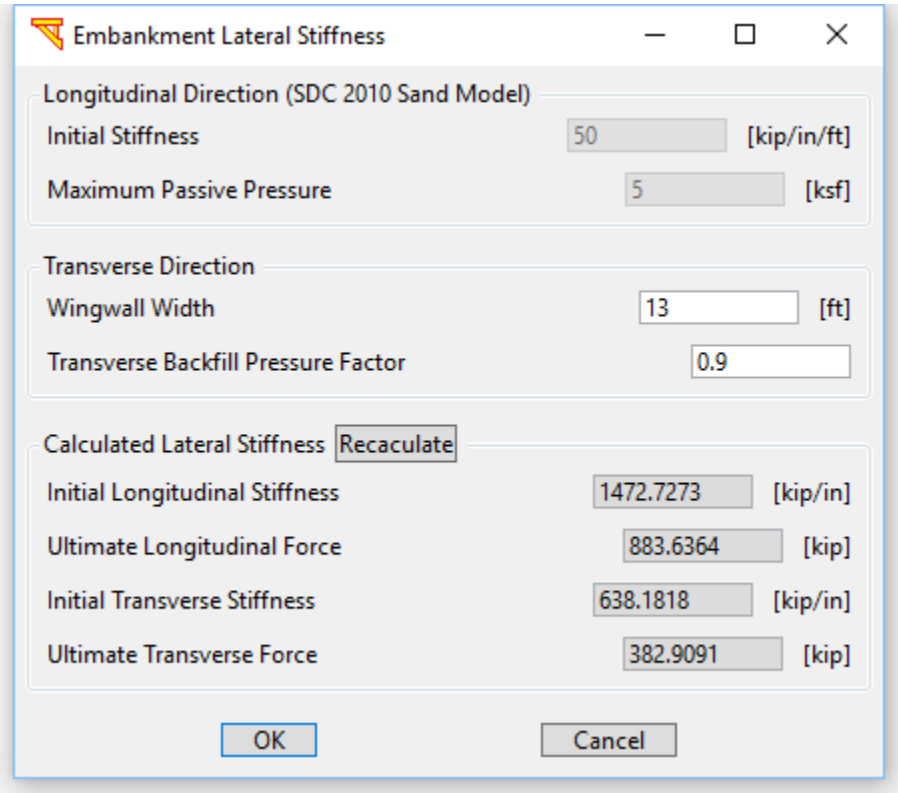

Fig. 86. Backfill horizontal properties for the SDC 2010 Sand Abutment Model

Table 5. SDC Abutment Properties

Abutment Model	Initial Stiffness (kip/in/ft)	Maximum Passive Pressure (ksf)
SDC 2004	20	5
SDC 2010 Sand	50	5
SDC 2010 Clay	25	5
EPP-Gap	User-defined	User-defined
HFD Model	*50 (sand); 25 (clay)	5.5

*Denotes average soil stiffness K50.

4.5 SDC 2010 Clay Abutment Model

This model is similar to the SDC 2004 abutment model but employs the parameters of the most recent SDC 2010 for a Clay backfill Embankment (Fig. 87). To define an SDC 2010 Clay Abutment Model, select **SDC 2010 Clay** for the abutment model type in Fig. 72. Table 5 shows the initial stiffness and the maximum passive pressure employed for the SDC 2010 Clay Abutment Model, compared to other similar abutment models.

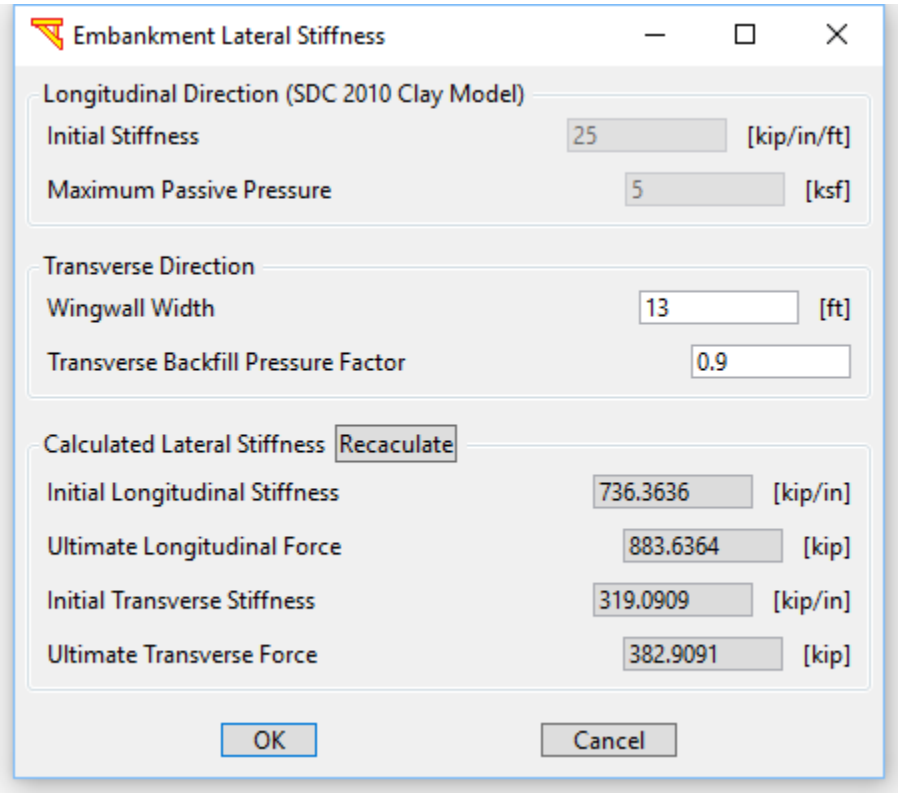

Fig. 87. Backfill horizontal properties of the SDC 2010 Clay Abutment Model

4.6 ElasticPP-Gap Model

This model is similar to the SDC 2004 Abutment Model but employs user-defined parameters for the stiffness and maximum resistance (Fig. 88). To define an EPP-Gap Abutment Model, select **EPP-Gap** for the abutment model type in Fig. 72.

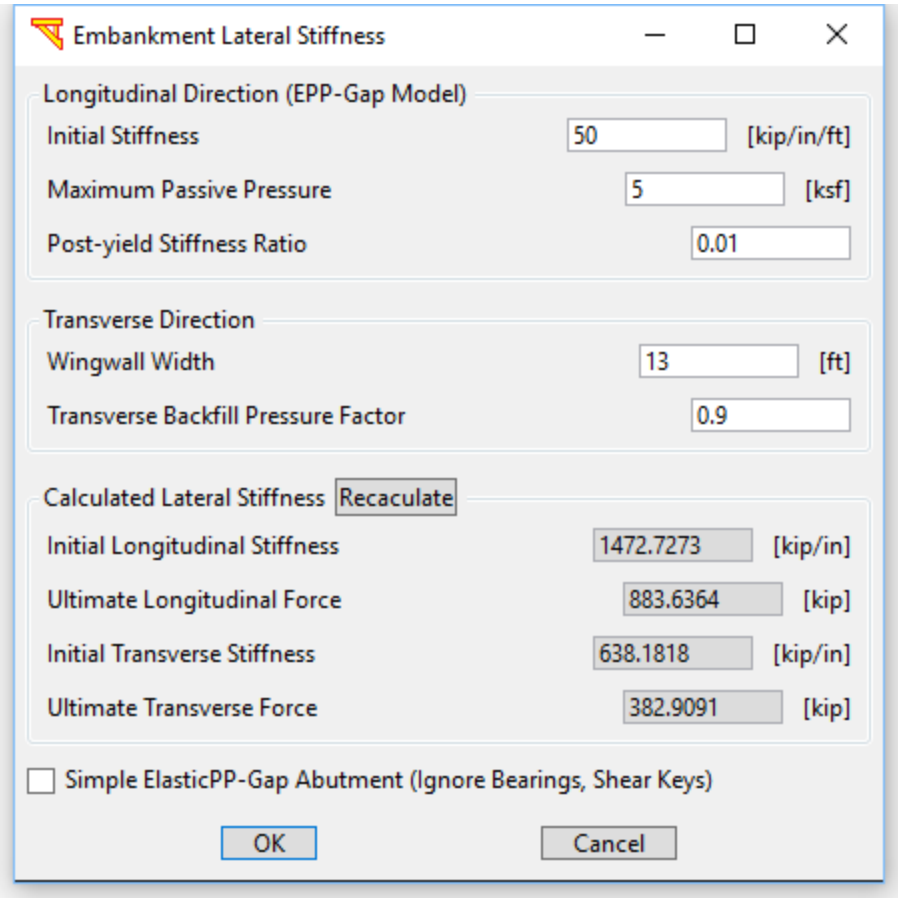

Fig. 88. Backfill horizontal properties of the EPP-Gap Abutment Model

4.7 HFD Model

As suggested by Shamsabadi et al. (2007, 2010), a Hyperbolic Force-Displacement (HFD) relationship is employed to represent abutment resistance to bridge displacement in the longitudinal direction (Fig. 89).

$$F(y) = \frac{F_{ult}(2K_{50}y_{max} - F_{ult})y}{F_{ult}y_{max} + 2(K_{50}y_{max} - F_{ult})y}$$

Where F is the resisting force, y is the longitudinal displacement, F_{ult} is the ultimate passive resistance and K_{50} is the secant stiffness at $F_{ult}/2$.

$$F(y) = \frac{\left(2K_{50} - \frac{F_{ult}}{y_{max}}\right)y}{1 + 2\left(\frac{K_{50}}{F_{ult}} - \frac{1}{y_{max}}\right)y}$$

In this HFD model, resistance appears after a user-specified gap is traversed, and the bridge thereafter gradually mobilizes the abutment's passive earth pressure strength. Herein, this strength is specified according to Shamsabadi et al. (2007, 2010) at 5.5 ksf (for a nominal 5.5 ft bridge deck height), with full resistance occurring at a passive lateral displacement of 3.6 in (the sand structural backfill scenario). Similarly, abutment resistance to the transverse bridge displacement is derived from the longitudinal hyperbolic force-displacement relationship according to the procedure outlined in Aviram et al. (2008).

To define an HFD abutment model, select **HFD Model** for the abutment model type. Click **Advanced** in **Embankment Lateral Stiffness** box to define the horizontal backfill properties (Fig. 89c). Parameters of the backfill soil are defined based on soil types (sand, clay, or User-defined), and the overall abutment stiffness/ or maximum passive pressure resist are calculated using the SDC equations.

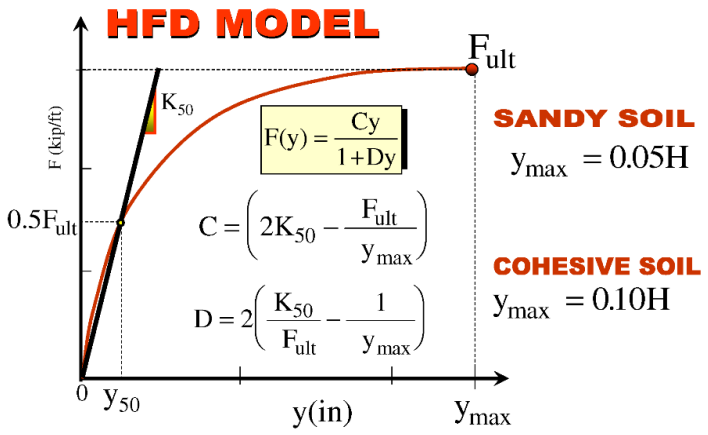

a)

Table 4. Suggested HFD Parameters for Abutment Backfills

Abutment backfill type	Pressure kPa (ksf)	Average soil stiffness kN/cm/m (K/in/ft)	Maximum displacement y_{max}/H
Granular[a]	265 (5.5)	290 (50)	0.05
Cohesive[a]	265 (5.5)	145 (25)	0.10

Note: Abutment backwall height = 1.67 m (5.5 ft).

[a]Compacted to at least 95% relative compaction per ASTM D-1557.

b)

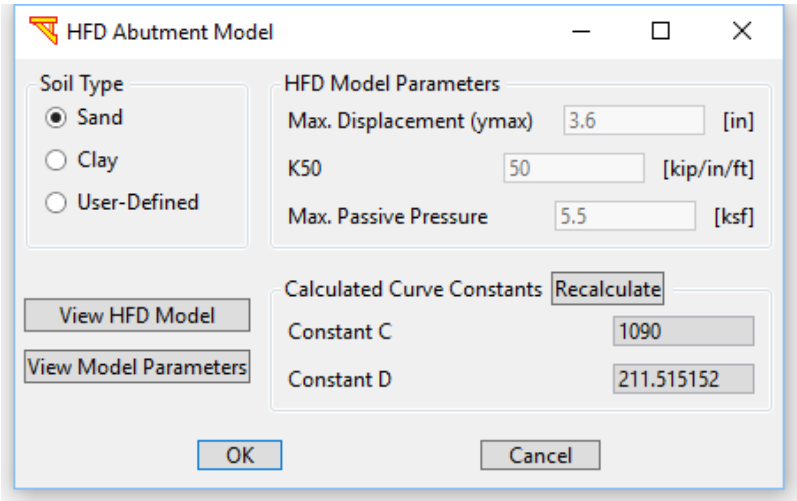

c)

Fig. 89. Definition of the HFD Abutment Model: a) HFD abutment model; and b) HFD parameters for abutment backfills suggested by Shamsabadi et al. (2007); and c) backfill properties of the HFD Model

5 COLUMN RESPONSES & BRIDGE RESONANCE

MSBridge provides features to view column lateral responses, abutment responses and bridge natural periods (Fig. 8 and Fig. 90).

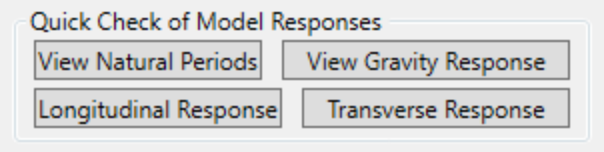

Fig. 90. Buttons to view column & abutment responses and bridge resonance

5.1 Bridge Natural Periods

Click **View Natural Periods (**Fig. 90**)** to view the natural periods and frequencies of the bridge (Fig. 91). A mode shape analysis is conducted in this case.

The user can copy and paste the values to their favorite text editor such as MS Excel (in Fig. 91, right-click and then click **Select All** (ctrl-a) to highlight, and then right-click and then click **Copy** (ctrl c) to copy to the clipboard).

5.2 Column Gravity Response

Click **View Gravity Response (**Fig. 90**)** to view the column internal forces and bending moments after application of own weight (Fig. 92).

5.3 Column & Abutment Longitudinal Responses

Click **Longitudinal Response (**Fig. 90**)** to view the column longitudinal responses (Fig. 93) and the abutment longitudinal responses (Fig. 94). A pushover up to 5% of drift ratio in the longitudinal direction is conducted in this case.

5.4 Column & Abutment Transverse Responses

Click **Transverse Response (**Fig. 90**)** to view the transverse column responses (Fig. 95) and the abutment transverse responses (Fig. 96). A pushover up to 4% of drift ratio in the transverse direction is conducted in this case.

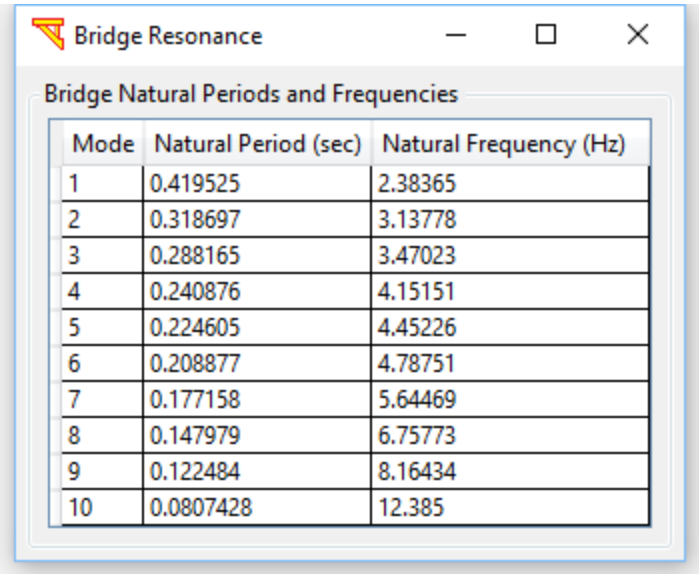

Mode	Natural Period (sec)	Natural Frequency (Hz)
1	0.419525	2.38365
2	0.318697	3.13778
3	0.288165	3.47023
4	0.240876	4.15151
5	0.224605	4.45226
6	0.208877	4.78751
7	0.177158	5.64469
8	0.147979	6.75773
9	0.122484	8.16434
10	0.0807428	12.385

Fig. 91. Natural periods and frequencies of bridge

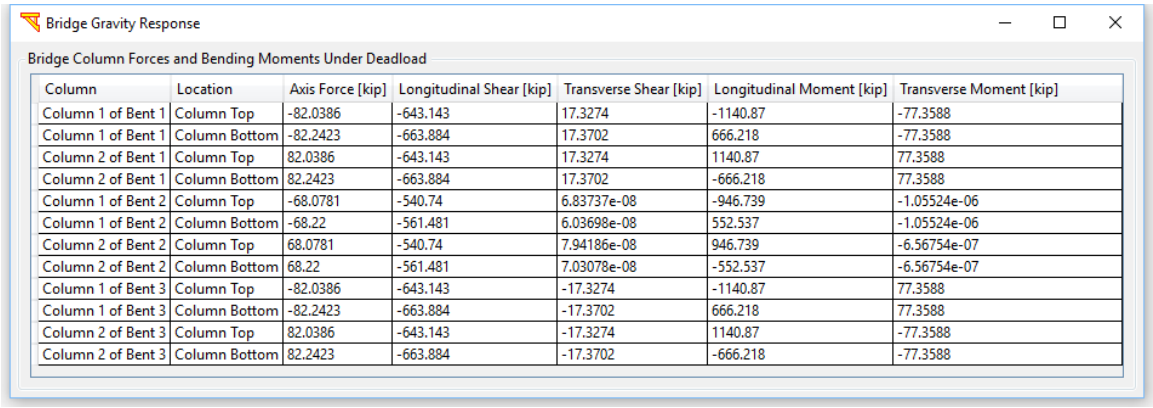

Column	Location	Axis Force [kip]	Longitudinal Shear [kip]	Transverse Shear [kip]	Longitudinal Moment [kip]	Transverse Moment [kip]
Column 1 of Bent 1	Column Top	-82.0386	-643.143	17.3274	-1140.87	-77.3588
Column 1 of Bent 1	Column Bottom	-82.2423	-663.884	17.3702	666.218	-77.3588
Column 2 of Bent 1	Column Top	82.0386	-643.143	17.3274	1140.87	77.3588
Column 2 of Bent 1	Column Bottom	82.2423	-663.884	17.3702	-666.218	77.3588
Column 1 of Bent 2	Column Top	-68.0781	-540.74	6.83737e-08	-946.739	-1.05524e-06
Column 1 of Bent 2	Column Bottom	-68.22	-561.481	6.03698e-08	552.537	-1.05524e-06
Column 2 of Bent 2	Column Top	68.0781	-540.74	7.94186e-08	946.739	-6.56754e-07
Column 2 of Bent 2	Column Bottom	68.22	-561.481	7.03078e-08	-552.537	-6.56754e-07
Column 1 of Bent 3	Column Top	-82.0386	-643.143	-17.3274	-1140.87	77.3588
Column 1 of Bent 3	Column Bottom	-82.2423	-663.884	-17.3702	666.218	77.3588
Column 2 of Bent 3	Column Top	82.0386	-643.143	-17.3274	1140.87	-77.3588
Column 2 of Bent 3	Column Bottom	82.2423	-663.884	-17.3702	-666.218	-77.3588

Fig. 92. Column internal forces and bending moments after application of own weight

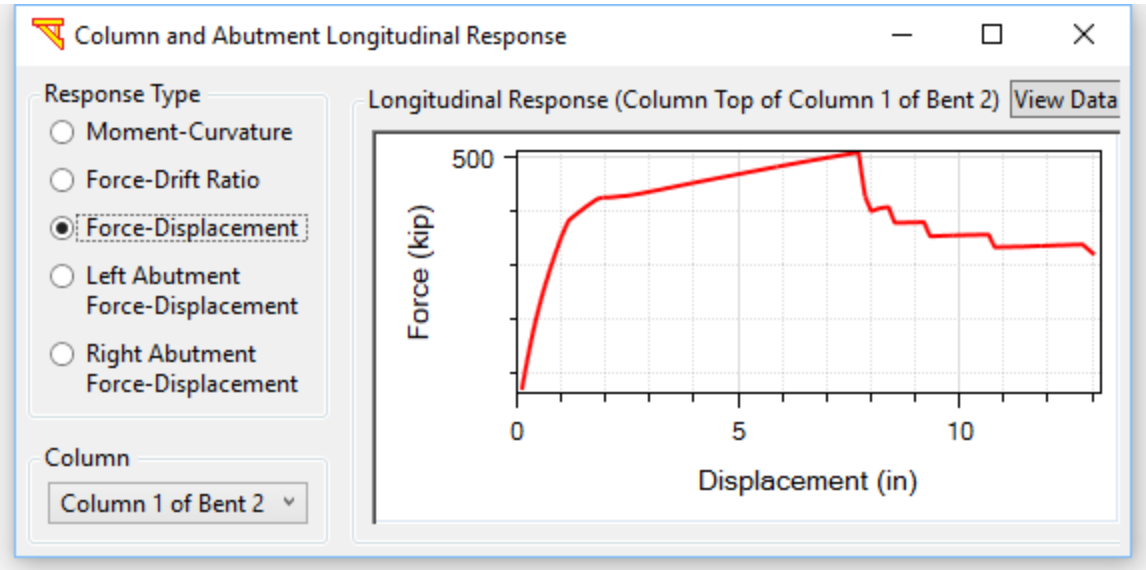

Fig. 93. Column longitudinal response

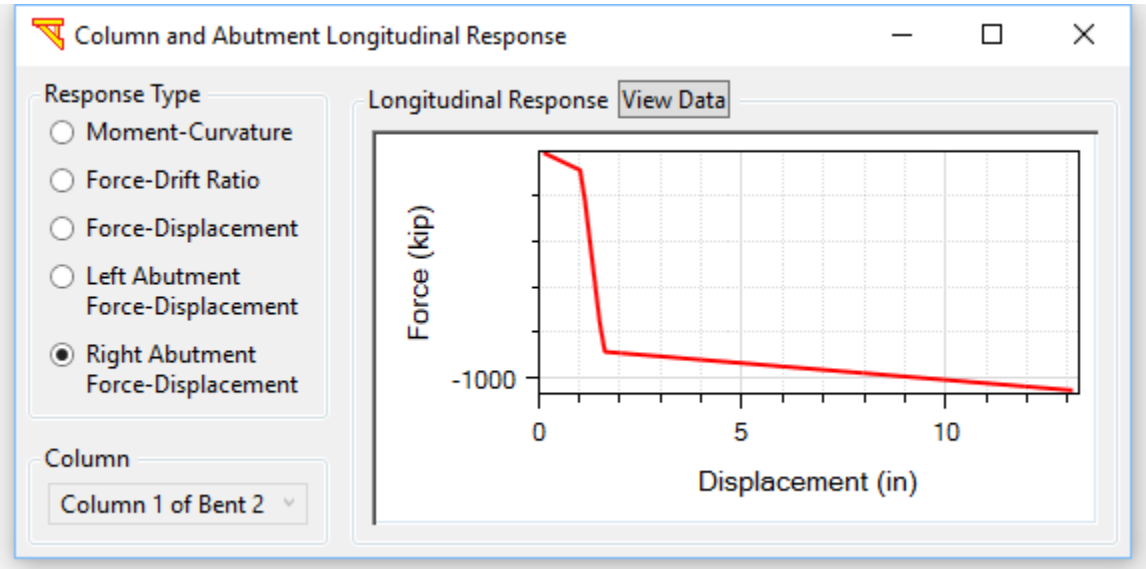

Fig. 94. Abutment longitudinal response

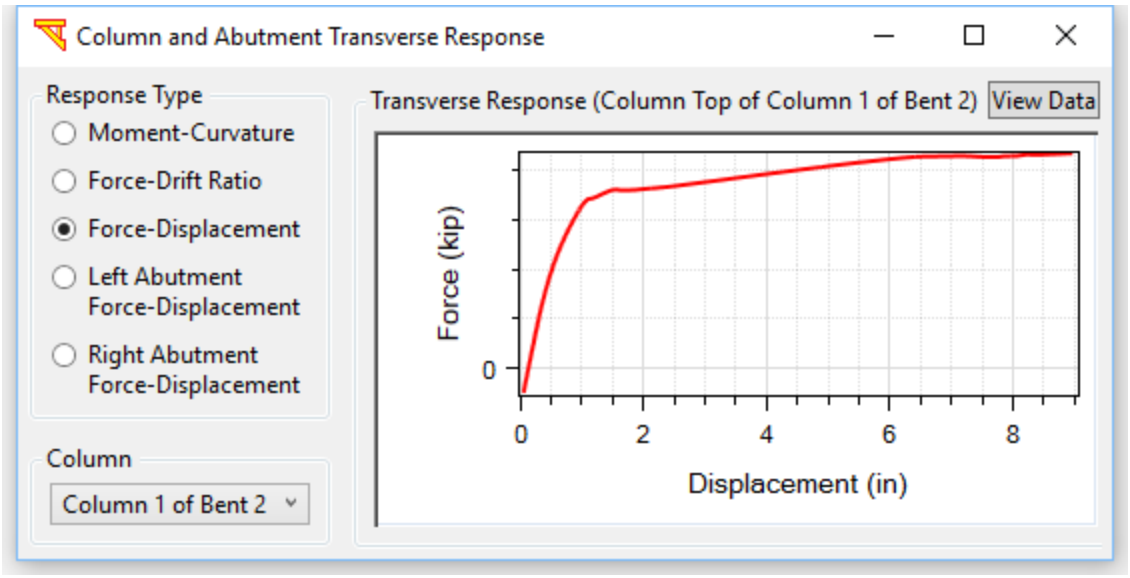

Fig. 95. Column transverse response

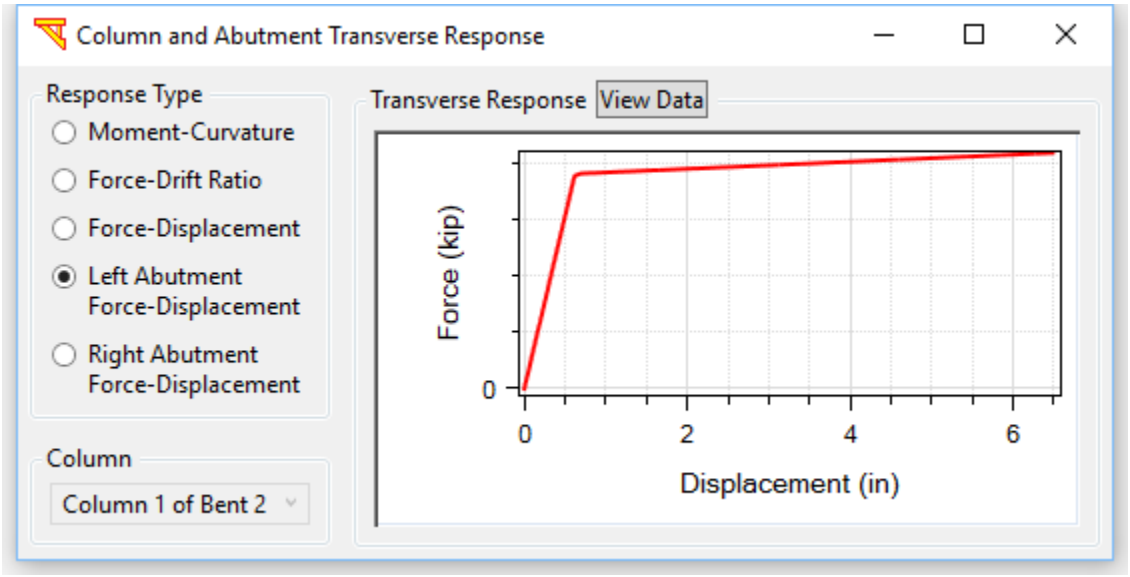

Fig. 96. Abutment transverse response

6 PUSHOVER & EIGENVALUE ANALYSES

6.1 Pushover Analysis

A load pattern must be defined to conduct a pushover analysis. As shown in Fig. 97, first, choose **Pushover** in the Analysis Options and then click **Change Pattern**. The load pattern window is shown in Fig. 98.

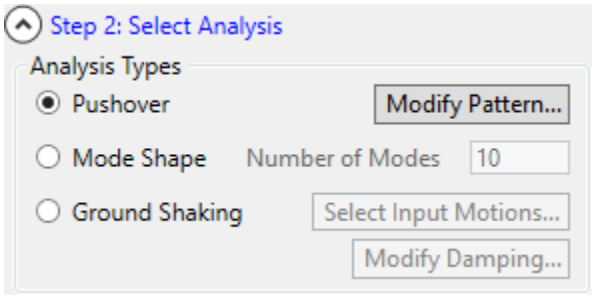

Fig. 97. Pushover analysis option

6.1.1 Input Parameters

This section presents the inputs needed to perform the pushover analysis. On this basis, three types of analysis are included as follow: i) Monotonic Pushover, ii) Cyclic Pushover, and iii) U-Push.

6.1.1.1 Monotonic Pushover

The pushover options include **Monotonic Pushover**, **Cyclic Pushover**, and **U-Push** (pushover by a user-defined loading pattern).

Two methods of pushover are available (Fig. 98): force-based and displacement-based. If **Force-Based Method** is chosen, please enter the parameters of force increment (per step): **Longitudinal (X) Force**, **Transverse (Y) Force**, **Vertical (Z) Force**, **Moment @ X**, **Moment @ Y**, and **Moment @ Z**.

If **Displacement-Based Method** is chosen, please enter the displacement increment parameters (per step): **Longitudinal Displacement**, **Transverse Displacement**, **Vertical Displacement**, **Rotation around X**, **Rotation around Y**, and **Rotation around Z**.

The pushover load/displacement linearly increases with step in a monotonic pushover mode. The pushover load/displacement is applied at the bridge deck center or the deck location at a bent.

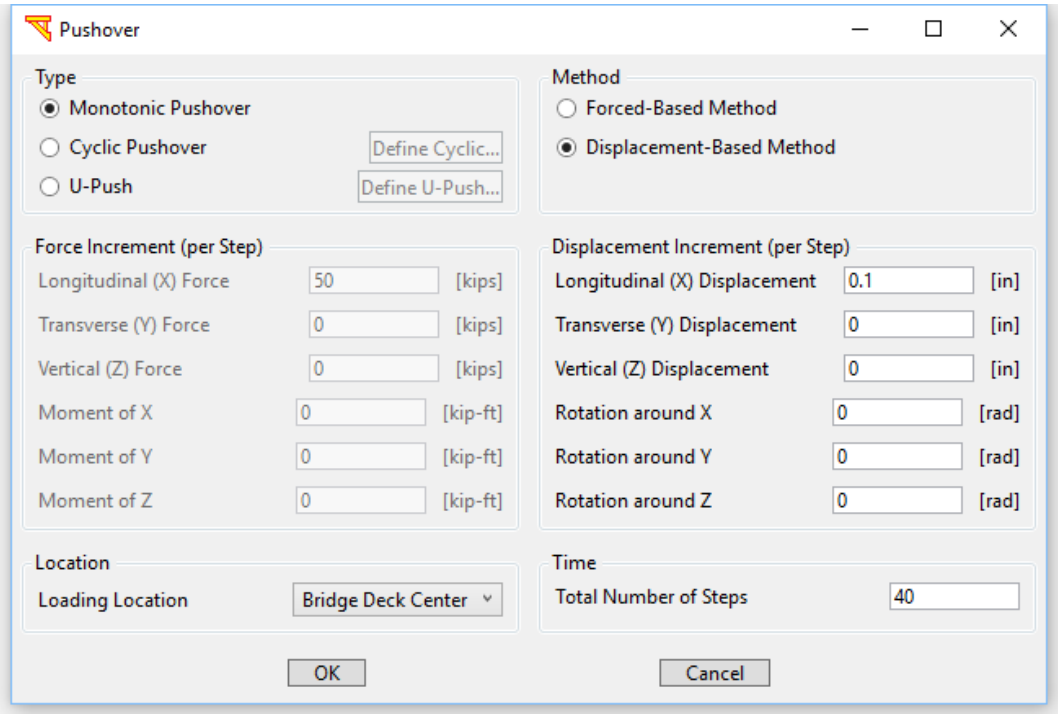

Fig. 98. Load pattern for monotonic pushover analysis

6.1.1.2 Cyclic Pushover

To conduct a Cyclic Pushover, click **Cyclic Pushover** in Fig. 98 and then define the **Number of Steps for the First Cycle** and **Step Increment per Cycle (**Fig. 99).

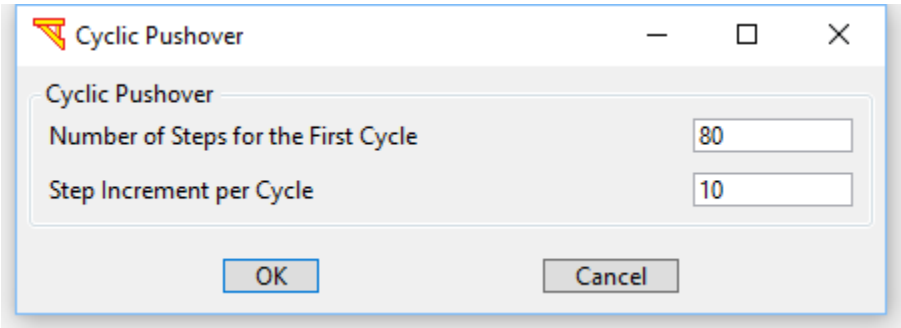

Fig. 99. Load pattern for cyclic pushover analysis

6.1.1.3 User-Defined Pushover (U-Push)

Click **U-Push** and then click **Define U-Push** to enter your load pattern (U-Push). In this case, the displacement or force parameters entered in Fig. 100 are used as the maximum values. The U-Push data entered are used as the factors (of the maximum displacement or the maximum force entered).

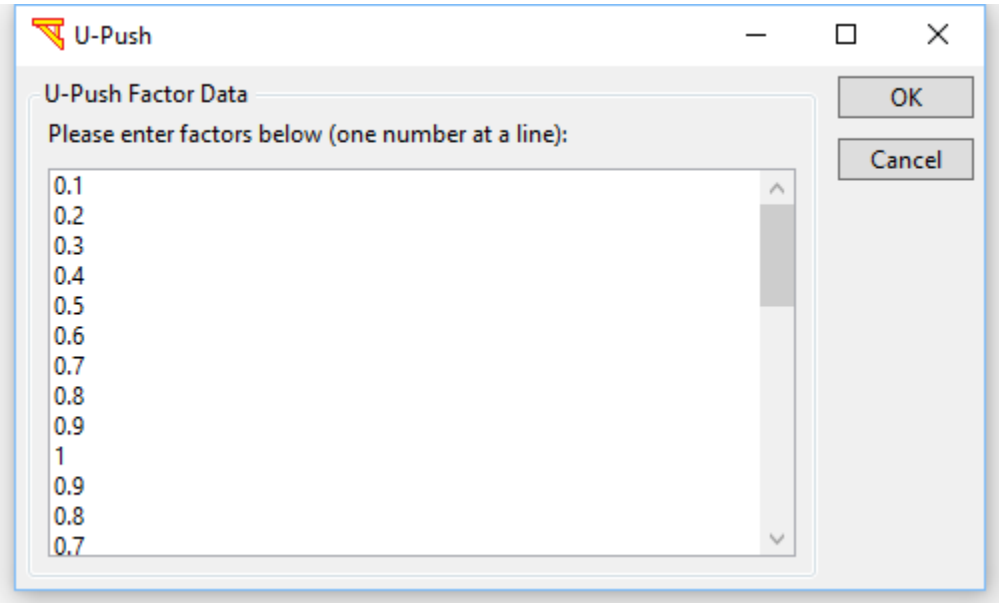

Fig. 100. User-defined pushover (U-Push)

6.1.2 Output for Pushover Analysis

Output windows for a pushover analysis include:

i) Response time histories and profiles for column (and pile shaft under grade)
ii) Response relationships (force-displacement as well as moment-curvature) for column (and pile shaft under grade)
iii) Abutment response time histories
iv) Deformed mesh, contour fill, plastic hinges, and animations.

6.1.2.1 Column Response Profiles

After performing the pushover analysis, the column response profiles can be accessed by clicking menu **Display** (Fig. 4) and then **Column Response Profiles (**Fig. 101**).**

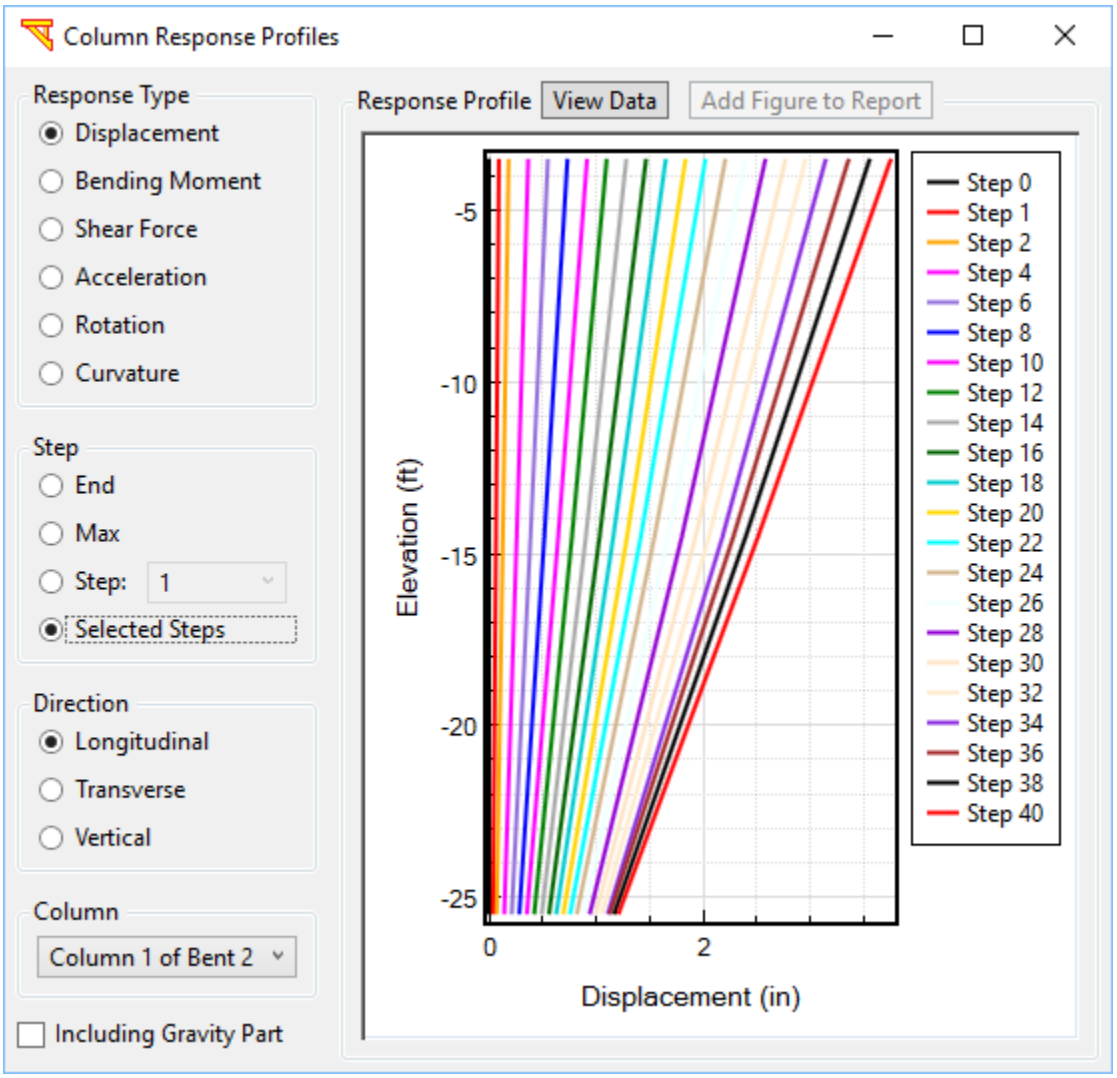

Fig. 101. Column response profiles

6.1.2.2 Column Response Time Histories

After performing the pushover analysis, the column response profiles can be accessed by clicking menu **Display** (Fig. 4) and then **Column Response Time Histories (**Fig. 102**).**

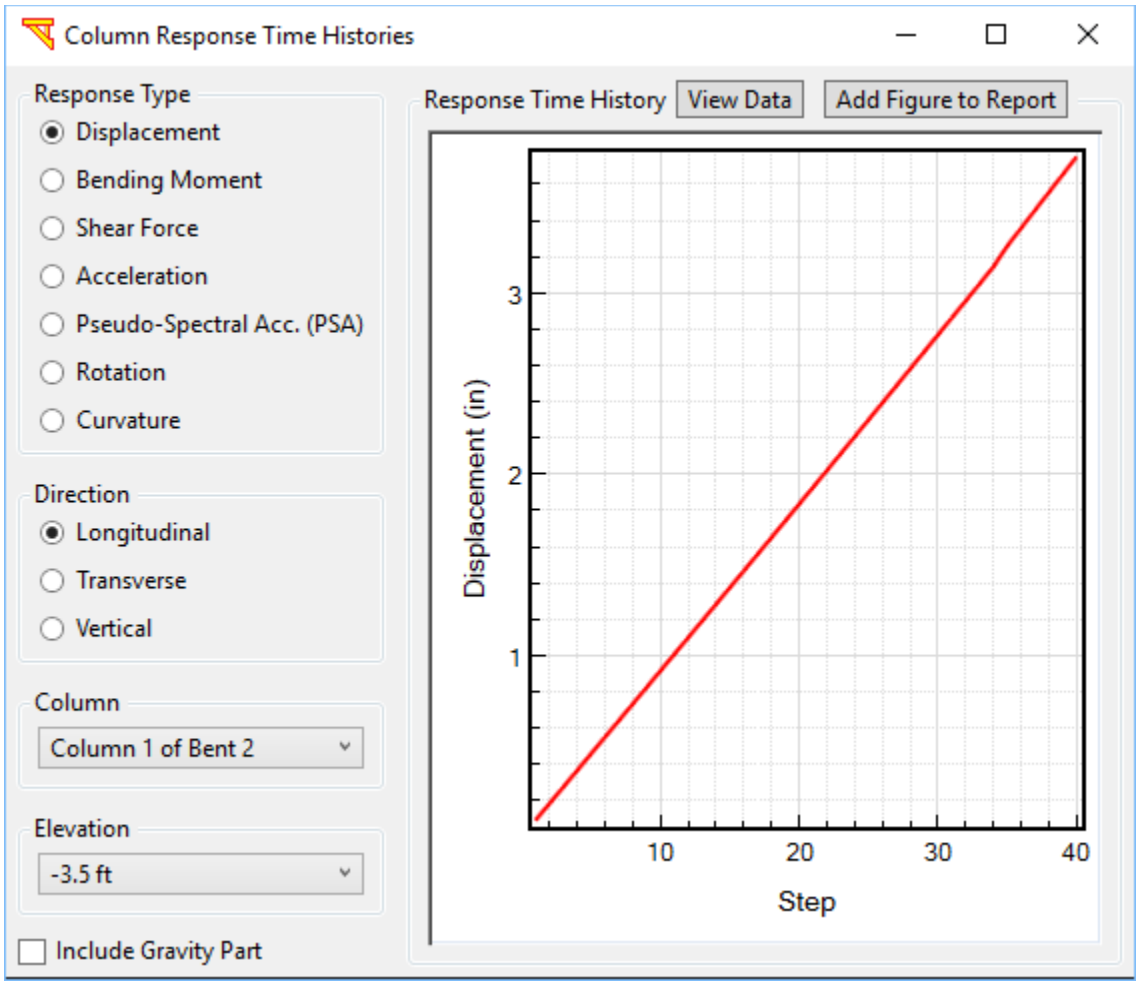

Fig. 102. Column response time histories

6.1.2.3 Column Response Relationships

After performing the pushover analysis, the column response profiles can be accessed by clicking menu **Display** (Fig. 4) and then **Column Response Relationships (**Fig. 103**).**

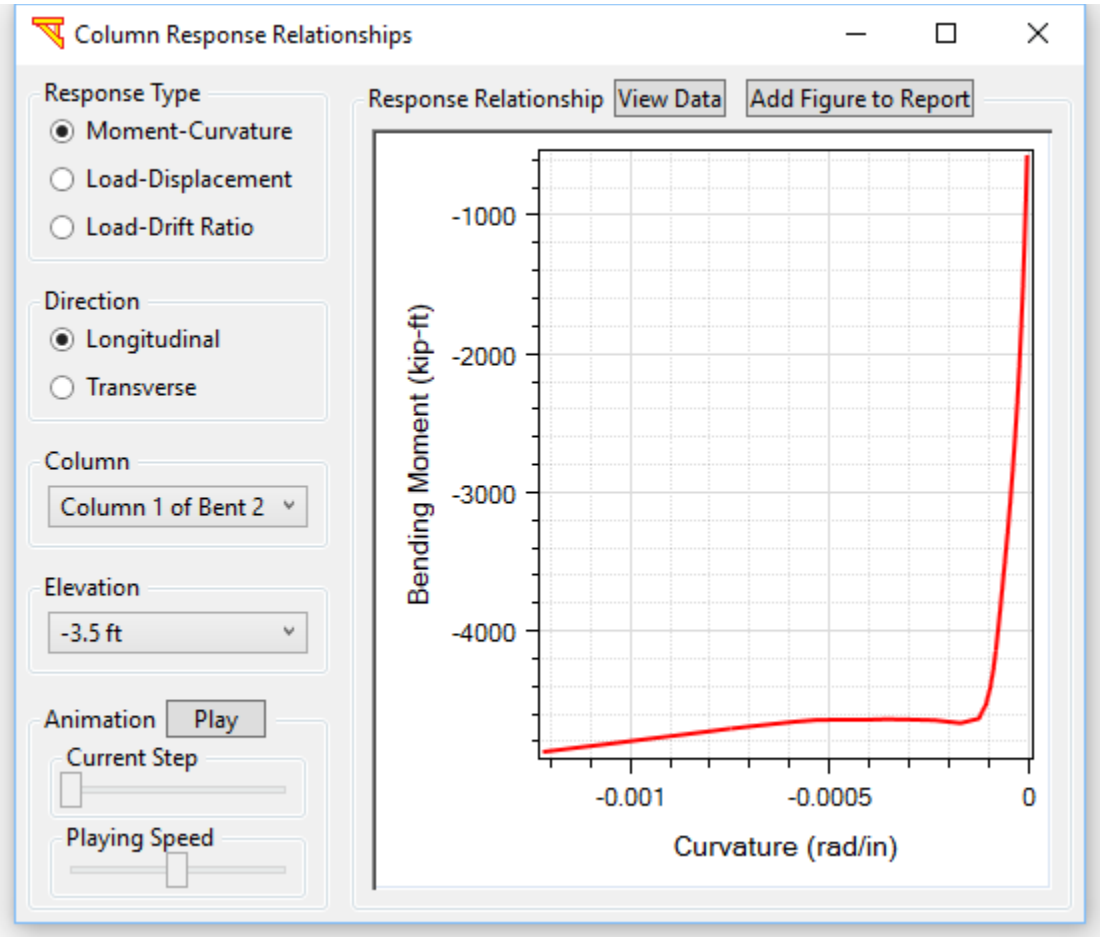

Fig. 103. Response relationships for column

6.1.2.4 Abutment Force-Displacement and Response Time Histories

After performing the pushover analysis, the column response profiles can be accessed by clicking menu **Display** (Fig. 4) and then **Abutment Response Time Histories (**Fig. 104**).**

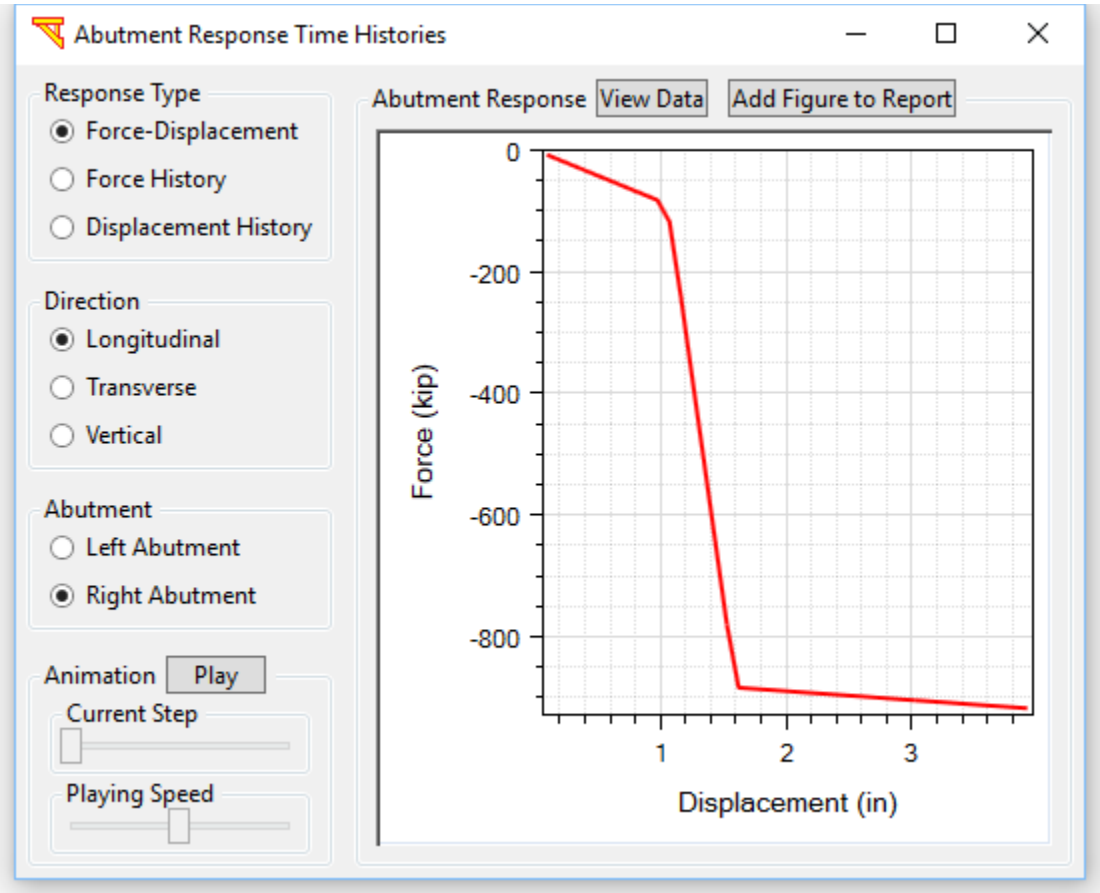

Fig. 104. Abutment response time histories

6.1.2.5 Deformed Mesh

After performing the pushover analysis, the column response profiles can be accessed by clicking menu **Display** (Fig. 4) and then **Deformed Mesh (**Fig. 105**).** The user can see the deformed mesh due to gravity or pushover for each defined step. Furthermore, the plastic hinges can be visualized as shown in Fig. 106.

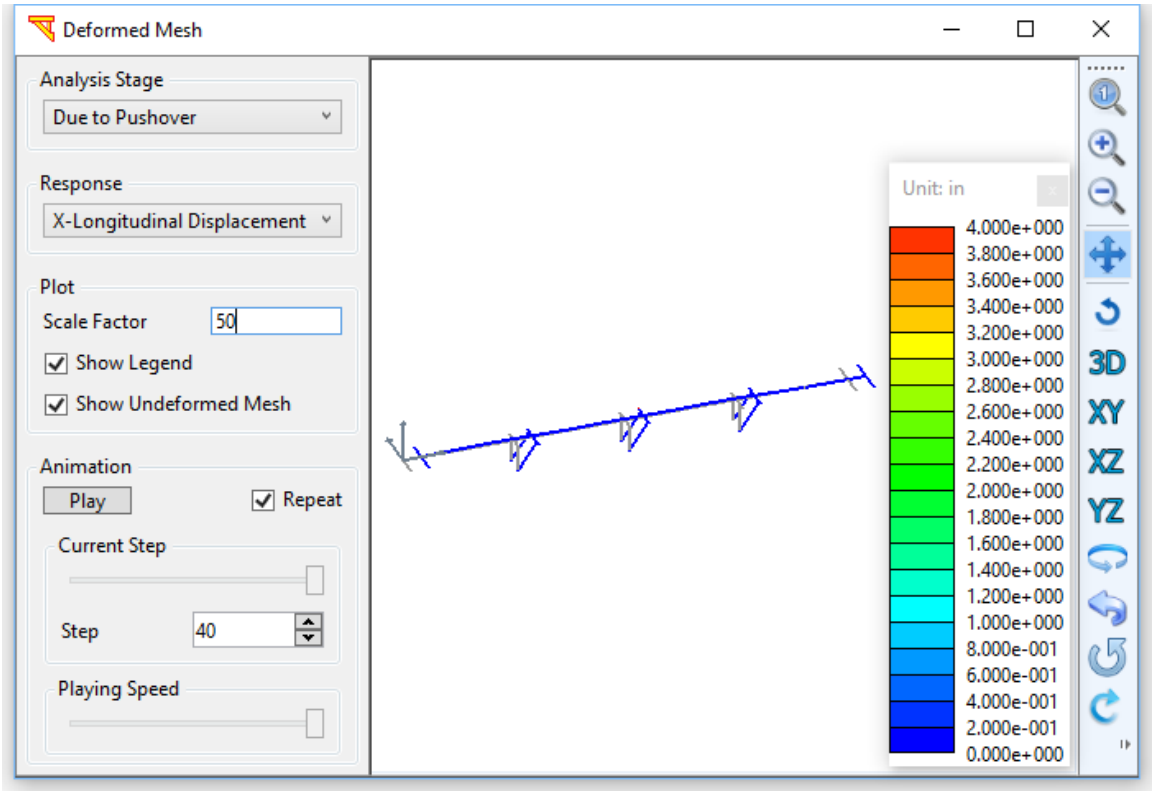

Fig. 105. Deformed mesh and contour fill

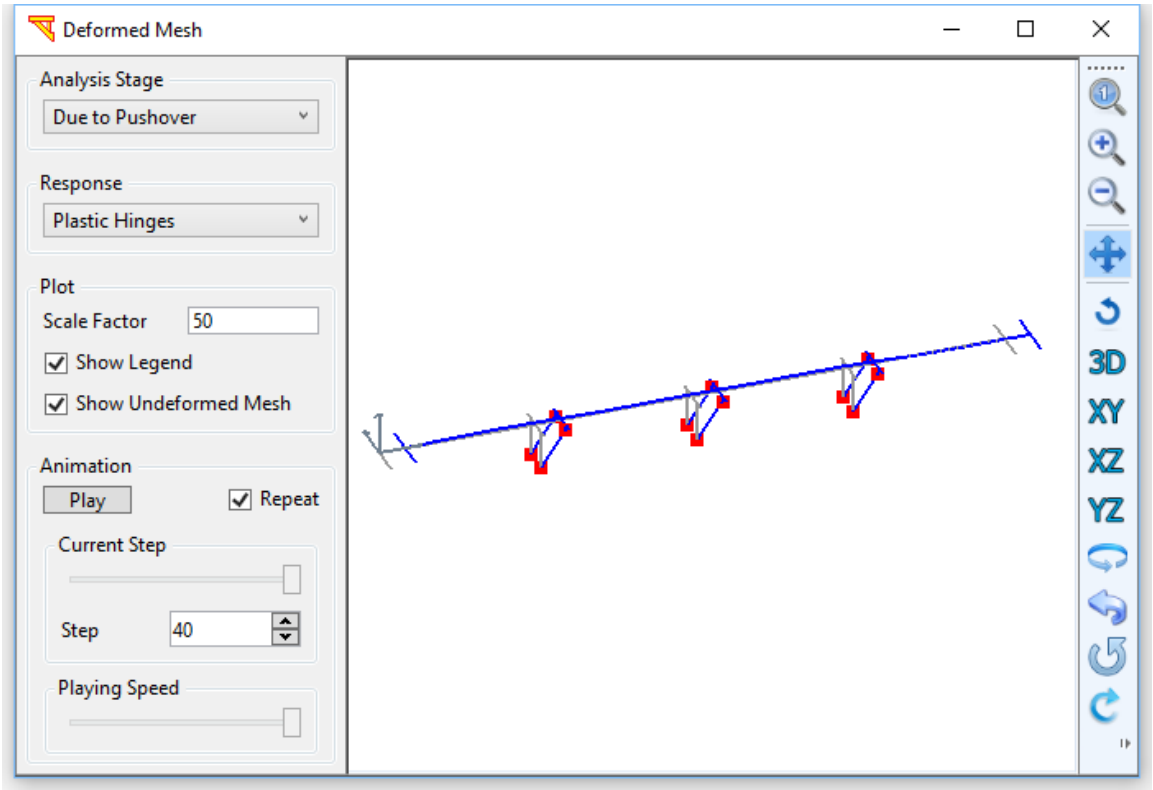

Fig. 106. Visualization of Plastic hinges (red dots represent plastic hinges developed)

6.2 Mode Shape Analysis

To conduct a mode shape analysis, please follow the steps shown in Fig. 107 and then click **Save Model & Run** Analysis. Fig. 108 shows the output window for a mode shape analysis, which can be accessed by clicking menu Display (Fig. 4) and then choosing Deformed Mesh. To switch between modes, move the slider or click the spin button to cycle through them.

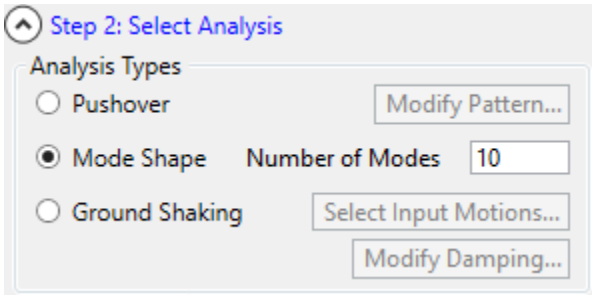

Fig. 107. Steps to perform a mode shape analysis

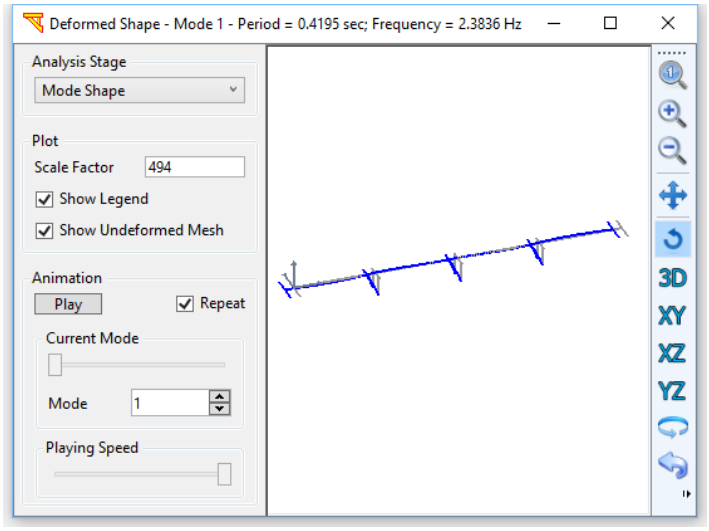

a)

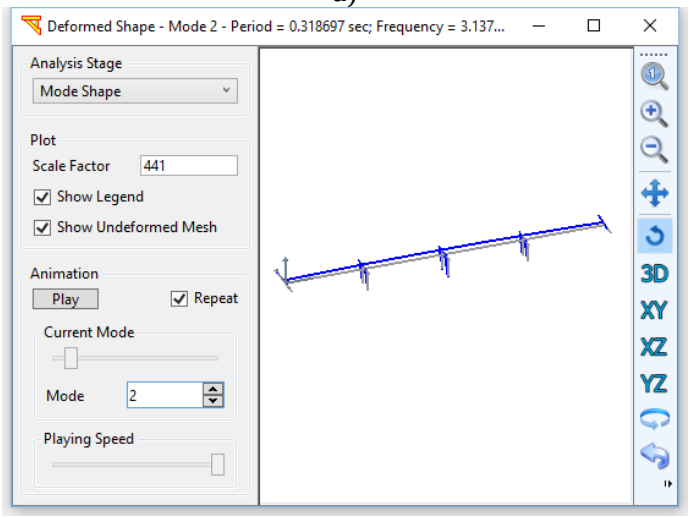

b)

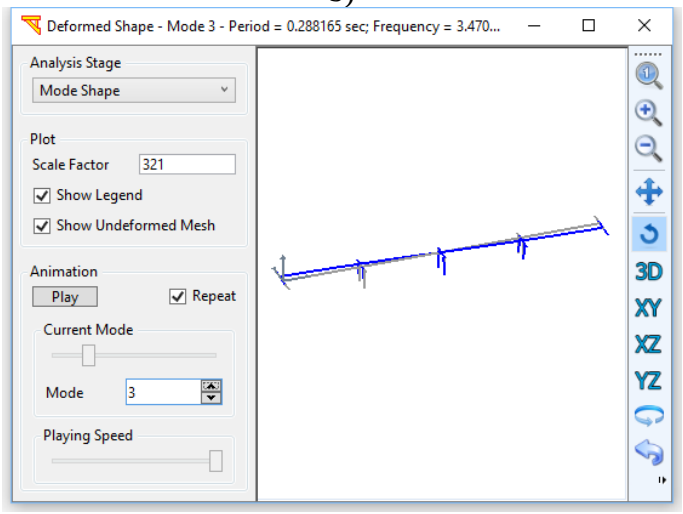

c)

Fig. 108. Mode shape analysis: a) first mode; b) second mode; c) third mode

7 GROUND SHAKING

To conduct a single earthquake analysis or multiple earthquake analyses, the "Ground Shaking" option under Analysis Options (Fig. 2 and Fig. 109) is used. For that purpose, the input earthquake excitation(s) must be specified. If only one earthquake record is selected out of a specified ensemble (suite) of input motions, then a conventional single earthquake analysis will be performed.

7.1 Definition/specification of input motion ensemble (suite)

This section presents the definition and specification of the input motions that represent a wide range of intensity measures to perform the analysis.

7.1.1 Available Ground Motions

A set of 10 motions are provided as the default input motion suite. The above ground motion data sets were resampled to a sampling frequency of 50 Hz (regardless of whether initial sampling frequency was 100 or 200 Hz) due to the computational demands of running full ground-structure analyses for an ensemble of motions. Standard interpolation methods were used to resample the time domain signals (so that the signal shape is preserved). The resampled records were then baselined to remove any permanent velocity and displacement offsets. Baselining was accomplished using a third order polynomial fitted to the displacement record.

In addition, four sets of input motions are also available (can be downloaded from the website: http://www.soilquake.net/msbridge):

Motion Set 1: These 100 motions were obtained directly from the PEER NGA database, and all files have been re-sampled to a time step of 0.02 seconds. This PBEE motion ensemble (Medina and Krawinkler 2004) obtained from the PEER NGA database (http://peer.berkeley.edu/nga/) consists of 100 3D input ground motions. Each motion is composed of 3 perpendicular acceleration time history components (2 lateral and one vertical). These motions were selected through earlier efforts (Gupta and Krawinkler, 2000; Mackie et al., 2007) to be representative of seismicity in typical regions of California. The moment magnitudes (Mw) of these motions range from 5.8-7.2 (distances from 0-60 km). The engineering characteristics of each motion and the ensemble overall may be viewed directly within **MSBridge**. The provided ground motions are based on earlier PEER research (Mackie and Stojadinovic 2005).

Motion Set 2: These motions (160 in total) were developed by Dr. Kevin Mackie from the 80 motions of Set1 (excluding the 20 motions of Set1 in the bin NEAR), to account for site classification.

Motion Set 3: These motions (80 in total) were developed by Dr. Jack Baker for PEER. Additional information about these motions is available at the website:

http://peer.berkeley.edu/transportation/projects/ground-motion-studies-for-transportation-systems/

Motion Set 4: These motions (260 in total) include the above **Set2** and **Set3** as well as the additional Bin NEAR of **Set1**.

Once an input motion data set is specified, the user interface will extract/calculate Intensity Measures (IMs) for each of these motions. In total, 11 different Intensity Measures are defined for each motion (and presented to the user in table and graphical formats), including quantities such as Peak Ground Acceleration (PGA), Peak Ground Velocity (PGV), Arias Intensity (AI), and so forth.

7.1.2 Specifications of Input Motions

To conduct a ground shaking analysis, input motions must be defined (Fig. 109). The window to define input motions is shown in Fig. 110. To select all motions, click **Select All**. To un-select all motions, click **De-select All.** To remove one motion, select the motion by clicking on it and then click **Delete**. To remove all motions, click **Remove All**.

To add a user-defined motion, click **Import** and then follow the simple steps to import a new motion (Fig. 111). The resulting motion will be added to the current suites of input motion. To obtain a completely new set of input motions, use **Delete All** to remove all existing input motions, and then use **Import** to add new motions.

To import a ground motion file, first, save the ground acceleration time history (easy in a notepad .txt file) with each new line being the next acceleration time step. This data in this file should have the acceleration units of g.

The finite element computations can be conducted for several earthquakes at a time. This is employed by specifying the **Number of Motions Running Simultaneously** (Fig. 110). You can select as many as eight records to be run at the same time to reduce the overall run time (for dual core machines or better).

Click **View Motion** to view the intensity measures and response spectra of the input motion being highlighted (Fig. 112). SRSS stands for Square Root of the Sum of the Squares of the two horizontal components. Click **Display Intensity Measures** to view the intensity measures of the input motion being highlighted (Fig. 113). The user can copy and paste the intensity measures to their favorite text editor such as MS Excel (in Fig. 113, right-click and then click **Select All** (ctrl-a) to highlight, and then right-click and then click **Copy** (ctrl c) to copy to the clipboard).

Click **View Histograms & Cumulative Distribution** to view the histogram and cumulative distribution plots for the whole input motion set (Fig. 114). The intensity measures include:

- PGA (Peak Ground Acceleration)
- PGV (Peak Ground Velocity)
- PGD (Peak Ground Displacement)
- $D_{5\text{-}95}$ (Strong Motion Duration)
- CAV (Cumulative Absolute Velocity)
- Arias Intensity
- SA (Spectral Acceleration; assuming 1 second period)
- SV (Spectral Velocity; assuming 1 second period)
- SD (Spectral Displacement; assuming 1 second period)
- PSA (Pseudo-spectral Acceleration)
- PSV (Pseudo-spectral Velocity)

The strong motion duration ($D_{5\text{-}95}$) is defined according to the time domain bounded by the 5% and 95% cumulative Arias intensity of the record. All of the spectral intensity measures are defined at effective viscous damping of 5% unless otherwise noted.

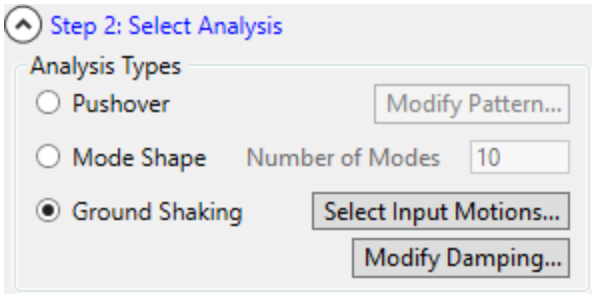

Fig. 109. Group shaking analysis

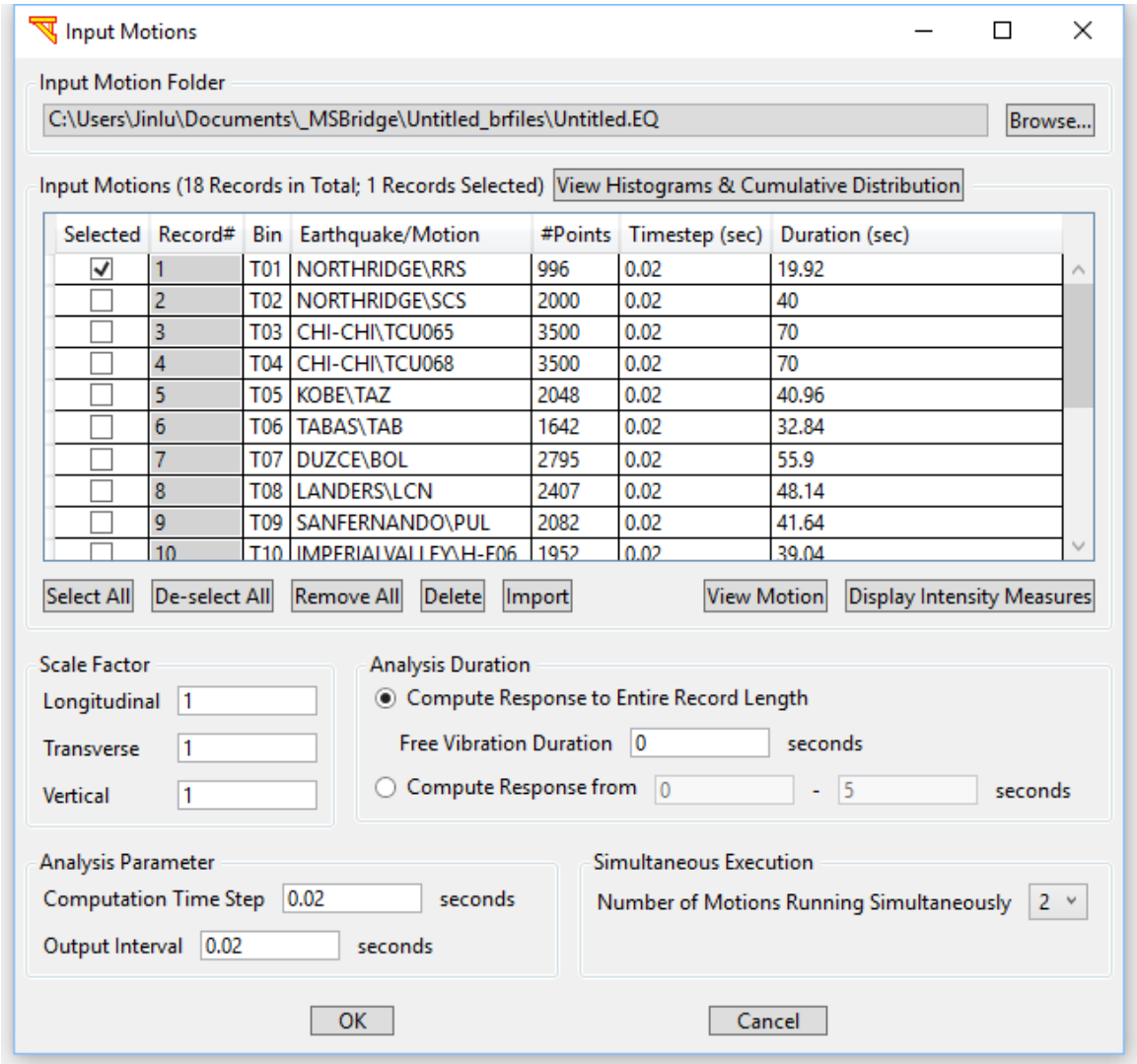

Fig. 110. Definition of input motions

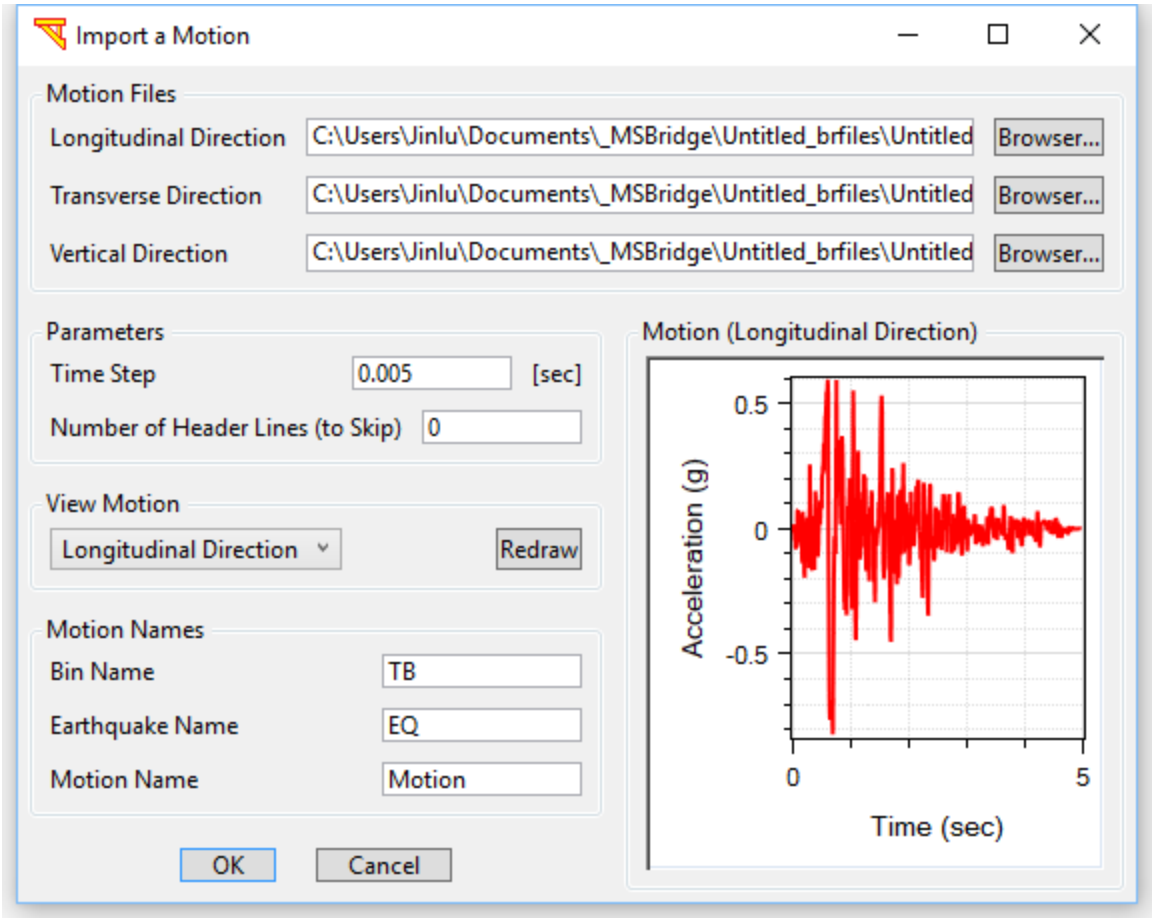

Fig. 111. Importing a user-defined motion

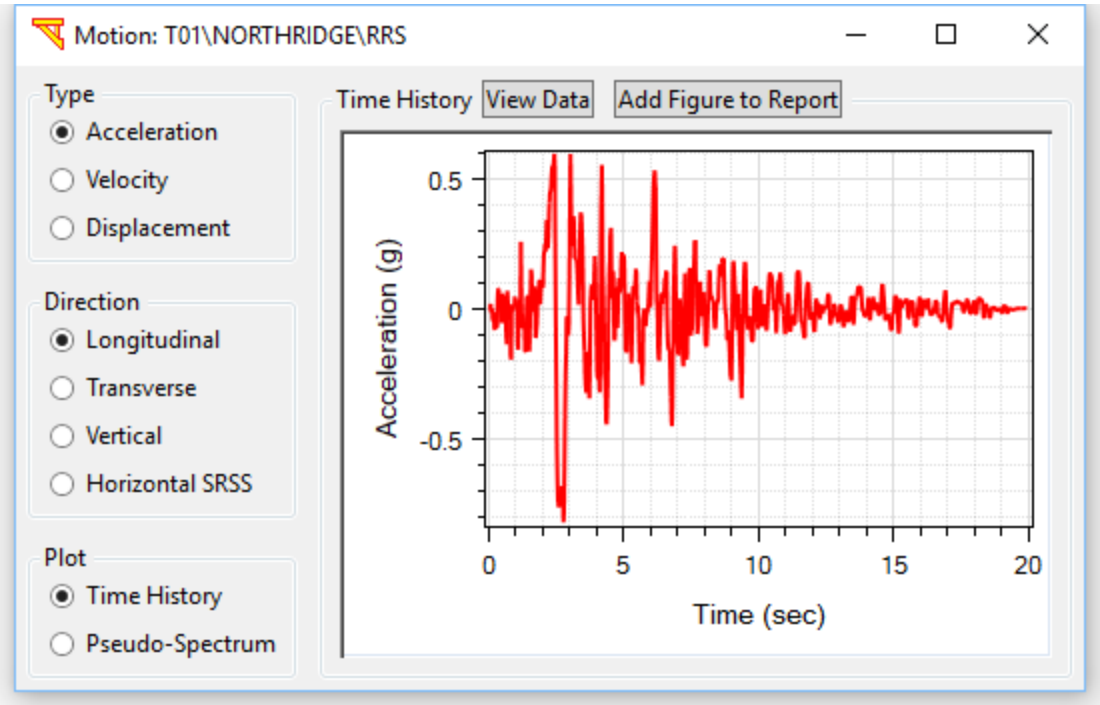

a)

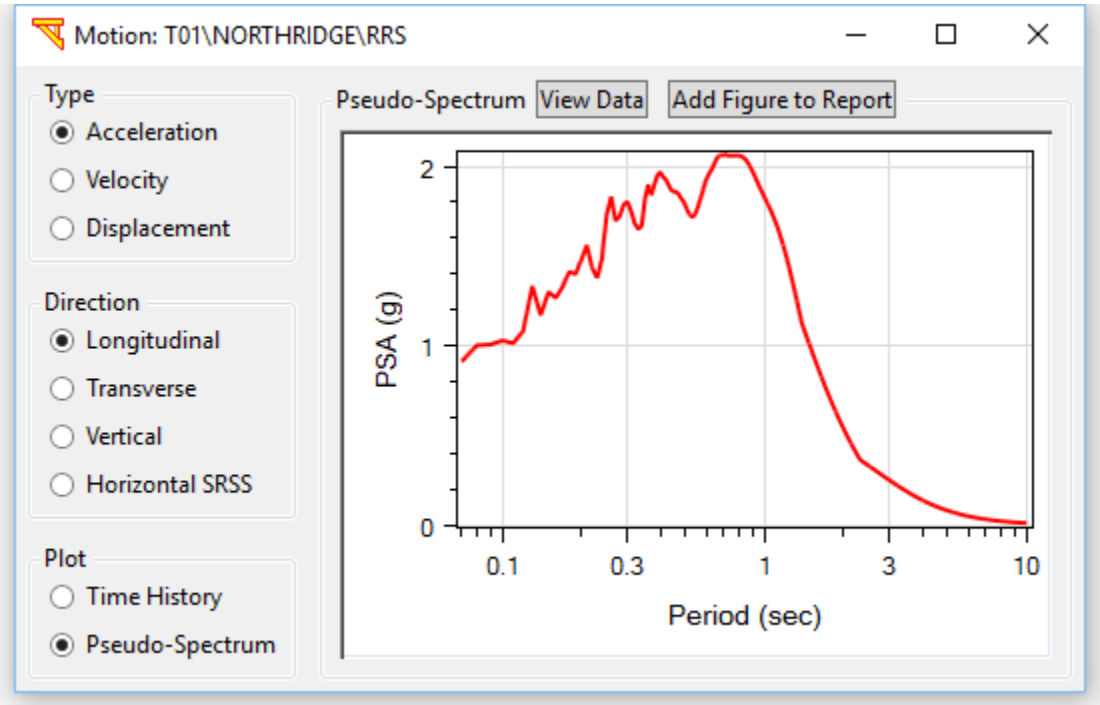

b)

Fig. 112. Ground motion: a) time histories; and b) response spectra

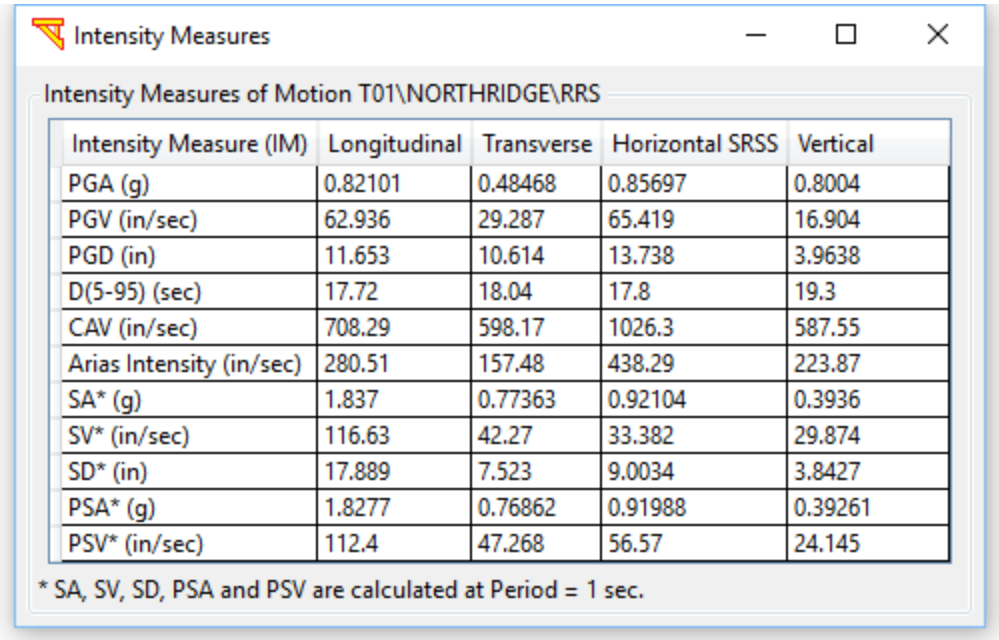

Fig. 113. Intensity measures of a ground motion

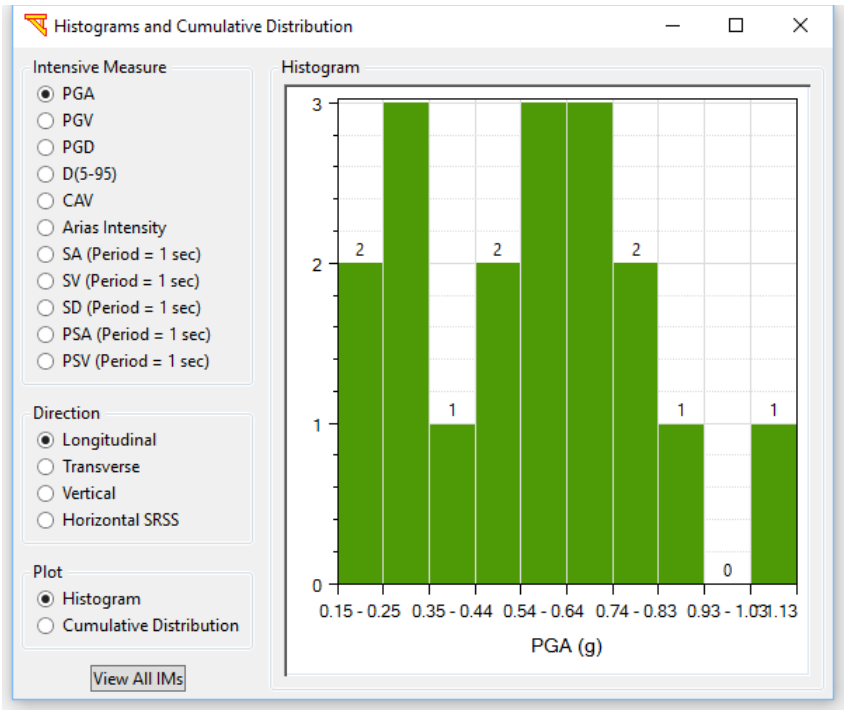

a)

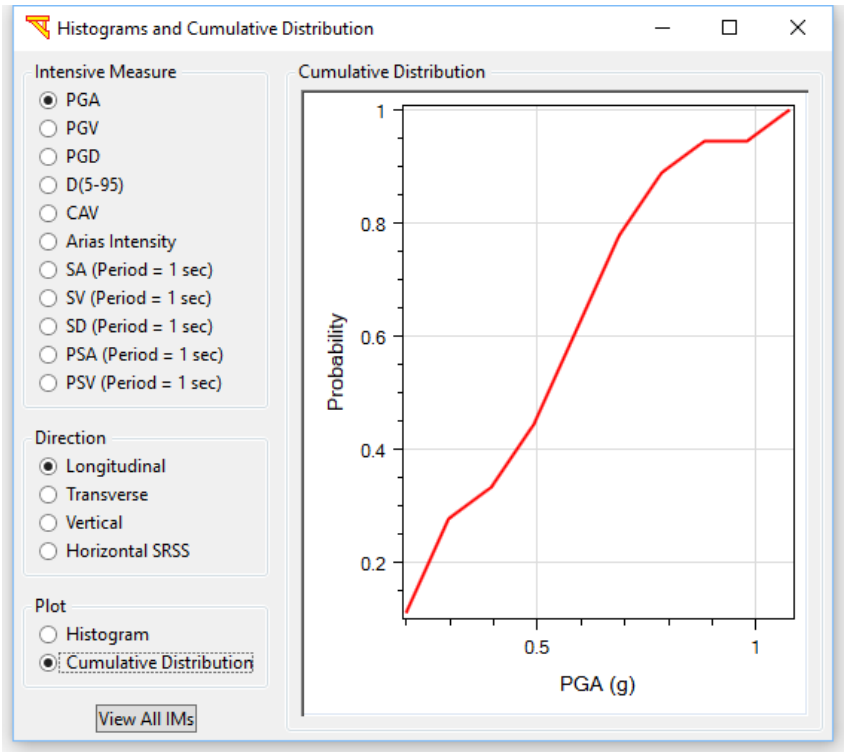

b)

Fig. 114. Histogram and cumulative distribution for a motion set: a) histogram; b) cumulative distribution

7.2 Rayleigh Damping

MSBridge employs Rayleigh damping, which takes the form:

$\mathbf{C} = A_m\mathbf{M} + A_k\mathbf{K}$

where **M** is the mass matrix, **C** is the viscous damping matrix, **K** is the initial stiffness matrix. A_m and A_k are two user-specified constants.

The damping ratio curve $\xi(f)$ is calculated based on the following equation:

$$\xi = \frac{A_m}{4\pi f} + A_k \pi f$$

where f is frequency.

(1) Specification of A_m and A_k By Defining Damping Ratios

Click **Change Damping** in the **MSBridge** main window to modify the Rayleigh damping coefficients (Fig. 115). The user can define damping coefficients (Fig. 115) by specifying two frequencies, f_1 and f_2 (must be between 0.1 and 50 Hz), and two damping ratios, ξ_1 and ξ_2 (suggested values are between 0.2% and 20%).

The Rayleigh damping parameters A_m and A_k are obtained by solving the following equations simultaneously:

$$\xi_1 = \frac{A_m}{4\pi f_1} + A_k \pi f_1$$

$$\xi_2 = \frac{A_m}{4\pi f_2} + A_k \pi f_2$$

(2) Direct Specification of A_m and A_k:

The user can also directly define Rayleigh damping coefficients A_m and A_k (Fig. 115).

7.3 Save Model and Run Analysis

After defining the finite element model, click **Save Model and Run Analysis**. The finite element computations will start, for several earthquakes at a time (Fig. 116) as specified in the **Input Motions** window (Fig. 110).

The user can modify the time integration scheme for the OpenSees analysis by clicking **Advanced** and then **OpenSees Parameters** (Fig. 70). Fig. 70 shows the default parameters which are used in the analysis.

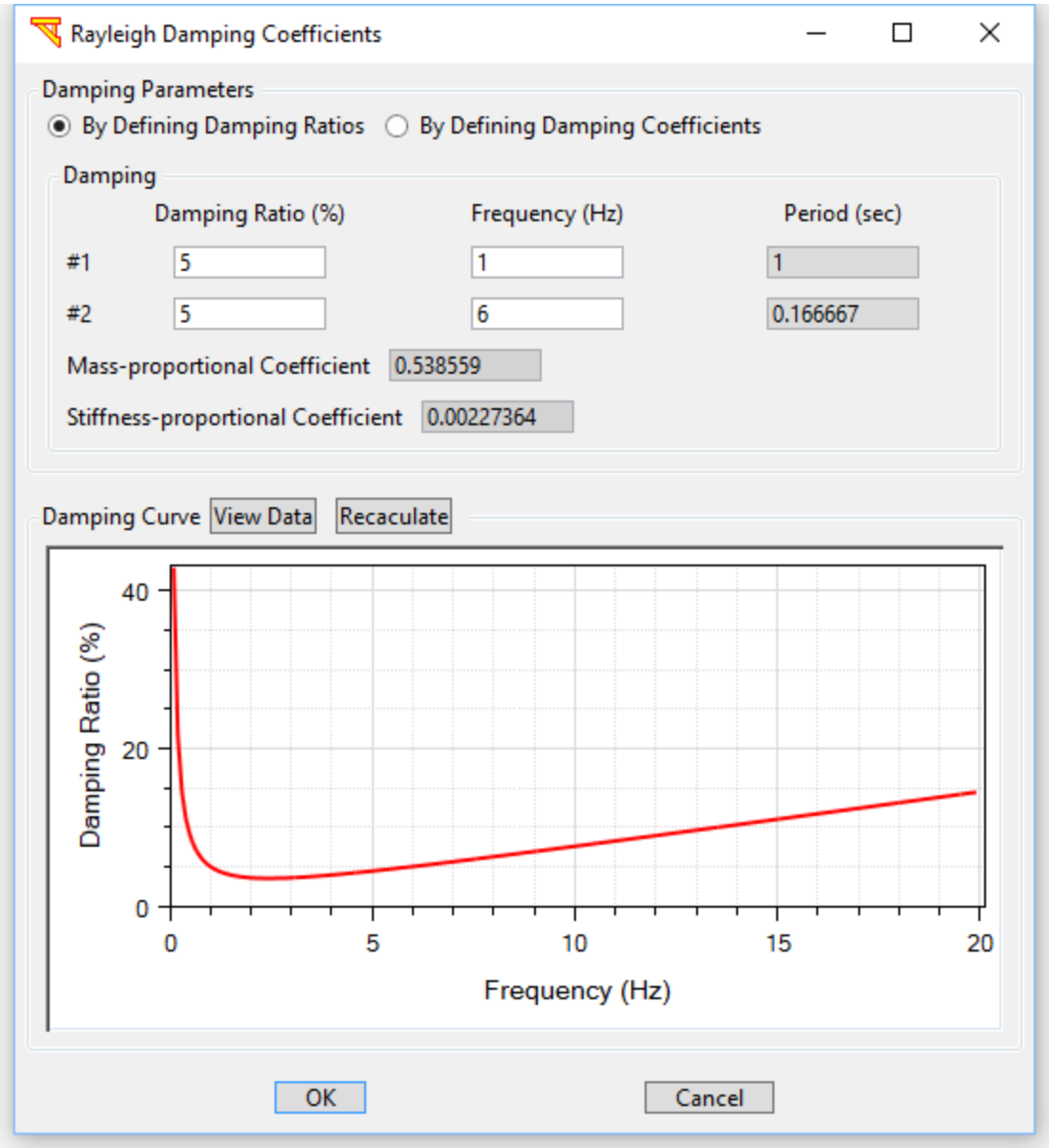

Fig. 115. Rayleigh damping

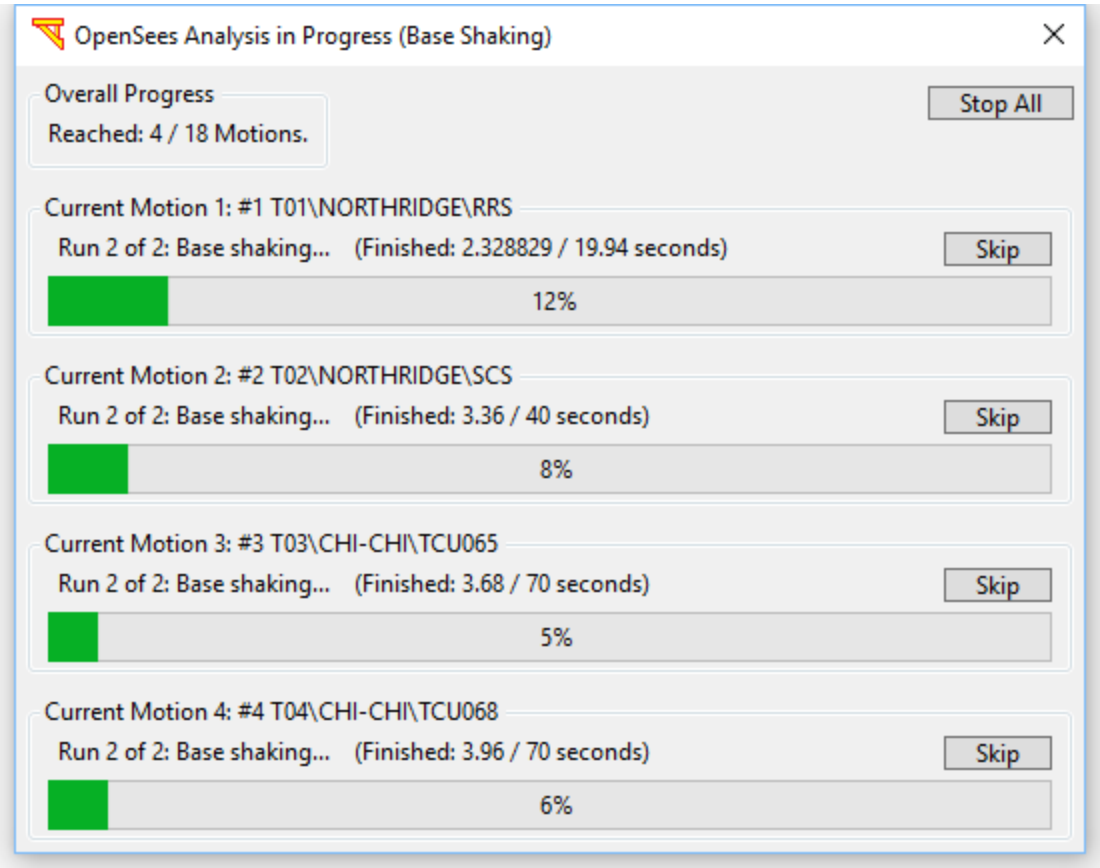

Fig. 116. Simultaneous execution of analyses for multiple motions

8 TIME HISTORY OUTPUT

This section presents the time history outputs after the FE analysis phase. The outputs are time history output quantities for each bridge element, the deformed mesh, and the maximum output quantities for all input motions.

8.1 Time History Output Quantities

At the end of the FE analysis phase, time histories and bridge responses will be available of the form:

i) Column Response Time Profiles
ii) Column Response Time Histories
iii) Column Response Relationships
iv) Abutment Responses
v) Deformed Mesh

In addition, for multiple earthquake analysis scenarios, Intensity Measures (IMs) and response spectra for each input motion are calculated and are available for display in Table and Figure formats. Engineering Demand Parameter (EDP) Quantities and Bridge peak accelerations for all employed shaking motions are also available for display against any of the computed IMs.

The post-processing capabilities can be accessed from Menu **Display** (Fig. 4). To display output for a different input motion, click Menu **Display** and then **Detailed Output: Please Select Input Motion** (Fig. 4d). The name of the selected input motion will also appear on the menu items (Fig. 4d).

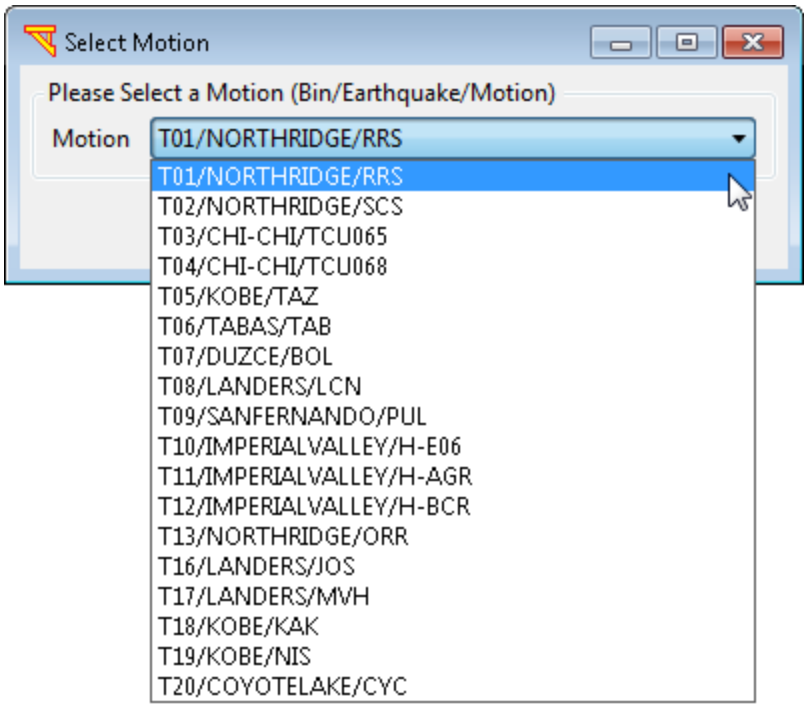

Fig. 117. Selection of an input motion

8.1.1 Deck Response Time Histories

The deck response time histories can be accessed by clicking menu **Display** (Fig. 4) and then **Deck Response Time Histories**. Fig. 118 shows the window for displaying the deck longitudinal displacement time histories.

8.1.2 Column Response Profiles

The column response profiles can be accessed by clicking menu **Display** (Fig. 4) and then **Column Response Profiles**. The column response window is shown in Fig. 119. The columns are labeled as:

i) **Column 1 of Bent 2** (see Fig. 1., the first bent starting after left abutment is denoted as “Bent 2”, the second as “Bent 3”, and so on)
ii) Column 2 of Bent 2
iii) (more if any)

Fig. 120 shows the bending moment in the longitudinal plane. The horizontal axis of the plot is the response name (e.g., displacement, bending moment, etc.) and the vertical axis is the elevation of the column. Zero elevation means the column base.

8.1.3 Column Response Time Histories

The column response time histories can be accessed by clicking menu **Display** (Fig. 4) and then **Column Response Time Histories**. Fig. 121 shows the window for displaying the column longitudinal displacement time histories.

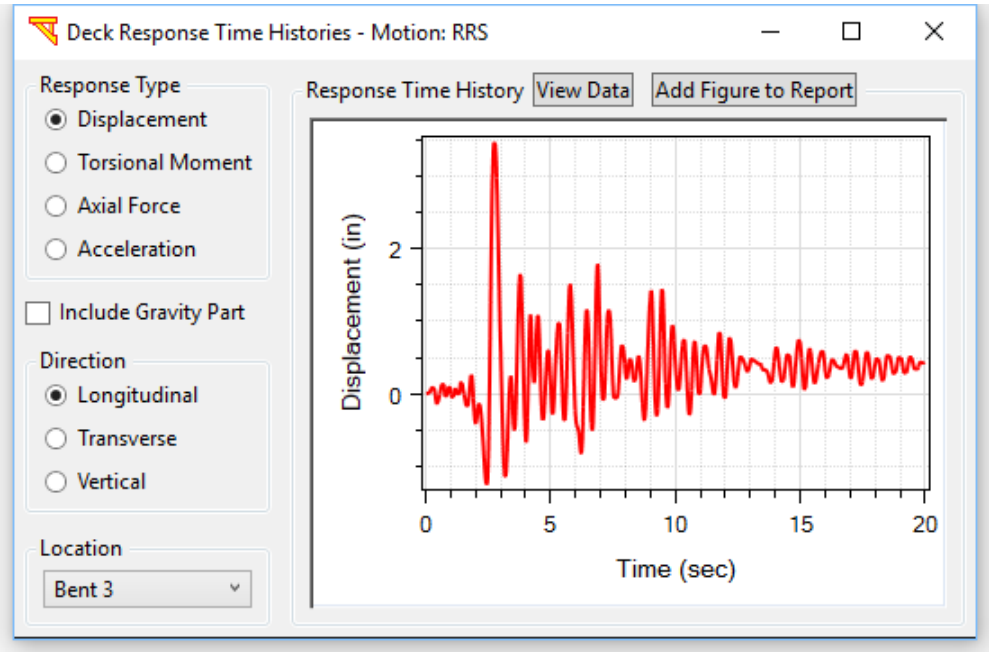

Fig. 118. Deck longitudinal displacement response time histories

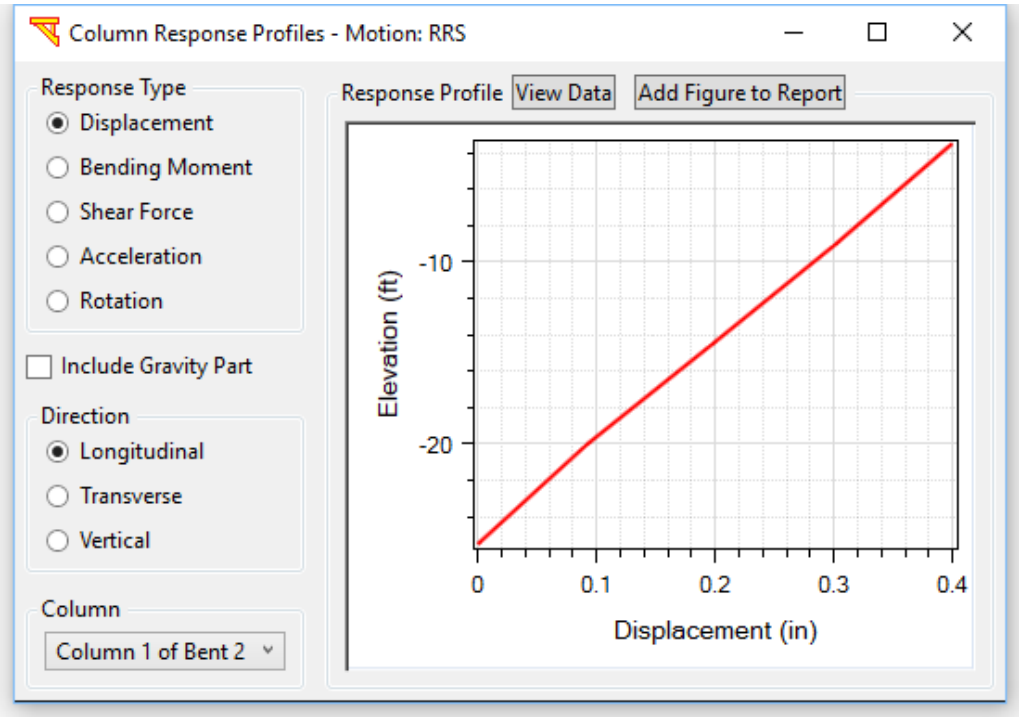

Fig. 119. Displacement profile in the longitudinal plane

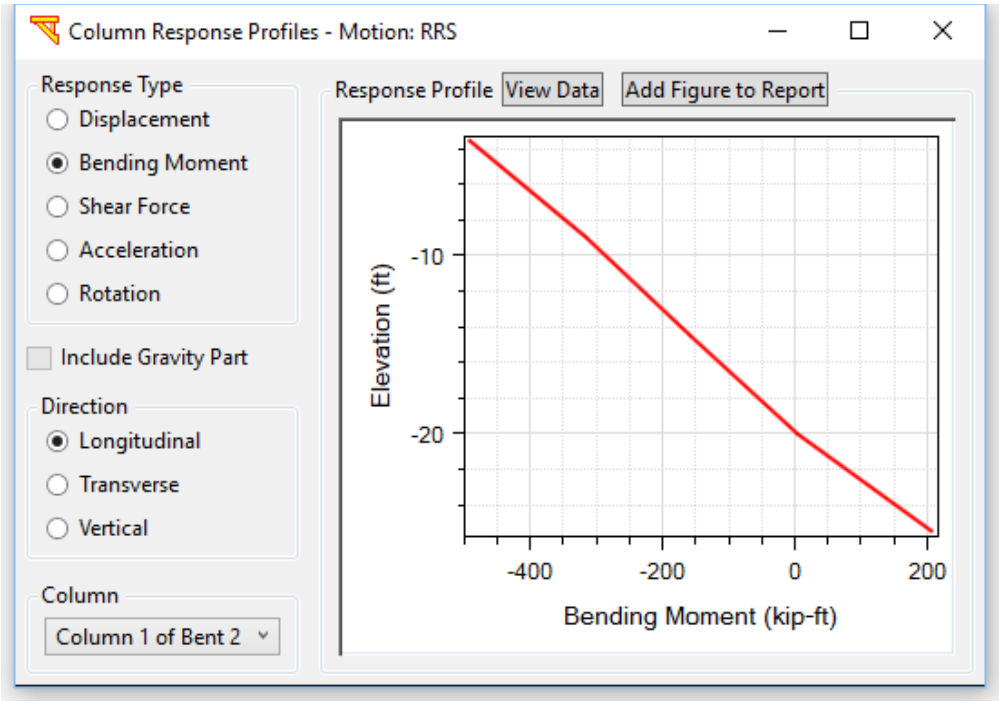

Fig. 120. Bending moment profile in the longitudinal plane

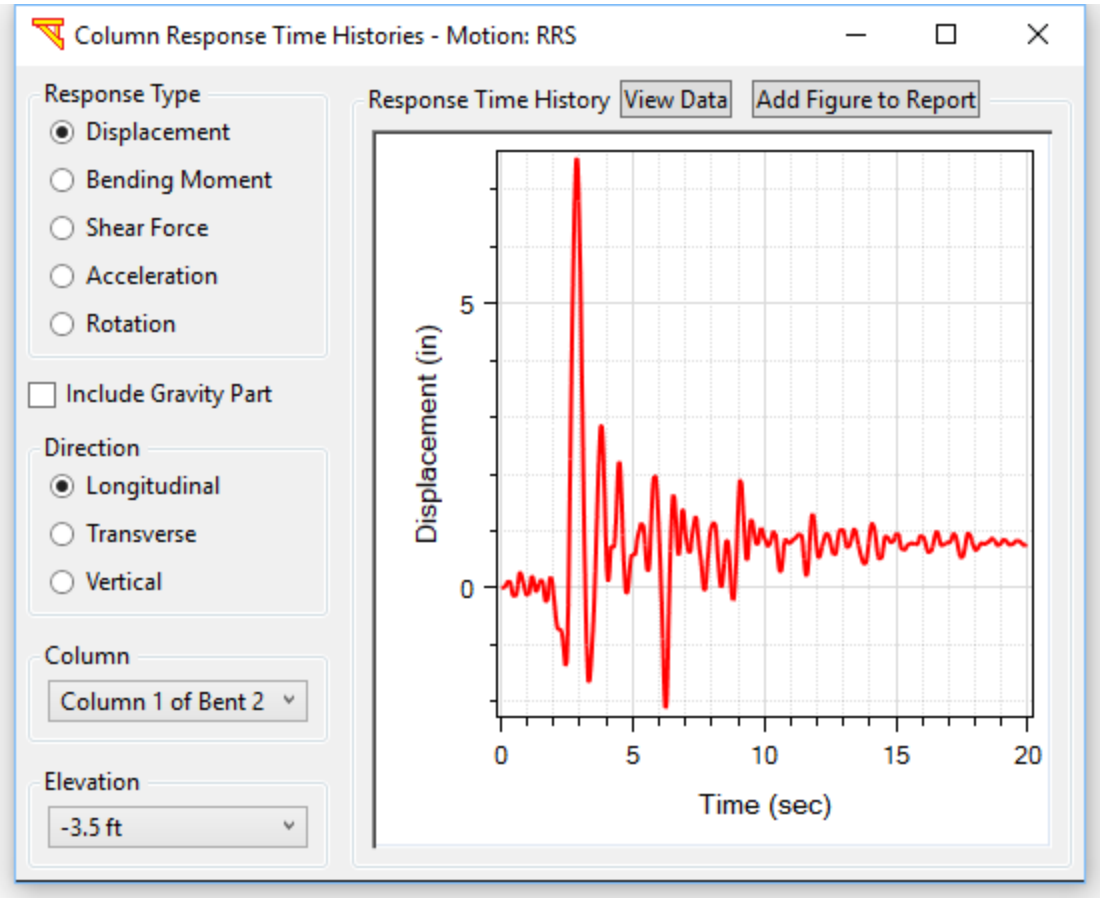

Fig. 121. Response time histories and profiles for column (and pile shaft): displacement is shown at the nodes.

8.1.4 Column Response Relationships

The column response relationships can be accessed by clicking menu **Display** (Fig. 4) and then **Column Response Relationships**.

The **Elevation** box includes all elevations (starting from column top). Zero elevation refers to the column base. Fig. 122 shows the longitudinal load-displacement curve at the column top. The load refers to the shear force of the beam-column element at the specified elevation. Fig. 123 shows the moment-curvature curve at the column top. The vertical axis is the bending moment and the horizontal axis is the curvature. To view the data for the plot, click **View Data**.

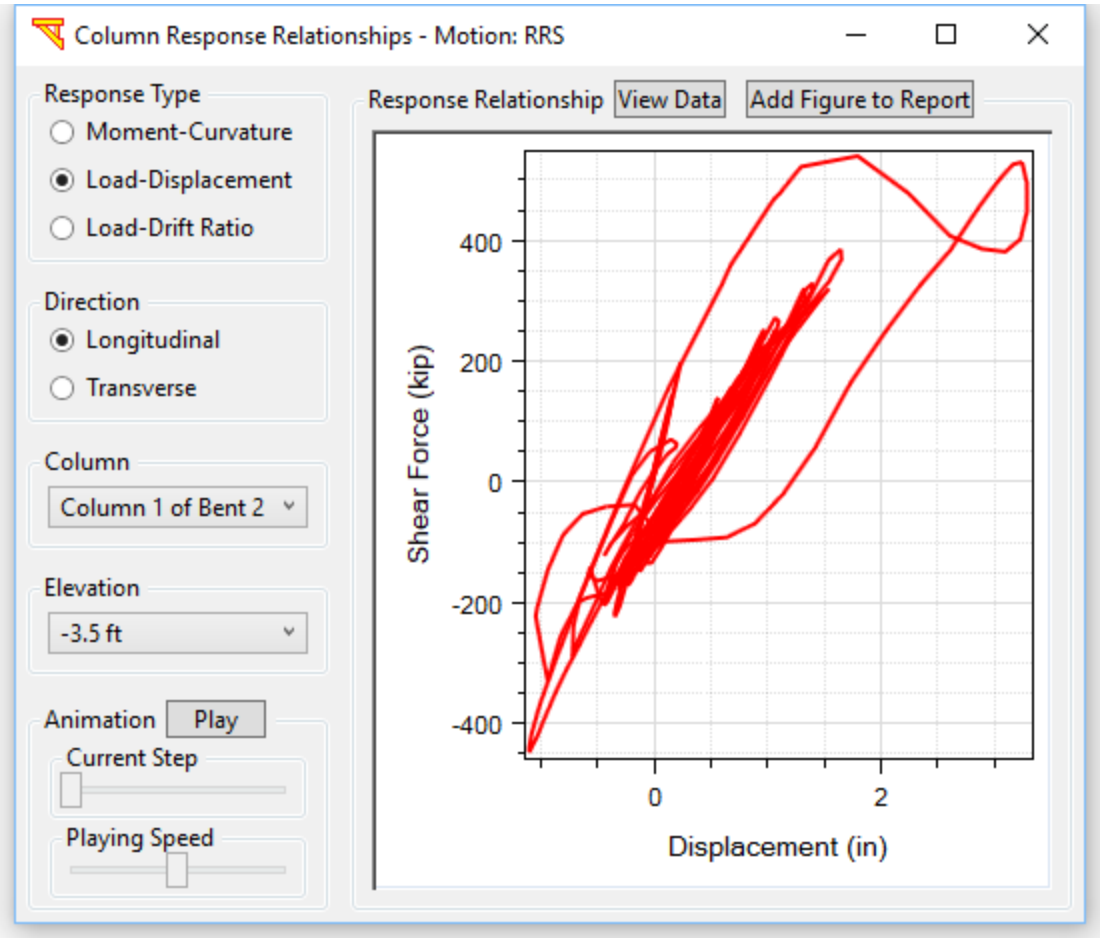

Fig. 122. Load-displacement curve at the column top

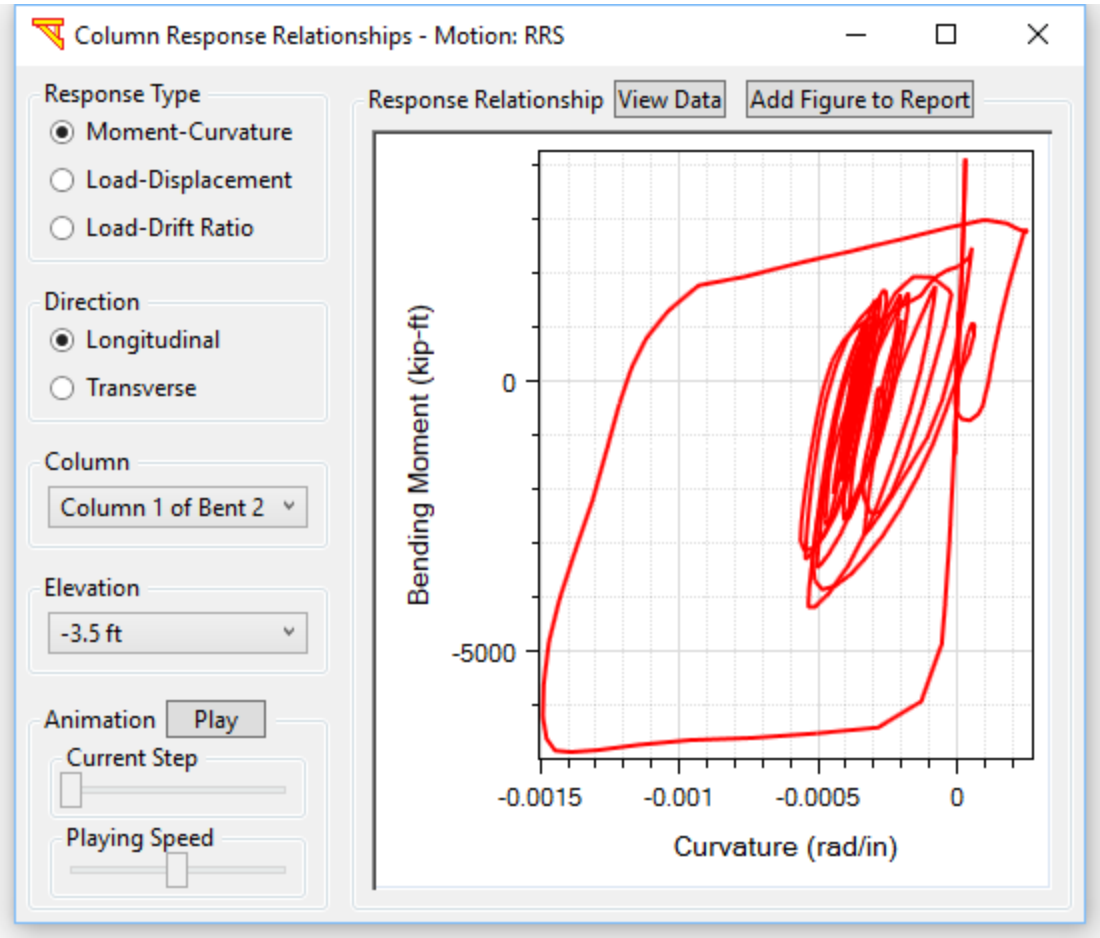

Fig. 123. Moment-curvature curve at the column top

8.1.5 Abutment Responses Time Histories

The abutment responses can be accessed by clicking menu **Display** and then **Abutment Response Time Histories**. The abutment responses window includes the following options:

i) **Force-Displacement Relationships**
ii) **Relative Deck-end/Abutment Displacement Time Histories**
iii) **Resisting Force Time Histories**

Three directions (longitudinal, transverse and vertical directions) of the above responses for both left and right abutments are all displayed. Fig. 124 shows the abutment response time histories. The force refers to the resisting force acting on deck-end and the displacement refers to the relative deck-end/abutment displacement.

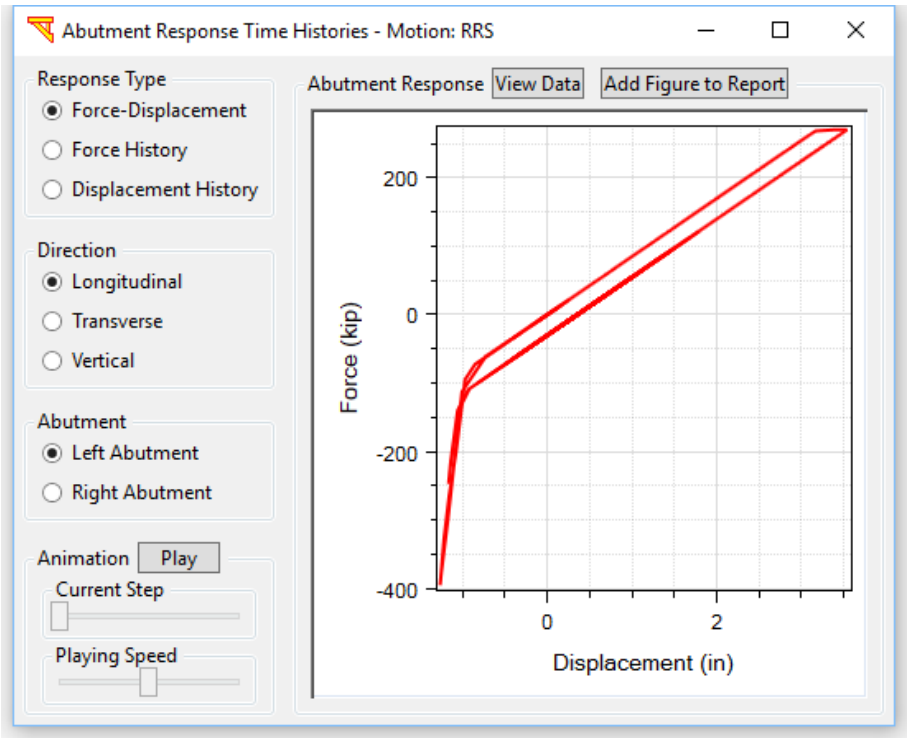

a)

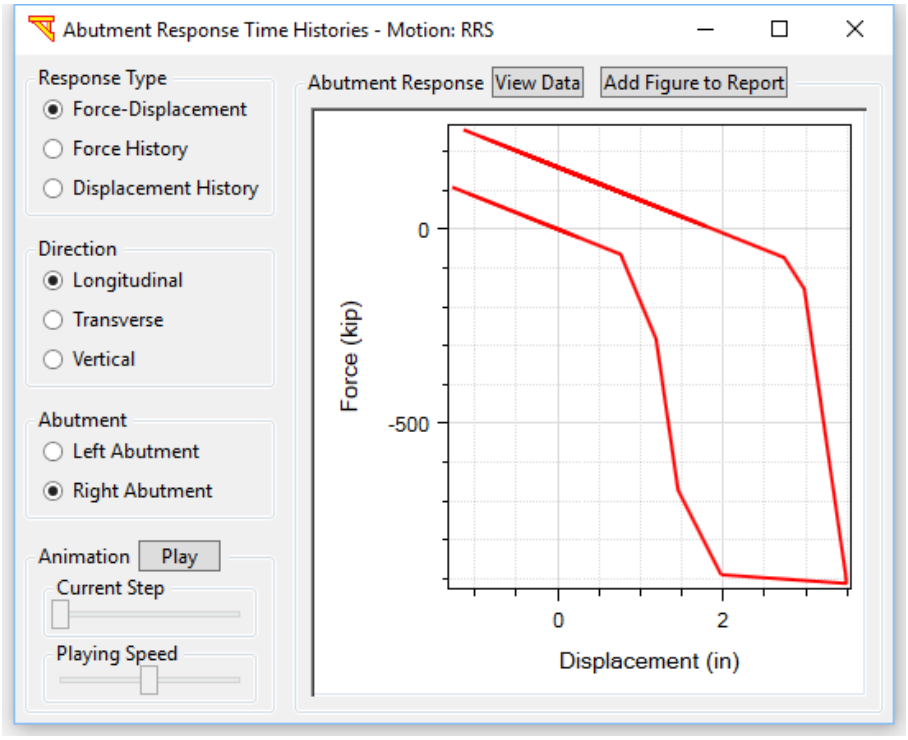

b)

Fig. 124. Abutment longitudinal force-displacement relationship: a) left abutment; and b) right abutment

8.1.6 Soil Spring Responses Time Histories

The soil spring responses can be accessed by clicking menu **Display** and then **Soil Spring Response Time Histories**. The soil spring responses window includes the following options (Fig. 125):

i) **Force-Displacement Curve**
ii) **Displacement Time History**
iii) **Force Time History**

Two directions (longitudinal and transverse directions) of the above responses for each soil spring are all displayed (Fig. 125).

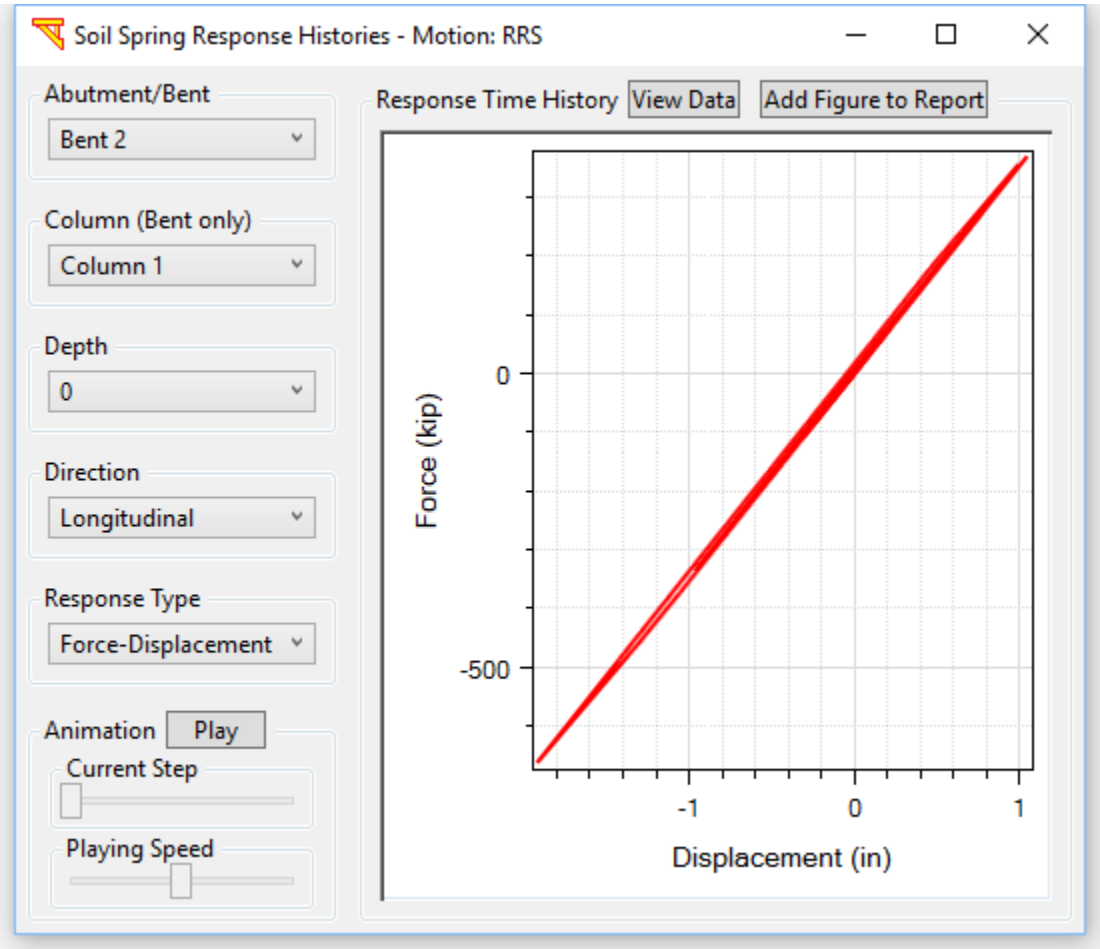

Fig. 125. Soil spring response time histories

8.1.7 Deck Hinge Responses Time Histories

The deck hinge responses can be accessed by clicking menu **Display** and then **Deck Hinge Response Time Histories**. The deck hinge responses window includes the following options (Fig. 126):

i) **Force-Displacement Curve**
ii) **Displacement Time History**
iii) **Force Time History**

Response time histories are shown for the cable and edge hinge elements for each hinge (Fig. 126).

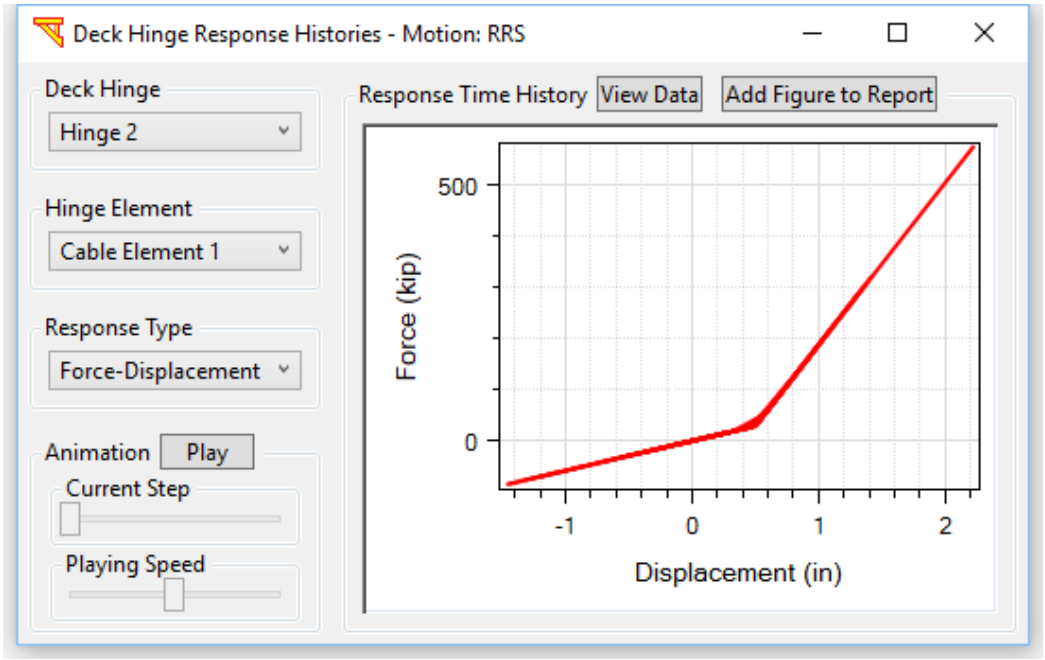

a)

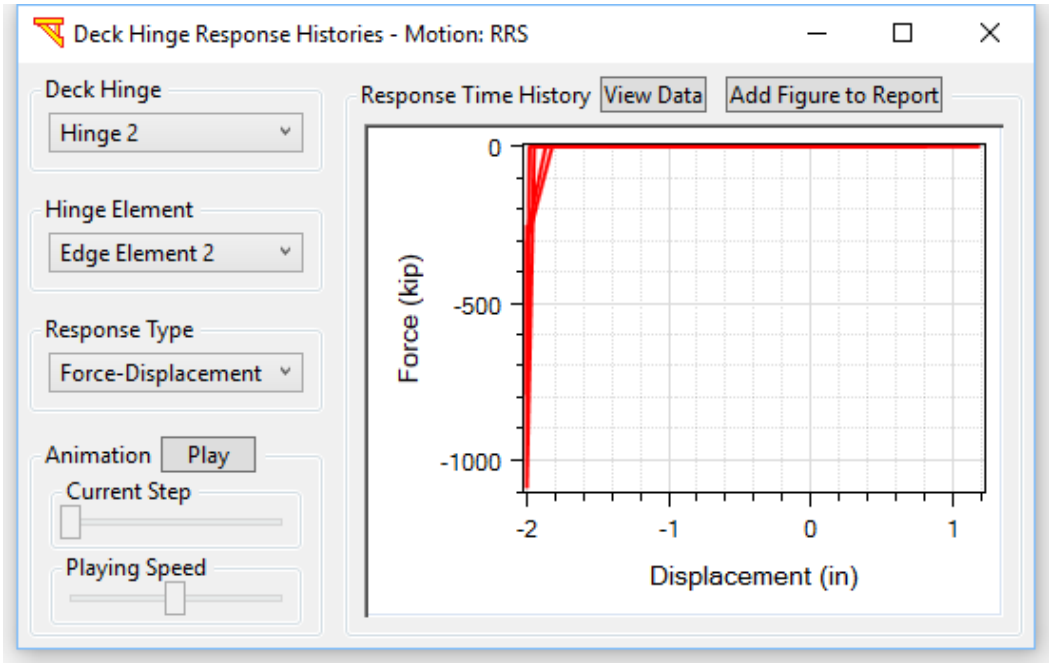

b)

Fig. 126. Deck hinge response time histories: a) cable element; b) edge element

8.1.8 Isolation Bearing Responses Time Histories

The isolation bearing responses can be accessed by clicking menu **Display** and then **Isolation Bearing Response Time Histories**. The isolation bearing responses window includes the following options (Fig. 127):

i) **Force-Displacement Curve**
ii) **Displacement Time History**
iii) **Force Time History**

Three translational directions and three rotational directions of the above responses for each bearing are displayed (Fig. 127).

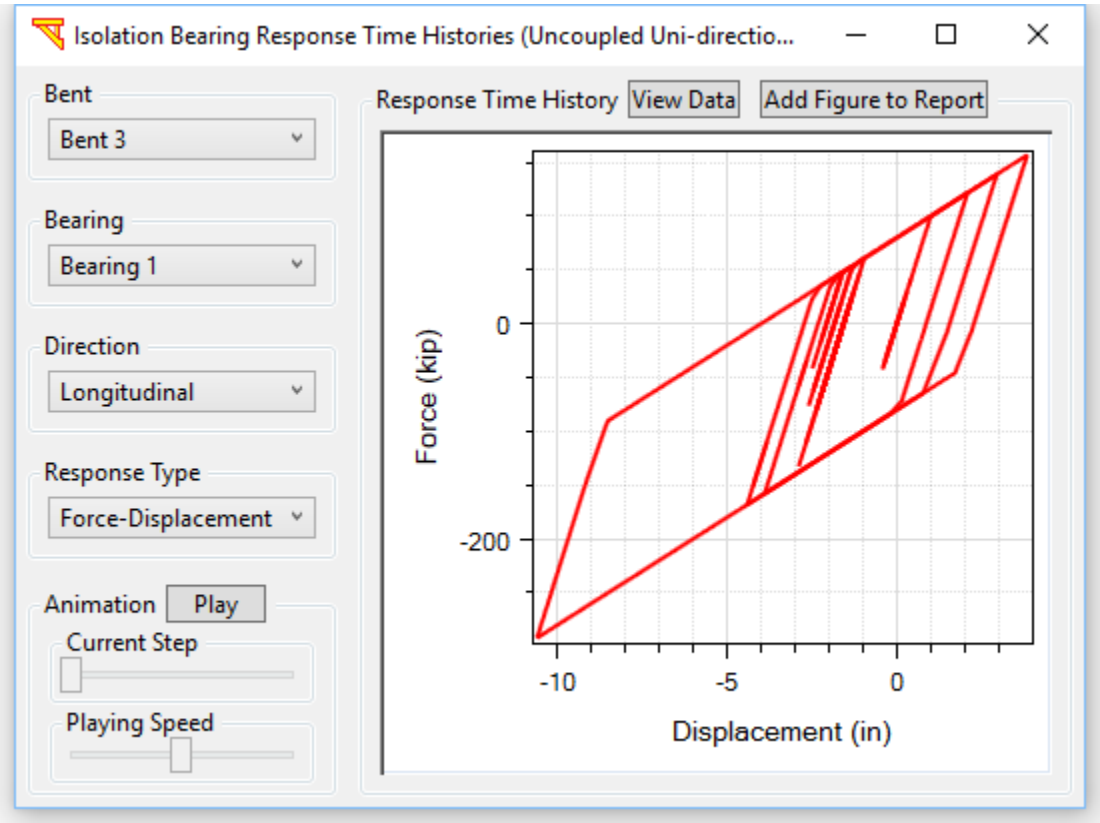

Fig. 127. Isolation bearing response time histories

8.2 Deformed Mesh and Animation

The deformed mesh can be accessed by clicking menu **Display** (Fig. 4) and then **Deformed Mesh**. The deformed mesh window is shown in Fig. 128.

Analysis stages include **Due to gravity** and **Due to pushover** (or **Due to base shaking**). The response types include

i) Deformed mesh
ii) Resultant Disp.
iii) X-Displacement
iv) Y-Displacement
v) Z-Displacement
vi) Plastic Hinges

In the Ground Shaking Analysis, the input motion is also animated at the deformed mesh window along with bridge displacement (Fig. 128).

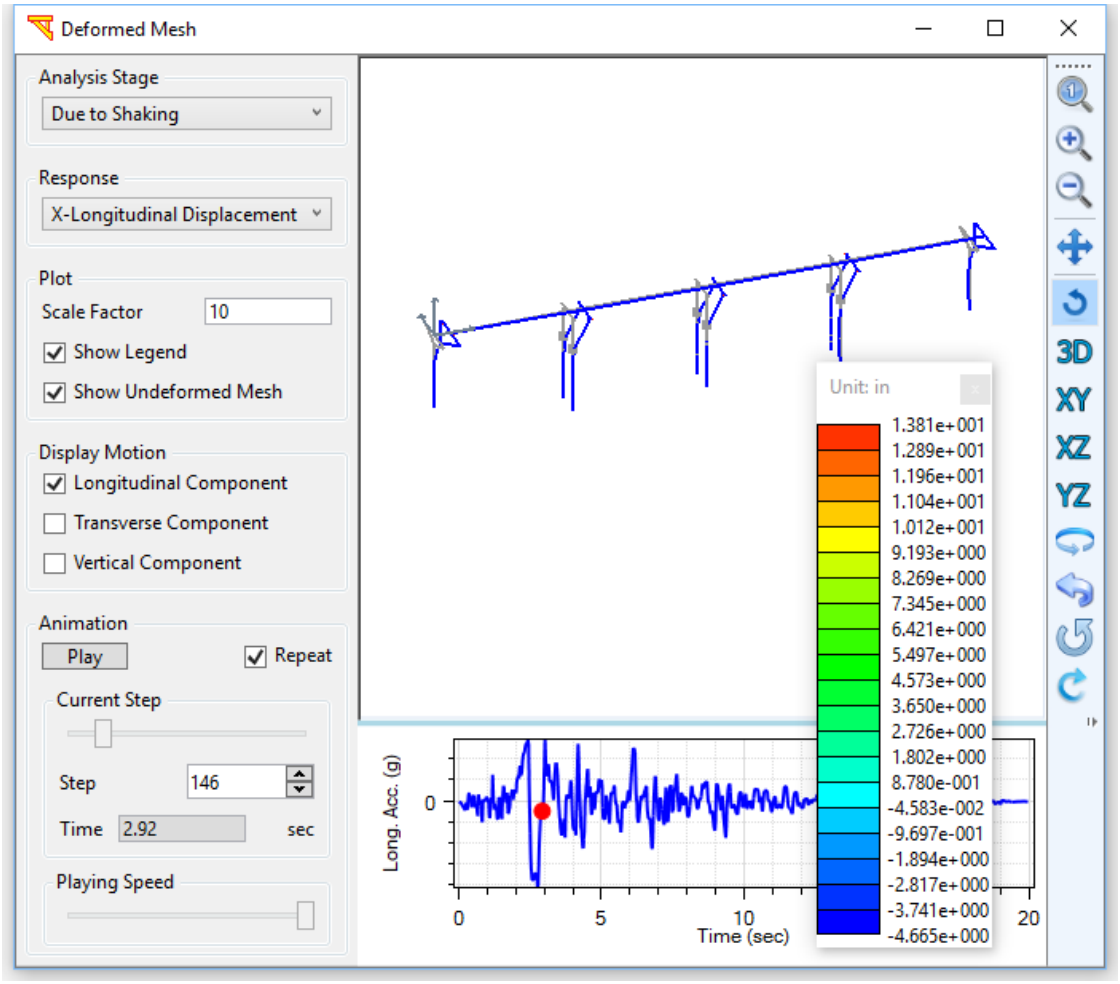

Fig. 128. Deformed mesh

Visualization of plastic hinges is available if the nonlinear beam-column element is used for the columns. In the Ground Shaking Analysis, the input motion is also animated at the deformed mesh window along with the development of plastic hinges (Fig. 129). In the current version, the visualization is implemented in such a way that a plastic hinge marker stays once the plastic hinge is developed. The plastic hinge is developed when rebar fails in tension or first concrete fiber reaches the maximum strain capacity.

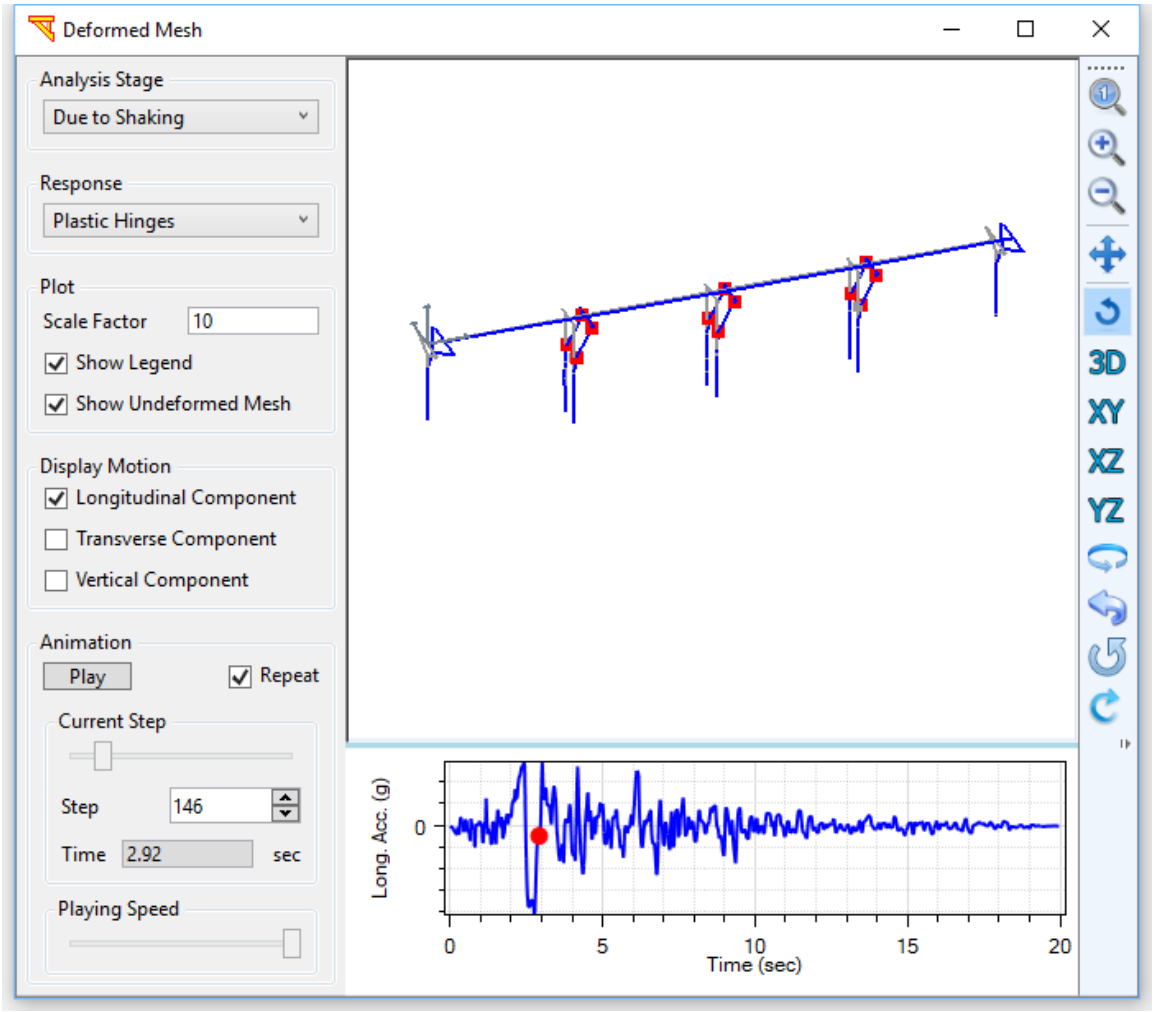

Fig. 129. Visualization of plastic hinges

8.3 Maximum Output Quantities

This section presents the maximum acceleration and displacements for all motions after performing time history analysis. In addition, the maximum column and abutments forces.

8.3.1 Bridge Peak Accelerations & Displacements for All Motions

The bridge peak accelerations and displacements for all input motions can be accessed by clicking menu **Display** (Fig. 4) and then **Bridge Peak Accelerations& Displacements for All Motions**. The window to display the bridge peak accelerations for all motions is shown in Fig. 130. The responses are available in the longitudinal and transverse directions as well as for the SRSS of the two horizontal directions (Fig. 130).
The figures in this window include:

i) Maximum bridge acceleration
ii) Maximum bridge displacement
iii) Bridge peak acceleration/input peak acceleration

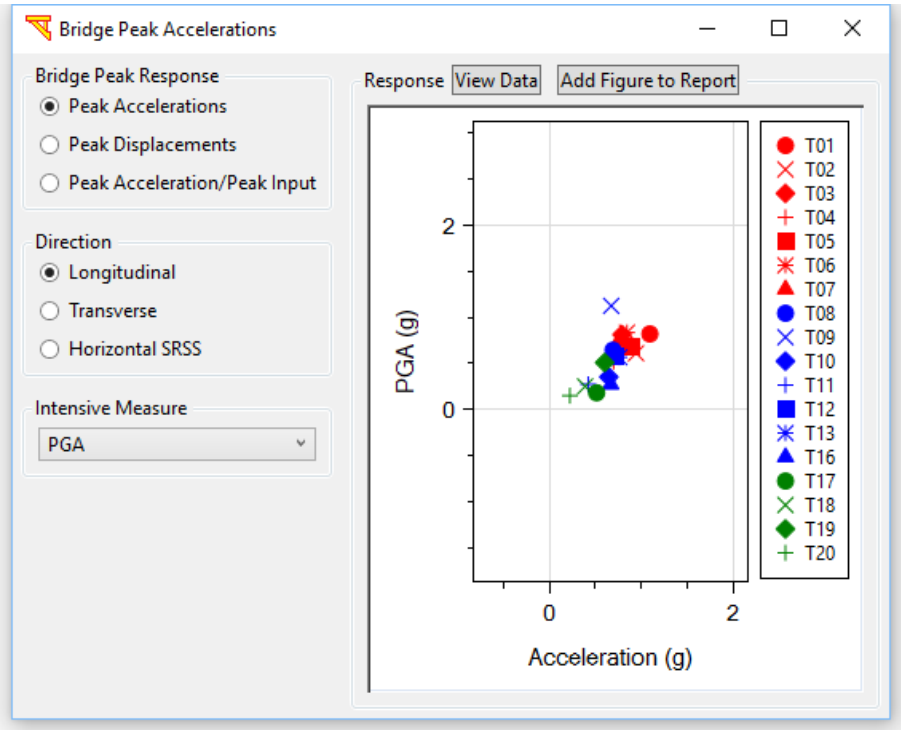

a)

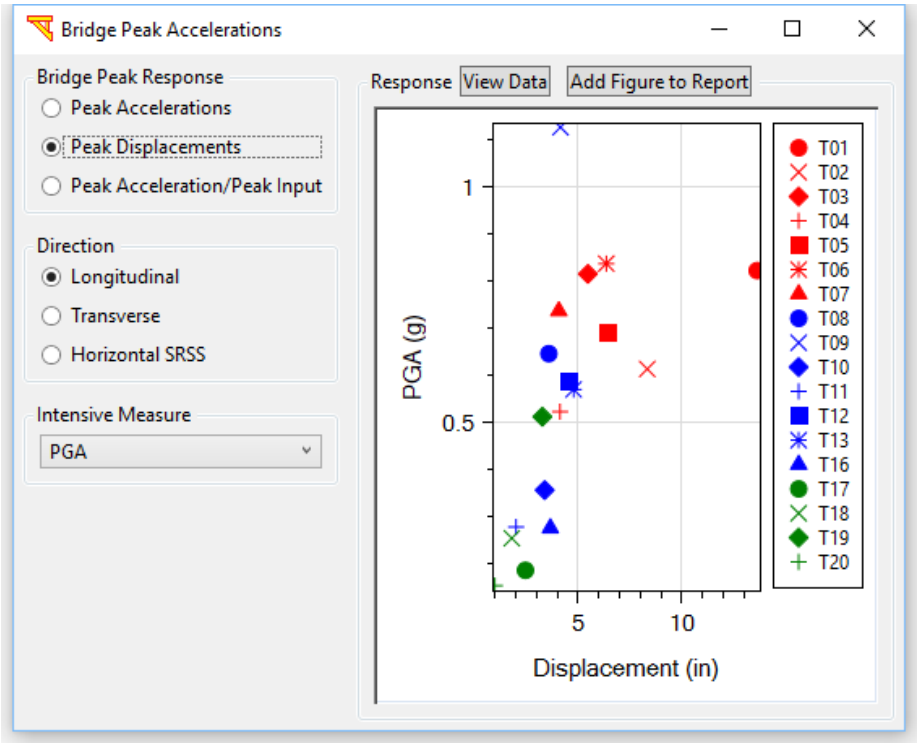

b)

Fig. 130. Bridge peak accelerations for all motions: a) maximum bridge accelerations; b) maximum bridge displacements

8.3.2 Maximum Column & Abutment Forces for All Motions

The maximum column & abutment forces for all input motions can be accessed by clicking menu **Display** (Fig. 4)and then **Maximum Column & Abutment Forces for All Motions**. The window to display the maximum column & abutment forces for all motions is shown in Fig. 131. The responses are available in the longitudinal and transverse directions as well as for the SRSS of the two horizontal directions (Fig. 131).

The figures in this window include:

i) Maximum column shear forces
ii) Maximum column bending moments
iii) Maximum abutment forces (left abutment)
iv) Maximum abutment forces (right abutment)

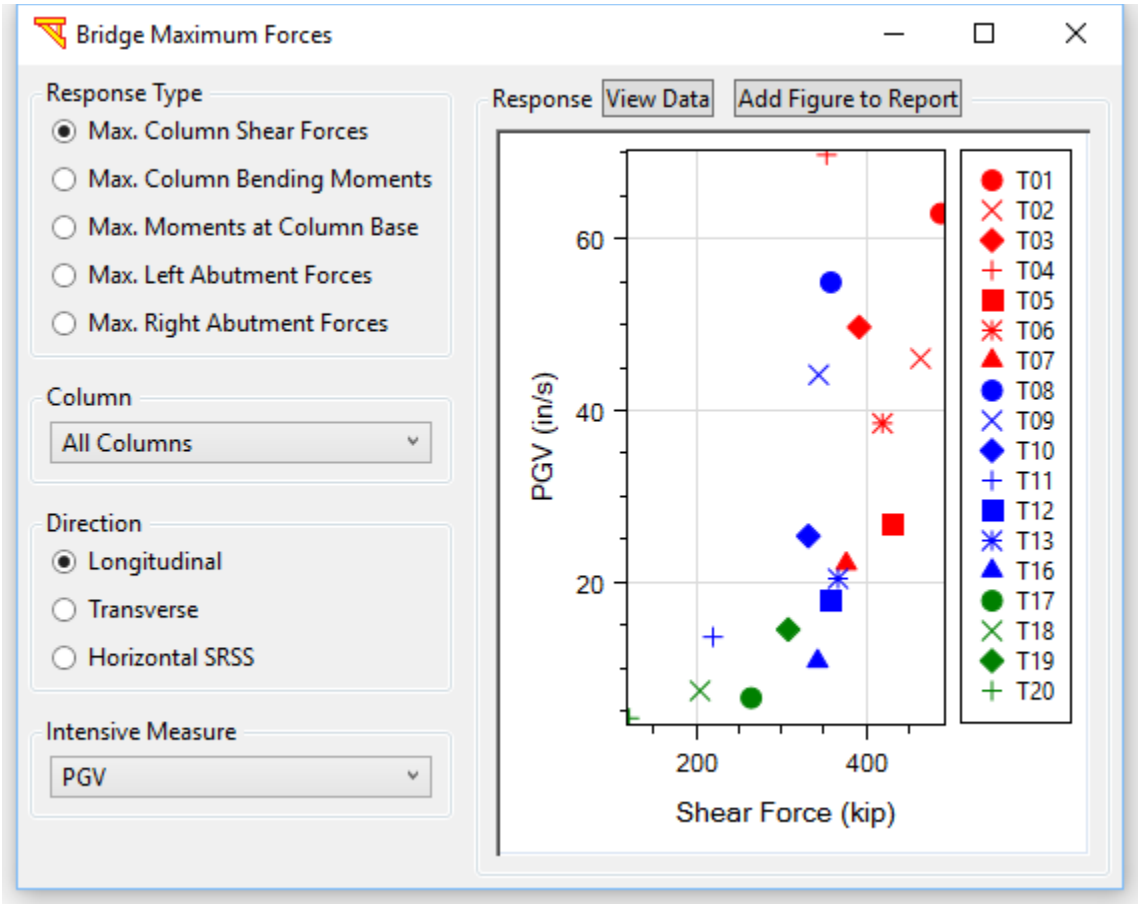

Fig. 131. Maximum column & abutment forces for all motions

9 EQUIVALENT STATIC ANALYSIS

Equivalent Static Analysis (ESA) option is available in **MSBridge** for the bridge longitudinal & transverse directions. The whole bridge system is employed in the bridge longitudinal ESA. And one single bent is employed in the bridge transverse ESA.

9.1 Bridge Longitudinal Direction

To conduct an Equivalent Static Analysis (ESA) for the bridge longitudinal direction, click **Longitudinal Direction** in the main window (Fig. 132). The elastic displacement demand output is shown in Fig. 133. The displacement demand output is available for the longitudinal components of the input motions.

To view the comparison of displacements from ESA and Time History Analysis (THA), click **Compare with THA**. The comparison result is shown in **Fig. 134**. However, the comparison is only available for ESA for the longitudinal components of the input motions (Fig. 133).
The procedure of the bridge longitudinal ESA is as follows:

1. Specify a load F of the total weight (see below for now to calculate the total weight), do pushover and get a displacement d
2. Calculate the Stiffness $K = F/d$
3. Calculate the Period $T = 2\pi$ sqrt(M/K)
4. From the spectral acceleration of the input motion, get Sa
5. Calculate $D_d = M*Sa/K$, and this is the elastic displacement demand.
6. Check the abutment displacement (D_d) compared to abutment yield displacement (D_y). If $D_d/D_y<2$, stop, D_d is the demand. If $D_d/D_y> 4$, set abutment spring to 0.1*its initial stiffness, recalculate the displacement demand (D_d). If $2 <D_d/D_y< 4$, linearly interpolate abutment stiffness between its full and 0.1 values and ratios of 2 and 4, then recalculate the displacement demand.

The whole bridge system is employed in the bridge longitudinal ESA. As such, the pushover load is applied at the bridge center along the bridge deck (longitudinal) direction.

The total weight is equal to the total deck weight plus ½ column weight. The deck weight should be distributed weight over span elements (or applied to nodes by tributary length). Column weight applied at the top column node or if more than one element is used per column, distributed to column nodes by tributary length.

9.2 Bridge Transverse Direction

To conduct an ESA for the bridge transverse direction, click Transverse Direction in the main window (Fig. 132). The output is shown in Fig. 135.
Only one single bent is employed in the bridge transverse ESA. As such, the pushover load is applied at the bent cap center along the bent cap direction (bridge transverse direction).
The total weight is equal to the deck weight of left half span and right half span for the bent plus ½ column weight.

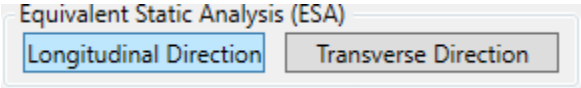

Fig. 132. Equivalent Static Analysis for the bridge longitudinal & transverse directions

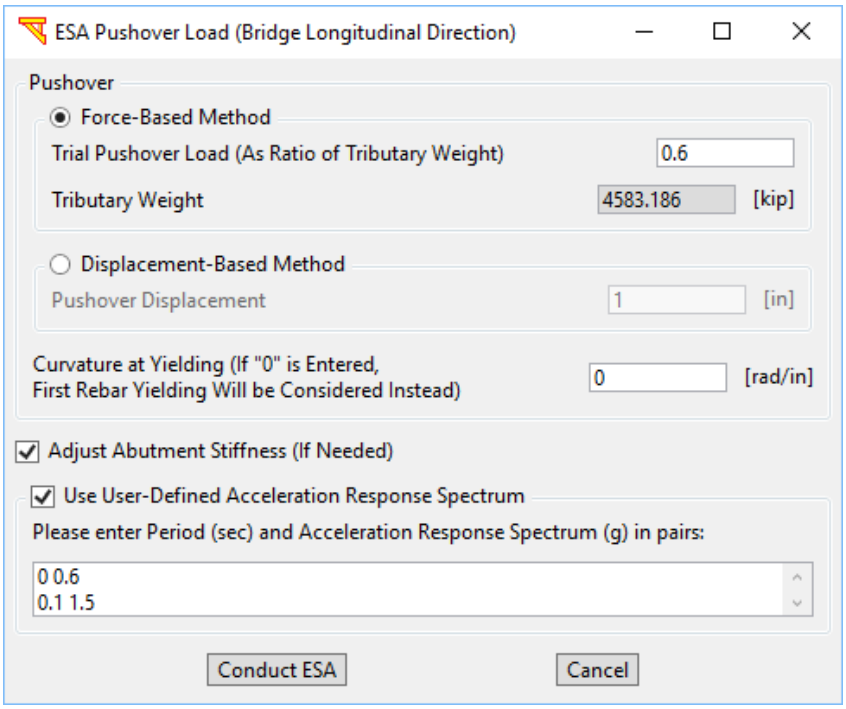

a)

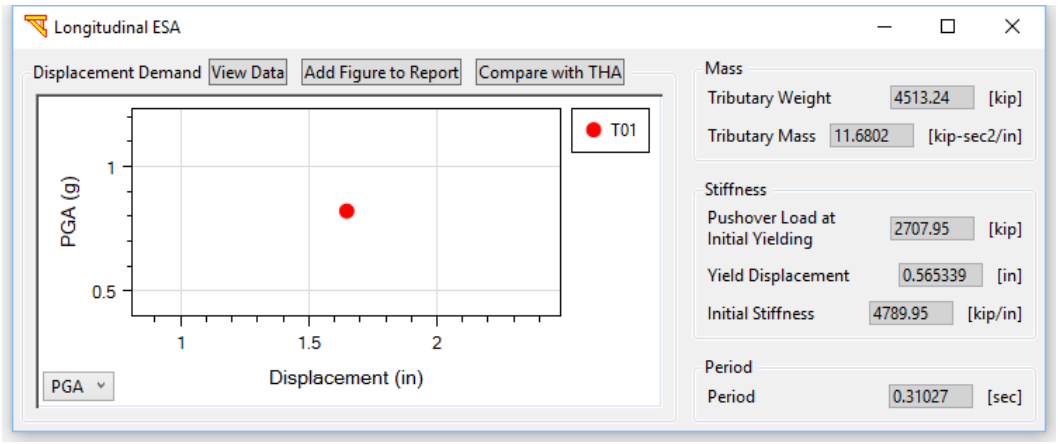

b)

Fig. 133. Longitudinal ESA: a) pushover load; b) elastic displacement demand

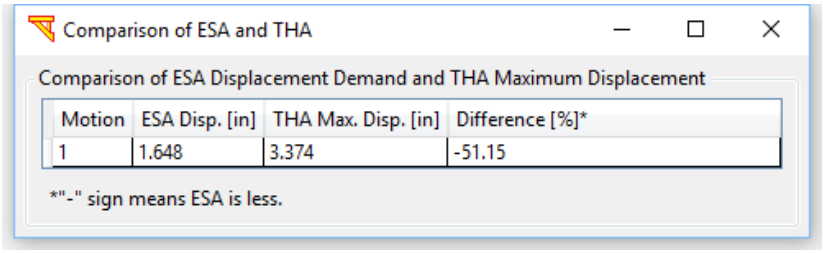

Fig. 134. Comparison of displacements from ESA and THA

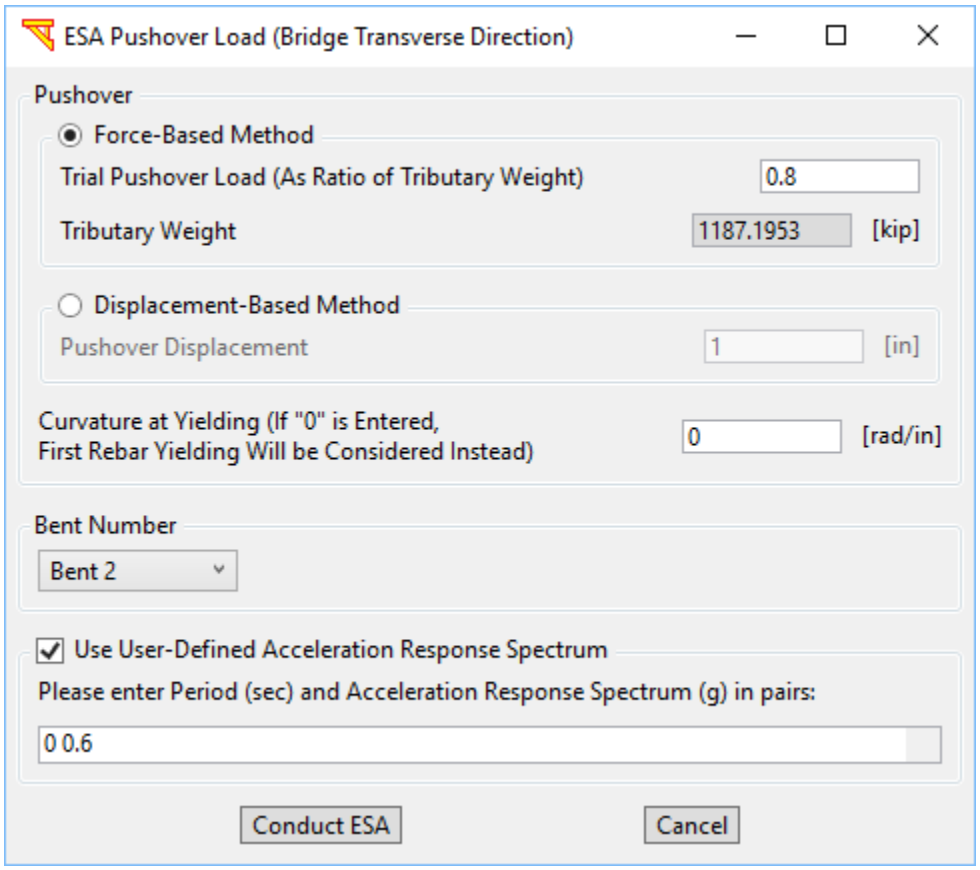

a)

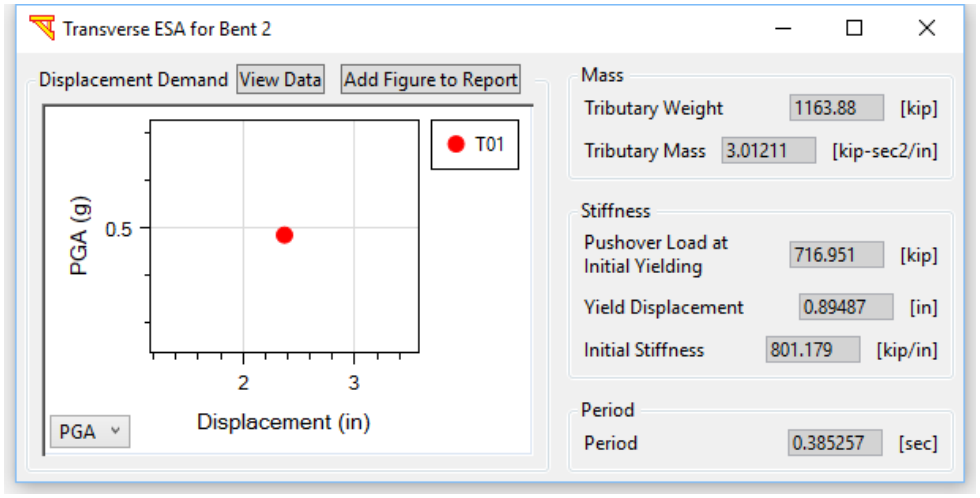

b)

Fig. 135. Transverse ESA: a) pushover load and bent number; b) elastic displacement demand

10 ANALYSIS OF IMPOSED DISPLACEMENTS

10.1 Imposed Soil Displacement

Imposed displacement option is available in MSBridge to study the soil movement for the bridge longitudinal, transverse and vertical directions. This option has been added to perform the pushover analysis with varying displacements along the pile height. Therefore, soil springs foundation model must be selected to activate this option. As such, the deformation due to liquefaction-induced lateral spreading can be applied as per Caltrans guidelines found in MTD 20-15 (Caltrans 2017).

To conduct the pushover analysis of soil movements, click **Imposed Displacement** in the main window (Fig. 2). The soil displacement profile layout is shown in Fig. 136. According to the simplified procedure (Caltrans 2017), application of the permanent lateral ground displacement follows the pattern displayed in Fig. 137, where the soil above the liquefied layer moves as a rigid block (constant displacement) and the displacement decreases constantly in the liquefied layer, with zero displacement below.

To define the normalized displacement profile, the displacement time history functions should be first defined, click **Define Time History Functions**. As such, each function corresponds to a value in the normalized displacement profile that will be reached after a certain number of steps (Fig. 138a). By default, **Function 1** and **Zero Displacement** are defined for the values of unity and zero, respetively, then the user should define the linearly interpolated functions along the thickness of the liquefied layer as according to the existing soil spring nodes. After that, the functions should be assigned at different nodes along the pile height (Fig. 138b). To do that, click **Define Layout.**

To account for a wide range of displacement values that resulted from applying different input motions and different values for each bent. Click **Define Displacement** to enter the displacement factors as according to the corresponding input motion (Fig. 139a) and click **Modify Displacement Factor** to enter the bent location factors (Fig. 139b). Fig. 140 shows the output in terms of the bridge deformed shape and pile response profile.

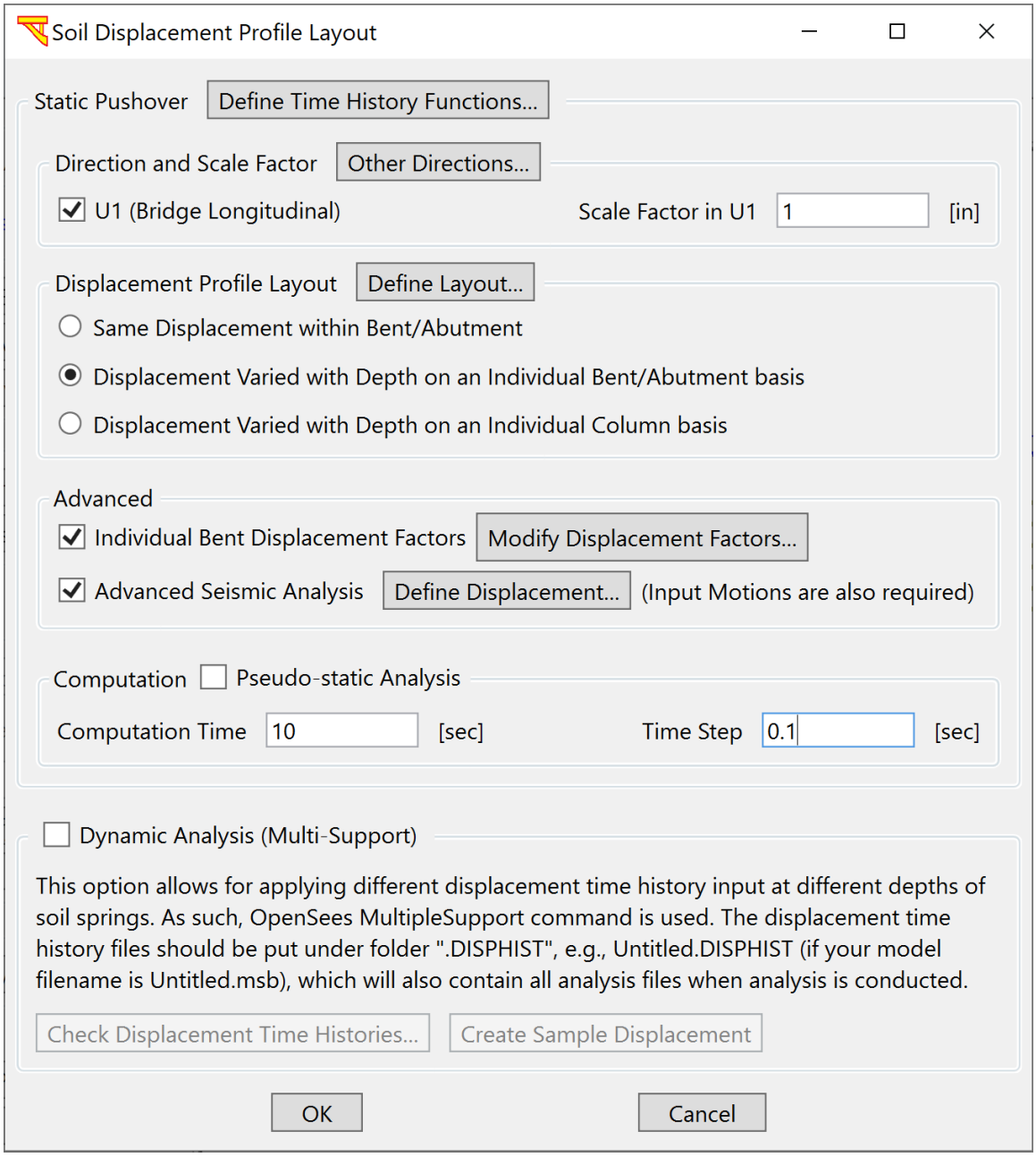

Fig. 136. Imposed displacement window

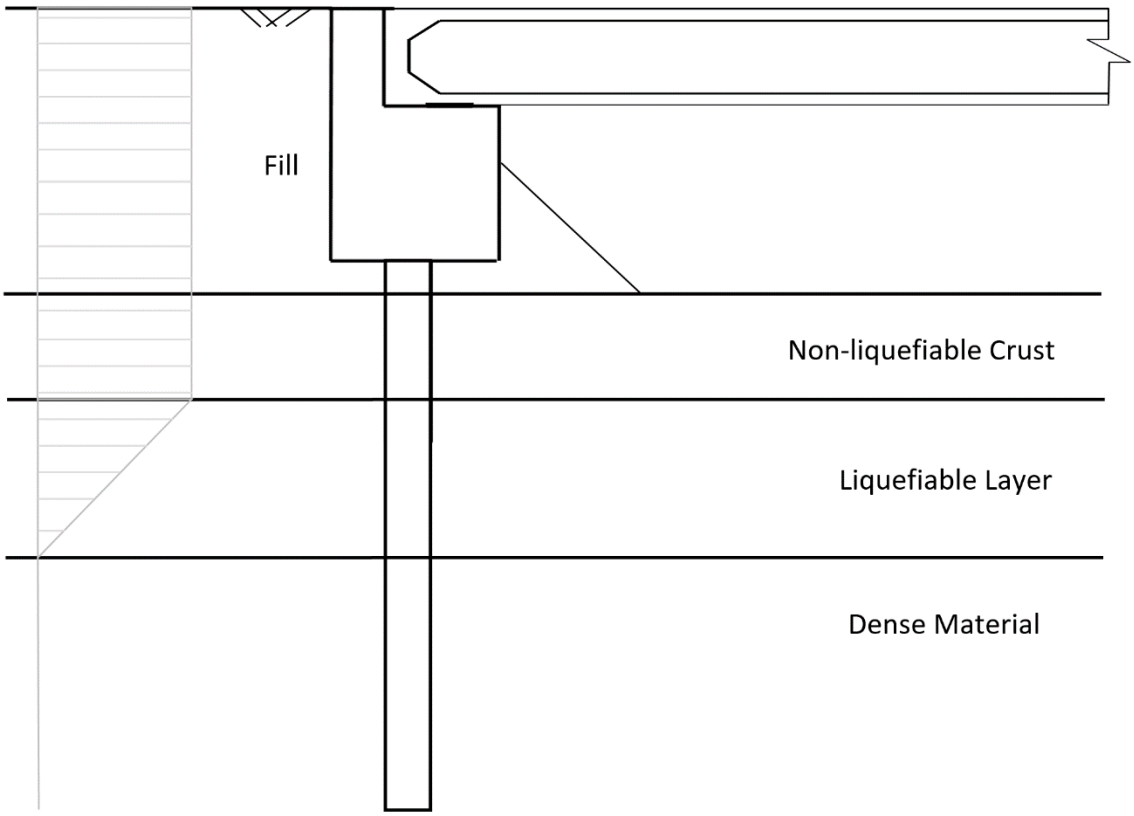

Fig. 137. Schematic abutment configuration and soil properties (not to scale)

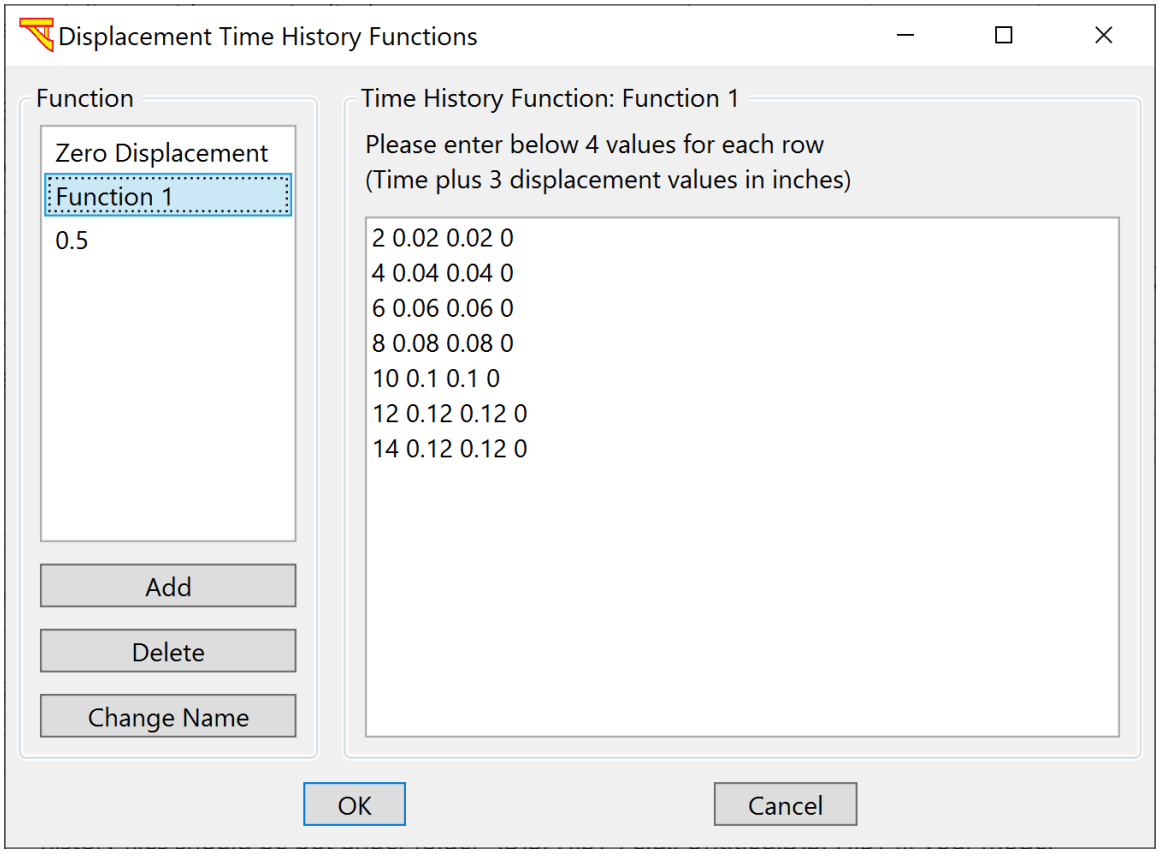
Displacement Time History Functions
Function
Zero Displacement
Function 1
0.5
Add
Delete
Change Name
Time History Function: Function 1
Please enter below 4 values for each row
(Time plus 3 displacement values in inches)
2 0.02 0.02 0
4 0.04 0.04 0
6 0.06 0.06 0
8 0.08 0.08 0
10 0.1 0.1 0
12 0.12 0.12 0
14 0.12 0.12 0
OK
Cancel

(a)

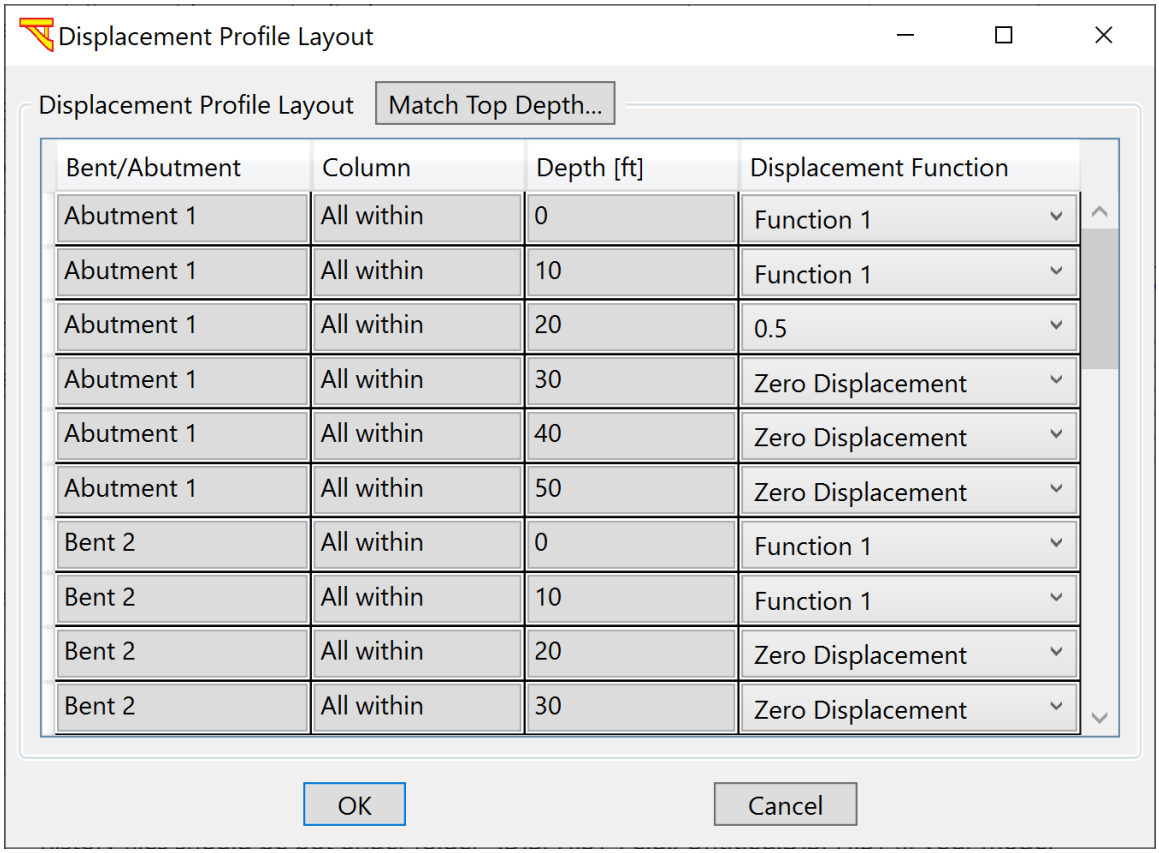

(b)

Fig. 138. Imposed displacement: (a) displacement time history functions; and (b) displacement profile layout

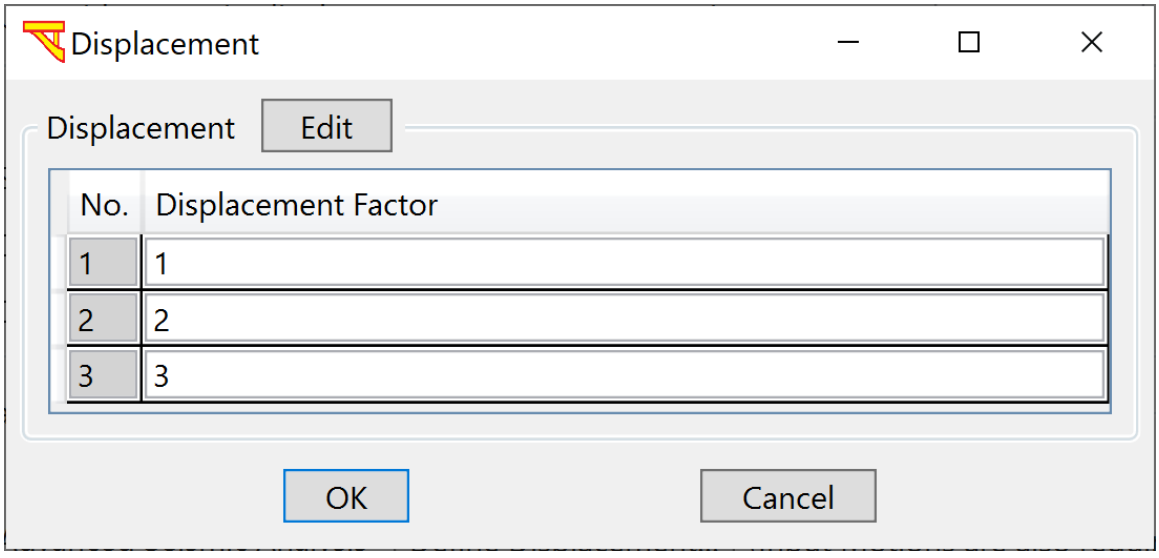

(a)

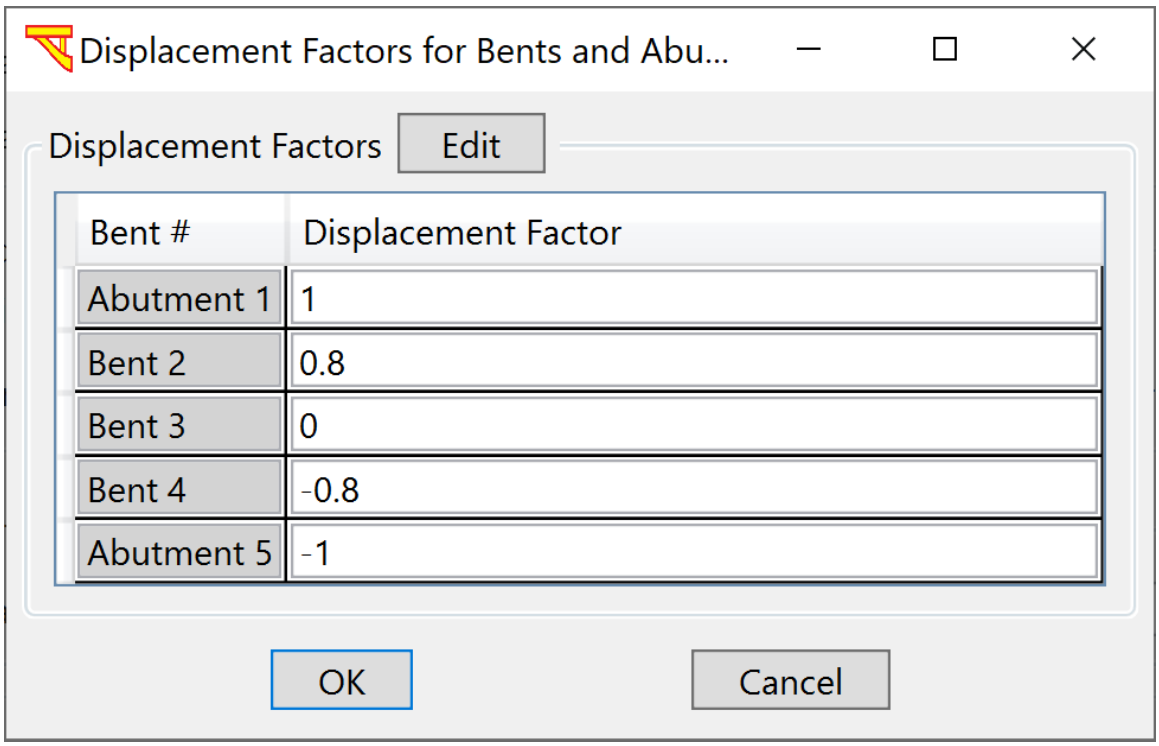

(b)

Fig. 139. Imposed displacement factors: (a) input motions factors; and (b) bents factors;

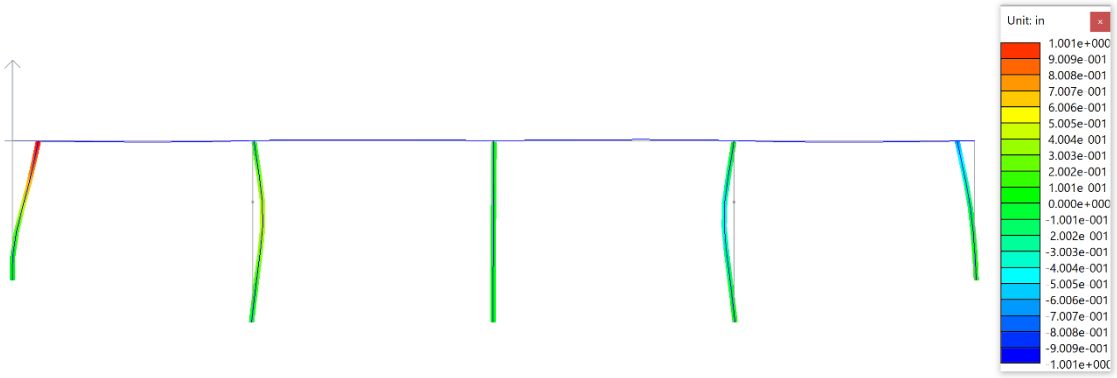

(a)

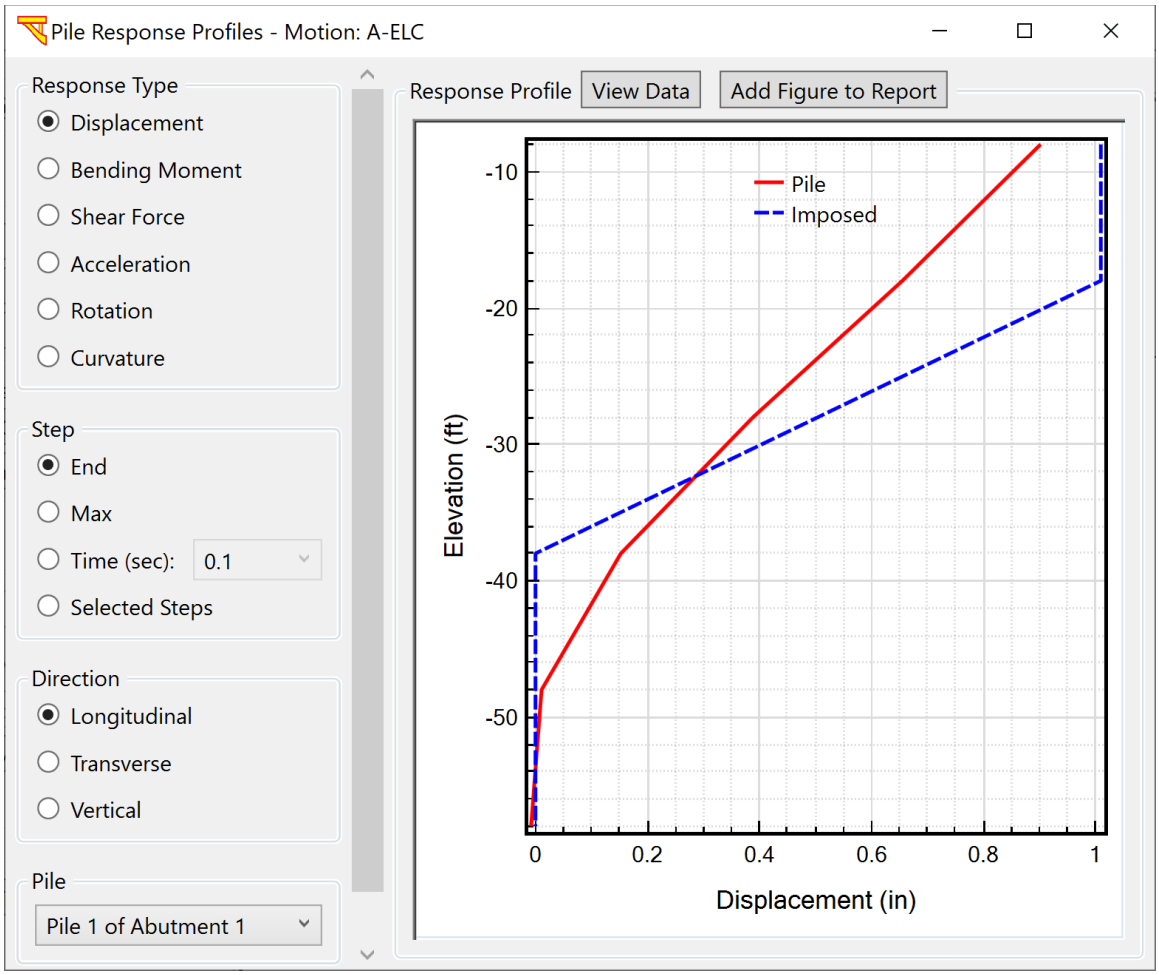

(b)

Fig. 140. An output of imposed displacement for the longitudinal bridge direction: a) deformed shape; and b) pile response profile

10.2 Pile Analysis

To conduct liquefaction analysis for single pile, click Pile Analysis in the main window (Fig. 2). The output is shown in Fig. 141. The displacement profile should be first defined. Click Imposed Soil Movement to enter the values of the imposed displacement, crust height, and the thickness of the liquefied layer (). As such, the profile will be defined as according to the MTD 20-15. Click **Pile-Head Loading** and **Analysis Options** to define the applied loading at the pile head and number of loading steps, respectively (Fig. 142).

To start the analysis, click Analyze. The results in terms of the pile response and soil spring response will be available as shown in Fig. 143.

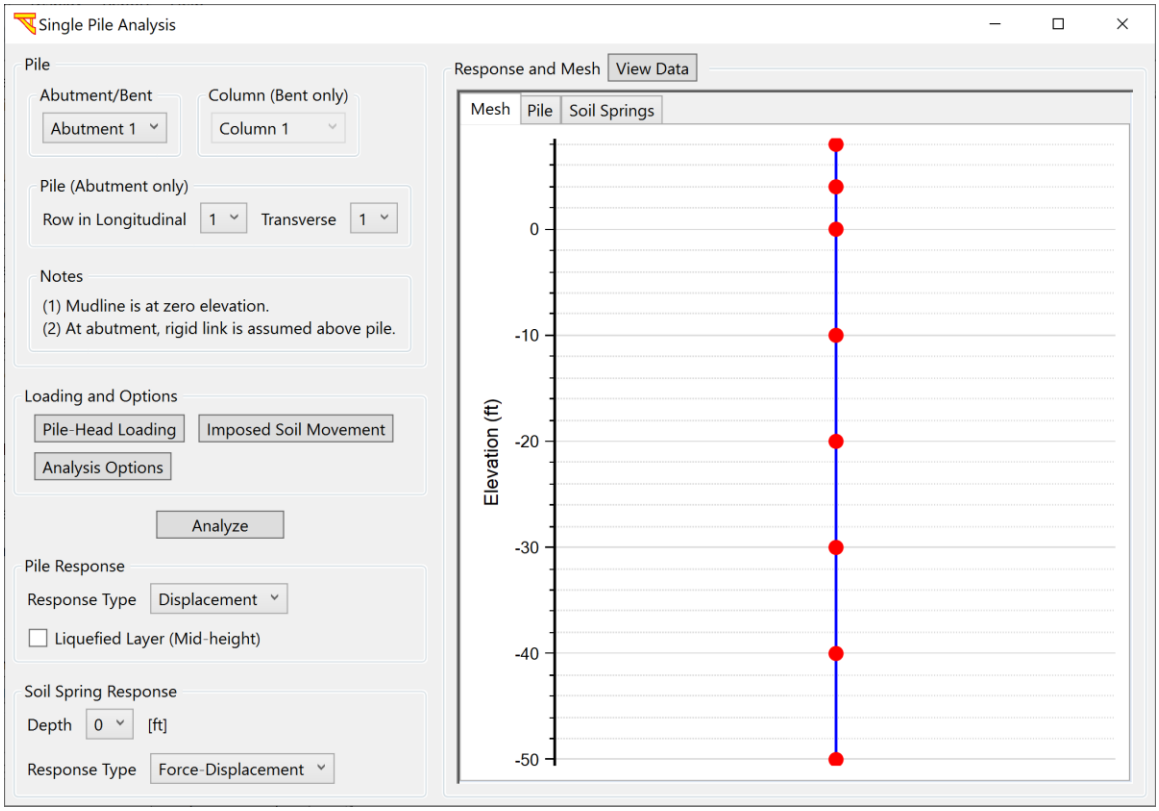

Fig. 141. Pile Analysis window

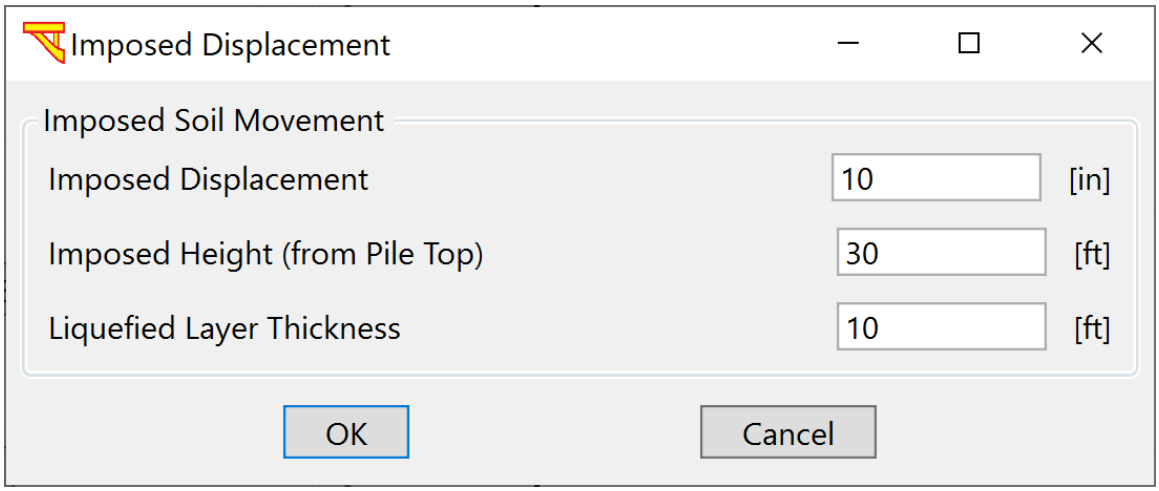

(a)

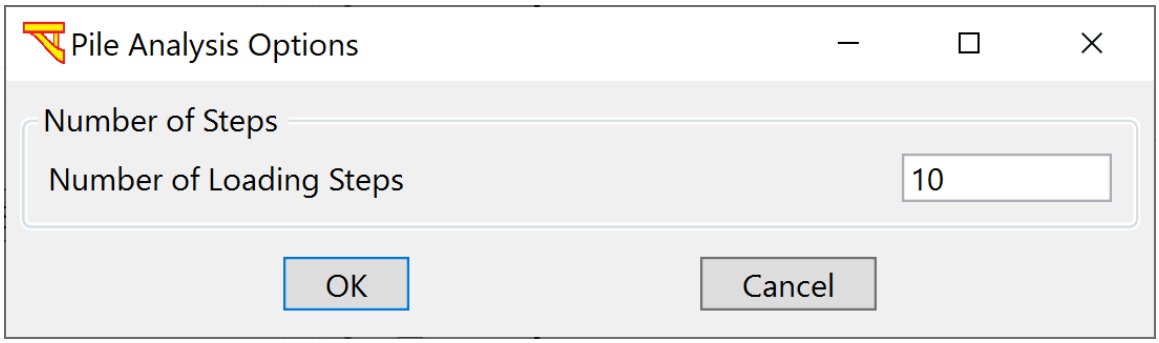

(b)

Fig. 142. Pile Analysis inputs: (a) Pile loading; and (b) Pile Analysis options

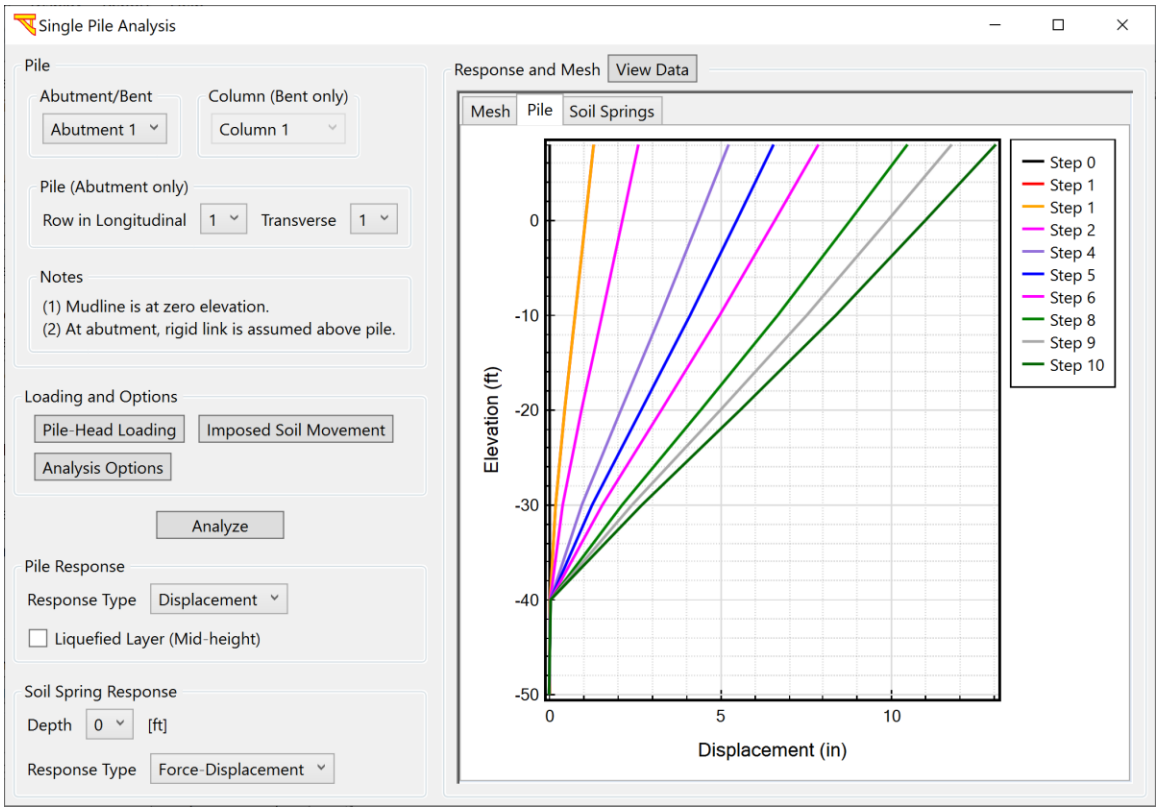
Single Pile Analysis
Pile
Abutment/Bent
Abutment 1
Column (Bent only)
Column 1
Pile (Abutment only)
Row in Longitudinal
1
Transverse
1
Notes
(1) Mudline is at zero elevation.
(2) At abutment, rigid link is assumed above pile.
Loading and Options
Pile-Head Loading
Imposed Soil Movement
Analysis Options
Analyze
Pile Response
Response Type
Displacement
Liquefied Layer (Mid-height)
Soil Spring Response
Depth
0
[ft]
Response Type
Force-Displacement
Response and Mesh
View Data
Mesh
Pile
Soil Springs
Elevation (ft)
0
-10
-20
-30
-40
-50
0
5
10
Displacement (in)
Step 0
Step 1
Step 1
Step 2
Step 4
Step 5
Step 6
Step 8
Step 9
Step 10

(a)

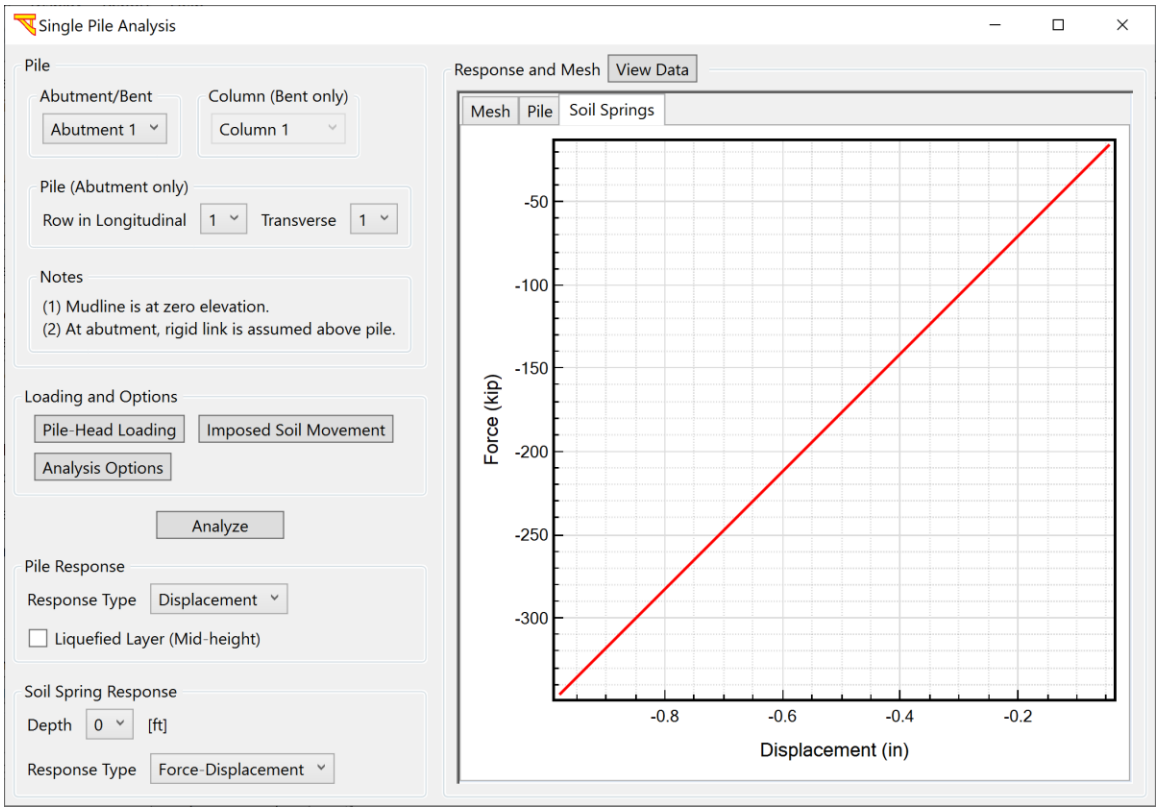

(b)

Fig. 143. Pile Analysis outputs: (a) Pile Response; and (b) Soil Spring Response

11 PBEE ANALYSIS (GROUND SHAKING)

To conduct a single earthquake analysis or a full PBEE analysis, click on the "Ground Shaking" option under Analysis Type (Fig. 2). For that purpose, the input earthquake excitation(s) must be specified. Input files at http://soilquake.net/msbridge that exercise this option include Examples 2 and 4. If only one earthquake record is selected out of a specified ensemble (suite) of input motions, then a conventional single earthquake analysis will be performed.

11.1 Theory and Implementation of PBEE Analysis

In the user interface, an implementation of the Pacific Earthquake Engineering Research (PEER) Center's performance-based earthquake engineering framework (Cornell and Krawinkler, 2000) is used to generate probabilistic estimates of repair cost and repair time. The PEER PBEE framework utilizes the total probability theorem to compute the desired probability distributions by disaggregating the task into several intermediate probabilistic models with different sources of randomness and uncertainty. The hazard model uses earthquake ground motion data to determine an intensity measure (IM). The demand model uses response from dynamic analysis to determine an engineering demand parameter (EDP). The damage model connects the EDP to a damage measure (DM). Then, the DM is linked to consequences that are termed the decision variables (DV). Repair cost and repair time can be thought of as two possible decision variable (DV) outcomes characterized probabilistically by the framework.

The complete analysis is accomplished using the local linearization repair cost and time methodology (LLRCAT), described by Mackie et al. (2010) and depicted conceptually in Fig. 144. In the LLRCAT methodology, each bridge system is disaggregated into independent structural or non-structural components or subassemblies defined as performance groups (PGs) that are damaged, assessed, and repaired together using a specific combination of different repair methods. Demands on the bridge system (and components) are determined using 3D nonlinear time history analysis under multiple-component earthquake excitation. The damage in each of the PGs is characterized according to several discrete damage states (DSs) that are defined by distributions of critical EDPs.

A feature of the LLRCAT implementation used is the introduction of a repair model between the original PEER abstraction of DM and DV. Jumping directly from DMs to repair costs is difficult to accomplish because it skips over the details of repair design and the variability of cost and time estimating. Creating these two additional models makes it easier to implement a step-by-step procedure for defining the models. The repair model and cost model are created through the process of schematic design of repairs and estimating the costs of those designs. Different repair methods are employed for the various damage states of each PG or bridge component. The repair methods for each PG require a combination of several repair quantities (Qs). Repair quantities for all PGs are then combined with due consideration of the correlation between components. Repair costs (RC) are obtained through a unit cost (UC). Repair times (RT) are obtained through

a production rate (PR). The PRs are in terms of crew working days (CWD), representing one working day for a normal sized crew and can be combined later by construction management experts to obtain total site construction times.

$$\text{Repair cost: } \lambda(RC > rc) = \int_{im}\int_{dm}\int_{edp} G(uc \cdot q \mid dm)\, dG(dm \mid edp)\, dG(edp \mid im) \left| d\lambda(im) \right|$$

$$\text{Repair time: } \lambda(RT > rt) = \int_{im}\int_{dm}\int_{edp} G(lpr \mid dm)\, dG(dm \mid edp)\, dG(edp \mid im) \left| d\lambda(im) \right|$$

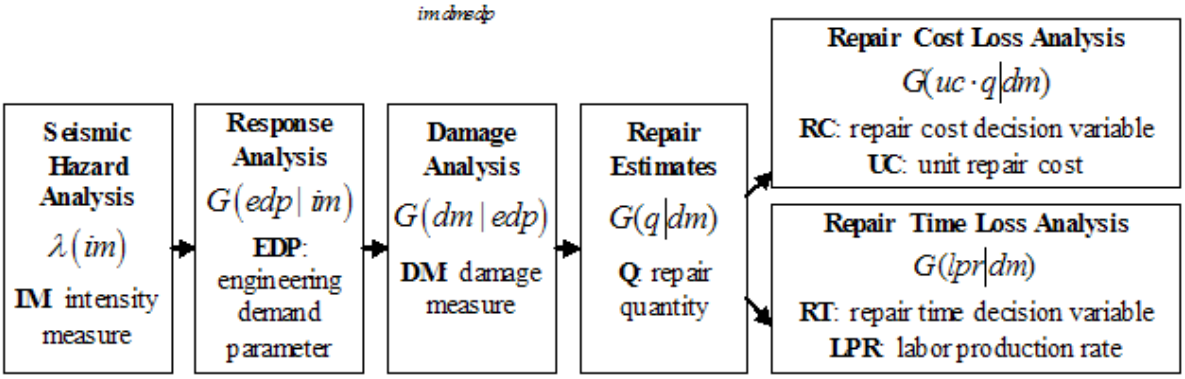

Fig. 144. Schematic procedure of the LLRCAT methodology for a single bridge component

The characterization and visualization of the ground motion suites using different choices of IMs will be discussed in Section 7.1. The FEM, parameter selection, analysis options, and outcomes that generated EDPs were similarly covered in Section 3. The bridge is then broken down into performance groups (PGs) for each major bridge superstructure, substructure, and foundation component. Each performance group represents a collection of structural components that act as a global-level indicator of structural performance and that contribute significantly to repair-level decisions. Performance groups are not necessarily the same as load-resisting structural components. For example, non-structural components may also form a performance group, since they also suffer damage and contribute to repair costs. The notion of a performance group also allows grouping several components together for related repair work. For example, it is difficult to separate all of the individual structural components that comprise a seat-type abutment (shear key, back wall, bearings, approach slab, etc.) as they all interact during seismic excitation and their associated repair methods are coupled. Therefore, the abutment repair group incorporates the fact that repairs to the back wall require excavation of the approach slab.

Performance groups also address the issue of potentially double counting related repair items. Some repair items require the same preparation work such as soil excavation. For example, both back wall repair and enlargement of an abutment foundation require at least 4 ft of excavation behind the back wall. If these repair items were in different PGs, then double counting the excavation would be a problem. Bundling these related repair methods within a PG allows for independent consideration of each PG. The correlation between repair items from the PGs is handled at the demand model level in the

methodology. A total of 11 PGs are considered: PG1: Max column drift ratio; PG2: Residual column drift ratio; PG3: Max relative deck-end/abutment displacement (left); PG4: Max relative deck-end/abutment displacement (right); PG5: Max bridge-abutment bearing displacement (left); PG6: Max bridge-abutment bearing displacement (right); PG7: Approach residual vertical displacement (left); PG8: Approach residual vertical displacement (right); PG9: Abutment residual pile cap displacement (left); PG10: Abutment residual pile top displacement (right); PG11: Column residual pile displacement at ground surface.

Discrete DSs are defined for each PG. Damage states are numbered sequentially in order of increasing severity. The DS0 damage state corresponds to the onset of damage when repair costs begin to accumulate. An upper limit to the quantities and costs is called DS∞ because it corresponds to the most severe possible damage state for the elements in a PG. DS∞ usually corresponds to complete failure and replacement of all the elements in the entire PG. The DSs are connected to structural demands obtained from finite element analysis results by way of an EDP specific to each PG. The repair quantities associated with each DS are developed more fully in the definition of the damage scenarios. All the PGs and DSs are linked to a single EDP in this implementation.

Based on previous work, the methodology was calibrated for defining the post-earthquake performance of select bridges that fall within the class of ordinary post-tensioned, box girder, reinforced concrete highway overpasses (Mackie et al. 2011). The three major components required for this calibration were damage scenarios that describe particular instances of earthquake damage, schematic design of bridge repairs to address the state of damage in the scenarios, and the link between repair design, methods and procedures, and subsequent quantities. There is a direct link between damage scenarios and the repair, i.e., there is a single repair procedure for a single state of damage. The repair quantity results were parameterized in terms of basic bridge geometry and properties so that they can be used to extrapolate loss modeling for other bridges in the same class (such as those that can be built within the user interface).

Data for time and monetary repair costs were obtained by estimating the costs of the damage and loss scenarios using published Caltrans construction estimation data, case studies from previous earthquakes, and interviews with Caltrans bridge engineers. Monetary costs were adjusted to 2007 values based on Caltrans cost index data. Repair costs are estimated for each damage scenario based on quantities of each repair item. Cost estimates accounted for variations in unit cost, and the details involved in estimating a combination of repairs together. The benefit of separating the Qs from costs is that the unit cost model is easily updated for new years of data, local economic conditions, site accessibility, and incentives.

Normalized costs of repair are obtained by using the repair cost ratio (RCR) between the cost of repair and the cost of replacement cost (does not include demolition). It is shown in %, and it can range between 0 and some number higher than 100% (there is no reason why it is bounded by replacement cost; this is purely an owner/operator decision). This ratio is useful for comparing the performance of different bridge design options for new

construction. For the evaluation of existing structures, the RCR including demolition costs might be more useful. Constructing a new bridge on the same site after an earthquake would require both demolitions of the damaged bridge and construction of its replacement. The costs of new construction used in the interface come from Caltrans bridge cost estimates used for planning purposes. They are based on the deck and type of construction, providing a range of cost/SF of deck area, circa 2007 to be consistent with the repair data used.

Repair time for the bridge can be expressed either as an approximation of repair duration or repair effort. The repair effort represents the total number of crew-workdays (CWD) required to complete the task. This is different from repair duration, which counts the total duration of the repair project. The repair duration includes the effect of scheduling concurrent on-site construction processes, while the repair effort does not. The repair duration can vary based on the amount and type of concurrent construction processes, schedule dependencies, availability of labor, and whether or not contract incentives are provided in order to decrease duration. Repair times are also computed on the basis of each repair quantity Q. For any repair item, a probability of 50% that Q > tolerance indicates that the associated repair time should be added to the total repair time for the project (the tolerance is set at a value of 3% of $Q_{n,max}$).

11.2 Input Necessary for User-defined PBEE Quantities

If the user is interested in providing user- or project-specific information in a PBEE analysis, the following paragraphs describe the data needed by the interface to execute the PBEE analysis and post-process the results. Performance groups need to be defined for each important component or subassembly of the system that has potential repair consequences. Performance groups are defined in terms of a single EDP that characterizes the response of this PG. Once this EDP metric has been defined and time history analysis performed to obtain a distribution of EDP realizations for different ground motions, the PBEE methodology can be implemented. The PBEE methodology requires definitions (by the user) of discrete damage states for each PG, a repair method with associated repair quantities for each discrete DS for each PG, and the corresponding costs and times required to execute the repair method.

The damage states are discrete and supplied in the form of what is commonly called a fragility curve. This is a misnomer, however, because the information required is the value of the EDP (not IM) required to trigger different probabilities of exceeding the given discrete DS. It is often assumed that said curves are well described by the lognormal probability distribution and therefore, the only parameters required are the two lognormal distribution parameters: lambda and beta. Lambda is the median and beta is the lognormal standard deviation. A PG can have as many discrete DS as are required to cover the full range of possible responses experienced by the PG. These should be input as is shown in Section 11.5.1.

Once the different states of damage have been established, damage scenarios need to be generated that show different possible “snapshots” of damage that the structure may be in

after an earthquake event. Once these scenarios have been generated (note the scenarios need to be detailed and include exact descriptions of the extent and depth of damage), they can be used to decide what repair method would be appropriate for each PG or group of PGs. Such information is specific to the type of structure, the discrete DSs, and the PGs. It is only obtainable from experts with past experience designing repair procedures given a damage scenario or snapshot. Once the repair methods have determined, specific details about the repair quantities (specific meaning square footage of deck, cubic yards of concrete, etc.) can be specified. The current data employed in the interface has repair quantities parameterized in terms of the common bridge design and geometric parameters, making it possible to solve for a variety of bridges within the class. However, any changes beyond these configurations would require numerical values for all the repair quantities to be input.

It is assumed that the repair quantity estimates for each PG and DS are also random quantities and can be described by a mean (or median) value and a coefficient of variation or lognormal standard deviation. In the interface, beta has been set as 0.4, but could be modified by the user in the future (if so desired). The repair quantities may then be handed over to a cost estimator, who would have the ability to access historical pricing and bid information. In addition, the type and magnitude of each repair quantity would correspond to standard DOT estimates and specifications procedures. Each repair quantity can then be bid, or an estimation of cost and effort/time/production rate made. These unit costs and production rates are also random quantities and can be described by a mean (or median) value and a coefficient of variation or lognormal standard deviation. The values currently in the interface all have a beta of 0.2 but could again be set by the user if desired. See more details about PERT criteria for the production rates in Mackie et al. (2008).
Modifying the default PBEE quantities (repair quantities, unit costs, and production rates) is detailed in Appendix E.

11.3 Definition/specification of PBEE input motion ensemble (suite)

This section presents the definition and specification of PBEE input motions. The input motions represent a wide range of intensity measures to perform the analysis. More details about the ground motions and their specifications can be found in chapter 7.

11.4 Save Model and Run Analysis

After defining the finite element model, click on "**Save model and run analysis**". The finite element computations will start, for several earthquakes at a time as specified in Fig. 110, the user can select as many as 8 records to be run at the same time in order to reduce the overall run time (for dual core machines or better). Fig. 116 shows the analysis progress for each record.

11.5 PBEE Analysis

Once the FE analysis of all motions in the ensemble is complete, click **PBEE Analysis** (Fig. 2) to display:

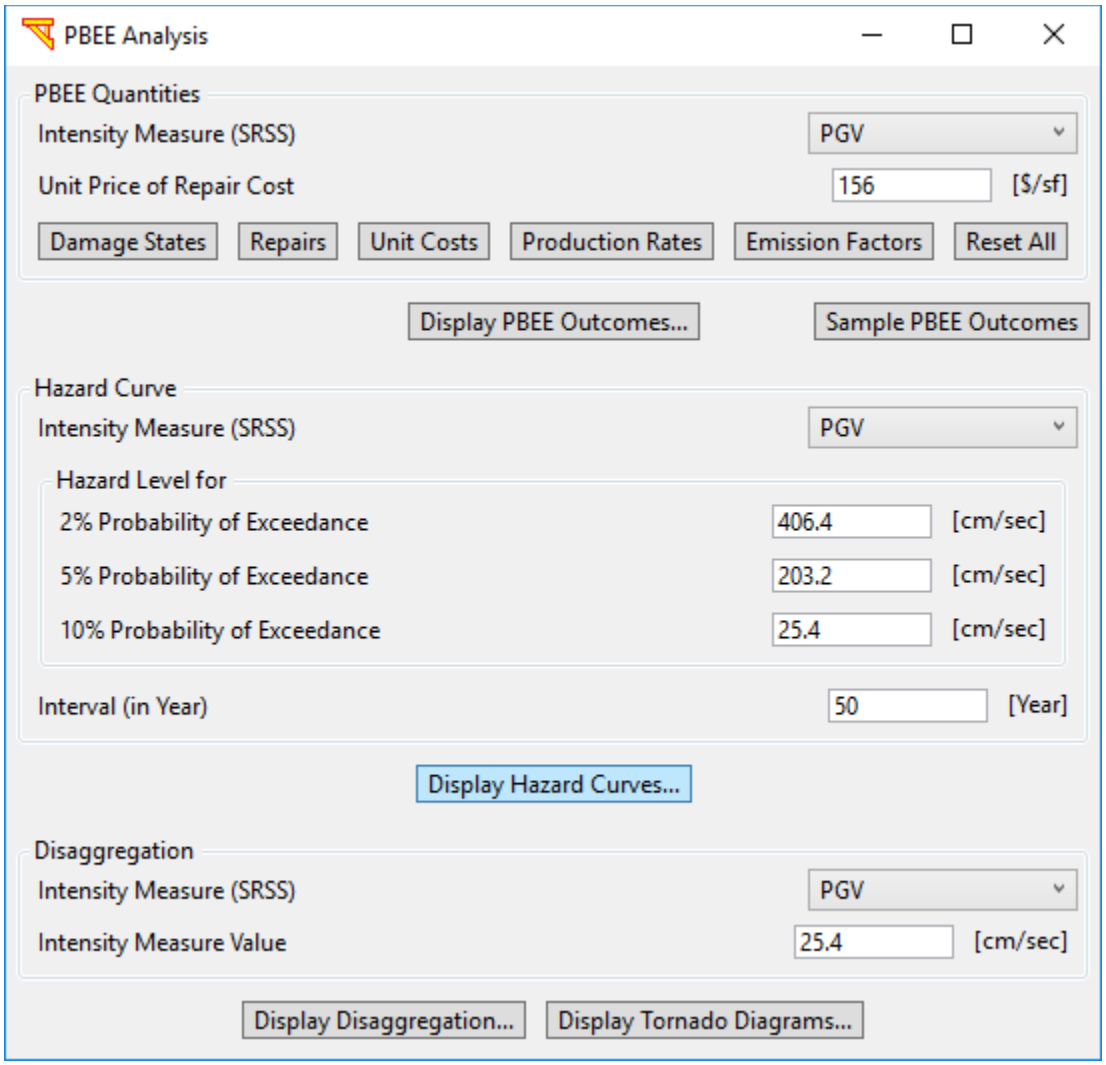

Fig. 145. PBEE analysis window

11.5.1 PBEE Quantities

In the figure above (Fig. 145), under Damage States (Fig. 146), Lambda is the median EDP that defines onset of the damage state and is one parameter of the assumed lognormal distribution of damage when conditioned in EDP. It has the same units as the EDP for the selected PG. Beta is the lognormal standard deviation and is the second parameter of the assumed lognormal distribution. Hence beta is dimensionless and has a typical range between 0 and 1 (although it is not bounded by 1). This parameter is closely related to the coefficient of variation (standard deviation normalized by the mean) under

certain conditions (small beta values). In addition, the Repairs, Unit Costs, Production Rates, and Emission Factors are displayed in Fig. 147-Fig. 150, respectively.

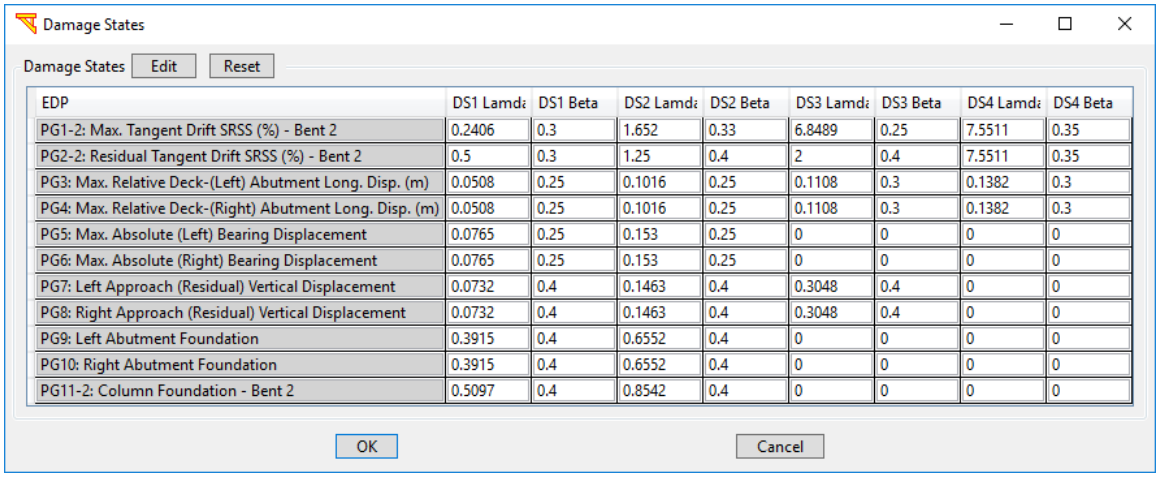

EDP	DS1 Lamda	DS1 Beta	DS2 Lamda	DS2 Beta	DS3 Lamda	DS3 Beta	DS4 Lamda	DS4 Beta
PG1-2: Max. Tangent Drift SRSS (%) - Bent 2	0.2406	0.3	1.652	0.33	6.8489	0.25	7.5511	0.35
PG2-2: Residual Tangent Drift SRSS (%) - Bent 2	0.5	0.3	1.25	0.4	2	0.4	7.5511	0.35
PG3: Max. Relative Deck-(Left) Abutment Long. Disp. (m)	0.0508	0.25	0.1016	0.25	0.1108	0.3	0.1382	0.3
PG4: Max. Relative Deck-(Right) Abutment Long. Disp. (m)	0.0508	0.25	0.1016	0.25	0.1108	0.3	0.1382	0.3
PG5: Max. Absolute (Left) Bearing Displacement	0.0765	0.25	0.153	0.25	0	0	0	0
PG6: Max. Absolute (Right) Bearing Displacement	0.0765	0.25	0.153	0.25	0	0	0	0
PG7: Left Approach (Residual) Vertical Displacement	0.0732	0.4	0.1463	0.4	0.3048	0.4	0	0
PG8: Right Approach (Residual) Vertical Displacement	0.0732	0.4	0.1463	0.4	0.3048	0.4	0	0
PG9: Left Abutment Foundation	0.3915	0.4	0.6552	0.4	0	0	0	0
PG10: Right Abutment Foundation	0.3915	0.4	0.6552	0.4	0	0	0	0
PG11-2: Column Foundation - Bent 2	0.5097	0.4	0.8542	0.4	0	0	0	0

Fig. 146. Damage states window

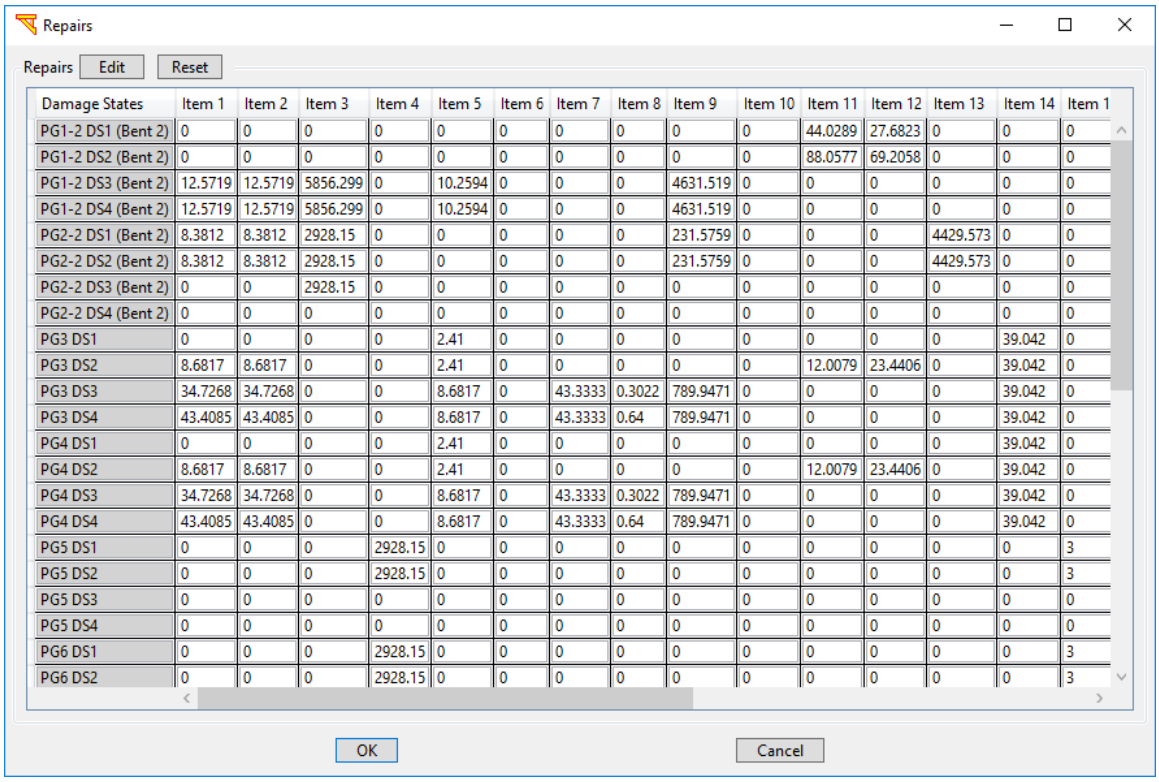

Damage States	Item 1	Item 2	Item 3	Item 4	Item 5	Item 6	Item 7	Item 8	Item 9	Item 10	Item 11	Item 12	Item 13	Item 14	Item 1
PG1-2 DS1 (Bent 2)	0	0	0	0	0	0	0	0	0	0	44.0289	27.6823	0	0	0
PG1-2 DS2 (Bent 2)	0	0	0	0	0	0	0	0	0	0	88.0577	69.2058	0	0	0
PG1-2 DS3 (Bent 2)	12.5719	12.5719	5856.299	0	10.2594	0	0	0	4631.519	0	0	0	0	0	0
PG1-2 DS4 (Bent 2)	12.5719	12.5719	5856.299	0	10.2594	0	0	0	4631.519	0	0	0	0	0	0
PG2-2 DS1 (Bent 2)	8.3812	8.3812	2928.15	0	0	0	0	0	231.5759	0	0	0	4429.573	0	0
PG2-2 DS2 (Bent 2)	8.3812	8.3812	2928.15	0	0	0	0	0	231.5759	0	0	0	4429.573	0	0
PG2-2 DS3 (Bent 2)	0	0	2928.15	0	0	0	0	0	0	0	0	0	0	0	0
PG2-2 DS4 (Bent 2)	0	0	0	0	0	0	0	0	0	0	0	0	0	0	0
PG3 DS1	0	0	0	0	2.41	0	0	0	0	0	0	0	0	39.042	0
PG3 DS2	8.6817	8.6817	0	0	2.41	0	0	0	0	0	12.0079	23.4406	0	39.042	0
PG3 DS3	34.7268	34.7268	0	0	8.6817	0	43.3333	0.3022	789.9471	0	0	0	0	39.042	0
PG3 DS4	43.4085	43.4085	0	0	8.6817	0	43.3333	0.64	789.9471	0	0	0	0	39.042	0
PG4 DS1	0	0	0	0	2.41	0	0	0	0	0	0	0	0	39.042	0
PG4 DS2	8.6817	8.6817	0	0	2.41	0	0	0	0	0	12.0079	23.4406	0	39.042	0
PG4 DS3	34.7268	34.7268	0	0	8.6817	0	43.3333	0.3022	789.9471	0	0	0	0	39.042	0
PG4 DS4	43.4085	43.4085	0	0	8.6817	0	43.3333	0.64	789.9471	0	0	0	0	39.042	0
PG5 DS1	0	0	0	2928.15	0	0	0	0	0	0	0	0	0	0	3
PG5 DS2	0	0	0	2928.15	0	0	0	0	0	0	0	0	0	0	3
PG5 DS3	0	0	0	0	0	0	0	0	0	0	0	0	0	0	0
PG5 DS4	0	0	0	0	0	0	0	0	0	0	0	0	0	0	0
PG6 DS1	0	0	0	2928.15	0	0	0	0	0	0	0	0	0	0	3
PG6 DS2	0	0	0	2928.15	0	0	0	0	0	0	0	0	0	0	3

Fig. 147. Repair quantities window

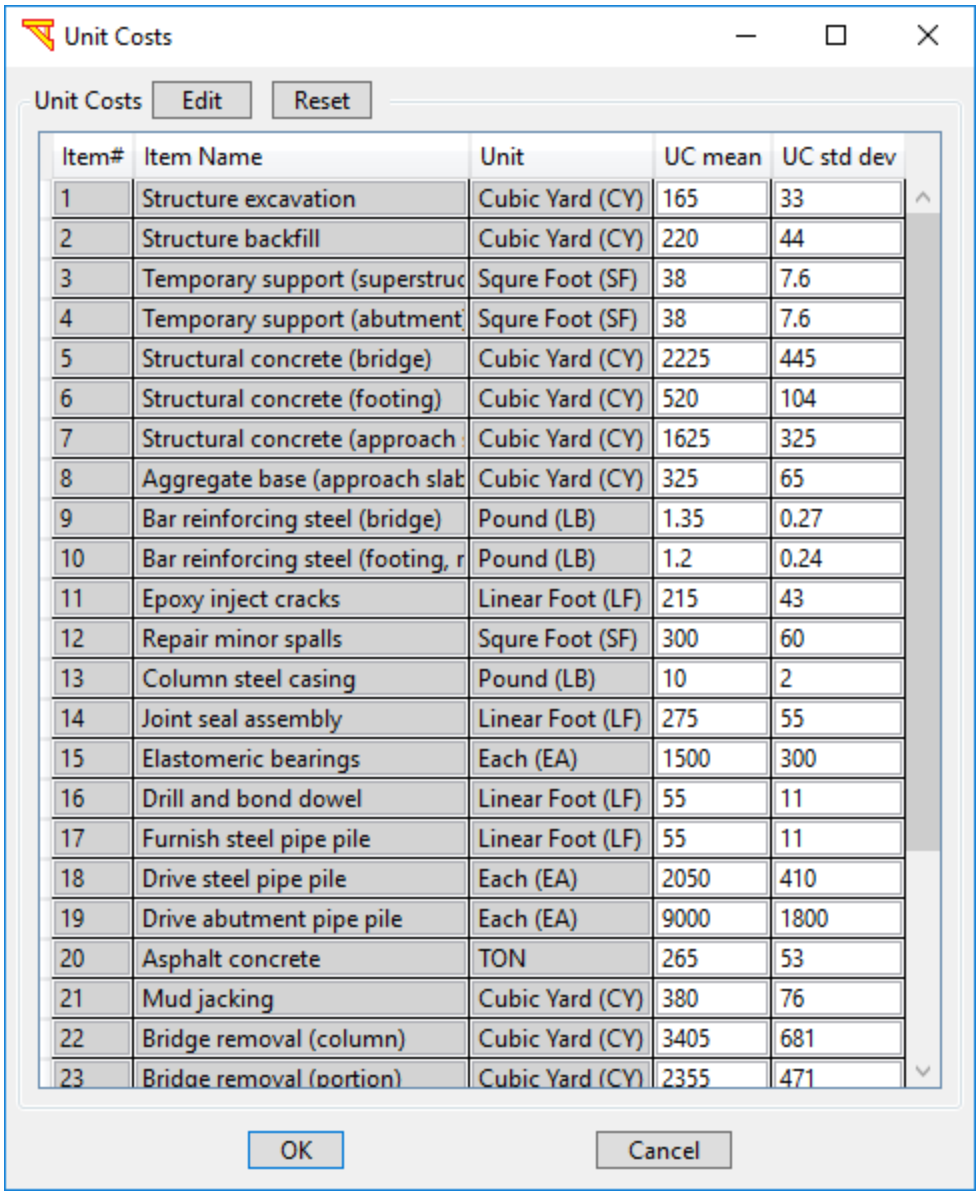

Fig. 148. Unit Costs window

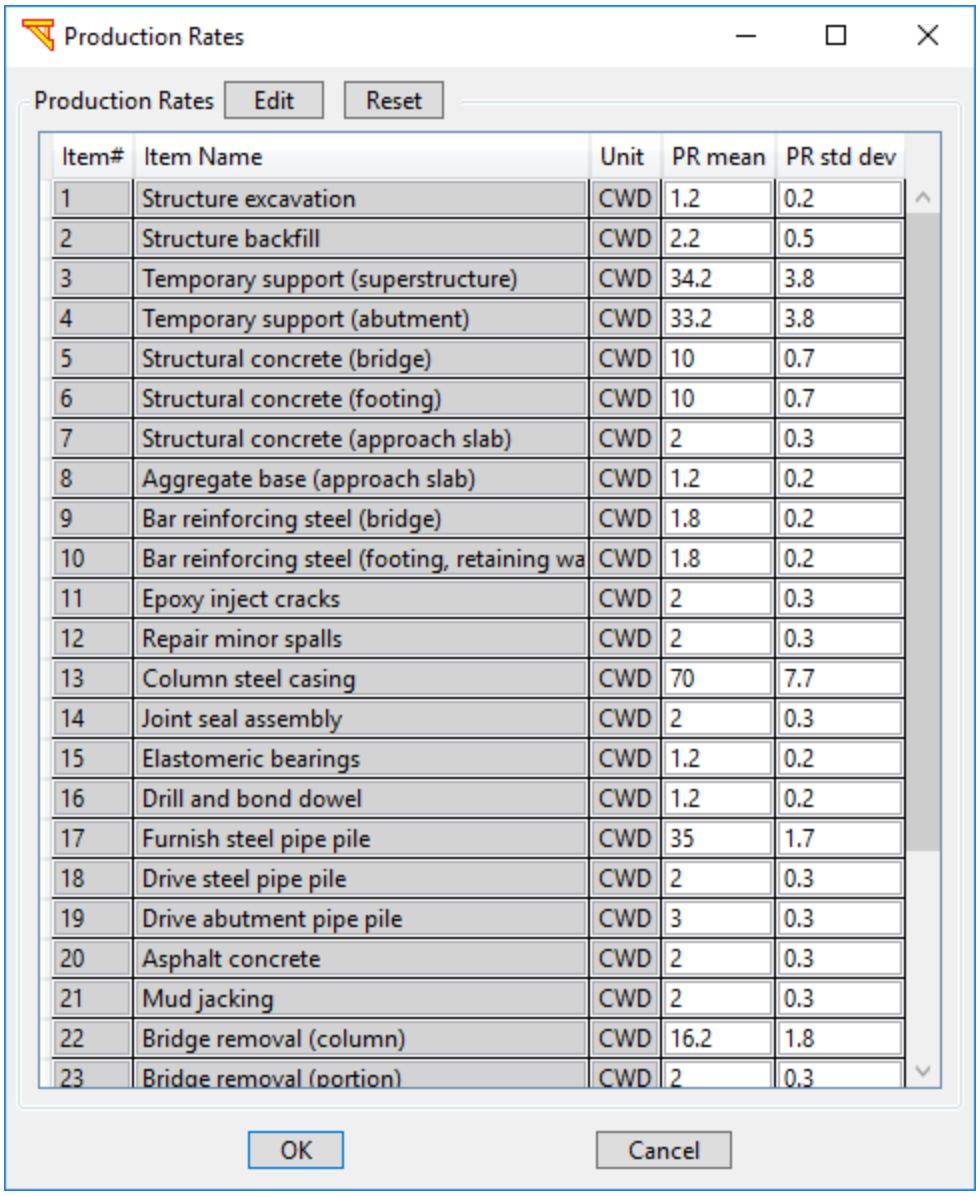

Fig. 149. Production Rates window

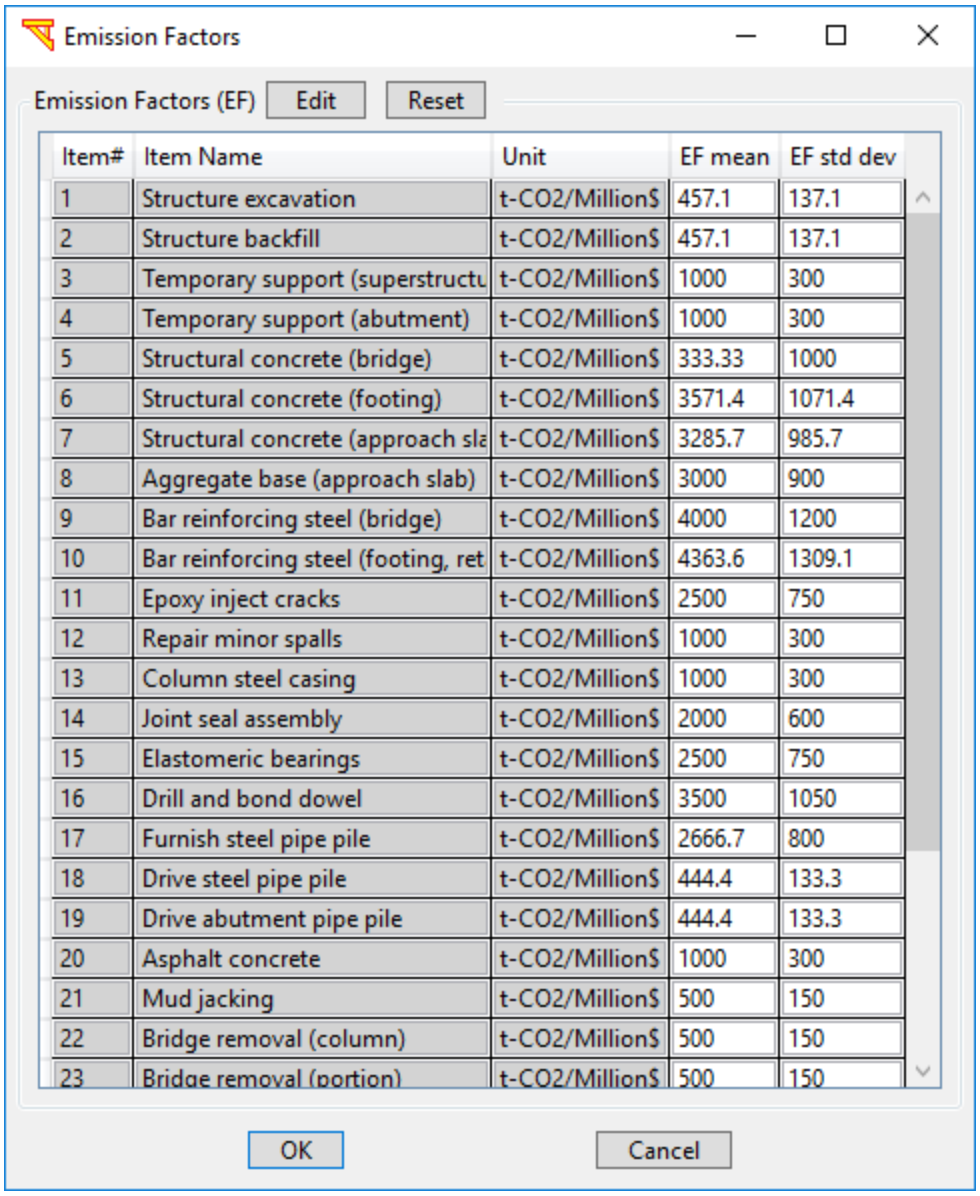

Fig. 150. Emission Factors window

11.5.2 Compute PBEE outcomes

Now, you can select any of the Intensity Measures (e.g., PGV above), and then click **Display PBEE outcomes** in Fig. 145 to display the probabilistic repair cost, Crew Working time in Days (CWD), and carbon footprint along with Standard Deviation, displayed for each PG (eleven of them) and each repair quantity (29 of them, see

Table 6), as shown below. See Section 12.3.1 for the detailed output.

Table 6. PBEE Repair Quantities

Item#	Item name
1	Structure excavation
2	Structure backfill
3	Temporary support (superstructure)
4	Temporary support (abutment)
5	Structural concrete (bridge)
6	Structural concrete (footing)
7	Structural concrete (approach slab)
8	Aggregate base (approach slab)
9	Bar reinforcing steel (bridge)
10	Bar reinforcing steel (footing, retaining wall)
11	Epoxy inject cracks
12	Repair minor spalls
13	Column steel casing
14	Joint seal assembly
15	Elastomeric bearings
16	Drill and bond dowel
17	Furnish steel pipe pile
18	Drive steel pipe pile
19	Drive abutment pipe pile
20	Asphalt concrete
21	Mud jacking
22	Bridge removal (column)
23	Bridge removal (portion)
24	Approach slab removal
25	Clean deck for methacrylate
26	Furnish methacrylate
27	Treat bridge deck
28	Barrier rail
29	Re-center column

11.5.3 Compute Hazard Curves

The user is also able to specify a Seismic Hazard for a particular geographic location of this bridge system in terms of specified values for any IM (e.g., derived from USGS seismicity maps). The interactive hazard deaggregation for a particular geographic location can be done using the USGS website (https://earthquake.usgs.gov/hazards/interactive/). In addition, the website can be found by Googling “interactive hazard deaggregation USGS”. The user interface provides default values for site hazard specific to a location in Northern California. The hazard values are provided at each of the 2%-, 5%-, and 10%-probability of exceedance in 50 years only for PGA and PGV. The user should input hazard values specific to the site being studied as well as the intensity measure selected for analysis. If an IM other than PGA or PGV is selected, the user interface will leave the three hazard level input boxes blank for user input as there are no readily available hazard

maps or conversions from PGA for an arbitrary IM. The default PGA hazard values were obtained from USGS hazard maps. These PGA values were converted to PGV values using the firm ground conversion of 48 in./sec/g. It is not meant to imply that switching between PGA and PGV (or any other IM) will yield equal hazard.

Once a desired local site seismicity is defined, users can click **Display Hazard Curves** (Fig. 145) to display the mean annual frequency of exceedance and return period. Please see Section 12.3.2 for the detailed output.

11.5.4 Compute Disaggregation

Users can also click **Display Disaggregation** (Fig. 145) to display the disaggregation by performance groups and repair quantities. Please see Section 12.3.3 for the detailed output. Only the disaggregation of the expected repair cost/time by performance group is possible due to the LLRCAT formulation. However, both expected, and variance disaggregation plots are available when disaggregating by repair quantity. The user can select the intensity measure and value on which to disaggregate. The default value is a PGV value equal to the 10% probability of exceedance in 50 years specified in the previous section.

12 TIME HISTORY AND PBEE OUTPUT

This section presents the time history results after the FE analysis phase that are used to calculate the EDP values needed for the PBEE outcomes.

12.1 Time History Output Quantities

At the end of the FE analysis phase, time histories and bridge responses will be available of the form:

v) Column Response Time Histories and Profiles
vi) Column Response Relationships
vii) Abutment Responses
viii) Deformed Mesh

In addition, for PBEE analysis scenarios, Intensity Measures (IMs) and response spectra for each input motion are calculated and are available for display in Table and Figure formats. Performance Group (PG) Quantities and Bridge peak accelerations for all employed shaking motions are also available for display against any of the computed IMs.

The post-processing capabilities can be accessed from Menu **Display** (Fig. 4). Fig. 151 shows the post-processing capabilities available in a base shaking analysis, respectively. More details about the time history outputs can be found in chapter 8.

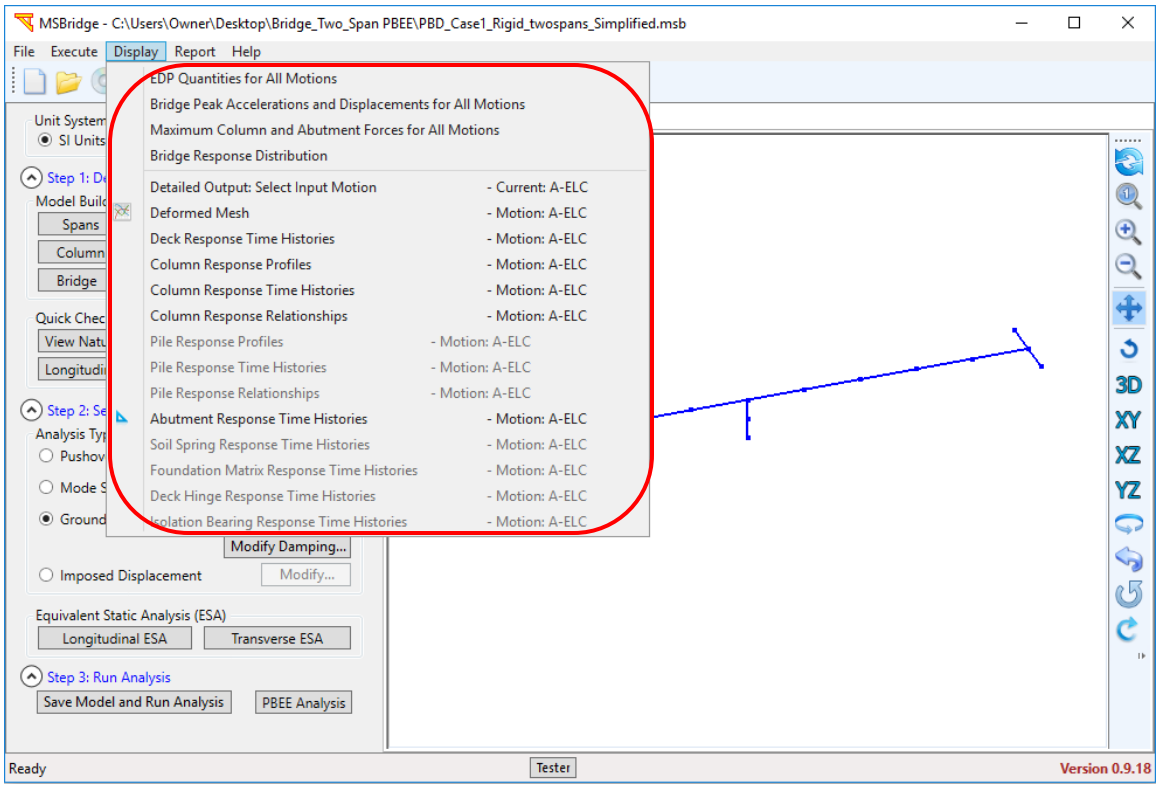

Fig. 151. Post-processing capabilities (menu options) available in a base shaking analysis

12.2 PBEE Output Quantities

At the end of the finite element analysis phase, the following output performance group quantities (for each earthquake record) are used in the next phase of PBEE analysis:

Table 7. PBEE Performance Groups

Performance Group (PG) #	Performance group names
1	Maximum column drift ratio
2	Residual column drift ratio
3	Maximum relative deck-end/abutment displacement (left)
4	Maximum relative deck-end/abutment displacement (right)
5	Maximum bridge-abutment bearing displacement (left)
6	Maximum bridge-abutment bearing displacement (right)
7	Approach residual vertical displacement (left)
8	Approach residual vertical displacement (right)
9	Abutment residual pile cap displacement (left)
10	Abutment residual pile top displacement (right)
11	Column residual pile displacement at ground surface

To account for the multi-span extension for the framework, the following notation (Eq. 4) is used for PG1, PG2, and PG11:

$$PGi - j \tag{4}$$

where i refers to the PG # as defined in Table 7, and j refers to column #.
In addition, Intensity Measures for the computed Free Field ground surface acceleration records are computed, so that outcomes can be either shown against the input base shaking IMs or the computed ground surface IMs (noted as Free-Field in the user interface). The sections below detail how the response quantities are obtained for each PG.

PG1: Maximum tangential drift ratio SRSS (column)
PG2: Residual tangential drift ratio SRSS (column)

The tangential drift ratio is defined as the maximum of a) displacement above the inflection point divided by the length of this distance, and b) displacement below the inflection point divided by the length of this distance. This takes care of rotation at the base, different boundary conditions, etc., so that the results are consistent when computing damage. The Square Root of Sum of Squares (SRSS) values of the two horizontal components are used. The tangential drift ratios are combined separately at each time step (to obtain SRSS).

PG1 (Max tangential drift ratio SRSS) is the maximum of the SRSS values of all time steps. PG2 (Residual tangential drift ratio SRSS) is the SRSS value at the last time step. The tangential drift ratio is in percentage.
To calculate the tangential drift ratio, the following 2 lines were added into the tcl file:

```
recorder Element -file A-ELC.dft -time -ele $columnEle tangentDrift
recorder Element -file A-ELC.ifp -time -ele $columnEle inflectionPoint
```

where `$columnEle` is the element # of the column (Only one forced-based beam-column element `nonlinearBeamColumn` is used for the column). In the `.dft` file, there will be five columns of data for each time step, and the first column is time. In the `.ifp` file, there will be three columns for each time step, and the first column is also time.

Subsequently, the tangential drift ratio is calculated using the code snippet shown in Fig. 152. For the tangential drift ratio in the longitudinal direction (X-direction or bridge longitudinal direction), the `tdx1` and `tdx2` variables are the second and third column (the first column is time), respectively, of the tangential drift recorder file (e.g., `A-ELC.dft`). The `tdxi` variable is the second column (the first column is time) of the inflection point recorder file (e.g., `A-ELC.ifp`).

For the transverse tangential drift ratio, the `tdx1` and `tdx2` variables are the fourth and fifth column of the `.dft` file and the `tdxi` variable is the third column of the `.ifp` file.

```
// tdx1 & tdx2 -- the tangent drift recorder file at time step i
// tdxi -- the inflection point recorder at time step i
// tdx - tangential drift ratio

if( fabs(tdxi) < 1e-20 ) {
    tdx = -tdx2/(H - tdxi);
}
else if ( fabs(H-tdxi) < 1e-20 ) {
    tdx = -tdx1 / tdxi;
}
else {
    tdx = __max(fabs(tdx1/tdxi), fabs(tdx2/(H-tdxi)));
    //tdx = -tdx*sgn(tdx2/(H-tdxi));
    if( fabs(tdx2/(H-tdxi)) < 1e-20 )
        tdx = 0;
    else if( (tdx2/(H-tdxi)) > 0)
        tdx = -tdx;
}
return tdx;
```

Fig. 152. Code snippet to calculate the tangential drift ratio of column

PG3: Maximum longitudinal relative deck-end/abutment displacement (left)
PG4: Maximum longitudinal relative deck-end/abutment displacement (right)

These two PGs are intended to address the issue of abutment impact into the backwall, so they are defined as only the motion of the deck into the abutment. Maximum absolute values in the longitudinal direction are used.

For example, for the right abutment, it is the relative longitudinal displacement of node B (deck-end node) in the direction of node C (abutment top node). A zero value is used for the times during which the deck-end node moves away from the abutment top node.

PG5: Maximum absolute bearing displacement (left abutment)
PG6: Maximum absolute bearing displacement (right abutment)

These two PGs are intended to address bearing damage whether or not an explicit representation of the bearings is included in the user-selected abutment model. Therefore, the EDP for the PG is based on the relative displacements of the deck-end node to the abutment top node. The SRSS values of the resulting two relative horizontal displacements are used, and both motions into the backwall and away from the backwall are considered.

PG7: Residual vertical displacement (left abutment)
PG8: Residual vertical displacement (right abutment)

This PG is used to gauge immediate repairs for rideability and is not a measure of the permanent slumping of the embankment (for example). Therefore, the EDP is calculated as the vertical displacement of the abutment top node relative to the deck-end node. The residual value is used (value at the final time step).

PG9: Residual pile cap displacement SRSS (left abutment)
PG10: Residual pile cap displacement SRSS (right abutment)

These PGs address possible damage below grade due to lateral translation of the piles and pile caps. While not a direct measure, pile cap displacement was selected as it would not require knowledge or observations of piles below grade. The EDP is defined by calculating the SRSS value of the 2 horizontal displacements of the abutment pile cap node. The residual is obtained from the value at the final time step.

PG11: Residual pile cap displacement SRSS (column)

This quantity is analogous to the two previous PG but is representative of response and damage at the abutment foundations. The EDP is obtained by calculating the SRSS value of the 2 horizontal displacements of the column pile cap node and taking the value at the final time step.

The PG (Performance Group) quantities for all input motions can be accessed by clicking menu **Display** (Fig. 4) and then **PG Quantities for All Motion** (Fig. 153). The window to display PG quantities is shown in Fig. 154.

The PG quantities are displayed against any of the 22 intensity measures (including 11 for the input acceleration and the other 11 for the free-field response). The PG quantities for each input motion are displayed by bin of the motion. When an IM is paired with an EDP and all the individual realizations are plotted, the result is typically termed a demand model, or probabilistic seismic demand model (PSDM). Previous research has demonstrated that the central values of PSDMs are often well described using a power-law relationship between EDP and IM. The parameters of such a power-law fit can be obtained using least squares analysis on the data. Therefore, when plotted in log-log space, the best-fit, or mean, the relationship is linear.

The mean (in log-log space) is shown along with the standard deviation (also in log-log space) of the power-law fit. If it is assumed that the EDP responses are lognormally distributed when conditioned on IM, then these curves can be interpreted as being defined by the two parameters of a lognormal distribution (the median can be related to the mean of the logarithm of the data and the lognormal standard deviation is as shown).

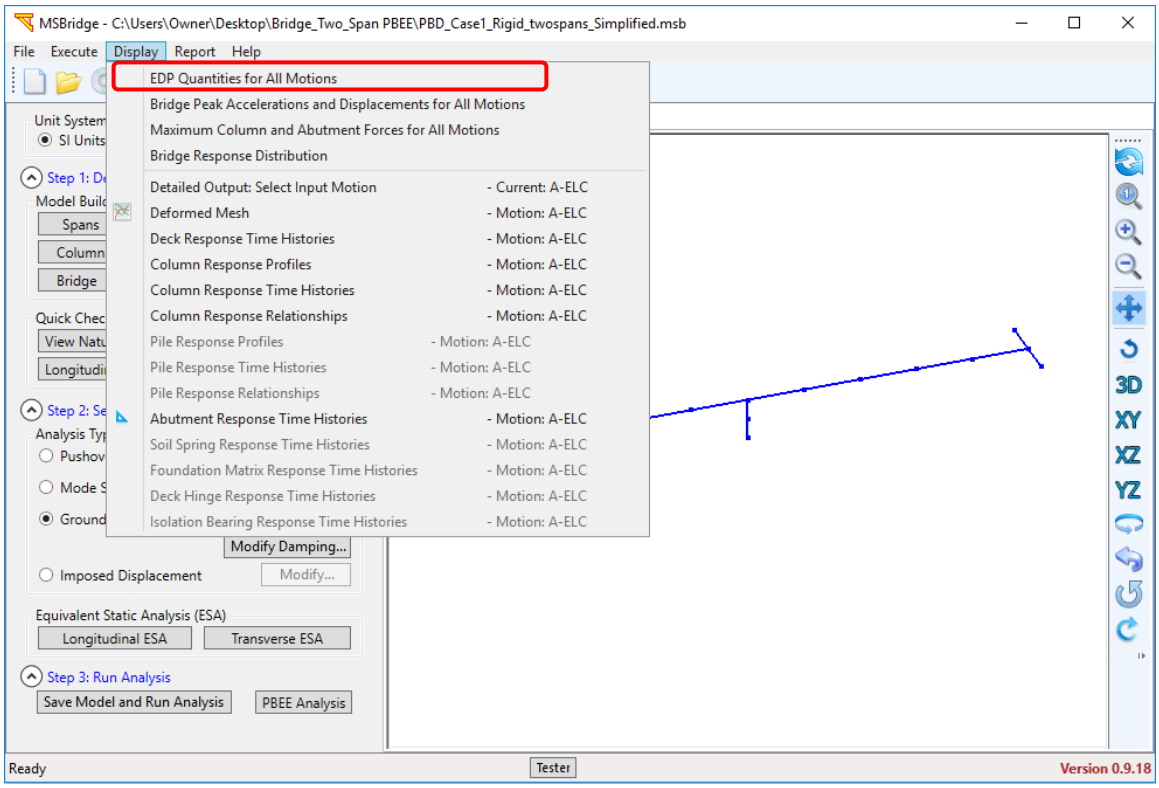

Fig. 153. Menu items to access the PG quantities for all motions

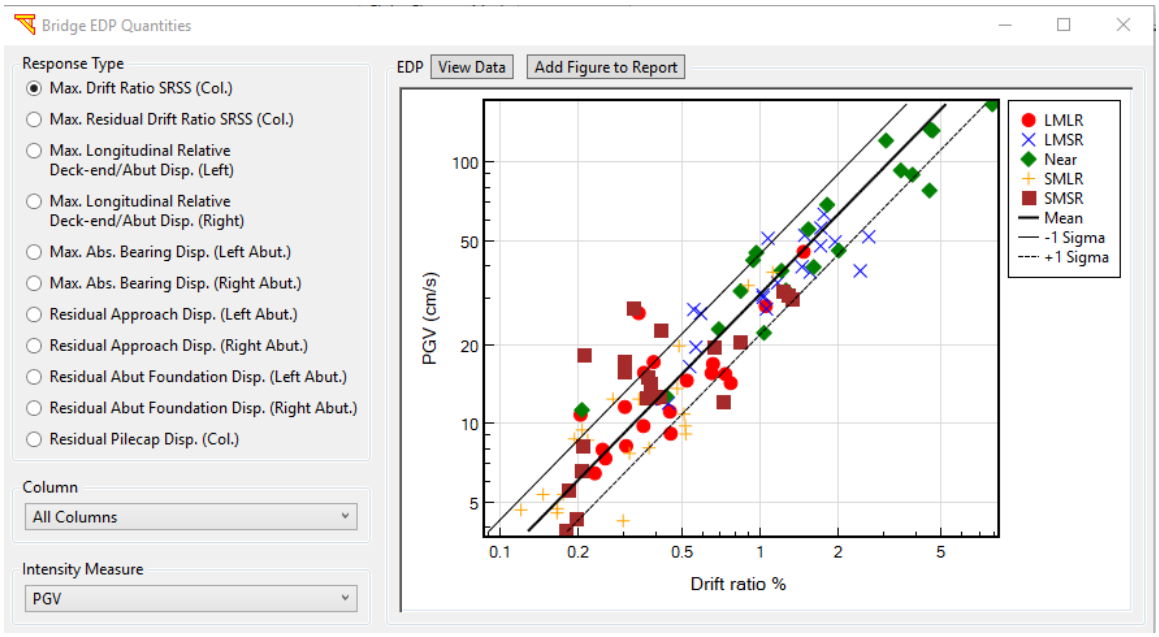

Fig. 154. PG quantities for all motions

12.3 PBEE Outcomes

This section displays the probabilistic repair cost, Crew Working time in Days (CWD), and carbon footprint along with Standard Deviation, displayed for each PG (eleven of them) and each repair quantity.

12.3.1 Repair Cost, Repair Time, and Carbon Footprint

The final PBEE results will be displayed against any intensity measure (e.g., PGV) in terms of:

- Contribution to expected repair cost ($) from each performance group (Fig. 155)
- Total repair cost ratio (%) (Fig. 156)
- Contribution to expected repair cost ($) from each repair quantity (Fig. 157)
- Contribution to repair cost standard deviation ($) from each repair quantity (Fig. 158)
- Total repair time (CWD) where CWD stands for Crew Working Day (Fig. 159)
- Contribution to expected repair time (CWD) from each repair quantity (Fig. 160)
- Contribution to expected carbon footprint (Mg CO_2 equivalent) from each performance group (Fig. 161)
- Contribution to expected carbon footprint (Mg CO_2 equivalent) from each repair quantity (Fig. 162)

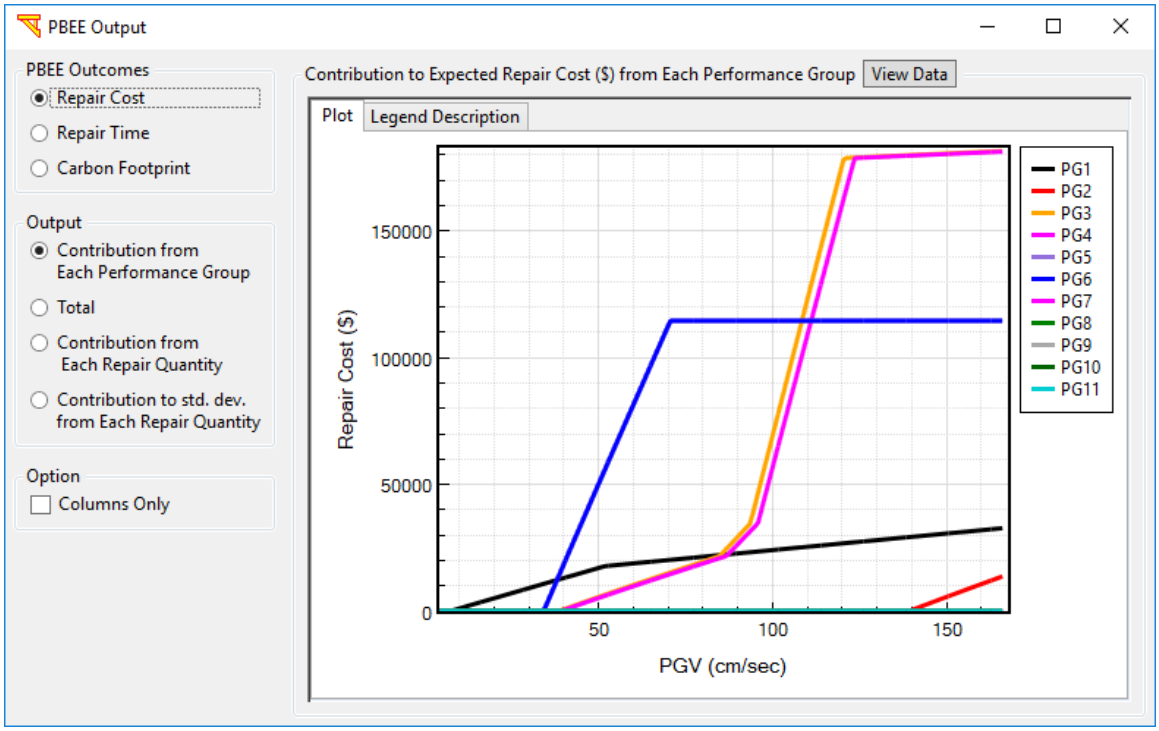

Fig. 155. Contribution to expected repair cost ($) from each performance group

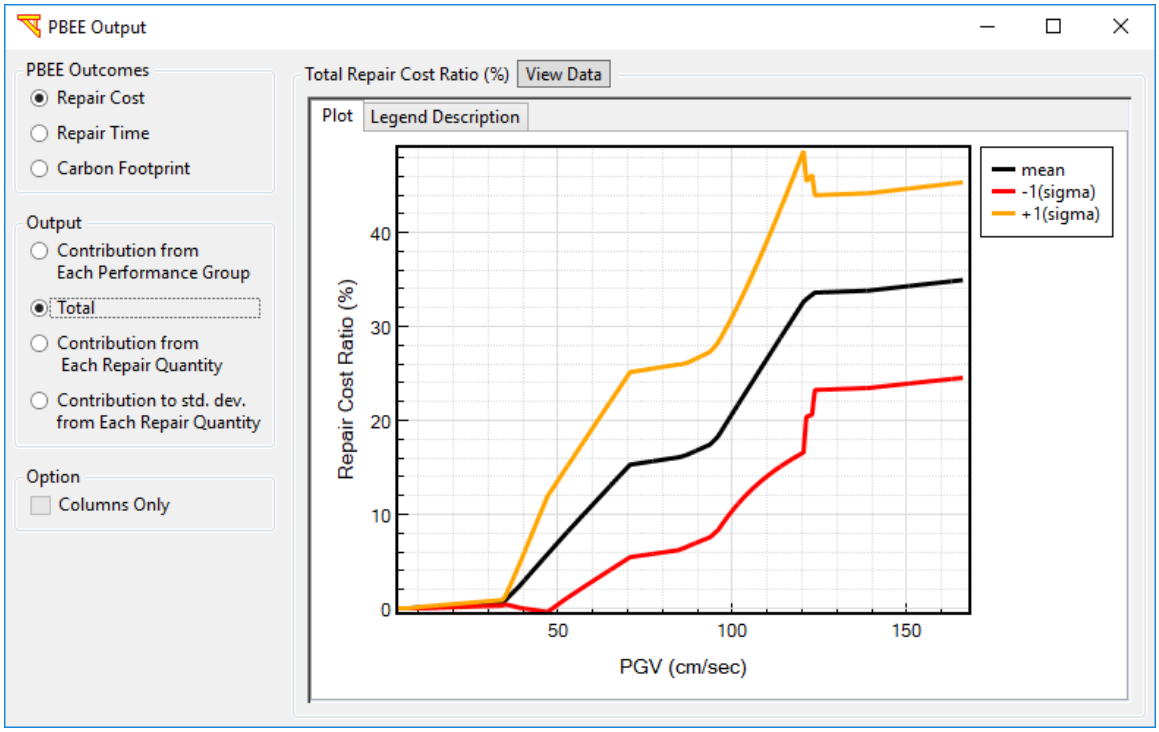

Fig. 156. Total repair cost ratio (%) as a function of intensity

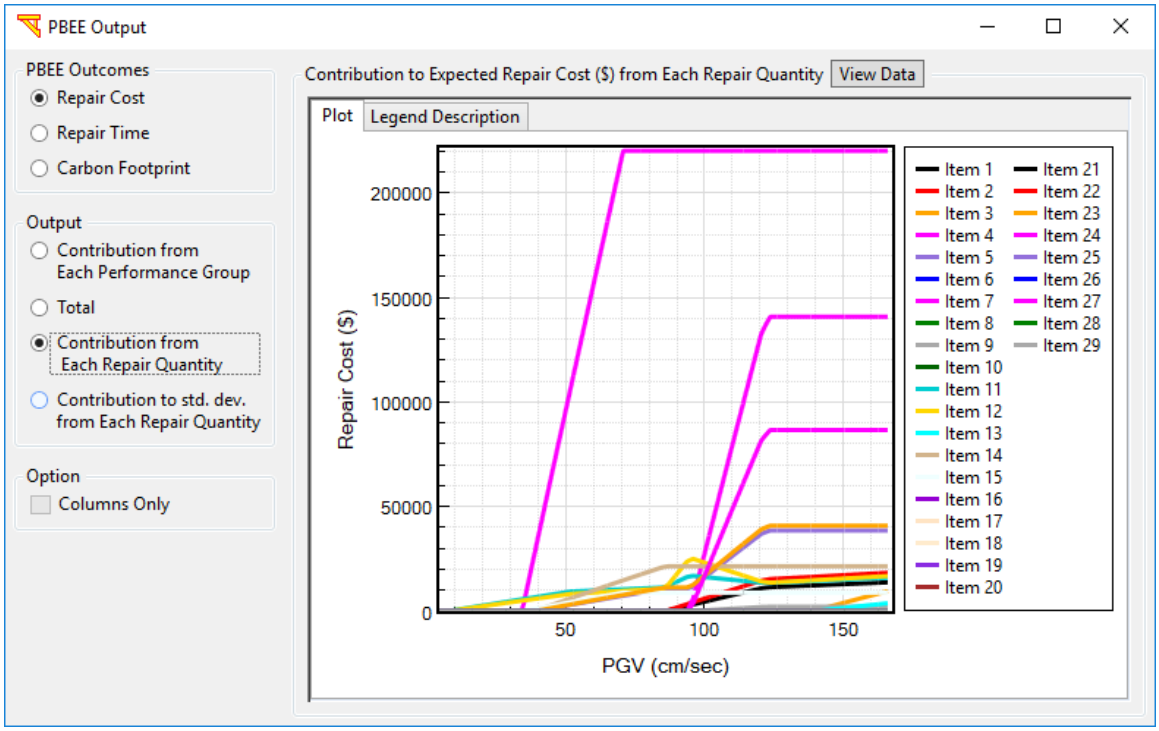

Fig. 157. Contribution to expected repair cost ($) from each repair quantity

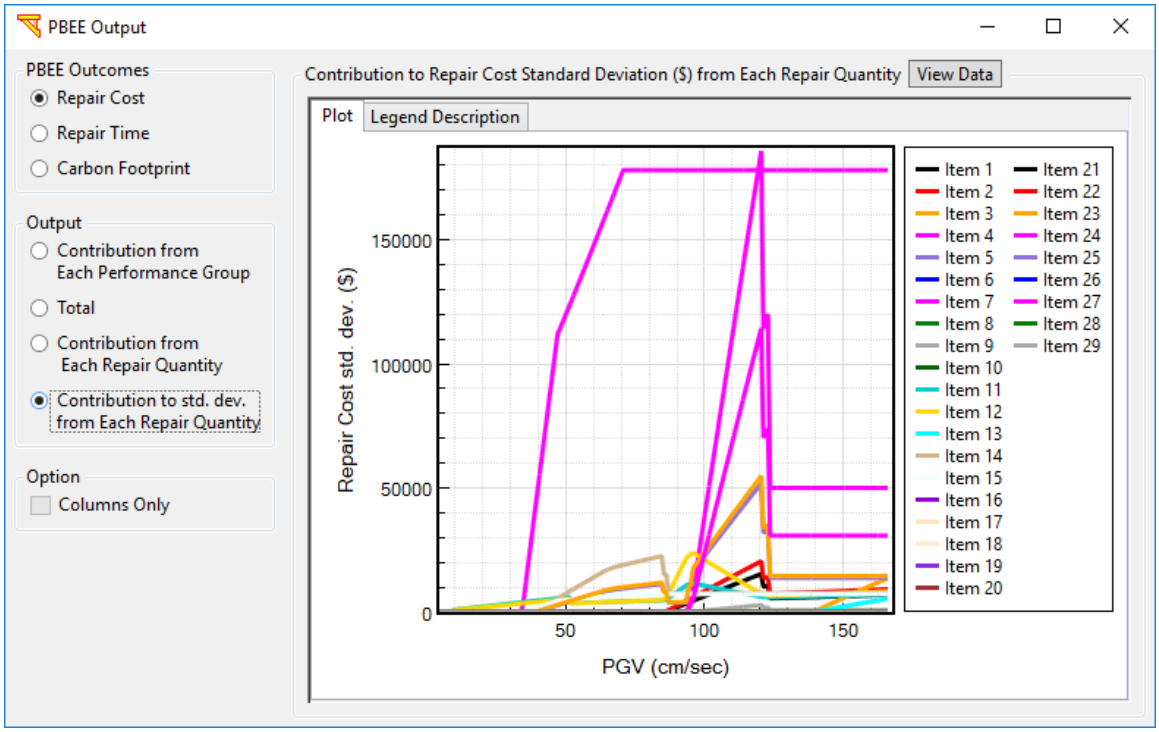

Fig. 158. Contribution to repair cost standard deviation ($) from each repair quantity

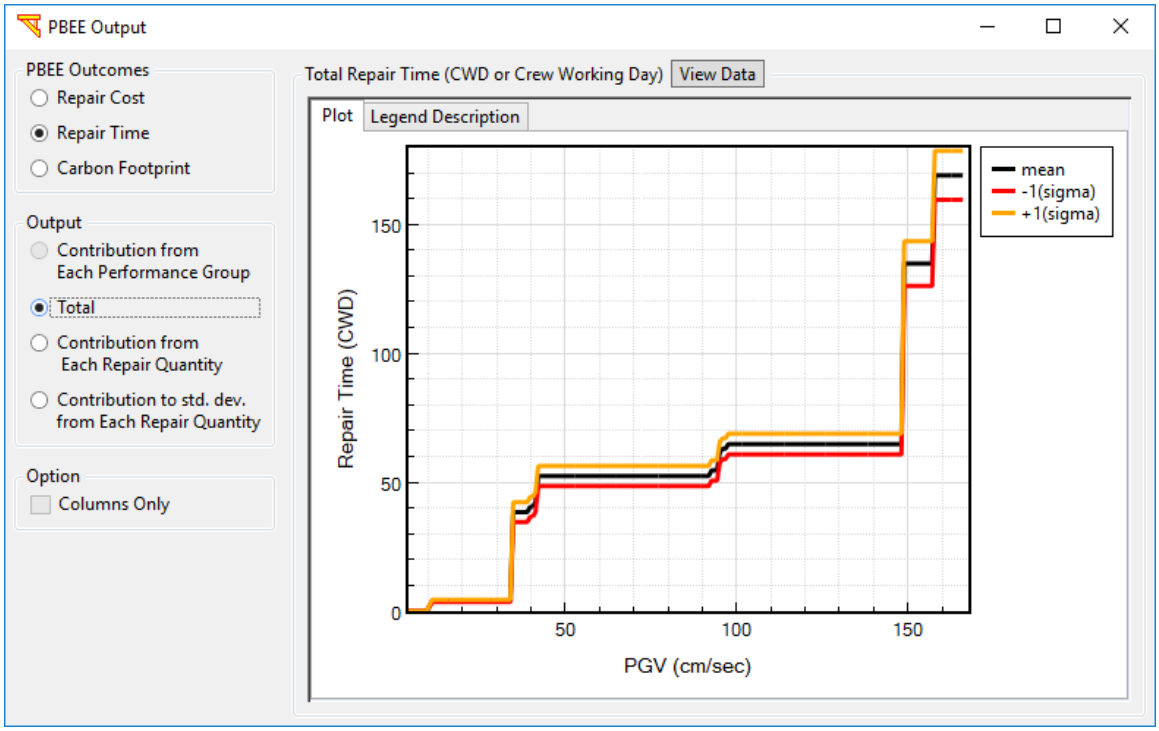

Fig. 159. Total repair time (CWD: Crew Working Day) as a function of intensity measure

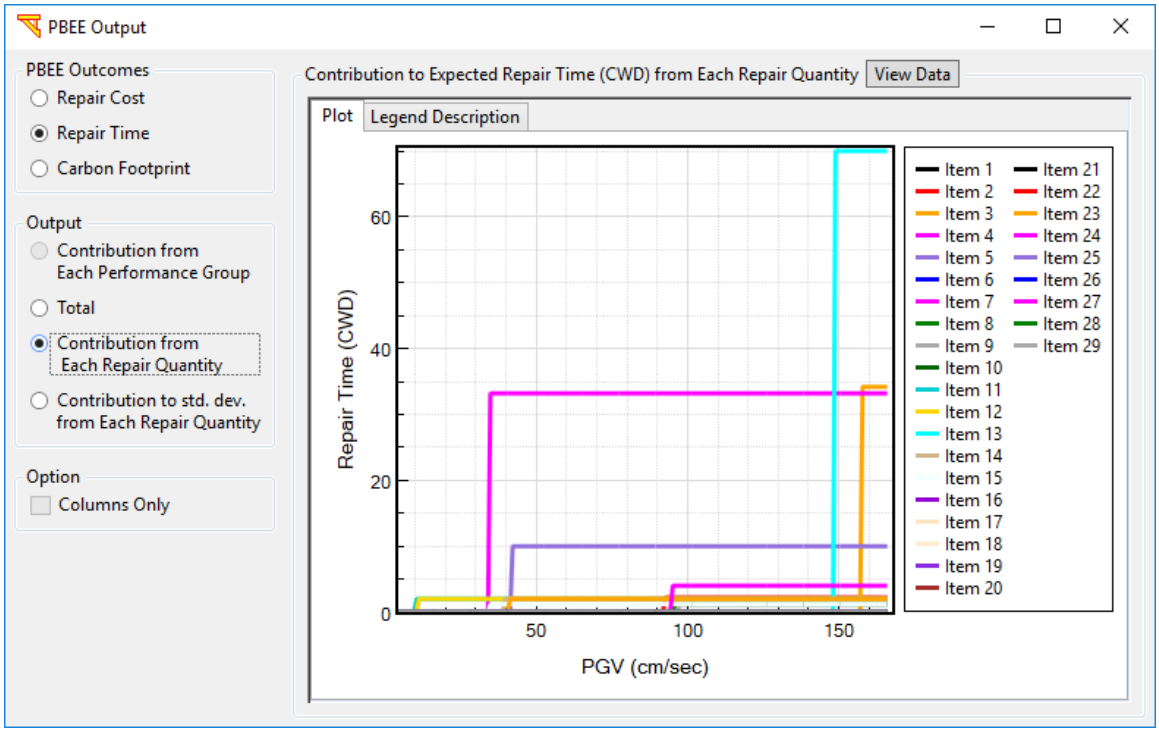

Fig. 160. Contribution to expected repair time (CWD) from each repair quantity

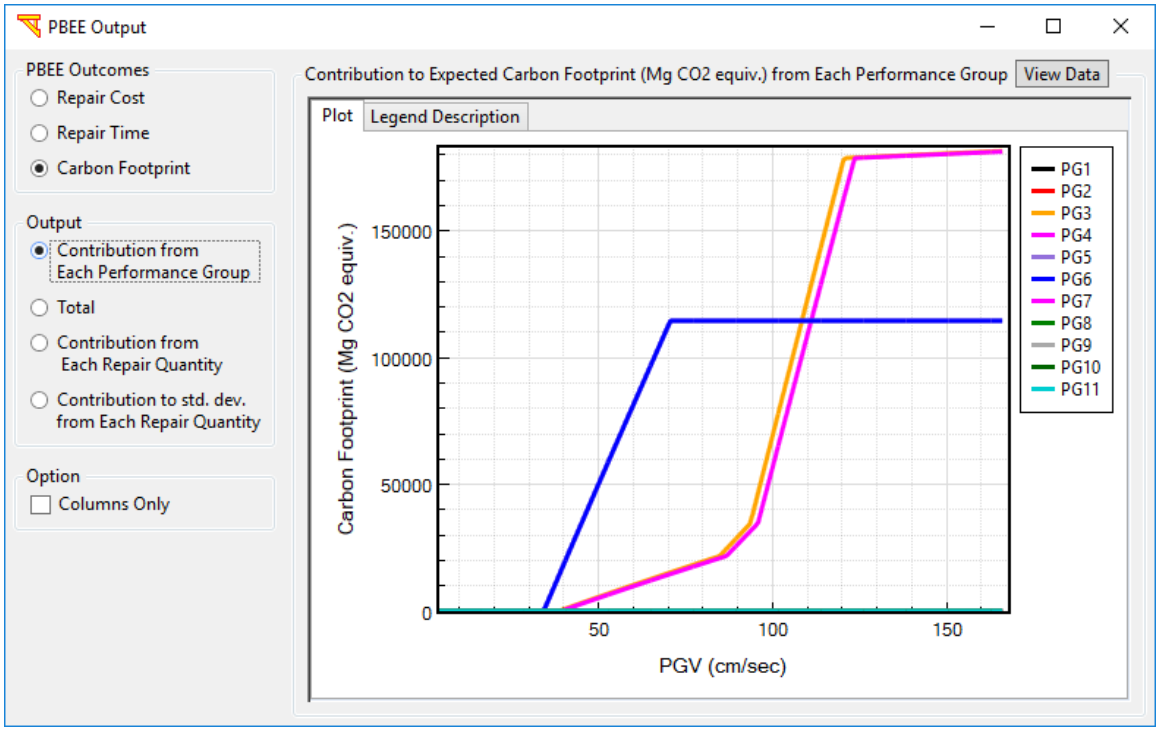

Fig. 161. Contribution to expected carbon footprint (Mg CO_2 equivalent) from each performance group

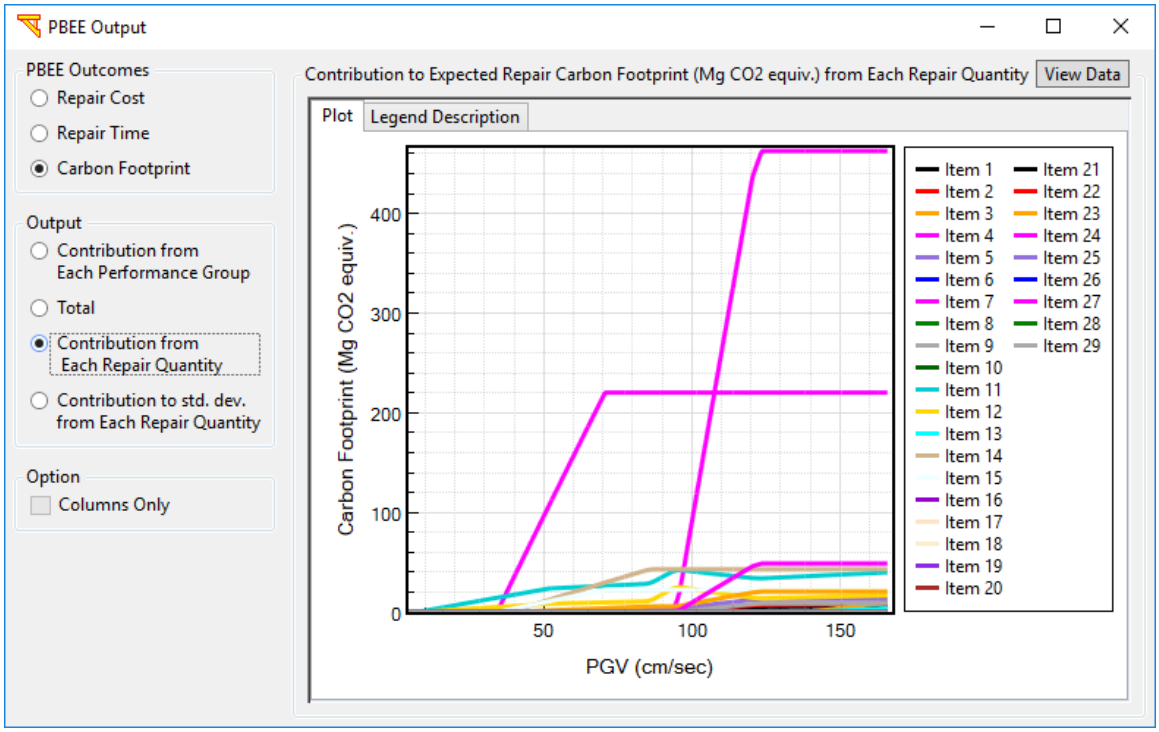

Fig. 162. Contribution to expected carbon footprint (Mg CO_2 equivalent) from each repair quantity

12.3.2 Hazard Curves

Based on the local site seismic hazard specified, losses are estimated and displayed graphically as:

- The defined local site hazard curve as a mean annual frequency (ν) of exceedance (ground motion) (Fig. 163)
- Return period against total repair cost ratio (Fig. 164)
- Mean annual frequency (MAF) of exceedance (loss) against total repair cost ratio RCR (Fig. 165)
- Return period against total repair time RT (Fig. 166)
- Mean annual frequency (MAF) of exceedance (loss) against total repair time (Fig. 167)

The median ground motion hazard curve is assumed to have a power-law form with two unknown parameters (k, k_0 in Eq. 5) in the range of the ground motion intensities bracketed by the 2%- and 10%-probability of exceedance IM values (im). The two-parameter fit (linear in log space) to the nonlinear (in log space) hazard curve tends to overpredict frequencies of exceedance for IM extremes both above and below the range of intensities considered. Therefore, care should be taken when extrapolating any resultant hazard curves to extremely low (or high) frequencies of exceedance. By using a least-squares fit in log space, the unknown parameters can be determined numerically

from the three values input by the user (2%-, 5%-, and 10%-probability of exceedance in 50 years). On the site hazard curves plotted in the interface, both the data points and the fitted curve are shown (Fig. 163).

$$\nu_I \quad (i_M) \not{m} k_0 (i \quad)^{\not{k}} \not{m} \tag{5}$$

The power-law fit to the hazard data is used to compute the loss hazards. The loss model (probability of exceeding RCR or RT conditioned on intensity levels) is integrated with the absolute value of the derivative of this IM hazard to obtain the loss hazard curve (MAF of exceeding either RCR or RT). Details of the numerical integration are presented in Mackie et al. (2008) and other sources.

The loss hazard curves (both for repair cost and repair time) are further integrated over intensity to yield mean annual loss. For example, in Fig. 165, the mean annual repair cost ratio expected for the bridge at the given site is 0.05% of the replacement cost.

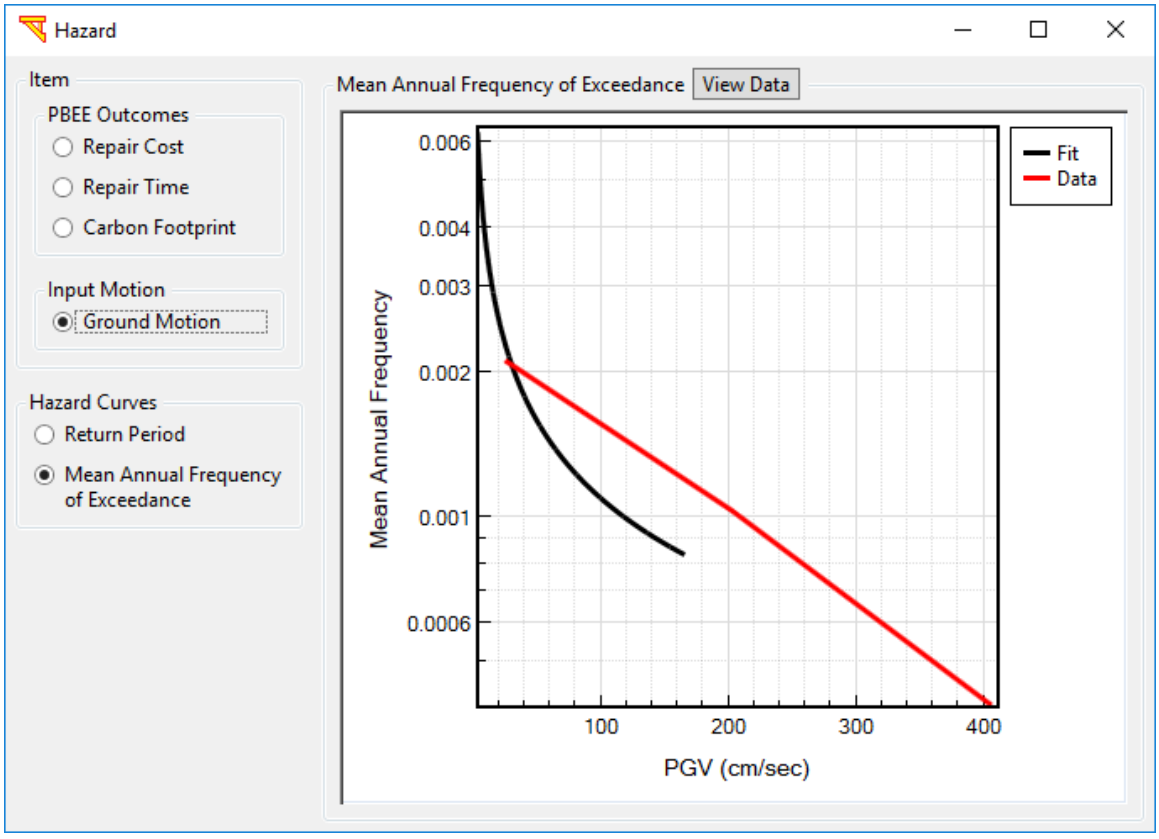

Fig. 163. Mean annual frequency of exceedance (ground motion)

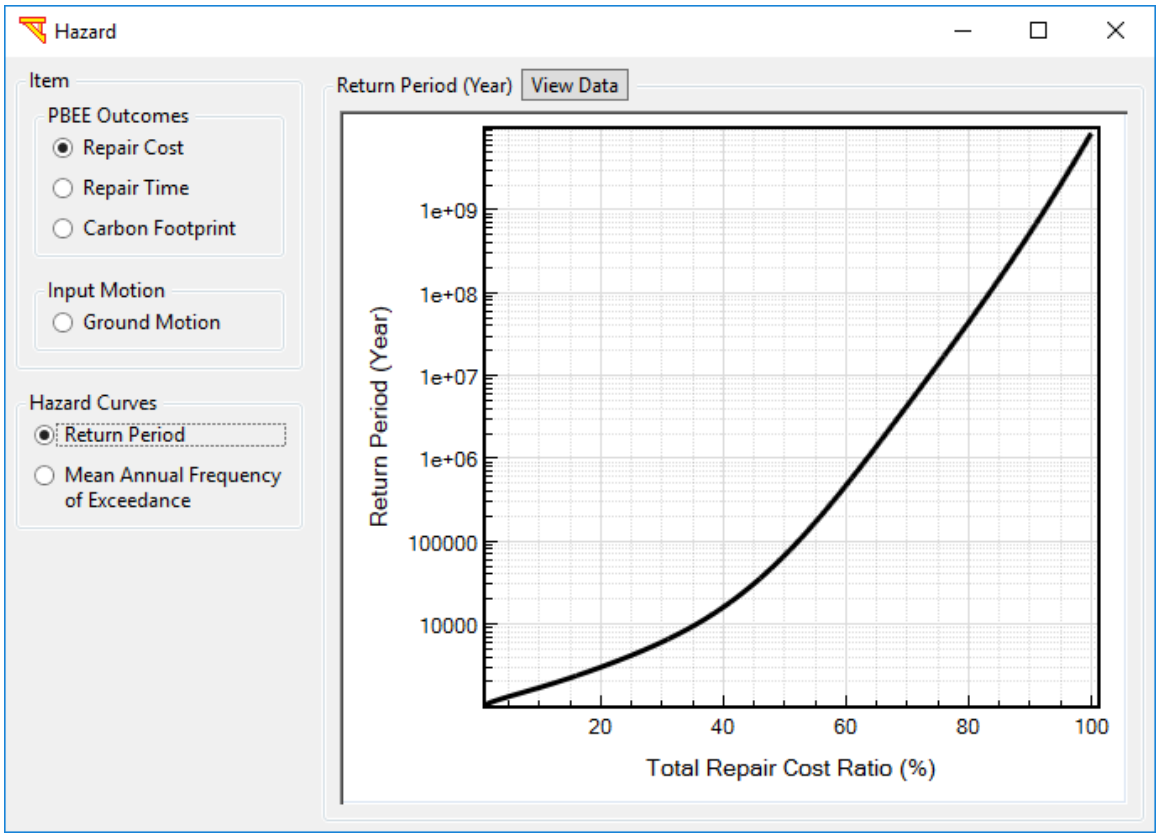

Fig. 164. Return period against total repair cost ratio

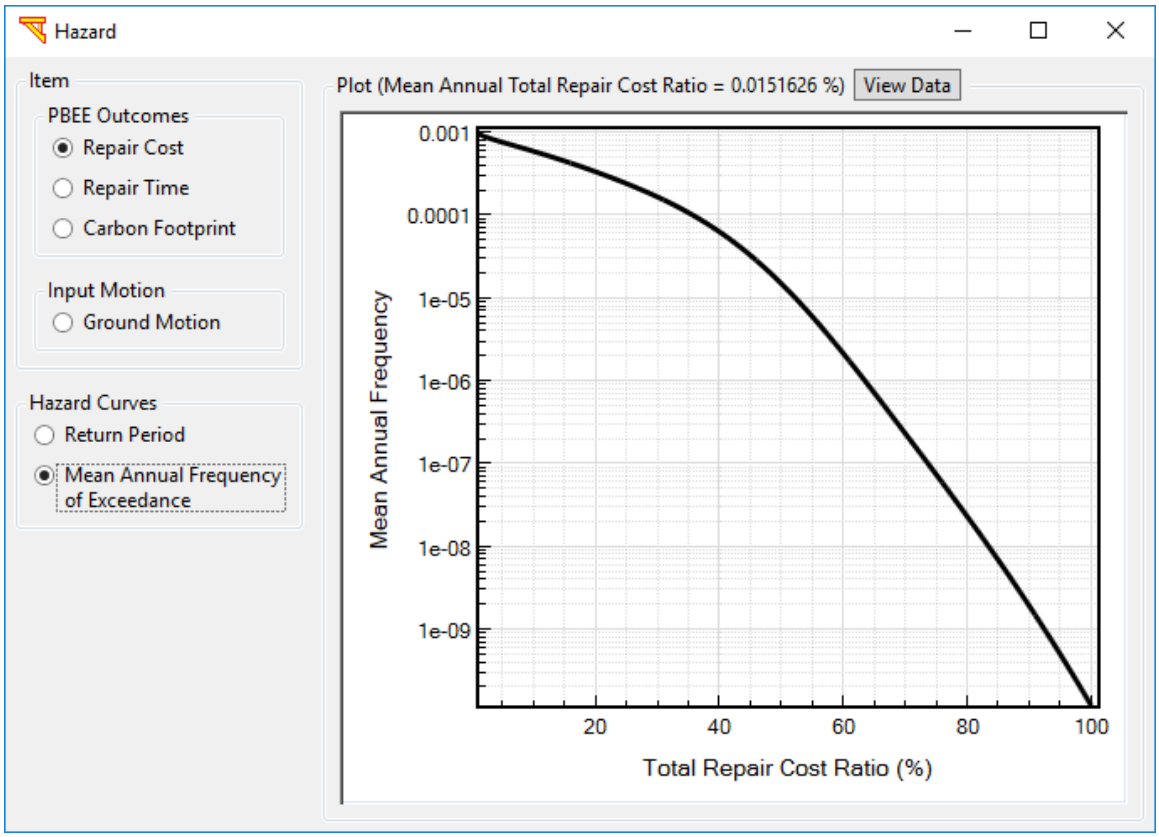

Fig. 165. Mean annual frequency of exceedance (loss) against total repair cost ratio

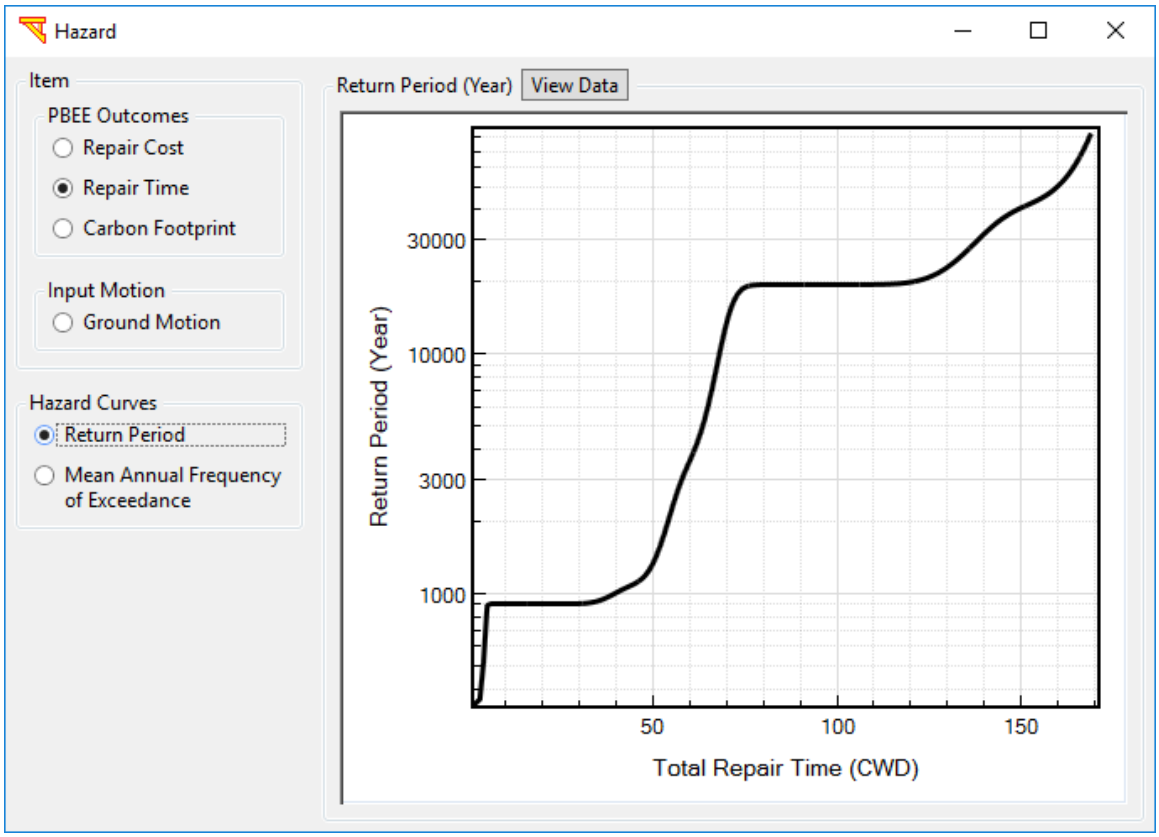

Fig. 166. Return period against total repair time

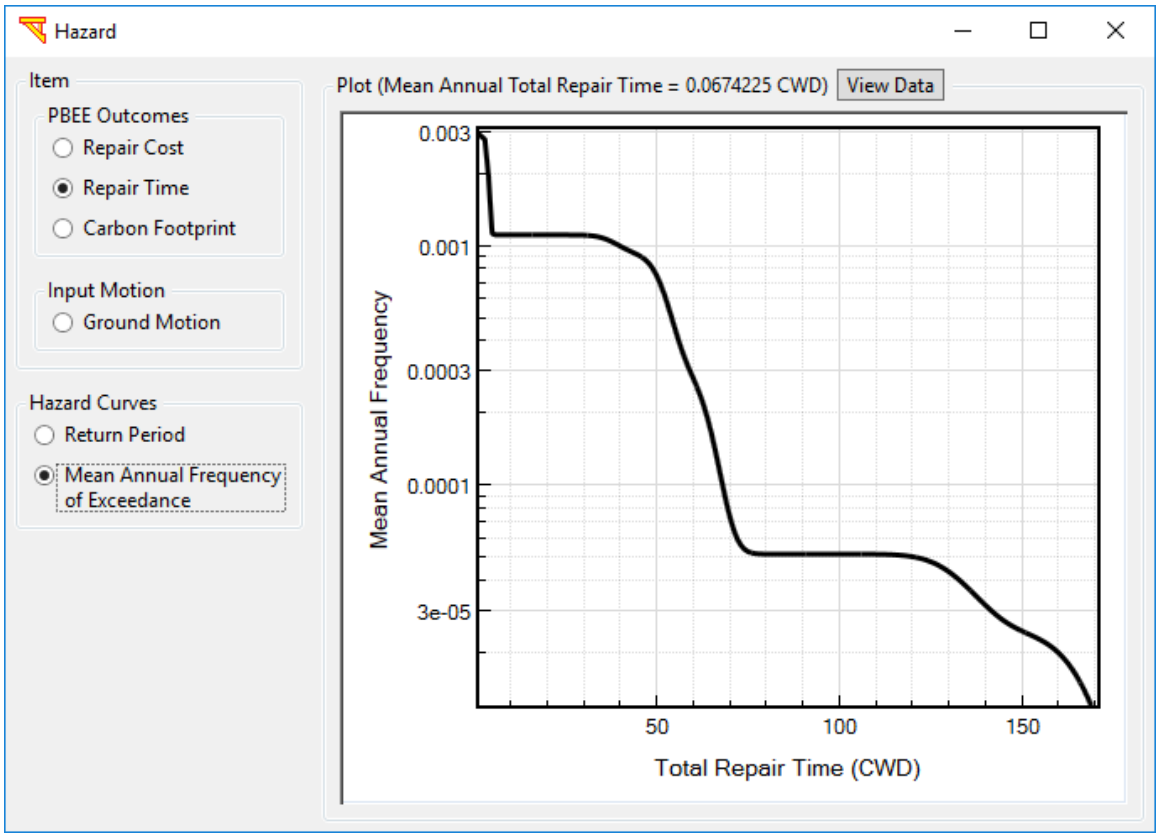

Fig. 167. Mean annual frequency of exceedance (loss) against total repair time

12.3.3 Disaggregation

Figs. 168-170 display the disaggregation (Fig. 145) of expected cost by performance group, the disaggregation of expected cost by repair quantities, and the disaggregation of expected time by repair quantities, respectively. In the figures below, the disaggregation is performed at an intensity of 100 cm/s (PGV) for all three figures (a user IM and value as shown in Fig. 145). This IM and its value are shown in the plot titles.

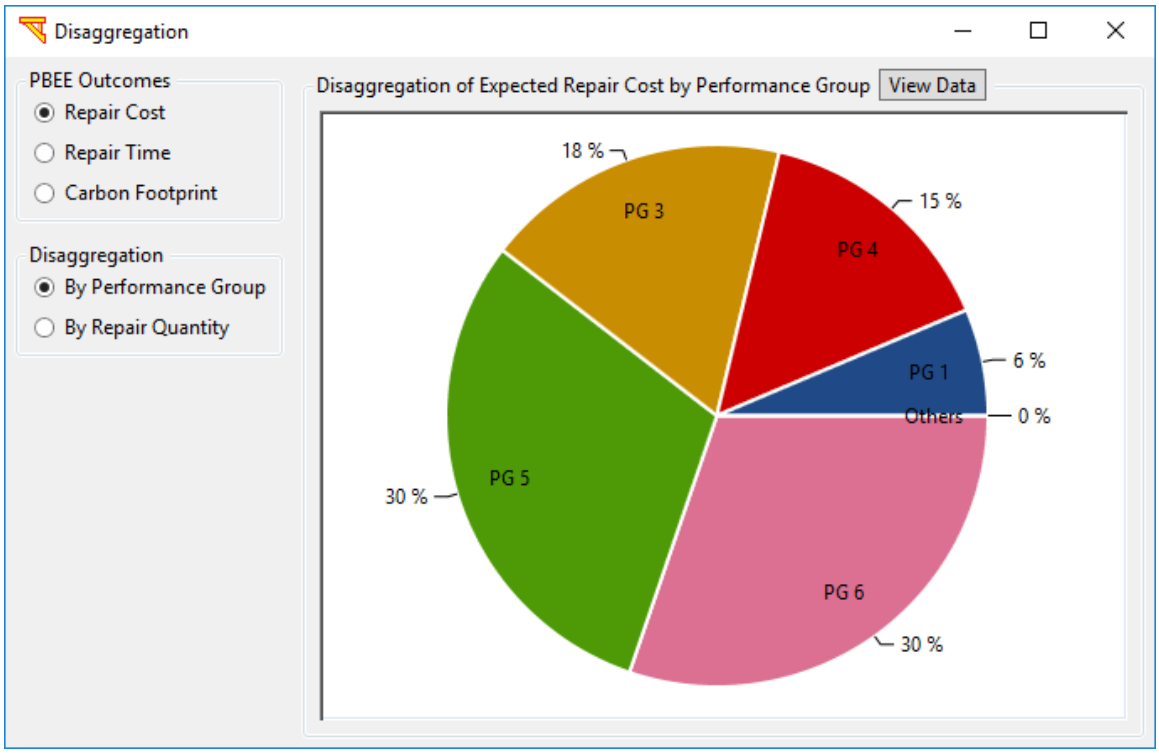

Fig. 168. Disaggregation of expected cost by performance group

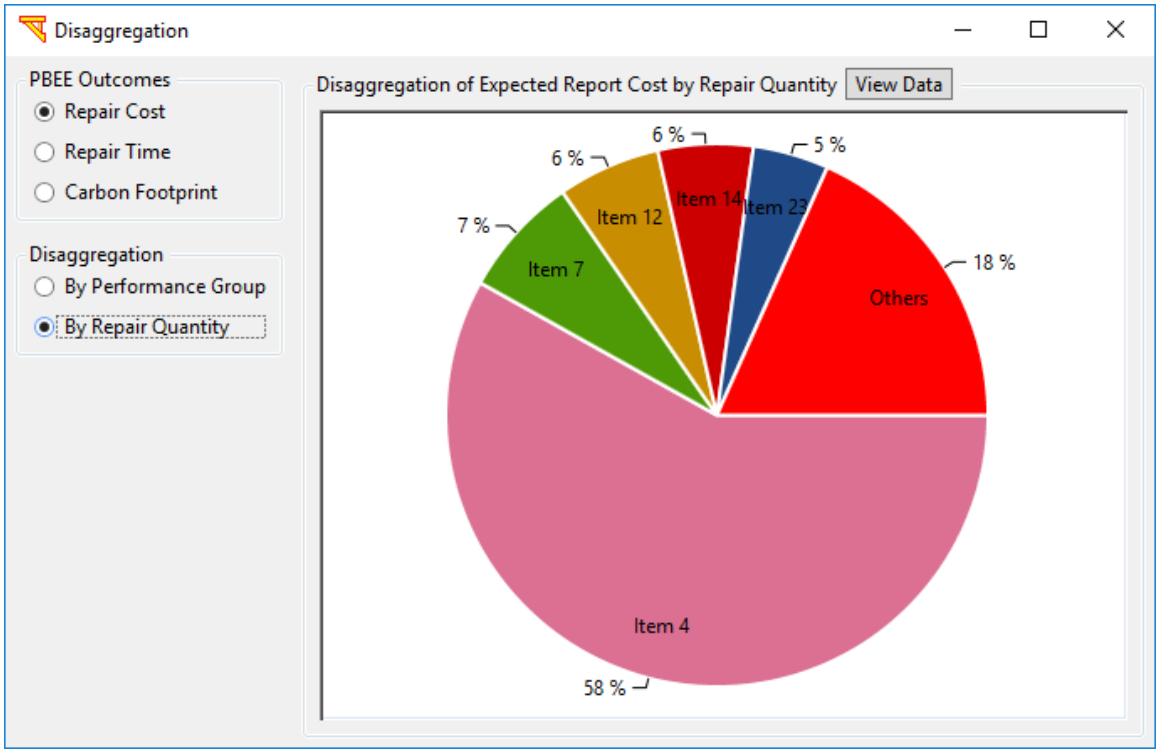

Fig. 169. Disaggregation of expected repair cost by repair quantities

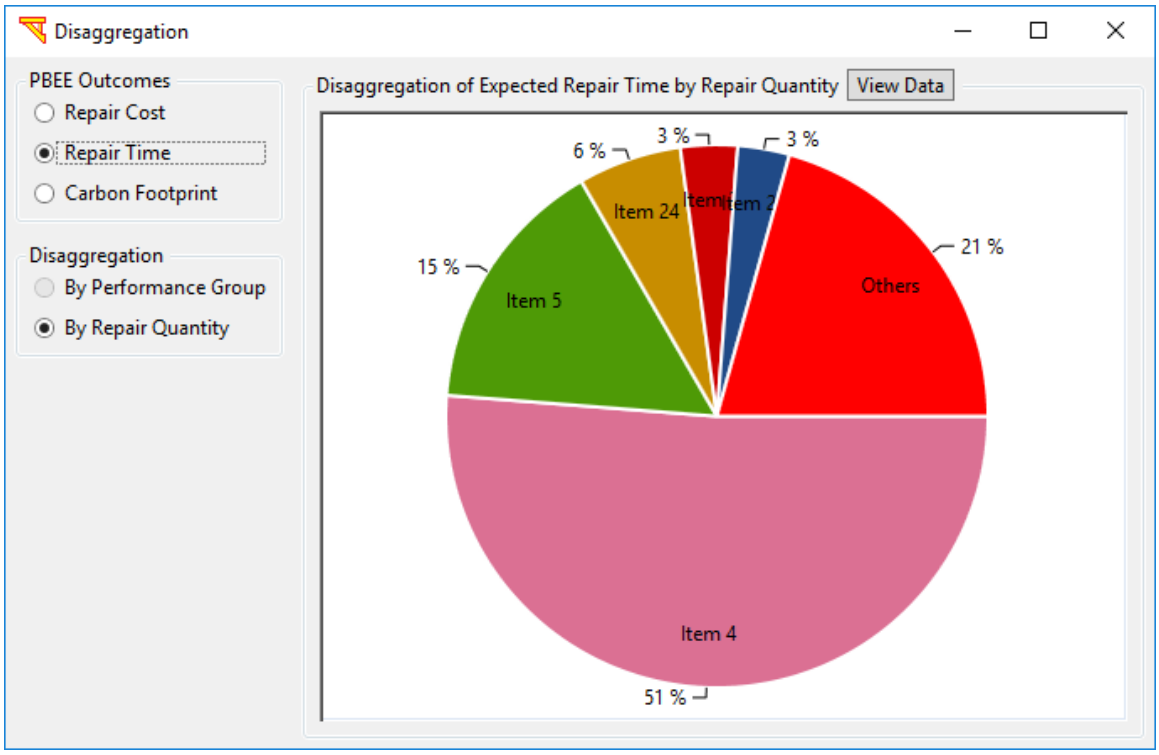

Fig. 170. Disaggregation of expected repair time by repair quantities

APPENDIX A CAPABILITIES ADDED IN THE CURRENT UPDATED VERSION

A number of capabilities and features have been added in the current version of MSBridge. These added features mainly allow MSBridge to address possible variability in the bridge deck, bent cap, column, foundation, and soil configuration/properties (on a bent-by-bent basis). Specifically, the capabilities implemented are:

(a) A different skew angle can be defined for each individual bent/abutment (in MSBridge, from main window -> **Advanced** -> check **Use Individual Skew Angles** -> **Bent and Abutments**).

(b) A different skew angle can be defined for each individual deck hinge (from main window -> **Advanced** -> **Define Deck Hinges**).

(c) Shear key option (using OpenSees **Bilin** material) is included in the deck hinge model. The shear key is not activated by default (From main window -> **Advanced** -> **Define Deck Hinges** -> **Modify**).

(d) Deck and bentcap are now connected by a rigid link (deck offset is activated in this case). A hinge with 6 Degrees of freedom (DOF's) of linear springs can be activated at the rigid link, at the location that the user specifies (From main window -> **Bentcap**).

(e) Box girder section graphical representation has been added (for efficient incorporation of the user-defined properties). (From main window -> **Deck** -> **Recalculate Section from Box Girder**)

(f) Option to couple longitudinal and transverse directions of isolation bearing nonlinear response has been added (From main window -> **Advanced** -> **Define Isolation Bearings** -> **Couple Longitudinal and Transverse Directions**).

(g) Definition of the bent cap properties is now allowed on a bent by bent basis (From main window -> **Bentcap**).

(h) Definition of the column properties is allowed for each individual column. This option gives the user great flexibility and control over assigning different nonlinear fiber sections to columns and pile shafts (Types I & II), (From main window -> **Column**).

(i) Oblong column cross-section with two circular steel cages has been added (From main window -> **Column** -> **Oblong**).

(j) For the circular cross-section, options for Bonded and Un-bonded Column Jackets (i.e., Casing as Fibers in the Bonded case) have been added (From main window -> **Column** -> **Circle** -> check **Activate Steel Jacket**).

(k) Option to improve computational analysis schemes has been added. Specifically, this option is mainly to allow automatic switching between time integration schemes to achieve convergence in highly nonlinear scenarios (From menu **Execute** -> **Advanced Option: OpenSees Parameters** -> check **Automatic Switching between Time Integration Schemes**).

Furthermore, the following options have been implemented:

(a) Concrete properties can be manually specified (instead of automatically calculated from the column geometry and reinforcement information) (From main window -> **Column** -> check **Update RC Properties** and click **Nonlinear Fiber Section**).

(b) Option to enter user-defined moment curvature (from main window -> **Column** -> check **User-Defined Moment Curvature** and click **Define Moment Curvature**).

(c) A separate steel material can be used for the steel jacket (From main window -> **Column** -> **Nonlinear Fiber Section**).

(d) Option to include the vertical soil springs for the Soil Springs foundation type (From main window -> **Foundation** -> click **Soil Springs** and then **Modify Soil Springs**).

(e) Option to calculate the vertical soil springs (for the Soil Springs foundation type) based on user-defined T-z and Q-z data (From main window -> **Foundation** -> click **Soil Springs** and then **Modify Soil Springs ->** click **Calculate from User T-z and Q-z**).

(f) Option to specify a yielding curvature as the yielding criterion for Longitudinal and Transverse ESA (From main window -> click **Longitudinal Direction** (or **Transverse Direction**).

(g) A different number of columns can be specified for each individual bent, with locations defined by column offsets (From main window -> **Bridge** -> check **Non-uniform Column Layout** -> **Columns**).

(h) Column base offset (zero by default) can also be defined, for modeling inclined columns (From main window -> **Bridge** -> check **Non-uniform Column Layout** -> **Columns** -> specify **Base Offset**).

(i) Different deck properties can be specified on a span-by-span basis (From main window -> **Deck**; from main window -> **Bridge** -> check **Non-uniform Column Layout**).

(j) For Horizontal Alignment, the global coordinate system can be rotated at the angle specified; or the bridge longitudinal direction can be chosen to coincide with the

chord connecting the two abutments (From main window -> **Spans** -> check **Horizontal Alignment** -> **Modify Horizontal Curve**).

(k) Option to include the bentcap overhang (the portion of the bent cap outside the columns) has been added (From main window -> **Bentcap**).

(l) Option to include the user-defined TCL code snippet for the nonlinear Fiber section has been added. This is an advanced option and the users must proceed with caution (From main window -> **Column** -> check **User-Defined Tcl Script for Nonlinear Fiber Section** -> **Define Fiber Section Tcl Script**).

(m) Different Foundation Matrix parameters can be assigned to each column base (From main window -> **Foundation** -> check **Foundation Matrix** -> **Modify Foundation Matrix**).

(n) Option to include pile cap masses and fixity conditions has been added, available only in the foundation types "Soil Springs" and "Foundation Matrix" (From main window -> **Advanced** -> **Pilecap Mass and Rotation Condition**).

(o) Option to include column P-Delta effect (included by default) has been added (From main window -> **Advanced** -> check/uncheck **Include P-Delta Effect**).

(p) Option to include Rayleigh (stiffness proportional component) damping for the abutments has been added, with no Rayleigh damping for the abutment stiffness as the default (From main window -> **Advanced** -> check/uncheck **Include Rayleigh Damping**).

(q) Deck-end fixity conditions can be directly applied (From main window -> **Advanced** -> **Deckend Fixity**)

(r) Visualization of pile response (profiles, time histories and relationships) has been added, available for the foundation type "Soil Springs" (From menu **Display** -> **Pile Response Profiles/Pile Response Time Histories/Pile Response Relationships**).

(s) Option to view OpenSees analysis log (From main menu -> **Execute** -> **OpenSees Analysis Log**).

(t) Multi-Linear abutment model has been added (From main window -> **Abutment** -> select **Elastic/Multi-Linear Abutment** -> **Modify Properties**).

(u) Option to include Rayleigh (stiffness proportional component) damping for the soil springs has been added, with no Rayleigh damping for the soil springs as the default (From main window -> **Advanced** -> check/uncheck **Include Rayleigh Damping**).

(v) Option to activate the linear behavior for the soil springs (From main window -> **Advanced** -> **Linear Soil Springs**).

(w) Option to choose a beam column element type for pile shafts (From main window -> **Mesh**).

APPENDIX B CALCULATION OF STEEL AND CONCRETE MATERIAL PROPERTIES

Steel Bars

By default, the Steel02 material is used to simulate steel bars. The format of the Steel02 command is as follows (McKenna et al. 2010):

uniaxialMaterial Steel02 $matTag $fy $E0 $b $R0 $cR1 $cR2

Where $fy is the steel yield strength, $E0 is Young's modulus of steel, and $b is the strain-hardening ratio (ratio between post-yield tangent and initial elastic tangent), $R0, $cR1, and $cR2 are parameters to control the transition from elastic to plastic branches.

The number of longitudinal bars is calculated as follows:

$$\#bars = \frac{\rho_s A_c}{A_b} \tag{6}$$

Where ρ_s is the longitudinal steel percentage, A_c the column cross-section area, A_b is the cross-section area of the steel bar.
If the number of longitudinal bars is known, the longitudinal steel percentage (reinforcement ratio) can be calculated:

$$\rho_s = \frac{A_s}{A_c} \tag{7}$$

Where A_s is the area of longitudinal steel, which is equal to the area of each bar times the number of bars. For example, the diameter of a #18 bar is 2.257 inches, so the area is four in^2. If there are 10 bars in a 36-inch diameter circular column, then

$$\rho_s = \frac{10(4)}{\frac{\pi}{4}36^2} = 0.039 \text{ or } 3.9\%.$$

The transverse steel percentage (reinforcement ratio) for a spirally confined circular column, currently the only type of column supported in the interface, is

$$\rho_t = \frac{\pi(d_{db}{}^2)}{s(d_{cc})} \tag{8}$$

Where d_{bt} is the diameter of the transverse spiral (always smaller than the diameter of the longitudinal bars). The spacing between transverse bars is s. The diameter of the confined core is d_{cc} which is the gross diameter minus twice the cover and minus the diameter of

the transverse bars (see Eq. 11). So for a #5 spiral spaced at 3 inches on center in the same column mentioned above.

$$\rho_t = \frac{\pi(\frac{5}{8})^2}{3(36 - 2(2) - \frac{5}{8})} = 0.0113 \text{ or } 1.3\%. \quad (9)$$

Currently, the transverse reinforcement does affect the shear response (through changes in the uniaxial constitutive model for the concrete core). However, the columns are modeled considering only flexurally dominated response (i.e., there is no accounting for shear flexibility or shear degradation directly). Additional relevant details on the parameters used in both the Cover and Core Concrete are included below.

Cover concrete

The Concrete02 material is used to simulate the concrete (for both cover and core). The format of the Concrete02 command is as follows:

uniaxialMaterial Concrete02 $matTag $fpc $epsc0 $fpcu $epsu $lambda $ft $Ets

Where $fpc is the concrete compressive strength, $epsc0 is the concrete strain at maximum strength, $fpcu is the concrete crushing strength, $epsu is the concrete strain at crushing strength (all of the above values are entered as negative), $lambda is the ratio between unloading slope at $epsu and initial slope, $ft is the tensile strength, and $Ets is tension softening stiffness (absolute value) (slope of the linear tension softening branch).

For cover concrete, $fpc is equal to the concrete unconfined strength, $epsc0 = 0.002, $fpcu = 0.0, $epscu = 0.006, $lambda = 0.1, $ft = (0.14)$fpc, and $Ets = $ft / $epsc0.

Core concrete

i) For core concrete of circular column cross-sections according to the Mander model, the procedure to calculate the confined concrete strength $fpc(= f_{cc}) is as follows:

$$f_{cc} = f_c'(-1.254 + 2.254\sqrt{1 + 7.94\frac{f_e'}{f_c'}} - 2\frac{f_e'}{f_c'}) \quad (10)$$

Where f_c' is the unconfined compressive strength and f_e' can be obtained from the following equation:

$$f_e' = \frac{1}{2}K_e\rho_t f_y \quad (11)$$

Where f_y is the steel yield strength, ρ_t is the transverse steel percentage, and K_e can be obtained from the following equation for circular columns confined by hoops:

$$K_e = \frac{(1 - \frac{S'}{2d_{cc}})^2}{(1 - \rho_{cc})} \quad (12)$$

Where:

$$\rho_{cc} = \frac{A_s}{A_{cc}} \quad (13)$$

An assumed value of the area of the confined core is used for default values. This area should be modified based on the expected compressive block in the column during lateral loading.

$$A_{cc} = \frac{\pi(d_{cc})^2}{4} \quad (14)$$

$$S' = \frac{\pi d_{bt}^2}{\rho_t d_{cc}} \quad (15)$$

Where d_{bt} is the transverse bar diameter

$$d_{cc} = D_L - 2c - d_{bt} \quad (16)$$

Where c is the clear cover (c = 1.5")

ii) $epsc0

$$epsc0 = \frac{2 f_{cc}}{E_c} \quad (17)$$

Where:

$$Ec = 0.043 w^{1.5} \sqrt{f_c'} \quad (18)$$

Where w is the concrete unit weight (unit: kg/m^3)

iii) $epsu (= $epsc$)

$$epscu = 0.004 + \varepsilon_s \frac{f_y}{f_c'} \rho_t \quad (19)$$

Where ε_s is the ultimate steel strain ($\varepsilon_s = 0.1$)

iv) \$fpcu (= f_{cu})

$$f_{cu} = \frac{f_{cc}(epscu)}{(epsc)} \left(\frac{(epscr)}{(epscr) - 1 + \left(\frac{(epscu)}{(epsc)}\right)^{(epscr)}} \right) \quad (20)$$

Where:

$$epsc = (epsc0)\left(1 + 5\left(\frac{f_{cc}}{f_c'} - 1\right)\right) \quad (21)$$

$$epscr = \frac{E_c}{E_c - \frac{f_{cc}}{(epsc)}} \quad (22)$$

Notes:

1. The information above is specific to the Steel02 and Concrete02 models of the Fiber section. Other options include (Fig. 25), Steel01 and Concrete01 (for more information please see the OpenSees documentation), and Elastic properties for the fibers. These options can be activated by clicking on the default Steel02 or Concrete02 sections (Fig. 25) and changing these options.

2. A different property may be specified for the Column below grade (for instance to roughly represent a large pile group as a large single column). If this option is selected (Fig. 7), the column below grade will have linear properties as specified by its diameter and Young's Modulus).

3. All the equations presented in this Appendix are based on the Mander model for spiral-reinforced circular concrete columns. The user may want to use their constitutive model or parameters. In this case, these parameters can be defined directly in Fig. 25.

APPENDIX C HOW TO INCORPORATE USER-DEFINED MOTIONS

1) Directory Structure of a Motion Set

Iput motions must be defined to conduct a base input acceleration analysis (Fig. 109). The window to define the input motions is shown in Fig. 110. Click **Browse** to select a motion set (Fig. 171). Click on the motion set name (e.g., **Motions**) and then click on **OK** to choose this motion set (Fig. 171).

In MSBridge, the input motions are organized in a format that the program can read. Specifically, the input ground motions are sorted into bins. Fig. 172 shows the directory structure of a motion set named **Motions**. The second level directories are bins (e.g., T01; see Fig. 171 and Fig. 172). The third level directories are earthquake names (e.g., earthquake NORTHRIDGE; see Fig. 172). And the fourth level directories are the input motion names (e.g., there is one input motion under earthquake NORTHRIDGE: RRS; see Fig. 172).

Each motion is composed of three perpendicular acceleration time history components (2 laterals and one vertical). As shown in Fig. 172, each motion folder contains six files categorized into two file types: the DATA files contain the time history (acceleration unit in g) of a component and the INFO files contain the characteristics of the corresponding component. Fig. 173 and Fig. 174 displays sample INFO & DATA files. The naming of these files usually has to follow the format below: Input motion name + angle (or "-UP" or "-DWN" for vertical component) + ".AT2" + ".data" (or ".info"). However, the following format is also allowed: Input motion name + "-E" or "-W" for horizontal components (or "-V" for vertical component).

Note that the filenames with the smaller angle will be used for the longitudinal direction and the other one (with the larger angle) will be used for the transverse direction (also, the filenames containing "-E" will be used for the longitudinal direction and the other one (containing "-W") will be used for the transverse direction.

The first two lines of each INFO file must follow the style of the example below:
{Data points NPTS}{996}
{Sampling period DT (sec)}{0.020000}

Where 996 and 0.02 are the number of data points, and the time step, respectively, of an input motion component.

2) Steps to Create an Input Motion

Based on the above description for the directory structure of a motion set, one can easily create an input motion (Fig. 175):

Step 1: create a folder and rename to your motion set name (e.g. MotionSet1; see Fig. 175).

Step 2: create a folder under the motion set folder and rename to your bin name (e.g., bin1).

Step 3: create a folder under the bin folder and rename to your earthquake name (e.g., Quake1).

Step 4: create a folder under the earthquake name and rename to your input motion name (e.g., MOTION1).

Step 5: create the six files (3 INFO files and 3 DATA files) for this input motion (Fig. 175).

Note: If you download the input motion files from the PEER NGA Database, there is no need to re-format the data into one column as shown in Fig. 174. Just copy the data points into the corresponding DATA files. And then make the INFO files containing the number of data points and the sampling period DT (2 lines) according to the header information.

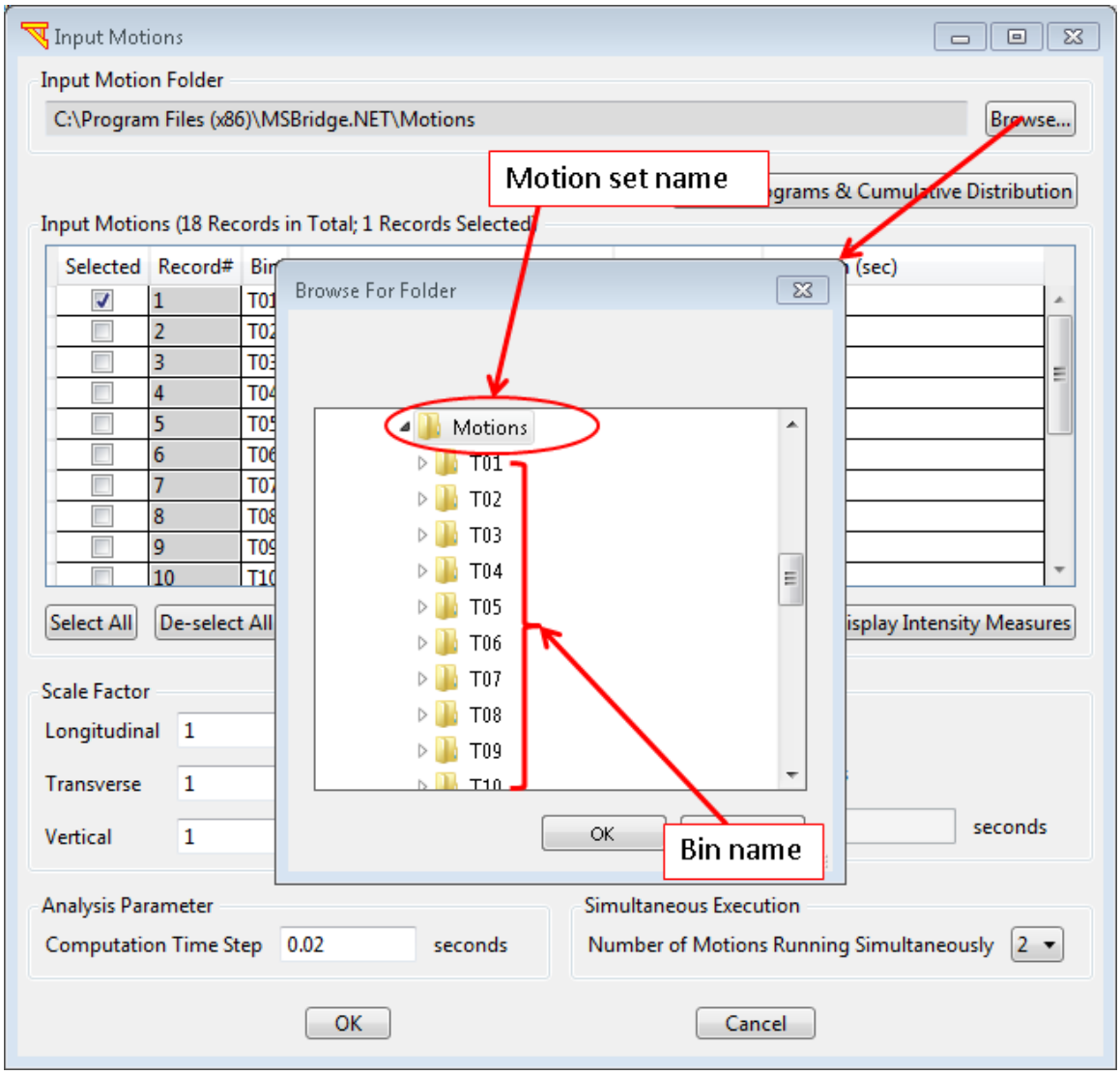

Fig. 171. Choosing a motion set

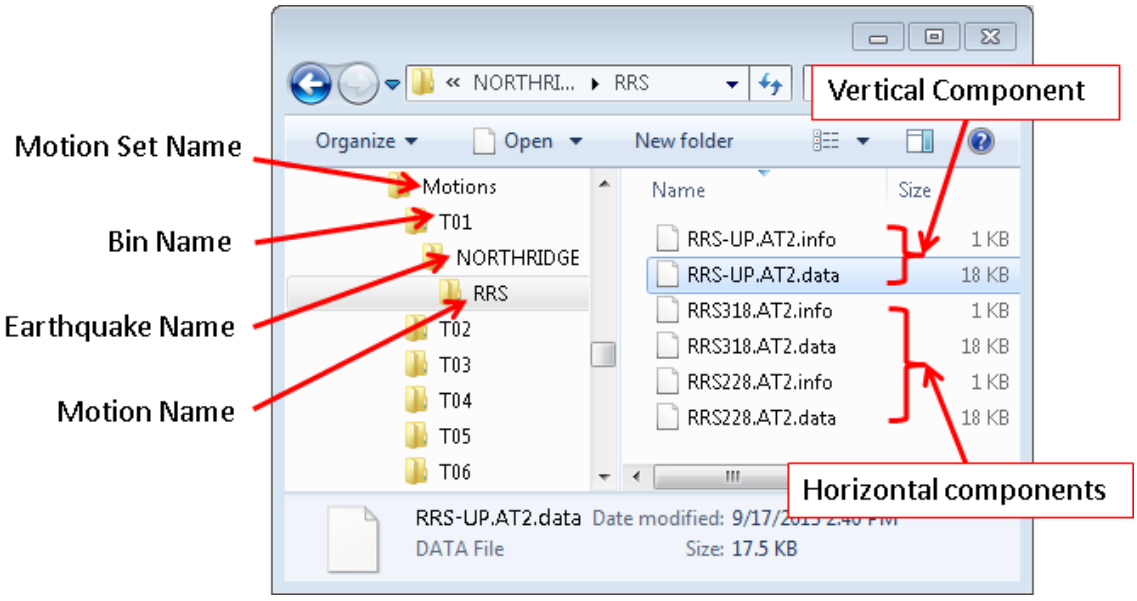

Fig. 172. The directory structure of a motion set

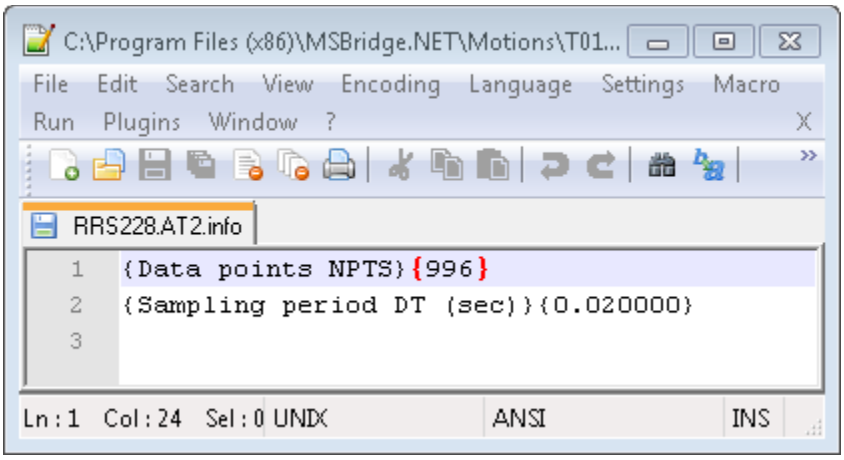

Fig. 173. Sample .info file

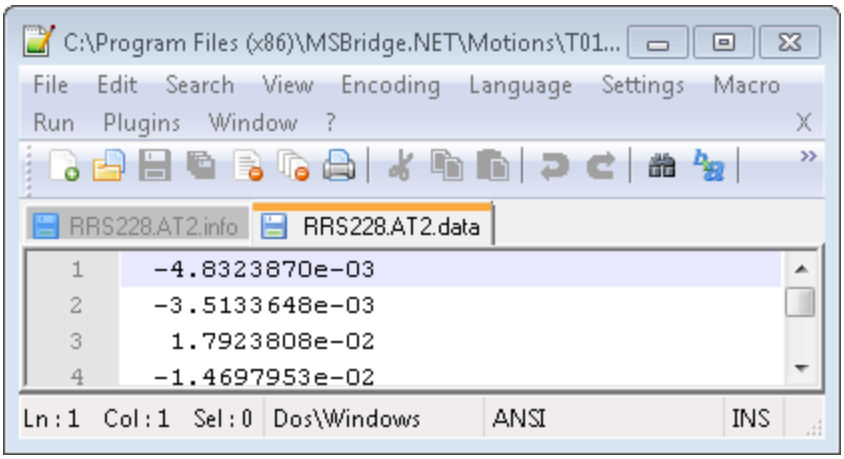

Fig. 174. Sample .data file

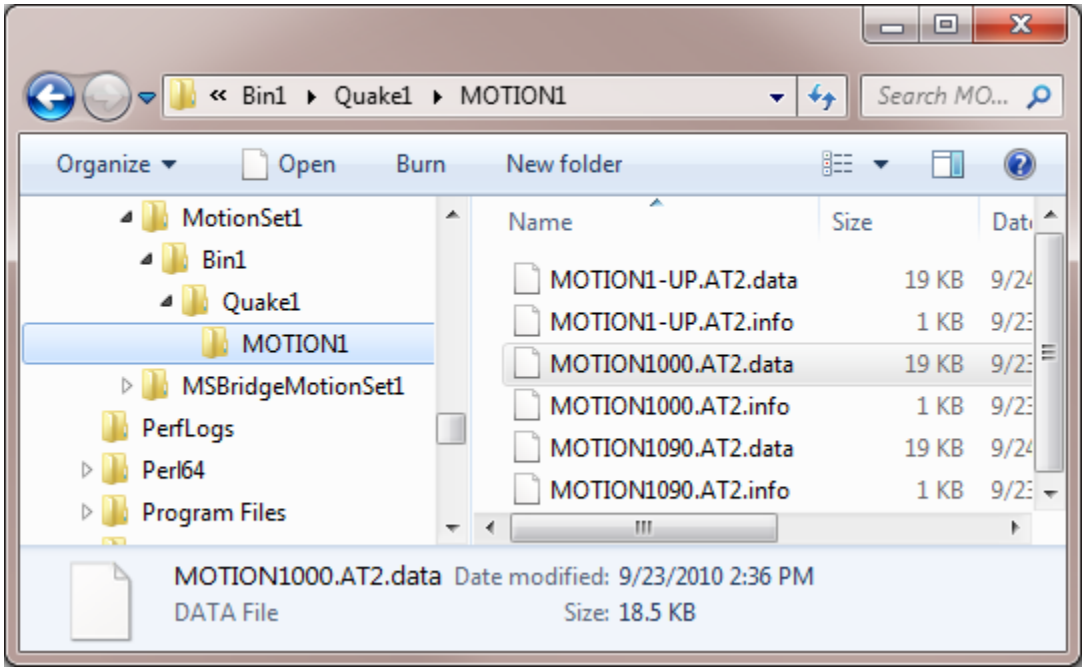

Fig. 175. Example of user-defined motion

APPENDIX D COMPARISON WITH SAP2000 FOR REPRESENTATIVE BRIDGE CONFIGURATIONS

A large portion of bridges in the current California bridge inventory share similar construction characteristics, especially those owned and maintained by the California Department of Transportation (CalTrans) (Mackie and Stojadinovic, 2007). Eleven bridge configurations were selected by Ketchum et al. (2004) as representative of typical statewide bridge construction in California. These bridge configurations are listed in Table 8.

Table 8. Typical Bridge Configurations in California (After Ketchum et al. 2004)

Bridge Type	Span Arrangement	Geometry	Bent Columns	Column Height	DeckWidth	Deck Depth
1	120'+150'+150'+150'+120'	Straight	1	22'	39'	6'
2	120'+150'+150'+150'+120'	Straight	3	22'	68'	6'
3	80'+100'+100'+100'+80'	Straight	1	22'	39'	4'
4	80'+100'+100'+100'+80'	Straight	3	22'	68'	4'
5	80'+100'+100'+100'+80'	Straight	1	22'	39'	5'-2"
6	80'+100'+100'+100'+80'	Straight	3	22'	68'	5'-2"
7	120'+120'	Straight	1	22'	39'	6'-2"
8	120'+120'	Straight	3	22'	68'	6'-2"
9	120'+150'+150'+150'+120'	1000' radius	1	22'	27'	6'
10	80'+100'+100'+100'+80'	30 skew	3	22'	68'	4'
11	120'+150'+150'+150'+120'	Straight	1	50'	39'	6'

The above models were built (without much effort) in **MSBridge** (Linear columns, Roller abutment model and Rigid-base were assumed; default values were used for other bridge parameters).

Linear analyses of monotonic pushover show both **MSBridge** and **SAP2000** gave identical results for all of the 11 bridge configurations shown in Table 8. For example, Fig. 176 shows the models built in **MSBridge** and SAP2000 for Bridge Type 1. Table 9 shows the displacement of the deck at each bent under the pushover load of 2000 kips applied at the deck center along the longitudinal and transverse directions. Fig. 177 and Table 10 show the comparison for Bridge Type 2. Fig. 178 and Table 11 show the comparison for Bridge Type 9. Fig. 179 and Table 12 show the comparison for a skewed bridge case (Bridge Type 10). Both **MSBridge** and **SAP2000** essentially gave the same result.

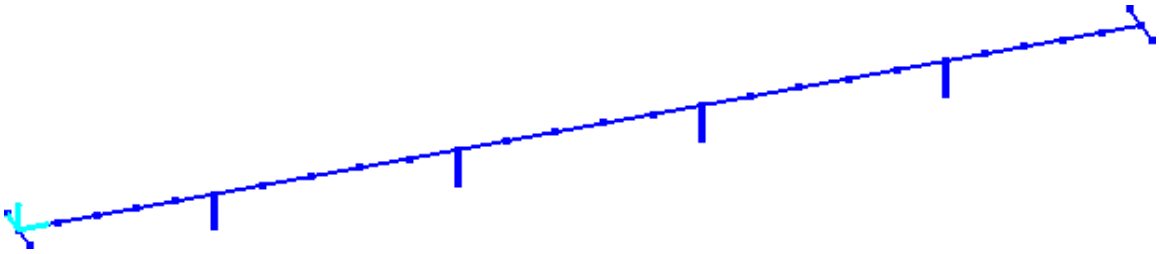

a)

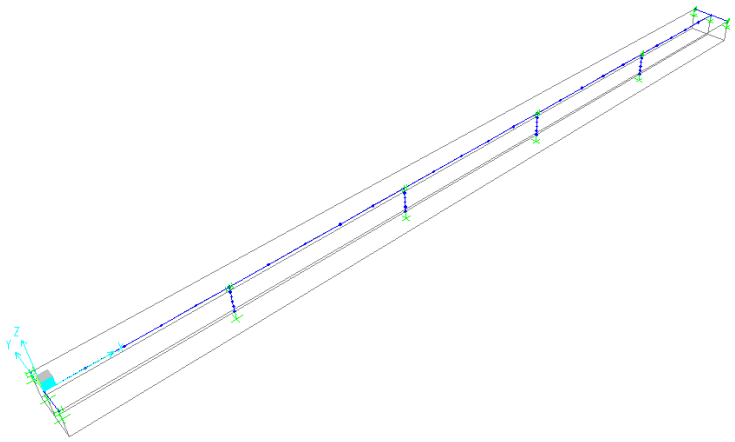

b)

Fig. 176. Bridge Type 1 model: a) **MSBridge**; b) **SAP2000**

Table 9. Deck displacement (unit: inches) of Bridge Type 1 under pushover (load of 2000 kips applied at deck center along both the longitudinal and transverse directions)

	Bent	Longitudinal Displacement	Transverse Displacement	Vertical Displacement
SAP2000	2	0.71745	0.68199	-0.05127
	3	0.73926	2.38939	-0.05235
	4	0.73025	2.15946	-0.05204
	5	0.70799	0.50487	-0.05278
MSBridge	2	0.71724	0.68326	-0.0513
	3	0.73941	2.39682	-0.0524
	4	0.73064	2.15976	-0.0520
	5	0.70873	0.50778	-0.0528
Difference	2	0%	0%	0%
	3	0%	0%	0%
	4	0%	0%	0%
	5	0%	1%	0%

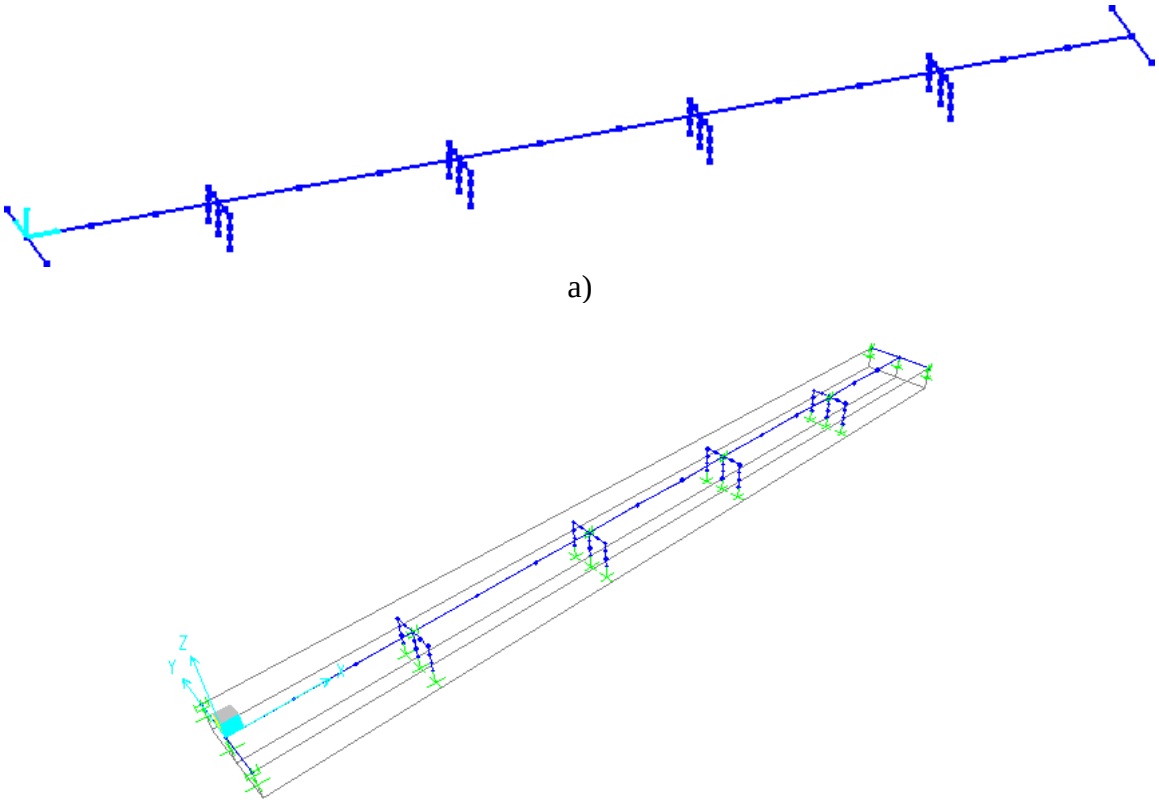

a)

b)

Fig. 177. Bridge Type 2 model: a) **MSBridge**; b) **SAP2000**

Table 10. Deck displacement (unit: inches) of Bridge Type 2 under pushover (load of 2000 kips applied at deck center along both the longitudinal and transverse directions)

	Bent	Longitudinal Displacement	Transverse Displacement	Vertical Displacement
SAP2000	2	0.3051	0.117	-0.0728
	3	0.3194	0.4988	-0.074
	4	0.3094	0.4082	-0.0737
	5	0.2946	0.0304	-0.0742
MSBridge	2	0.3053	0.1159	-0.073102
	3	0.3201	0.5099	-0.074236
	4	0.3104	0.4097	-0.074008
	5	0.2961	0.03116	-0.074469
Difference	2	0%	1%	0%
	3	0%	2%	0%
	4	0%	0%	0%
	5	1%	3%	0%

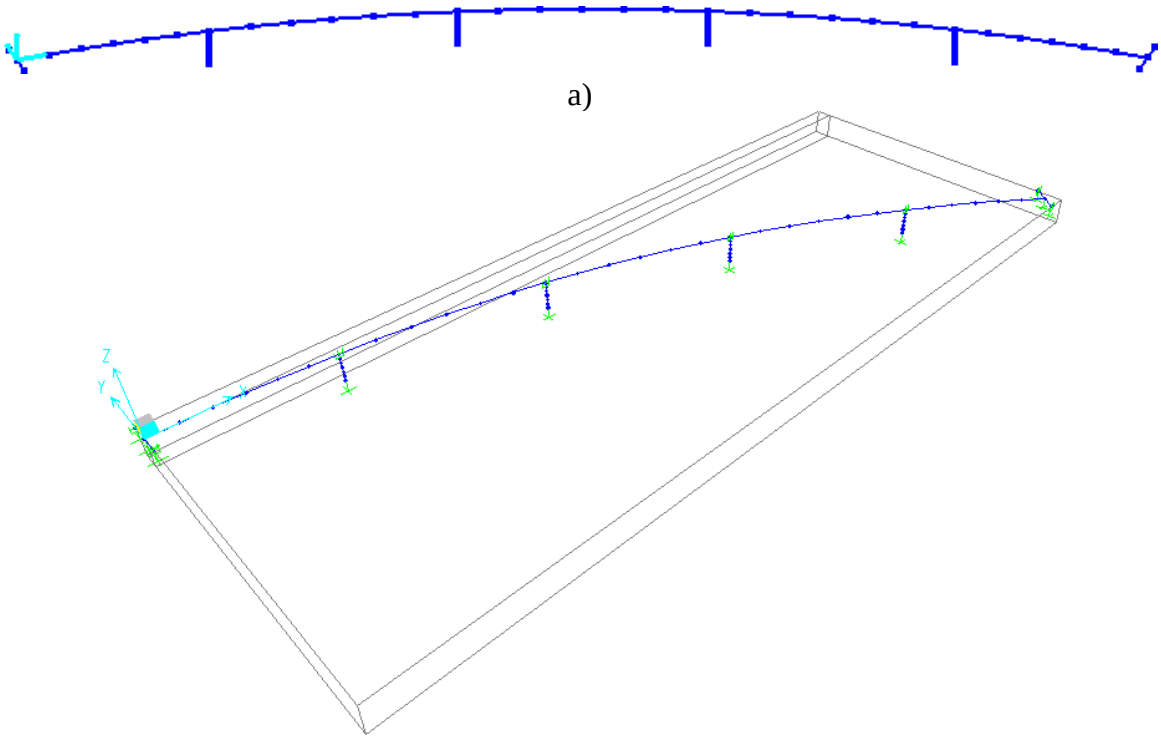

a)

b)

Fig. 178. Bridge Type 9 model: a) **MSBridge**; b) **SAP2000**

Table 11. Deck displacement (unit: inch) of Bridge Type 9 under pushover (load of 1000 kips applied at deck center along both the longitudinal and transverse directions)

	Bent	Longitudinal Displacement	Transverse Displacement	Vertical Displacement
SAP2000	2	0.4862	0.1208	-0.0410
	3	0.7547	1.3601	-0.0423
	4	0.7268	1.3913	-0.0422
	5	0.0953	0.2112	-0.0415
MSBridge	2	0.4881	0.1240	-0.0410
	3	0.7571	1.3630	-0.0423
	4	0.7266	1.3950	-0.0422
	5	0.0956	0.2149	-0.0415
Difference	2	0%	3%	0%
	3	0%	0%	0%
	4	0%	0%	0%
	5	0%	2%	0%

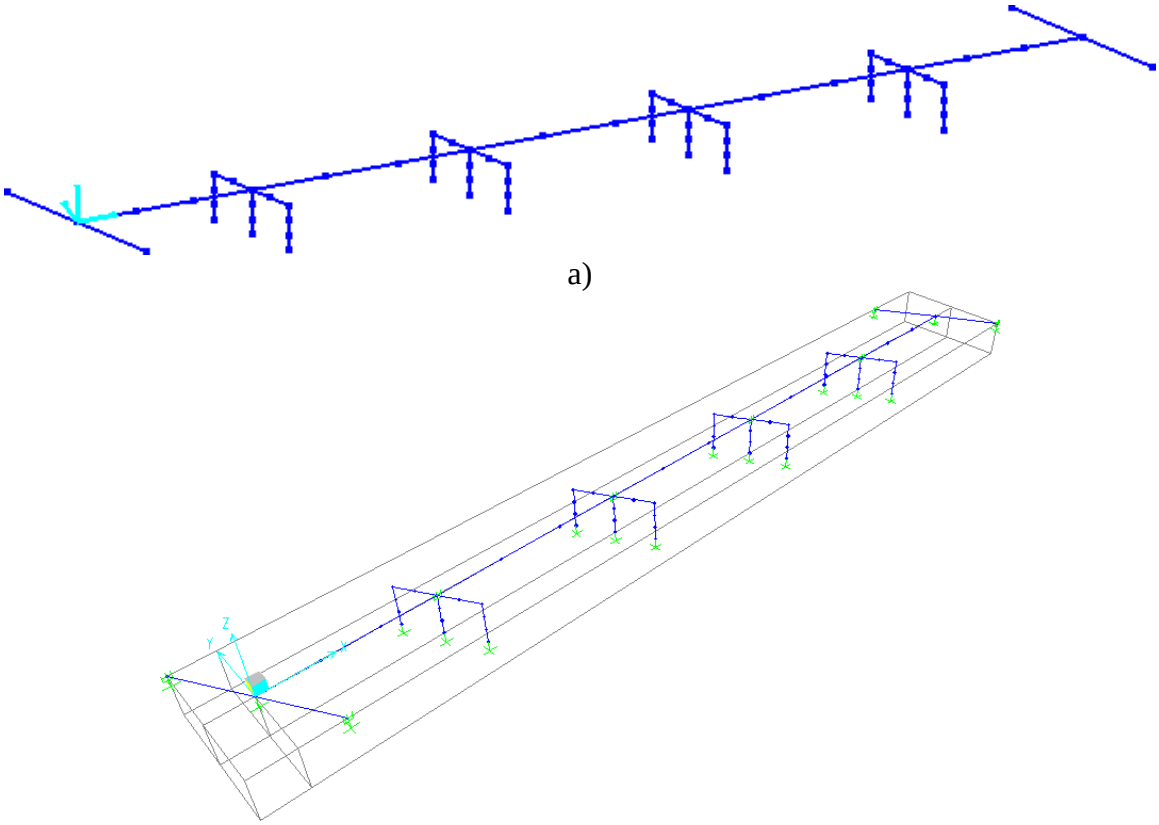

a)

b)

Fig. 179. Bridge Type 10 model: a) **MSBridge**; b) **SAP2000**

Table 12. Deck displacement (unit: inch) of Bridge Type 10 under pushover (load of 2000 kips applied at deck center along both the longitudinal and transverse directions)

	Bent	Longitudinal Displacement	Transverse Displacement	Vertical Displacement
SAP2000	2	0.3910	0.3054	-0.0456
	3	0.4018	0.4871	-0.0472
	4	0.3935	0.4210	-0.0476
	5	0.3811	0.1755	-0.0474
MSBridge	2	0.3931	0.2917	-0.0457
	3	0.4046	0.4991	-0.0472
	4	0.3970	0.4309	-0.0477
	5	0.3852	0.1853	-0.0475
Difference	2	1%	5%	0%
	3	1%	2%	0%
	4	1%	2%	0%
	5	1%	5%	0%

REFERENCES

Aviram, A., Mackie, K.R., and Stojadinovic, B. (2008).Effect of Abutment Modeling on the Seismic Response of Bridge Structures, Earthquake Engineering and Engineering Vibration 7(4), 395-402.

Berry, M.P., and Eberhard, M.O. (2007). Performance Modeling Strategies for Modern Reinforced Concrete Bridge Columns, Report No. 2007/07, Pacific Earthquake Engineering Research Center, University of California, Berkeley, California.

Kotsoglu, A., and Pantazopoulou, S. (2006). Modeling of Embankment Flexibility and Soil-structure Interaction in Integral Bridges, Proceedings of First European Conference on Earthquake Engineering and Seismology, September 3-8, Geneva, Switzerland.

Caltrans, 1999, xSection User Manual, California Department of Transportation, Sacramento, California.

Caltrans SDC, 2004. Caltrans Seismic Design Criteria, Version 1.3, California Department of Transportation, Sacramento, California.

Caltrans SDC, 2006. Caltrans Seismic Design Criteria, Version 1.4, California Department of Transportation, Sacramento, California.

Caltrans SDC, 2010. Caltrans Seismic Design Criteria, Version 1.6, California Department of Transportation, Sacramento, California.

Caltrans, 2017. Bridge Memo to Designer (MTD) 20-15: "Lateral Spreading Analysis for New and Existing Bridges." California Department of Transportation, Sacramento, CA 95816.

Caltrans, 2018. Highway Design Manual, 6th Edition, California Department of Transportation, Sacramento, California.

Elgamal, A., Yang, Z., Parra, E., and Ragheb, A. 2003.Modeling of cyclic mobility in saturated cohesionless soils. International Journal of Plasticity, 19(6), 883-905.

Elgamal, A., and Lu, J. 2009. A Framework for 3D finite element analysis of lateral pile system response, Proceedings of the 2009 International Foundation Congress and Equipment Expo, Contemporary Topics in In Situ Testing, Analysis, and Reliability of Foundations, ASCE GSP 186, M. Iskander, D. F. Laefer, and M. H. Hussein, Editors, Orlando, Florida, March 15-19, pp. 616-623.

Elgamal, A., Jinchi Lu, J., and Forcellini, D. 2009a. Mitigation of liquefaction-induced lateral deformation in a sloping stratum: 3D numerical simulation, Journal of

geotechnical and geoenvironmental engineering, ASCE, Vol. 135, No. 11, November, 1672-1682.

Elgamal, A., Lu, J., Yang, Z. and Shantz, T. 2009b. Scenario-focused three-dimensional computational modeling in geomechanics, Alexandria, Egypt, October 3-5, 4 iYGEC'09 - 4th International Young Geotechnical Engineers' Conference, 2 - 6 October, ISSMGE.

Elgamal, A. (2010). Calibrated 3D computational modeling of soil-structure systems and liquefaction scenarios, Proc. Fifth Intl. Conf. on Recent Advances in Geotechnical Earthquake Engineering and Soil Dynamics, May 24-29, San Diego, CA.

Lam, I. P., and Martin, G. R. (1986), "Seismic Design of Highway Bridge Foundations, FHWA Report," Federal Highway Administration, Washington D.C.

Lu J., 2006. Parallel finite element modeling of earthquake site response and liquefaction, Ph.D. Thesis, Department of Structural Engineering, University of California, San Diego, La Jolla, CA.

Mackie, K.R., and Stojadinovic, B. (2005). "Fragility basis for California highway overpass bridge seismic decision making." PEER Report No. 2005/02, Pacific Earthquake Engineering Research Center, University of California, Berkeley.

Mackie, K. and Stojadinovic, B. (2006). Seismic Vulnerability of Typical Multi-span California Highway Bridges, Proceedings of the Fifth National Seismic Conference on Bridges and highways, September 18-20, San Francisco.

Mackie, K.R., Wong, J-M., and Stojadinovic, B. (2008)."Integrated probabilistic performance-based evaluation of benchmark reinforced concrete bridges." PEER Report No. 2007/09, Pacific Earthquake Engineering Research Center, University of California, Berkeley.

Mackie, K.R., Wong, J-M., and Stojadinovic, B. (2010). Post-earthquake bridge repair cost and repair time estimation methodology. Earthquake Engineering and Structural Dynamics, 39(3): 281-301.

Mackie, K.R., Wong, J-M., and Stojadinovic, B. (2011). Bridge damage and loss scenarios calibrated by schematic design and cost estimation of repairs. Earthquake Spectra, 27: 1127-1145.

Maroney, B.H., and Chai, Y.H. (1994). Seismic Design and Retrofitting of Reinforced Concrete Bridges, Proceedings of 2nd International Workshop, Earthquake Commission of New Zealand, Queenstown, New Zealand.

Mander, J.B., Priestley, M.J.N., and Park, R. (1988). Theoretical Stress-Strain Model for Confined Concrete, Journal of the Structural Division ASCE, 114, pp. 1804-1826.

Mazzoni, S., McKenna, F., Scott, M. H., Fenves, G. L., et al. (2009). Open System for Earthquake Engineering Simulation, User Command-Language Manual, Pacific Earthquake Engineering Research Center, University of California, Berkeley, OpenSees version 2.0, May.

Megally, S.H., Seible, F., Bozorgzadeh, A., Restrepo, J. and Silva, P.F. (2003). Response of Sacrificial Shear Keys in Bridge Abutments to Seismic Loading, Proceedings of the FIB Symposium on Concrete Structures in Seismic Regions, May 6-9, Athens, Greece.

Shamsabadi, A., Rollins, K.M, and Kapuskar, M. (2007).Nonlinear Soil-Abutment-Bridge Structure Interaction for Seismic Performance-Based Design, Journal of Geotechnical and Geoenvironmental Engineering, 133(6), 707-720, June.

Shamsabadi, A., Khalili-Tehrani, P., Stewart, J.P., and Taciroglu, E. (2010).Validated Simulation Models for Lateral Response of Bridge Abutments with Typical Backfills, J. Bridge Eng., 15(3), 302-311, May.

Werner, S.D. (1994). Study of Caltrans' Seismic Evaluation Procedures for Short Bridges, Proceedings of the 3rd Annual Seismic Research Workshop, Sacramento, California.

Yang, Z., Elgamal, A., and Parra, E. 2003.A computational model for cyclic mobility and associated shear deformation, Journal of Geotechnical and Geoenvironmental Engineering, 129 (12), 1119-1127.

Zhang, J., and Makris, N. (2002). Kinematic Response Functions and Dynamic Stiffnesses of Bridge Embankments, Earthquake Engineering & Structural Dynamics, 31(11), pp. 1933-1966.